PŘÍLOHA 1

Predictive relevance of miR-34a, miR-224 and miR-342 in patients with advanced squamous cell carcinoma of the lung undergoing palliative chemotherapy

VLASTIMIL KULDA[1], MARTIN SVATON[2], PETR MUKENSNABL[3], KRISTYNA HRDA[1,2],
PAVEL DVORAK[4], ZBYNEK HOUDEK[4], KATERINA HOUFKOVA[4], RADANA VRZAKOVA[1],
VACLAV BABUSKA[1], MILOS PESEK[2] and MARTIN PESTA[4,5]

Departments of [1]Medical Chemistry and Biochemistry, [2]Pneumology and Phthisiology, [3]Pathology and [4]Biology;
[5]Biomedical Centre, Faculty of Medicine in Pilsen, Charles University, 30166 Pilsen, Czech Republic

Abstract. Attributing to their pathophysiological role and stability in biological samples, microRNAs (miRNAs) have the potential to become valuable predictive markers for non-small cell lung cancer (NSCLC). Samples of biopsy tissue constitute suitable material for miRNA profiling with the aim of predicting the effect of palliative chemotherapy. The present study group included 81 patients (74 males, 7 females, all smokers or former smokers) with the squamous cell carcinoma (SCC) histological subtype of NSCLC at a late stage (3B or 4). All patients received palliative chemotherapy based on platinum derivatives in combination with paclitaxel or gemcitabine. The expression of 17 selected miRNAs was measured by reverse transcription-quantitative polymerase chain reaction in tumor tissue macrodissected from formalin-fixed paraffin-embedded (FFPE) tissue samples. To predict the effect of palliative chemotherapy, the association between gene expression levels and overall survival (OS) time was analyzed. From the 17 miRNAs of interest, low expression levels of miR-342 and high expression levels of miR-34a and miR-224 were associated with a reduced OS time in subgroups of patients based on smoking status and treatment modality. Using cluster analysis, associations between combinations of miR-34a, -224 and -342 expression levels with patient survival were identified. The present study revealed that patients with the simultaneous high expression of miR-224 and -342 had a similar prognostic outcome to those with the low expression of miR-224 and -342, which was significantly reduced, compared with patients exhibiting high expression of either miR-224 or miR-342 with low expression of the other. We hypothesize that the effect of a particular miRNA is dependent on the expression level of other members of the miRNA network. This finding appears to complicate survival analyses based on individual miRNAs as markers. In conclusion, the present study provides evidence that specific miRNAs were associated with OS time, which may be candidate predictors for the effectiveness of palliative treatment in SCC lung cancer patients. This objective can be better achieved by combining more markers together than by using individual miRNAs.

Introduction

Lung cancer is the most common type of cancer, with high mortality rates worldwide (1); the incidence in the Czech Republic was 86.9 cases in men and 38.0 in women per 100,000 people in 2011 (2). Approximately 85% of all lung cancer cases are non-small cell lung cancer (NSCLC), which includes two major histological subtypes: Squamous cell carcinoma (SCC) and adenocarcinoma. SCC represents ~25-30% of cases of NSCLC (3). The prognosis for patients with advanced SCC is poorer than that of those with adenocarcinoma (4).

Chemotherapy is an essential modality of palliative treatment for inoperable SCC at advanced stages. The response rate to chemotherapy varies widely from patient to patient; therefore, it is of interest to find biomarkers that predict the effect of cytostatic therapeutics. The resistance of cancer cells to chemotherapy can be caused by the increased export of anticancer drugs out of the cells, improved DNA repair ability or apoptosis resistance (5). The expression of genes participating in these processes is regulated by the microRNA (miRNA/miR) network. miRNAs are small non-coding RNA molecules of ~22 nucleotides that participate in the post-transcriptional regulation of gene expression (6). The human genome encodes >2,500 miRNAs (7), which target ~60% of mammalian genes and are abundant in a number of human cell types (8) (see miRNA database available online at www.mirbase.org).

The aim of the present study was to evaluate the association of the expression of miRNAs involved in the processes resulting in chemotherapy resistance with the overall survival (OS) time of patients with advanced SCC receiving palliative

Correspondence to: Dr Martin Pesta, Department of Biology, Faculty of Medicine in Pilsen, Charles University, 76 Alej Svobody, 30166 Pilsen, Czech Republic
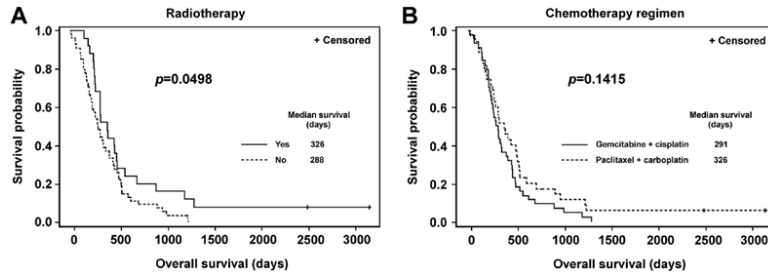E-mail: martin.pesta@lfp.cuni.cz

Figure 1. Association between the treatment modality and OS time for non-small cell lung cancer patients, as determined with the Kaplan-Meier method. All patients were treated with chemotherapy. (A) There were significantly longer OS times in the subgroup of patients who underwent chemotherapy combined with radiotherapy, compared with the patients who underwent chemotherapy without radiotherapy. (B) OS was independent of the chemotherapy regimen received. OS, overall survival.
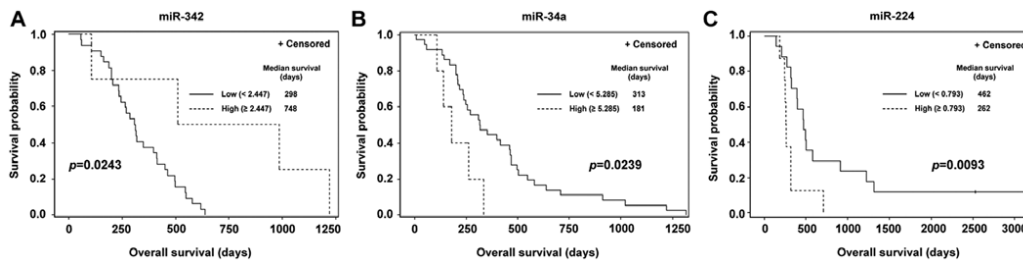

Figure 2. Association of miRNA expression with OS in the subgroups of non-small cell lung cancer patients (Kaplan-Meier curves). (A) Low expression of miR-342 was associated with shorter OS time in the subgroup of smokers. (B) High expression of miR-34a was associated with shorter OS time in the subgroup of patients treated with chemotherapy based on platinum derivatives in combination with gemcitabine. (C) High expression of miR-224 was associated with shorter OS time in a subgroup of patients who underwent chemotherapy combined with radiotherapy. OS, overall survival; miR, microRNA.
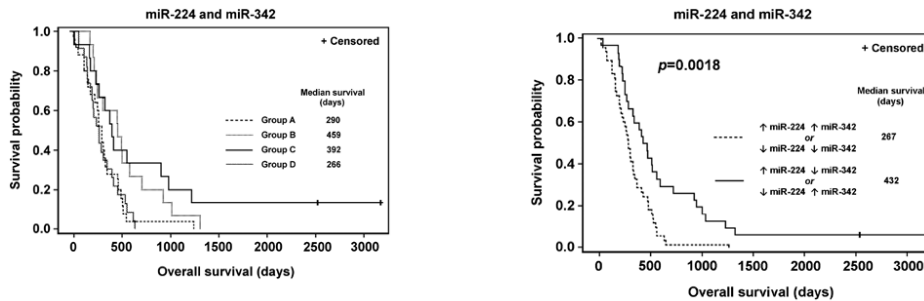

Figure 3. Kaplan-Meier curves for the overall survival of patients stratified into four groups according to the expression of miR-224 and -342: Group A, high miR-224 and -342; group B, high miR-224 and low miR-342; group C, low miR-224 and high miR-342; and group D, low miR-224 and -342. miR, microRNA.

Figure 4. Comparison of survival of two groups of patients created by putting groups with similar survival from Fig. 3 together (group A and D vs. group B and C). Patients with the high expression of both miR-224 and -342 or low expression of both miR-224 and -342 have significantly shorter OS times than those with the high expression of either miR-224 and -342 and the low expression of the other. miR, microRNA.

family member 8 expression; the inconsistency of these studies will be discussed in the following paragraph.

In the present study, low levels of miR-342 indicated a poorer outcome in patients with a history of smoking, independent of treatment modality. Xie *et al* (21) demonstrated that miR-342 was downregulated in NSCLC and acted as a tumor suppressor through the repression of RAP2B, member of RAS oncogene family. Similarly, Tai *et al* (22) identified

that miR-342 was capable of indirectly regulating MYC activity via the direct repression of E2F transcription factor 1. Takahashi *et al* (23) investigated how cigarette smoking altered plasma miRNA profiles; they identified that there was a decrease in plasma miR-342 in subjects who quit smoking, compared with smokers.

Table I. Analyzed miRNAs and their involvement in pathogenesis and treatment of NSCLC.

Symbol	miRBase accession no.	Cat. no. 4427975 assay ID	Relation to NSCLC	(Refs.)
miR-15b	MIMAT0000417	000390	Regulates cisplatin resistance and metastasis by targeting PEBP4 in lung adenocarcinoma cells	(35)
miR-21	MIMAT0000076	000397	Regulates NSCLC cell invasion and chemo-sensitivity through SMAD7	(36)
miR-27a	MIMAT0000084	000408	Higher expression levels in advanced NSCLC patients resistant to EGFR-TKI	(37)
miR-34a	MIMAT0000255	000426	Sensitizes lung cancer cells to cisplatin via p53/miR-34a/MYCN axis	(38)
miR-99a-3p	MIMAT0004511	002141	Promotes proliferation, migration and invasion of NSCLC cell lines	(39)
miR-106a	MIMAT0000103	000578	Confers cisplatin resistance in non-small cell lung cancer A549 cells	(40)
miR-107	MIMAT0000104	000443	Regulates cisplatin chemosensitivity of A549 non small cell lung cancer cell lines by targeting cyclin dependent kinase 8	(41)
miR-143	MIMAT0000435	002249	Regulates cell apoptosis in lung cancer by targeting PKCε	(42)
miR-150	MIMAT0000451	000473	Downregulation induces cell proliferation inhibition and apoptosis in NSCLC by targeting BAK1	(43)
miR-192	MIMAT0000222	000491	Regulates chemo-resistance of lung adenocarcinoma for gemcitabine and cisplatin combined therapy by targeting Bcl-2	(44)
miR-193a-3p	MIMAT0000459	002250	Suppresses the metastasis of NSCLC by downregulating the ERBB4/PIK3R3/mTOR/S6K2 signaling pathway	(45)
miR-211	MIMAT0000268	000514	Promotes NSCLC proliferation by targeting SRCIN1	(46)
miR-218	MIMAT0000275	000521	Regulates cisplatin chemosensitivity in NSCLC by targeting RUNX2	(47)
miR-221	MIMAT0000278	000524	Overexpressed in aggressive NSCLC and regulates TRAIL resistance through PTEN and TIMP3	(48)
miR-224	MIMAT0000281	002099	Is implicated in lung cancer pathogenesis through targeting caspase-3 and caspase-7	(19)
miR-342-3p	MIMAT0000753	002260	Suppresses proliferation and invasion of NSCLC by targeting RAPB2	(21)
miR-375	MIMAT0000728	000564	Predictive for response for non-small cell lung cancer treated with cisplatin-vinorelbine A	(49)
RNU6B	-	001093	Reference gene	(50)

miR/miRNA, microRNA; NSCLC, non-small cell lung cancer.

subgroups of patients with different chemotherapy regimens (Fig. 1B).

Association of miRNA expression with OS time. The Cox regression hazard model was used to determine the association between the levels of miRNA expression with OS time. From the 17 miRNAs of interest, in the subgroup of smokers, the low expression of miR-342 (P=0.0500) and high expression level of miR-34a and miR-224 (P=0.0338 and P=0.0400, respectively) were associated with a shorter OS time. High expression levels of miR-34a were associated with shorter OS time in the subgroup of patients treated with platinum derivate-based chemotherapy in combination with gemcitabine (P=0.0364). High expression levels of miR-224 were associated with shorter OS time in the subgroup of patients who underwent chemotherapy combined with radiotherapy (P=0.0250).

For the statistically significant miRNA markers, optimal cut-off values were identified and Kaplan-Meier survival distribution functions for OS were generated. Statistically significant differences in OS time between subgroups with marker expression levels below and above the cut-off value were obtained for miR-342 in the subgroup of smokers (P=0.0243; Fig. 2A), miR-34a in a subgroup of patients that were treated with gemcitabine in chemotherapy regimen (P=0.0239; Fig. 2B) and miR-224 in the subgroup of patients that underwent chemotherapy combined with radiotherapy (P=0.0093; Fig. 2C). Statistical values obtained from the Kaplan-Meier analyses are summarized in Table III.

miRNAs associated with OS (miR-34a, -224 and -342) were the subject of the subsequent cluster analysis. Pairs of these miRNAs (miR-34a and -224, miR-34a and -342, and miR-224 and -342) were analyzed for their association with

Table II. Clinicopathological characteristics of patients with squamous cell carcinoma of the lung (n=81).

Characteristic	Patients, n (%)
Sex	
Male	74 (91.4)
Female	7 (8.6)
Age, years	
<55	11 (13.6)
55-65	41 (50.6)
>65	29 (35.8)
Smoking status	
Non-smoker	0 (0)
Ex-smoker	42 (51.9)
Smoker	39 (48.1)
Clinical stage	
3B	42 (51.9)
4	39 (48.1)
Eastern Cooperative Oncology	
Group performance status	
0	2 (2.5)
1	58 (71.6)
2	18 (22.2)
3	3 (3.7)
Radiotherapy	
Yes	25 (30.9)
No	56 (69.1)
Chemotherapy	
Paclitaxel and carboplatin	35 (43.2)
Gemcitabine and cisplatin	46 (56.8)

OS time. For each pair of miRNAs, patients were stratified into groups according to the miRNA expression being above (high) or below (low) the cut-off value: Group A (high miR-224 and high miR-342); group B (high miR-224 and low miR-342); group C (low miR-224 and high miR-342); and group D (low miR-224 and low miR-342). Initially, the cut-off value obtained from univariate analysis was used also for cluster analysis; however, this led to a highly disproportional distribution of patients among subgroups. Therefore, a median was used as a cut off value for cluster analysis.

Fig. 3 demonstrates the Kaplan-Meier survival distribution functions of patients stratified into groups according to the expression of miR-224 and miR-342. There are two pairs of groups with similar OS distributions; Fig. 4 includes a comparison of the OS of two groups of patients created by combining the groups from Fig. 3 with similar survival outcomes (group A/D vs. group B/C). There was a significant difference in survival between these groups (P=0.0018), as detailed in Table IV. The same approach was used to analyze the other pairs of miRNAs; however, no significance was identified. All three miRNAs were analyzed together in the same manner (miR-34a, -224 and -342). Patterns of expression

associating patients with significantly shorter survival times were identified (Fig. 5; Table IV).

Identification of potential target genes for miR-34a, -224 and -342. Using DIANA-TarBase v7.0 and DIANA-miRPath v3.0 bioinformatic tools (11,12), 6 overlapping target genes with P<0.05 were identified between miR-34a, -224 and -342. These genes, including GNAS complex locus (GNAS), insulin like growth factor 1 receptor (IGF1R), cyclin D1 (CCND1), cyclin G2 (CCNG2), serpin family E member 1 (SERPINE1) and ribonucleotide reductase regulatory subunit M2 (RRM2), are associated with cell cycle regulation, p53 signaling and DNA repair.

Discussion

miRNAs may have the potential to become accurate, easily measurable biomarkers, with features convenient for diagnostic testing methods, including stability in FFPE tissue blocks, blood, and potentially, other bodily fluids (16). The present study focused on patients with the NSCLC SCC subtype with an advanced-stage SCC. The included patients were unable to undergo surgical resection and received palliative treatment only. For these patients, there were multiple treatment modalities. The main clinical concern in such cases is deciding which therapeutic regimen is indicated. However, in the group of patients in the present study, it was only possible to analyze the potential predictors for the treatment response to platinum base derivatives in combination with either paclitaxel or gemcitabine, with or without the application of radiotherapy.

Initially, the present study focused on a univariate analysis of the association between miRNA expression and OS time. Subsequently, a multivariate analysis was performed that included the miRNAs that had been identified to exhibit associations with OS. On the basis of the results of the present study, we hypothesize that the effect of a single miRNA may depend on the level of expression of other members of the miRNA network, to be further discussed.

Higher levels of miR-224 indicated shorter OS times for patients with chemotherapy combined with radiotherapy in the present study. Cui *et al* (17) reported that miR-224 expression was significantly upregulated in NSCLC tissues and suggested it performed its oncogenic role in lung cancer pathogenesis through targeting caspase-3 and -7. Wang *et al* (18) identified through microarray analysis that miR-224 expression was upregulated in cisplatin-resistant cell lines, and demonstrated that miR-224 could promote cisplatin resistance via regulating the G_1/S cell cycle transition and apoptosis by targeting p21. These findings indicated the association of miR-224 with the effect of chemotherapy based on DNA damage, and its potential as a predictor for the response to treatment. However, Zhu *et al* (19) reported that miR-224 expression levels were downregulated in NSCLC compared with non-cancerous lung tissue. These authors also observed that decreased miR-224 expression was significantly associated with lymph node metastasis, an advanced tumor-node-metastasis stage and a reduced OS time (19). Furthermore, Wang *et al* (20) recently identified that miR-224 was significantly upregulated in NSCLC tissues and hypothesized that miR-224 expression promotes NSCLC cell proliferation by downregulating Ras association domain

Table III. Association between the level of miRs and overall survival time as determined by Kaplan-Meier estimation.

					Below cut-off		Above cut-off		
Patient group	Treatment	Marker	Patients, n	Cut-off	n	Median, days	n	Median, days	P-value
Smokers only	Chemotherapy	miR-342	36	2.447	32	298	4	748	0.0243
Smokers and ex-smokers	Gemcitabine and cisplatin	miR-34a	41	5.285	36	313	5	181	0.0239
Smokers and ex-smokers	Chemotherapy and radiotherapy	miR-224	25	0.793	17	462	8	262	0.0093

miR, microRNA.

Table IV. Association between combinations of miRs and OS (Kaplan-Meier estimation).

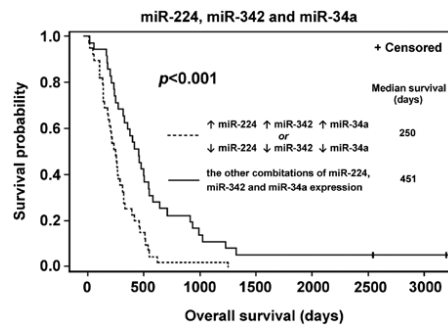| Expression pattern	Patients, n	Median OS, days
miR-342 and -224		
High miR-224 and -342, or low miR-224 and -342	48	267
High miR-224 and low miR-342, or low miR-224 and high miR-342	30	432
miR-342, -224 and -34a		
High miR-224, -342 and -34a, or low miR-224, -342 and -34a	39	250
Other combinations	35	451

OS, overall survival; miR, microRNA.

Figure 5. Comparison of the OS of two groups of patients based on patterns of miR-224, -342 and -34a expression. Patients with the high or low expression of all three miRs exhibit a significantly shorter OS time than those with other combinations of miR-224, -342 and -34a expression. OS, overall survival; miR, microRNA.

miR-34a is a member of the miR-34 family that is associated with the p53 pathway, and is implicated in cell death/survival signaling (24). The miR-34 family is transcriptionally activated by p53; in turn, p53 is a direct miR-34a target. However, the effect of miR-34a on p53 depends on the cellular context (25). miR-34a can have also a positive effect on p53 transcriptional activity and protein stability by targeting multiple p53 inhibitor genes (including MDM4, p53 regulator, sirtuin 1, metastasis associated 1 family member 2, histone deacetylase 1 and YY1 transcription factor) (26). A previous study identified that miR-34a inhibits cell proliferation (27). Expression of the miR-34 family was downregulated in tumor tissue compared with normal tissue, and low levels of miR-34a expression were associated with a higher probability of relapse in surgically resected NSCLC (28). However, higher levels of circulating miR-34a were observed in patients with NSCLC compared with healthy controls (29). Higher levels of miR-34a indicated a shorter OS time in patients receiving palliative platinum derivate-based chemotherapy in combination with gemcitabine in the present study.

Multivariate analysis was performed with the miRNAs (miR-34a, -224 and -342) that were identified as associated with OS. The most notable finding was that patients with the high expression of miR-224 and -342 exhibited similar outcomes to those with low expression of miR-224 and -342, which was significantly shorter than that of patients with high expression of either miR-224 or miR-342 and the low expression of the other (Figs. 3 and 4).

We hypothesize that the effect of a single miRNA is dependent on the level of expression of the other members of the miRNA network. It has been established that an miRNA can have a predominantly oncogenic role in one type of cancer and a tumor suppressive role in another; for instance, miR-224 was identified to be a tumor suppressor in prostate cancer (30), whereas in other types of malignancy, including gastric (11,31) and colorectal cancer (32), an oncogenic role for miR-224 was described. The ambiguous role of miR-224 was also observed within the SCC histological subtype of NSCLC in the present study. Tumor progression occurs as a result of the dysregulation of a number of protein-coding genes and epigenetic processes,

including the deregulation of a number of miRNAs. Therefore, to understand the role of one particular miRNA, it is necessary to determine the levels of the other 'co-players'. In the present study, OS time was influenced by the mutual association of miR-224 and -342. The high level of miR-224 can be associated with adverse or favorable outcomes, depending on the simultaneous level of miR-342. These findings could explain the inconsistent results of previously published studies on miR-224 expression in NSCLC. In 2014, Zhu *et al* (19) reported that miR-224 was significantly downregulated in NSCLC and that a decrease in miR-224 expression was significantly associated with shorter OS time (19). Also in NSCLC, Cui *et al* (33) identified that miR-224 was significantly upregulated, with the increased expression of miR-224 promoting cell migration, invasion, and proliferation. As aforementioned, the present study also identified that the high expression levels of miR-224 were associated with shorter OS time in one subgroup of patients, specifically those who underwent chemotherapy combined with radiotherapy.

Using bioinformatic tools, the present study identified overlapping experimentally validated target genes for miR-34a, -224 and -342. Notably, all overlapping target genes identified in the present study (GNAS, IGF1R, CCND1, CCNG2, SERPINE1, and RRM2) are involved in processes associated with carcinogenesis, including cell cycle regulation, p53 signaling and DNA repair. This may explain the complicated mutual dependency of those miRNAs in relation to tumor progression and the effectiveness of treatment. We hypothesize that these molecules could be involved in competing endogenous RNA crosstalk, where RNA transcripts co-regulate each other by competing for shared miRNAs, thereby titrating miRNA availability (34). However, one limitation of the present study is the absence of immunoprecipitation data and reporter assays, which are methods that may confirm the interactions among the set of 3 miRNAs and 6 target genes. Nevertheless, the results of the present study may provide a stimulus for further research in this area.

With cluster analysis, novel associations between miR-34a, -224 and -342 that affected patient survival time were identified in the present study. The result may demonstrate that the effort to find a particular miRNA as a perfect marker for a particular event may be fruitless due to the complex interactions between RNA transcripts. In order to understand all aspects of the effect of miRNAs on the regulation of gene expression in cancer and their associations with phenotype and treatment outcome, miRNA profiling and deep bioinformatic analysis will be necessary. Only this approach can facilitate the future application of miRNAs in clinical practice. miRNAs can generally be assessed with more precision and ease than the mRNAs of coding genes, as miRNA analysis is less demanding in terms of the quality and quantity of isolated RNA, features that may be problematic in RNA samples extracted from FFPE tissue (16). FFPE tissue samples are routinely taken and analyzed during standard lung cancer management, which is why miRNAs may become clinically applicable predictors of the effectiveness of palliative treatment in patients with lung cancer. Nevertheless, the findings of the present study demonstrated that, due to the complex network of interactions, this objective could be achieved by combining more markers together rather than by using individual miRNAs. On the basis of the results of the current study, miR-224, -342 and -34a could be members of this panel of predictors of treatment efficacy.

References

1. Torre LA, Siegel RL and Jemal A: Lung Cancer Statistics. Adv Exp Med Biol 893: 1-19, 2016.
2. Institute of Health Information and Statistics of the Czech Republic: Czech Health Statistics Year Book 2013. UZIS CR, Prague, 2014.
3. Travis WD: Pathology of lung cancer. Clin Chest Med 32: 669-692, 2011.
4. Socinski MA, Obasaju C, Gandara D, Hirsch FR, Bonomi P, Bunn P, Kim ES, Langer CJ, Natale RB, Novello S, *et al*: Clinicopathologic features of advanced squamous NSCLC. J Thorac Oncol 11: 1411-1422, 2016.
5. Olaussen KA and Postel-Vinay S: Predictors of chemotherapy efficacy in non-small-cell lung cancer: A challenging landscape. Ann Oncol 27: 2004-2016, 2016.
6. Inamura K and Ishikawa Y: MicroRNA in lung cancer: Novel biomarkers and potential tools for treatment. J Clin Med 5: pii: E36, 2016.
7. Griffiths-Jones S, Saini HK, van Dongen S and Enright AJ: miRBase: Tools for microRNA genomics. Nucleic Acids Res 36 (Database Issue): D154-D158, 2008.
8. Friedman RC, Farh KK, Burge CB and Bartel DP: Most mammalian mRNAs are conserved targets of microRNAs. Genome Res 19: 92-105, 2009.
9. Sobin LH, Gospodarowicz MK and Wittekind Ch: TNM Classification of Malignant Tumours. 7th edition. Wiley-Blackwell, Chichester, 2010.
10. Kalfert D, Pesta M, Kulda V, Topolcan O, Ryska A, Celakovsky P, Laco J and Ludvikova M: MicroRNA profile in site-specific head and neck squamous cell cancer. Anticancer Res 35: 2455-2463, 2015.
11. Smid D, Kulda V, Srbecka K, Kubackova D, Dolezal J, Daum O, Kucera R, Topolcan O, Treska V, Skalicky T and Pesta M: Tissue microRNAs as predictive markers for gastric cancer patients undergoing palliative chemotherapy. Int J Oncol 48: 2693-2703, 2016.
12. Mazumdar M and Glassman JR: Categorizing a prognostic variable: Review of methods, code for easy implementation and applications to decision-making about cancer treatments. Stat Med 19: 113-132, 2000.
13. Faraggi D and Simon R: A simulation study of cross-validation for selecting an optimal cutpoint in univariate survival analysis. Stat Med 15: 2203-2213, 1996.
14. Vlachos IS, Paraskevopoulou MD, Karagkouni D, Georgakilas G, Vergoulis T, Kanellos I, Anastasopoulos IL, Maniou S, Karathanou K, Kalfakakou D, *et al*: DIANA-TarBase v7.0: Indexing more than half a million experimentally supported miRNA:mRNA interactions. Nucleic Acids Res 43 (Database Issue): D153-D159, 2015.
15. Vlachos IS, Zagganas K, Paraskevopoulou MD, Georgakilas G, Karagkouni D, Vergoulis T, Dalamagas T and Hatzigeorgiou AG: DIANA-miRPath v3.0: Deciphering microRNA function with experimental support. Nucleic Acids Res 43: W460-W466, 2015.
16. Khan J, Lieberman JA and Lockwood CM: Variability in, variability out: Best practice recommendations to standardize pre-analytical variables in the detection of circulating and tissue microRNAs. Clin Chem Lab Med 55: 608-621, 2017.
17. Cui R, Kim T, Fassan M, Meng W, Sun HL, Jeon YJ, Vicentini C, Tili E, Peng Y and Scarpa A: MicroRNA-224 is implicated in lung cancer pathogenesis through targeting caspase-3 and caspase-7. Oncotarget 6: 21802-21815, 2015.
18. Wang H, Zhu LJ, Yang YC, Wang ZX and Wang R: MiR-224 promotes the chemoresistance of human lung adenocarcinoma cells to cisplatin via regulating G_1/S transition and apoptosis by targeting p21(WAF1/CIP1). Br J Cancer 111: 339-354, 2014.

19. Zhu D, Chen H, Yang X, Chen W, Wang L, Xu J and Yu L: Decreased microRNA-224 and its clinical significance in non-small cell lung cancer patients. Diagn Pathol 9: 198, 2014.
20. Wang L, Liu W, Zhang YP and Huang XR: The miR-224 promotes non-small cell lung cancer cell proliferation by directly targeting RASSF8. Eur Rev Med Pharmacol Sci 21: 3223-3231, 2017.
21. Xie X, Liu H, Wang M, Ding F, Xiao H, Hu F, Hu R and Mei J: miR-342-3p targets RAP2B to suppress proliferation and invasion of non-small cell lung cancer cells. Tumour Biol 36: 5031-5038, 2015.
22. Tai MC, Kajino T, Nakatochi M, Arima C, Shimada Y, Suzuki M, Miyoshi H, Yatabe Y, Yanagisawa K and Takahashi T: miR-342-3p regulates MYC transcriptional activity via direct repression of E2F1 in human lung cancer. Carcinogenesis 36: 1464-1473, 2015.
23. Takahashi K, Yokota SI, Tatsumi N, Fukami T, Yokoi T and Nakajima M: Cigarette smoking substantially alters plasma microRNA profiles in healthy subjects. Toxicol Appl Pharmacol 272: 154-160, 2013.
24. Rokavec M, Li H, Jiang L and Hermeking H: The p53/miR-34 axis in development and disease. J Mol Cell Biol 6: 214-230, 2014.
25. Okada N, Lin CP, Ribeiro MC, Biton A, Lai G, He X, Bu P, Vogel H, Jablons DM, Keller AC, *et al*: A positive feedback between p53 and miR-34 miRNAs mediates tumor suppression. Genes Dev 28: 438-450, 2014.
26. Navarro F and Lieberman J: miR-34 and p53: New insights into a complex functional relationship. PLoS One 10: e0132767, 2015.
27. Ma ZL, Hou PP, Li YL, Wang DT, Yuan TW, Wei JL, Zhao BT, Lou JT, Zhao XT, Jin Y and Jin YX: MicroRNA-34a inhibits the proliferation and promotes the apoptosis of non-small cell lung cancer H1299 cell line by targeting TGFβR2. Tumour Biol 36: 2481-2490, 2015.
28. Gallardo E, Navarro A, Viñolas N, Marrades RM, Diaz T, Gel B, Quera A, Bandres E, Garcia-Foncillas J, Ramirez J and Monzo M: miR-34a as a prognostic marker of relapse in surgically resected non-small-cell lung cancer. Carcinogenesis 30: 1903-1909, 2009.
29. Franchina T, Amodeo V, Bronte G, Savio G, Ricciardi GR, Picciotto M, Russo A, Giordano A and Adamo V: Circulating miR-22, miR-24 and miR-34a as novel predictive biomarkers to pemetrexed-based chemotherapy in advanced non-small cell lung cancer. J Cell Physiol 229: 97-99, 2014.
30. Goto Y, Nishikawa R, Kojima S, Chiyomaru T, Enokida H, Inoguchi S, Kinoshita T, Fuse M, Sakamoto S, Nakagawa M, *et al*: Tumour-suppressive microRNA-224 inhibits cancer cell migration and invasion via targeting oncogenic TPD52 in prostate cancer. FEBS Lett 588: 1973-1982, 2014.
31. Zhang Y, Li CF, Ma LJ, Ding M and Zhang B: MicroRNA-224 aggravates tumor growth and progression by targeting mTOR in gastric cancer. Int J Oncol 49: 1068-1080, 2016.
32. Adamopoulos PG, Kontos CK, Rapti SM, Papadopoulos IN and Scorilas A: miR-224 overexpression is a strong and independent prognosticator of short-term relapse and poor overall survival in colorectal adenocarcinoma. Int J Oncol 46: 849-859, 2015.
33. Cui R, Meng W, Sun HL, Kim T, Ye Z, Fassan M, Jeon YJ, Li B, Vicentini C, Peng Y, *et al*: MicroRNA-224 promotes tumor progression in nonsmall cell lung cancer. Proc Natl Acad Sci USA 112: E4288-E4297, 2015.
34. Tay Y, Rinn J and Pandolfi PP: The multilayered complexity of ceRNA crosstalk and competition. Nature 505: 344-352, 2014.
35. Zhao Z, Zhang L, Yao Q and Tao Z: miR-15b regulates cisplatin resistance and metastasis by targeting PEBP4 in human lung adenocarcinoma cells. Cancer Gene Ther 22: 108-114, 2015.
36. Lin L, Tu HB, Wu L, Liu M and Jiang GN: MicroRNA-21 regulates non-small cell lung cancer cell invasion and chemo-sensitivity through SMAD7. Cell Physiol Biochem 38: 2152-2162, 2016.
37. Wang S, Su X, Bai H, Zhao J, Duan J, An T, Zhuo M, Wang Z, Wu M, Li Z, *et al*: Identification of plasma microRNA profiles for primary resistance to EGFR-TKIs in advanced non-small cell lung cancer (NSCLC) patients with EGFR activating mutation. J Hematol Oncol 8: 127, 2015.
38. Song C, Lu P, Sun G, Yang L, Wang Z and Wang Z: miR-34a sensitizes lung cancer cells to cisplatin via p53/miR-34a/MYCN axis. Biochem Biophys Res Commun 482: 22-27, 2017.
39. Chen C, Zhao Z, Liu Y and Mu D: microRNA-99a is down-regulated and promotes proliferation, migration and invasion in non-small cell lung cancer A549 and H1299 cells. Oncol Lett 9: 1128-1134, 2015.
40. Ma Y, Li X, Cheng S, Wei W and Li Y: MicroRNA-106a confers cisplatin resistance in non-small cell lung cancer A549 cells by targeting adenosine triphosphatase-binding cassette A1. Mol Med Rep 11: 625-632, 2015.
41. Zhang Z, Zhang L, Yin ZY, Fan XL, Hu B, Wang LQ and Zhang D: miR-107 regulates cisplatin chemosensitivity of A549 non small cell lung cancer cell line by targeting cyclin dependent kinase 8. Int J Clin Exp Pathol 7: 7236-7241, 2014.
42. Zhang N, Su Y and Xu L: Targeting PKCε by miR-143 regulates cell apoptosis in lung cancer. FEBS Lett 587: 3661-3667, 2013.
43. Gu XY, Wang J, Luo YZ, Du Q, Li RR, Shi H and Yu TP: Down-regulation of miR-150 induces cell proliferation inhibition and apoptosis in non-small-cell lung cancer by targeting BAK1 in vitro. Tumour Biol 35: 5287-5293, 2014.
44. Cao J, He Y, Liu HQ, Wang SB, Zhao BC and Cheng YS: MicroRNA 192 regulates chemo-resistance of lung adeno-carcinoma for gemcitabine and cisplatin combined therapy by targeting Bcl-2. Int J Clin Exp Med 8: 12397-12403, 2015.
45. Yu T, Li J, Yan M, Liu L, Lin H, Zhao F, Sun L, Zhang Y, Cui Y, Zhang F, *et al*: MicroRNA-193a-3p and -5p suppress the metastasis of human non-small-cell lung cancer by downregulating the ERBB4/PIK3R3/mTOR/S6K2 signaling pathway. Oncogene 34: 413-423, 2015.
46. Ye L, Wang H and Liu B: miR-211 promotes non-small cell lung cancer proliferation by targeting SRCIN1. Tumour Biol 37: 1151-1157, 2016.
47. Xie J, Yu F, Li D, Zhu X, Zhang X and Lv Z: MicroRNA-218 regulates cisplatin (DPP) chemosensitivity in non-small cell lung cancer by targeting RUNX2. Tumour Biol 37: 1197-1204, 2016.
48. Garofalo M, Di Leva G, Romano G, Nuovo G, Suh SS, Ngankeu A, Taccioli C, Pichiorri F, Alder H, Secchiero P, *et al*: miR-221&222 regulate TRAIL resistance and enhance tumorigenicity through PTEN and TIMP3 downregulation. Cancer Cell 16: 498-509, 2009.
49. Berghmans T, Ameye L, Willems L, Paesmans M, Mascaux C, Lafitte JJ, Meert AP, Scherpereel A, Cortot AB, Cstoth I, *et al*: Identification of microRNA-based signatures for response and survival for non-small cell lung cancer treated with cispl-atin-vinorelbine A ELCWP prospective study. Lung Cancer 82: 340-345, 2013.
50. Fiedler SD, Carletti MZ and Christenson LK. Quantitative RT-PCR methods for mature microRNA expression analysis. Methods Mol Biol 630: 49-64, 2010.

PŘÍLOHA 2

Původní práce

Může vyšetření lymfatických uzlin metodou One-Step Nucleic Acid Amplification zpřesnit staging plicních nádorů?

J. Vodička[1], Š. Vejvodová[1], M. Pešta[2,6], P. Mukenšnabl[3], V. Špidlen[1], V. Kulda[4], K. Houfková[2], O. Topolčan[5]

[1] Chirurgická klinika, Univerzita Karlova, Lékařská fakulta v Plzni, Fakultní nemocnice Plzeň
[2] Ústav biologie, Univerzita Karlova, Lékařská fakulta v Plzni
[3] Šiklův ústav patologie, Univerzita Karlova, Lékařská fakulta v Plzni, Fakultní nemocnice Plzeň
[4] Ústav lékařské chemie a biochemie, Univerzita Karlova, Lékařská fakulta v Plzni
[5] Oddělení nukleární medicíny – centrální laboratoř pro imunoanalýzu, Fakultní nemocnice Plzeň
[6] Biomedicínské centrum, Univerzita Karlova, Lékařská fakulta v Plzni

Souhrn

Úvod: Cílem práce je porovnání senzitivity detekce mikrometastáz v hilových a mediastinálních lymfatických uzlinách primárních (nemalobuněčných) a sekundárních (metastázy kolorektálního karcinomu) nádorů plic pomocí standardního histopatologického vyšetření v barvení hematoxylin-eosin, imunohistochemického vyšetření s protilátkou proti cytokeratinu 19 a metodou One-Step Nucleic Acid Amplification.

Metoda: Při radikální chirurgické léčbě nemalobuněčných primárních plicních karcinomů a metastáz kolorektálního karcinomu byly u 100 pacientů zařazených do studie v období 2015–2017 podle standardního schématu odebrány hilové a mediastinální lymfatické uzliny. Tyto uzliny pak byly v podélné ose děleny na 4 stejné části, přičemž část první a třetí zleva byla určena k vyšetření metodou One-Step Nucleic Acid Amplification, část druhá a čtvrtá k histologickému vyšetření. Při histologickém vyšetření byly příslušné části uzlin nejprve vyšetřeny standardním postupem v barvení hematoxylin-eosin a následně pak i imunohistochemicky s protilátkou proti cytokeratinu 19. Metoda One-Step Nucleic Acid Amplification byla prováděna soupravou firmy Sysmex (Kobe, Japonsko), jejím principem je detekce mRNA (messenger ribonucleic acid) cytokeratinu 19 reverzní transkripcí spojenou s izotermickou amplifikací.

Výsledky: Celkem bylo nemocným zařazeným do studie odebráno a uvedenou metodikou vyšetřeno 1426 lymfatických uzlin. Shodné výsledky vyšetření hematoxylinem-eosinem, imunohistochemií s protilátkou proti cytokeratinu 19 a One-Step Nucleic Acid Amplification byly zaznamenány u 78 nemocných (78 %). Mikrometastázy v lymfatických uzlinách byly metodou One-Step Nucleic Acid Amplification při negativitě ostatních metod prokázány u 16 pacientů (16 %). Pouze ve 3 případech (3 %) bylo vyšetření hematoxylinem-eosinem, resp. imunohistochemií s protilátkou proti cytokeratinu 19 pozitivní při negativitě metody One-Step Nucleic Acid Amplification. Výsledky imunohistochemie s protilátkou proti cytokeratinu 19 prakticky přesně kopírovaly výsledky vyšetření hematoxylinem-eosinem (97 %).

Závěr: Výsledky studie prokázaly vyšší procento detekovaných mikrometastáz v hilových a mediastinálních lymfatických uzlinách při vyšetření metodou One-Step Nucleic Acid Amplification ve srovnání s hematoxylin-eosinem a imunohistochemií s protilátkou proti cytokeratinu 19 (upstaging 16 %). Ukazuje se tak, že vyšetření lymfatických uzlin pomocí metody One-Step Nucleic Acid Amplification může mít určitý potenciál zpřesnit staging plicních nádorů, naopak imunohistochemie s protilátkou proti cytokeratinu 19 změny stagingu téměř nepřináší. Je však nezbytné potvrdit tento předpoklad v dalších studiích, resp. na větším souboru nemocných. Dalším úkolem je také pečlivým sledováním nemocných zjistit souvislost mikrometastáz detekovaných v lymfatických uzlinách metodou One-Step Nucleic Acid Amplification s jejich follow-up.

Klíčová slova: karcinom plic – lymfatické uzliny – H&E – IHC CK19 – OSNA

Summary

Can the One-Step Nucleic Acid Amplification method of lymph nodes examination make the staging of pulmonary tumours more precise?

J. Vodicka, S. Vejvodova, M.Pesta, P. Mukensnabl, V. Spidlen,V. Kulda, K. Houfkova, O. Topolcan

Introduction: The aim of this article is to compare the sensitivity of detecting micrometastases in hilar and mediastinal lymph nodes in case of primary (non-small cell) and secondary (metastases of colorectal carcinoma) pulmonary tumours using standard histopathological examination with haematoxylin-eosin staining, immunohistochemistry examination with Anti-Cytokeratin 19 antibody and examination based on the One-Step Nucleic Acid Amplification method.

Method: During radical surgical treatment of primary non-small cell lung carcinoma and pulmonary metastases of colorectal carcinoma, hilar and mediastinal lymph nodes of 100 patients enrolled in the study in the period from 2015 to 2017 were extracted based on a standard classification. These lymph nodes were subsequently divided along the longitudinal axis into 4 identical parts where part one and three on the left were intended for examination based on the One-Step Nucleic Acid Amplification method, whereas parts two and four were subjected to histopathological examination. In evaluating the respective parts of the nodes by histological examination, the nodes were first examined by a standard procedure that involves haematoxylin-eosin staining, followed by immunohistochemistry examination with Anti-Cytokeratin 19 antibody. The One-Step Nucleic Acid Amplification method was performed in the kit supplied by Sysmex (Kobe, Japan) and is based on the detection of cytokeratin 19 mRNA (messenger ribonucleic acid) by reverse transcription coupled with isothermal amplification.

Results: A total of 1,426 lymph nodes of the patients enrolled in the study were extracted and examined using the above mentioned methodology. In 78 patients (78%), identical results were obtained using haematoxylin-eosin staining, immunohistochemistry with Anti-Cytokeratin 19 and One-Step Nucleic Acid Amplification. Micrometastases in the lymph nodes using the One-Step Nucleic Acid Amplification method in the absence of the other methods were proven in 16 patients (16%). Only in 3 cases (3%), the examination by haematoxylin-eosin staining, or immunohistochemistry with Anti-Cytokeratin 19, was positive while One-Step Nucleic Acid Amplification was negative. The results obtained by immunohistochemistry with Anti-Cytokeratin 19 antibody were practically the same as those obtained by haematoxylin-eosin staining (97%).

Conclusion: The results of the study have demonstrated a higher percentage of metastases detected in hilar and mediastinal lymph nodes if the One-Step Nucleic Acid Amplification method of examination was used compared to haematoxylin-eosin staining and immunohistochemistry with Anti-Cytokeratin 19 antibody (upstaging in 16%). This shows that the examination of lymph nodes using the One-Step Nucleic Acid Amplification method can have a certain potential to make the pulmonary tumours staging more accurate. On the other hand, immunohistochemistry with Anti-Cytokeratin 19 antibody seems to be not so useful. However, it is necessary to prove this hypothesis in follow-up studies, or where applicable, in a larger cohort of patients. Another task is to ascertain, by careful patient monitoring, the influence of the micrometastases detected in their lymph nodes using the One-Step Nucleic Acid Amplification method on these patients' follow-up.
Key words: lung cancer – lymph nodes – H&E – IHC CK19 – OSNA assay

ÚVOD

Detekce nádorových buněk v hilových a mediastinálních lymfatických uzlinách (LU) u nemocných s primárními a sekundárními nádory plic je v současné době limitována možnostmi standardních histopatologických metod. Možnými cestami zvýšení detekce mikrometastáz v regionálních LU mohou být jednak průkaz nádorových buněk imunohistochemickým vyšetřením s protilátkou proti cytokeratinu 19 (IHC CK19), jednak molekulárně genetická metoda OSNA (One-Step Nucleic Acid Amplification), která detekuje mRNA CK19 (messenger ribonucleic acid cytokeratinu 19). Cytokeratin 19 (CK19) je intermediální filamentum cytoskeletu epiteliálních buněk, které je přítomno jak v normálních epiteliálních buňkách, tak v buňkách epiteliálních tumorů a jejich metastáz, nikoli ale v LU. Průkaz CK19 nebo mRNA pro CK19 v LU je tak ukazatelem jejich metastatického postižení nádorovými buňkami epiteliálního původu [1–3].

Hlavním cílem níže prezentované prospektivní studie bylo ověření možnosti zpřesnění patologické TNM (pTNM) klasifikace primárních a sekundárních plicních nádorů senzitivnější detekcí mikrometastáz v LU prostřednictvím IHC CK19 a metody OSNA ve srovnání se standardním histopatologickým vyšetřením hematoxylinem-eosinem (H&E).

METODA

Soubor pacientů

Do prospektivní studie probíhající v období let 2015 až 2017 byli zařazeni pacienti s operabilním nemalobuněčným plicním karcinomem (NSCLC) a plicními metastázami kolorektálního karcinomu, tj. s nádory, u kterých již byla prokázána exprese CK19 [1]. Soubor, jehož bližší charakteristiky uvádí Tab. 1, tvořilo 100 pacientů.

Operační postup

Operačním přístupem byla vždy posterolaterální torakotomie. Rozsah výkonu se odvíjel od typu nádoru, jeho velikosti a lokalizace a v případě metastáz i od jejich počtu. Při NSCLC byla standardním výkonem anatomická plicní resekce v rozsahu lobektomie, bilobektomie či pneumonektomie. Plicní metastázy byly odstraňovány buď klínovitou resekcí (na svorce, staplerem), nebo precizní laserovou excizí pomocí Nd:YAG laseru MY 40 1.3 o vlnové délce laserového pa-

prsku 1318 nm. Nedílnou součástí každé operace byla systematická hilová a mediastinální lymfadenektomie (SMLA) podle zavedeného schématu The International Association for the Study of Lung Cancer (IASLC) z roku 2009 [4].

Zpracování lymfatických uzlin

LU byly ihned po odebrání v podélné ose děleny na 4 stejné části, přičemž část první a třetí zleva byly určeny k vyšetření metodou OSNA, část druhá a čtvrtá k H&E, resp. IHC CK19. Velmi malé LU byly v podélné ose pouze půleny, jedna polovina analogicky připadla k vyšetření metodou OSNA, druhá k H&E, resp. IHC CK19. Dělení vyšetřovaných LU je standardním postupem a je dáno technologií zpracování LU pro jednotlivá vyšetření, kdy vyšetření jednou metodou vylučuje jejich ná-

Tab. 1: Charakteristiky souboru
Tab. 1: Patient characteristics

Proměnné	Počet	%
Pohlaví		
Muži	63	63,0
Ženy	37	37,0
Typ operace		
Pneumonektomie	6	6,0
Bilobektomie	6	6,0
Lobektomie	74	74,0
Klínovitá resekce, laserová excize	14	14,0
Typ tumoru		
Nemalobuněčný plicní karcinom	80	80,0
Metastáza kolorektálního karcinomu	20	20,0
Histologický typ NSCLC		
Adenokarcinom	45	56,25
Skvamózní karcinom	33	41,25
Adenoskvamózní karcinom	2	2,5
pT status NSCLC		
T1a	20	25,0
T1b	22	27,5
T2a	26	32,5
T2b	6	7,5
T3	5	6,25
T4	1	1,25

Vysvětlivka: NSCLC – nemalobuněčný plicní karcinom

sledné použití pro metodu druhou [5,6–9]. Z metodických důvodů byly části LU určené k vyšetření metodou OSNA sloučeny vždy v rámci jedné uzlinové zóny (dle schématu IASLC 2009) do jednoho vyšetření.

Histopatologické a imunohistochemické vyšetření

Při histopatologickém vyšetření byly z příslušných částí LU připraveny standardním způsobem tkáňové bločky, z nichž se pak zhotovily 3–4 µm tenké histologické řezy, které se následně obarvily základním histologickým barvením hematoxylin-eosin. Takto připravené řezy pak byly hodnoceny mikroskopicky. Po provedení tohoto základního histopatologického vyšetření byly vzorky vyšetřeny imunohistochemicky s protilátkou CK19.

Metoda OSNA

Při vyšetření metodou OSNA byly příslušné části LU zpracovány v několika krocích podle pokynů výrobce diagnostické soupravy LYNOAMP BC OSNA (Sysmex, Kobe, Japonsko). Vlastní stanovení přítomnosti mRNA CK19, resp. počtu jejích kopií, jakožto markeru epiteliálních buněk, bylo provedeno v přístroji RD100i. Detekce mRNA CK19 spočívá v současné reverzní transkripci (RT) a amplifikaci pomocí 3 párů primerů při teplotě 65 °C metodou LAMP (Loop Mediated Isothermal Amplification). Každá analýza skupiny LU obsahovala maximálně 600 mg tkáně. V případě větší hmotnosti byla tkáň LU rozdělena na vzorky do 600 mg. Průměrná hmotnost analyzované skupiny LU byla 310 mg, nejmenší LU vážila 20 mg, nejtěžší 4,46 g a byla rozdělena na části o hmotnosti do 600 mg. Uvedený postup respektuje firemní manuál LYNOAMP BC OSNA. Diagnostická souprava obsahuje pro každý test pozitivní a negativní kontrolu, má certifikaci in vitro diagnostických prostředků (IVD). Výsledek reakce umožňuje určit nepřítomnost nádorových buněk (cut off <250 kopií mRNA CK19/µl), přítomnost mikrometastázy (cut off 250–5000 kopií mRNA CK19/µl) nebo makrometastázy (cut off >5000 kopií mRNA CK19/µl). Hodnoty cut

off byly stanoveny dle firemního manuálu LYNOAMP BC OSNA a byly použity v předchozích studiích detekce nádorových buněk v LU pacientů s nádory plic [5,7,10–12].

Statistická analýza

Základní deskriptivní statistika byla provedena na základě klinicko-patologických dat pacientů, kteří souhlasili se vstupem do studie. Pro porovnání metod byly použity Vennovy diagramy.

VÝSLEDKY

Celkem bylo při 100 radikálních operacích odebráno během SMLA 1426 LU při průměru 14,3 LU na osobu (5–32 LU). Shodných výsledků vyšetření LU metodami H&E, IHC CK19 a OSNA bylo v našem souboru dosaženo u 78 osob (78 %), z toho negativních u 59 osob, pozitivních ve smyslu metastatického postižení LU u 19 osob. Zaznamenali jsme 16 případů (16 %) pozitivních nálezů při vyšetření metodou OSNA, které byly H&E i IHC CK19 negativní. Ve 3 případech (3 %) byla vyšetření H&E a IHC CK19 pozitivní při negativitě metody OSNA. Shodně po jednom případu (vždy 1 %) jsme zaznamenali negativní výsledek vyšetření H&E při pozitivitě IHC CK19 a OSNA, negativní výsledek IHC CK19 při pozitivitě vyšetření H&E a OSNA a pozitivní výsledek IHC CK19 při negativitě vyšetření H&E a OSNA (Graf 1).

Ve skupině NSCLC (80 osob) bylo shody mezi vyšetřeními H&E, IHC CK19 a OSNA dosaženo u 61 pacientů (76,3 %), negativní u 43 osob, pozitivní u 18 osob. Pozitivních nálezů metodou OSNA při negativitě vyšetření H&E, resp. IHC CK19 bylo 13 (16,3 %). Tři případy (3,8 %) byly H&E i IHC CK19 pozitivní při negativitě metody OSNA. Shodně po jednom případu (vždy 1,3 %) jsme zaznamenali negativní výsledek vyšetření H&E při pozitivitě IHC CK19 a OSNA, negativní výsledek IHC CK19 při pozitivitě vyšetření H&E

Graf 1: Porovnání shody výsledků vyšetření pacientů metodami H&E, IHC CK19 a OSNA pomocí Vennových diagramů
Graph 1: Comparison of identical examination results of patients using the H&E, IHC CK19 and OSNA methods by Venn diagrams
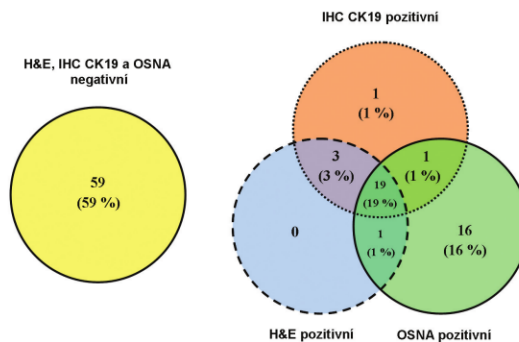
Vysvětlivky: H&E – hematoxylin-eosin; IHC CK19 – imunohistochemické vyšetření s protilátkou proti cytokeratinu 19; OSNA – One-Step Nucleic Acid Amplification

Tab. 2: Změny pTNM stagingu v závislosti na výsledcích vyšetření H&E, IHC CK19 a OSNA
Tab. 2: Changes in the pTNM staging depending on H&E, IHC CK19 and OSNA results

	H&E		IHC CK19		OSNA		Případy	Komentář
Shoda H&E, IHC CK19 a OSNA							78 (78 %)	
Rozdíly mezi H&E, IHC CK19 a OSNA							22 (22 %)	
	TNM	St	TNM	St	TNM	St		
NSCLC	T1aN0	IA	T1aN0	IA	T1aN2	IIIA	2	
	T1bN0	IA	T1bN0	IA	T1bN1	IIA	4	
	T1bN0	IA	T1bN0	IA	T1bN2	IIIA	1	Vyšší stadium dle OSNA
	T2aN0	IB	T2aN0	IB	T2aN1	IIA	2	
	T2aN0	IB	T2aN0	IB	T2aN2	IIIA	4	
	T1aN1	IIA	T1aN1	IIA	T1aN0	IA	1	
	T1aN2	IIIA	T1aN2	IIIA	T1aN0	IA	1	Nižší stadium dle OSNA
	T2aN2	IIIA	T2aN2	IIIA	T2aN0	IB	1	
	T1bN0	IA	T1bN2	IIIA	T1bN0	IA	1	Vyšší stadium dle IHC CK19
	T3N2	IIIA	T3N0	IIB	T3N2	IIIA	1	Nižší stadium dle IHC CK19
	T2aN0	IB	T2aN1	IIA	T2aN1	IIA	1	Vyšší stadium dle IHC CK19 a OSNA
Metastázy	N0	-	N0	-	N1	-	2	N pozitivní status dle OSNA
	N0	-	N0	-	N2	-	1	

Vysvětlivky: NSCLC – nemalobuněčný plicní karcinom; H&E – hematoxylin-eosin; IHC CK19 – imunohistochemické vyšetření s protilátkou proti cytokeratinu 19; OSNA – One-Step Nucleic Acid Amplification; TNM – klasifikace maligních nádorů

a OSNA a pozitivní výsledek IHC CK19 při negativitě vyšetření H&E a OSNA.

Ve skupině plicních metastáz (20 osob) bylo shody mezi vyšetřeními H&E, IHC CK19 a OSNA dosaženo u 17 pacientů (85 %), negativní u 16 osob, pozitivní u 1 osoby. Pozitivní nálezy metodou OSNA při negativitě vyšetření H&E a IHC CK19 byly 3 (15 %).

Z 16 případů pozitivních nálezů metodou OSNA při H&E, resp. IHC CK19 negativitě se jednalo o 13 případů NSCLC a 3 případy plicních metastáz kolorektálního karcinomu. V 8 případech měli tito nemocní nádorovou diseminací postiženy LU etáže N1, v 5 případech etáže N2 a ve 3 případech etáže N1 i N2. Ve 13 případech se jednalo o nález mikrometastázy v LU, ve dvou případech makrometastázy a v jednom případě jak mikrometastázy, tak makrometastázy.

Dopad neshod detekce nádorových buněk v LU metodami H&E, IHC CK19 a OSNA na pTNM staging ukazuje Tab. 2.

DISKUZE

Doporučené postupy pro léčbu jak primárních, tak sekundárních plicních nádorů se odvíjejí nejen od morfologické diagnózy nádoru, ale i od klinického stadia nemoci. Zásadní je proto co nejpřesnější určení stadia onemocnění podle TNM klasifikace (staging), aby mohla být zvolena nejvhodnější léčebná strategie [13]. Nedílnou součástí radikální léčby těchto nádorů je tak nejen jejich chirurgické odstranění, ale i odběr a následné vyšetření regionálních LU, které má v procesu stagingu stěžejní roli. Jednou z možných cest zpřes-

nění stagingu by mohlo být rutinní zavedení metody OSNA, resp. IHC CK19 do tohoto procesu. V dostupných literárních pramenech je použití metody OSNA v současnosti nejvíce zmiňováno v souvislosti s vyšetřováním regionálních LU u nemocných s karcinomem prsu. Podle většiny autorů poskytuje srovnatelné výsledky se standardním histopatologickým vyšetřením (míra shody 94–96 %, senzitivita 88–93 %, specificita 92–96 %) [5–8,10,14]. Studie zabývající se touto problematikou u nemocných s kolorektálním karcinomem přinesly obdobné výsledky (míra shody 96–97 %, senzitivita 86–96 %, specificita 97–100 %) [3,5,15–18]. Ve prospěch metody hovoří, vedle vyšetření celé homogenizované LU vylučující minutí nádorových buněk při přípravě histologického řezu, také velmi nízká míra falešné pozitivity, resp. negativity [5,15,19,23,26,27]. Existují ale i studie zpochybňující přínos metody OSNA, ať již pro nižší přesnost či vyšší cenu [20,21].

V případě primárních plicních nádorů jsou dosavadní literární údaje o aplikaci metody OSNA velmi sporé, jedná se jen o několik recentních publikací, problematikou plicních metastáz se dosud nezabývala žádná studie [1,11,12,22]. Masai a kol. sledovali expresi CK19 u primárních plicních nádorů a plicních metastáz karcinomu prsu, přičemž CK19 detekovali u 88 % pacientů s plicním karcinomem a u téměř 91 % nemocných s metastázami karcinomu prsu. Současně prokázali při uzlinové diseminaci zmíněných nádorů expresi CK19 v takto postižených LU [1]. Z výsledků této práce jsme vycházeli při volbě nádorů, resp. nemocných, kteří byli předmětem naší studie. Hayama a kol. srovnávali senzitivitu metod OSNA a H&E při vyšetřování LU u primárního plicního karcinomu. Jejich výsledky odpovídají

předchozím studiím s karcinomem prsu, resp. kolorektálním karcinomem (senzitivita OSNA 100 %, specificita 92 %), váha této studie je však podle našeho mínění znatelně snížena velmi malým počtem vyšetřených osob (20), resp. LU (pouhých 40) [11]. Poněkud větší soubor prezentoval Inoue se spolupracovníky, kteří vyšetřili 165 LU u 49 nemocných s rovněž příznivými výsledky (pozitivní prediktivní hodnota OSNA 95 %, negativní prediktivní hodnota 99 %, přesnost 99 %) [12]. Asi dosud největší soubor vyšetřovaných publikovali Nakagawa a kol., kteří zkoumali 410 LU u 111 nemocných s nemalobuněčným plicním karcinomem. Míru shody mezi H&E vyšetřením a metodou OSNA nalezli v necelých 93 % s citlivostí přes 79 % [22]. My jsme, ve srovnání s těmito studiemi, dosáhli významně většího počtu vyšetřených LU u 1 pacienta – průměrně 14,3. Podobně vysokého počtu odebraných LU na 1 pacienta dosáhli z recentních studií pouze Croner a kol. a Güller a kol. (shodně 14) [17,23].

Shodných výsledků vyšetření H&E, IHC CK19 a OSNA bylo v našem souboru dosaženo u 78 % případů (mezi H&E a OSNA v 80 %), což je sice méně, než udávají nejlepší výsledky recentních studií (93–97 %) [7,15–19,22,24], avšak tento rozdíl byl dán vyšším počtem OSNA pozitivních nálezů (16 případů – 16 %) při negativitě ostatních metod. Pouze ve 3 případech (3 %) bylo vyšetření H&E, resp. IHC CK19 pozitivní při negativitě metody OSNA, což je procento odpovídající zjištěním ostatních autorů, které si ve shodě s nimi vysvětlujeme, kromě pochopitelně různé senzitivity a specificity použitých vyšetřovacích metod, také nutným dělením LU [19,22,25].

V souladu s nálezy Chena a kol., Güllera a kol. a dalších jsme i v našem souboru pozorovali větší počet odhalených mikrometastáz metodou OSNA ve srovnání s vyšetřením H&E, resp. IHC CK19 [17,19,25–28]. Zde však vyvstává otázka stanovení správné hodnoty cut off pro určení přítomnosti mikrometastázy v LU. Naprostá většina všech autorů (včetně nás) automaticky používala hodnotu 250 kopií mRNA CK19/μl, kterou převzala ze studií zabývajících se diseminací karcinomu prsu (zde má OSNA pozitivní mikrometastáza velikost 0,2–2 mm). U jiných typů nádorů však může být tato hodnota zcela odlišná, což by pochopitelně výrazně ovlivnilo veškeré výsledky. Je proto zcela nezbytné provést další, nejlépe multicentrické studie, které by určily, zda lze jednu hodnotu cut off použít pro více typů nádorů či nikoli [5]. Tamaki a kol., Buglioni a kol. a další také poukazují na možnou predikci postižení dalších etáží LU při pozitivitě vyšetření metodou OSNA, přičemž riziko tohoto postižení stoupá s počtem detekovaných kopií mRNA CK19 v pozitivní LU [7,10,24,29]. Tomu v zásadě odpovídají i naše výsledky, kdy z 11 osob s OSNA pozitivními N1 LU měly 3 osoby (27,3 %) pozitivní i N2 LU. Míra upstagingu 16 % dosažená v našem souboru použitím metody OSNA (resp. 17 % při započtení 1 případu pozitivity IHC CK19 a OSNA) odpovídá literárním údajům uvádějícím rozmezí 2–25 % [17,18,23,30]. Relevantní otázkou v této souvislosti však také je, do jaké míry ovlivní odhalení, resp. přítomnost mikrometastáz v LU

follow-up těchto nemocných. Souhlasíme s Osakou a kol., že toto musí být předmětem dalšího zkoumání, resp. pečlivého sledování těchto pacientů [26].

Oproti našemu očekávání se ukázalo, že IHC CK19 nevede k zásadním změnám stagingu. V celých 97 % případů výsledky IHC CK19 přesně kopírovaly výsledky vyšetření H&E. To je v rozporu se zjištěními Vogelaara a kol., podle nichž doplnění IHC CK19 k H&E zvýší staging o 36 % a při kombinaci IHC CK19 a OSNA dokonce o 46,5 % [30]. Určitý přínos by snad mohla mít IHC CK19 alespoň v detekci exprese CK19 určitými nádory (LU) pro rozhodnutí o zařazení metody OSNA do vyšetřovacího procesu. Podle Vilardella a kol., resp. Takamota a kol. může totiž dojít v důsledku předchozí onkologické léčby k poklesu či ztrátě exprese CK19 nádory (LU), což je např. u karcinomu prsu poměrně častý jev [31,32]. Nicméně např. Osako a kol. si myslí, že schopnost metody OSNA detekovat metastázy v LU není ani po předchozí chemoterapii snížena ve srovnání s H&E [6]. Případnou ztrátu exprese CK19 nádory, resp. LU, po neoadjuvantní onkologické léčbě lze na druhou stranu využít jinak – pokud exprese CK19 závisí na životaschopnosti nádorových buněk, tak její ztráta může sloužit jako přesnější marker pro posouzení účinnosti oné onkologické léčby, resp. prognózy pacientů podstupujících neoadjuvantní léčbu [5].

ZÁVĚR

Dosažené výsledky ukazují, že vyšetření LU odebraných při SMLA během radikální operace primárních či sekundárních plicních nádorů pomocí metody OSNA může mít, na základě senzitivnější detekce mikrometastáz v LU, určitý potenciál zpřesnit pTNM staging těchto nádorů. Samozřejmě je nezbytné potvrdit tento předpoklad v dalších studiích, resp. na větším souboru nemocných. Zásadním úkolem je dále pečlivým sledováním zjistit souvislost mezi mikrometastázami v LU detekovanými metodou OSNA a follow-up nemocných.

Seznam zkratek

CK19 – cytokeratin 19
H&E – hematoxylin-eosin
IASLC – The International Association for the Study of Lung Cancer
IHC CK19 – imunohistochemické vyšetření s protilátkou proti cytokeratinu 19
LAMP – Loop Mediated Isothermal Amplification
LU – lymfatické uzliny
mRNA – messenger ribonucleic acid
Nd:YAG – Neodymium-doped Yttrium Aluminium Garnet
NSCLC – nemalobuněčný plicní karcinom
OSNA – One-Step Nucleic Acid Amplification
RT – reverzní transkripce
SMLA – systematická hilová a mediastinální lymfadenektomie
TNM – klasifikace maligních nádorů

Konflikt zájmů
Autoři článku prohlašují, že nejsou v souvislosti se vznikem tohoto článku ve střetu zájmů a že tento článek nebyl publikován v žádném jiném časopise.

Etické aspekty
Studie byla před svým zahájením schválena společnou etickou komisí Univerzity Karlovy, Lékařské fakulty v Plzni a Fakultní nemocnice Plzeň a všichni pacienti zařazení do studie s tím předem podepsali informovaný souhlas.

LITERATURA

1. Masai K, Nakagawa K, Yoshida A, et al. Cytokeratin 19 expression in primary thoracic tumors and lymph node metastases. Lung-Cancer 2014;86:318–23.
2. Zhang X, Xie J, Yu C, et al. RNA expressionof CK19, EGFR and LUNX in patients with lung cancer micrometastasis. Exp Ther Med 2014;7:360–4.
3. Yamamoto N, Daito M, Hiyama K, et al. An optimal mRNA marker for OSNA (One-step nucleic acid amplification) based lymph node metastasis detection in colorectal cancer patients. Jpn J ClinOncol 2013;43:264–70.
4. Rusch VW, Asamura H, Watanabe H, et al. Members of IASLC Staging Committee. The IASLC lung cancer staging project: a proposal for a new international lymph node map in the forthcoming seventh edition of the TNM classification for lung cancer. J Thorac Oncol. 2009;4:568–77.
5. Tamaki Y. One-step nucleic acid amplification (OSNA): where do we go withit? Int J ClinOncol 2017;22:3–10.
6. Osako T, Tsuda H, Horii R, et al. Molecular detection of lymph node metastasis in breast cancer patients treated with preoperative systemic chemotherapy: a prospective multicentre trial using the one-step nucleic acid amplification assay. Br J Cancer 2013;109:1693–8.
7. Buglioni S, Di Filippo F, Terrenato I, et al. Quantitative molecular analysis of sentinel lymph node may be predictive of axillary node status in breast cancer classified by molecular subtypes. PLOS One 2013;8:e58823.
8. Le Frère-Belda MA, Bats AS, Gillaizeau F, et al. Diagnostic performance of one-step nucleic acid amplification for intraoperative sentinel node metastasis detection in breast cancer patients. Int J Cancer 2012;130:2377–86.
9. Matsuzuka T, Takahashi K, Kawakita D, et al. Intraoperative molecular assessment for lymph node metastasis in head and neck squamous cell carcinoma using one-step nucleic acid amplification (OSNA) assay. Ann Surg Oncol 2012;19:3865–70.
10. Osako T, Iwase T, Kimura K, et al. Sentinel node tumour burden quantified based on cytokeratin 19 mRNA copy number predicts non-sentinel node metastases in breast cancer: molecular whole-node analysis of all removed nodes. Eur J Cancer 2013;49:1187–95.
11. Hayama M, Chida M, Karube Y, et al. One-step nucleic acid amplification for detection of lymph node metastasis in lung cancer. Ann Thorac Cardiovasc Surg 2014;20:181–4.
12. Inoue M, Hiyama K, Nakabayashi K, et al. An accurate and rapid detection of lymph node metastasis in non-small cell lung cancer patients based on one-step nucleic acid amplification assay. Lung Cancer 2012;78:212–8.
13. Benej M, Čapov I, Wechsler J, et al. Reevaluace stagingu nodálního statusu nemalobuněčného karcinomu plic (NSCLC) levého horního laloku v intencích revidovaných ESTS doporučení a našich zkušeností. Onkologie 2015;9:142–5.
14. Chaudhry A, Williams S, Cook J, et al. The real-time intra-operative evaluation of sentinel lymp hnodes in breast cancer patients using One Step Nucleic Acid Amplification (OSNA) and implications for clinical decision-making. Eur J SurgOncol 2014;40:150–7.
15. Croner RS, Schellerer V, Demund H, et al. One step nucleic acid amplification (OSNA) – a new method for lymph node staging in colorectal carcinomas. J Transl Med 2010;8:83.
16. Yamamoto H, Sekimoto M, Oya M, et al. OSNA-based novel molecular testing for lymph node metastases in colorectal cancer patients: results from a multicenter clinical performance study in Japan. Ann Surg Oncol 2011;18:1891–8.
17. Güller U, Zettl A, Worni M, et al. Molecular investigation of lymph nodes in colon cancer patients using one-step nucleic acid amplification (OSNA): a new road to better staging? Cancer 2012;118:6039–45.
18. Yamamoto H, Tomita N, Inomata M, et al. OSNA-assisted molecular staging in colorectal cancer: A prospective multicenter trial in Japan. Ann SurgOncol 2016;23:391–6.
19. Cserni G. Intraoperative analysis of sentinel lymph nodes in breast cancer by one-step nucleic acid amplification. J ClinPathol 2012;65:193–9.
20. Huxley N, Jones-Hughes T, Coelho H, et al. A systematic review and economic evaluation of intraoperative tests [RD-100i one-step nucleic acid amplification (OSNA) system and Metasin test] for detecting sentinel lymph node metastases in breast cancer. Health Technol Assess 2015;19:1–215.
21. Oezkan F, Khan AM, Hager T, et al. OSNA: A fast molecular test based on CK19 mRNA concentration for assessment of EBUS-TBNA samples in lung cancer patients. ClinLungCancer 2016;17:198–204.
22. Nakagawa K, Asamura H, Tsuta K, et al. The novel one-step nucleic acid amplification (OSNA) assay for the diagnosis of lymph node metastasis in patient swith non-small cell lung cancer (NSCLC): Results of a multicenter prospective study. LungCancer 2016;97:1–7.
23. Croner RS, Geppert CI, Bader FG, et al. Molecular staging of lymph node-negative colon carcinomas by one-step nucleic acid amplification (OSNA) results in upstaging of a quarter of patients in a prospective, European, multicentre study. Br J Cancer 2014;110:2544–50.
24. Sagara Y, Ohi Y, Matsukata A, et al. Clinical application of the one-step nucleic acid amplification method to detect sentinel lymph node metastasis in breast cancer. Breast Cancer 2013;20:181–6.
25. Chen JJ, Chen JY, Yang BL, et al. Comparison of molecular analysis and touch imprint cytology for the intraoperative evaluation of sentinel lymph nodes in primary breast cancer: results of the China Breast Cancer Clinical Study Group (CBCSG) 001c trial. Eur J SurgOncol 2013;39:442–9.
26. Osako T, Iwase T, Kimura K, et al. Incidence and possible pathogenesis of sentinel node micrometastases in ductal carcinoma in situ of the breast detected using molecular whole lymph node assay. Br J Cancer 2012;106:1675–81.
27. Osako T, Iwase T, Kimura K, et al. Intraoperative molecular assay for sentinel lymph node metastasis in early stage breast cancer: a comparative analysis between one-step nucleic acid amplification whole node assay and routine frozen section histology. Cancer 2011;117:4365–74.
28. Remoundos DD, Ng VV, Wilson HA, et al. The use of one step nucleic-acid amplification (OSNA) in clinical practice: a single-centre study. Breast 2013;22:162–7.
29. Tamaki Y, Sato N, Homma K, et al. Japanese One-Step Nucleic Acid Amplification Study Group. Routine clinical use of the one-step nucleic acid amplification assay for detection of sentinel lymph node metastases in breast cancer patients: results of a multicenter study in Japan. Cancer 2012;118:3477–83.
30. Vogelaar FJ, Reimers MS, van der Linden RL, et al. The diagnostic value of One-Step Nucleic acid Amplification (OSNA) for sentinel lymph nodes in colon cancer patients. Ann Surg Oncol 2014;21:3924–30.
31. Vilardell F, Novell A, Martin J, et al. Importance of assessing CK19 immunostaining in core biopsies in patients subjected to sentinel node study by OSNA. Virchows Arch 2012;460:569–75.
32. Takamoto K, Shimazu K, Naoi Y, et al. One-Step Nucleic Acid Amplification Assay for detection of axillary lymph node metastases in breast cancer patients treated with neoadjuvant chemotherapy. Ann SurgOncol 2016;23:78–86.

doc. MUDr. Josef Vodička, Ph.D.
Chirurgická klinika FN v Plzni a LF UK v Plzni
alej Svobody 80
304 60 Plzeň
e-mail: vodicka@fnplzen.cz

PŘÍLOHA 3

Article

Prognostic Significance of Lymph Node Examination by the OSNA Method in Lung Cancer Patients—Comparison with the Standard Histopathological Procedure

Josef Vodicka [1], Martin Pesta [2,3,*], Vlastimil Kulda [4], Katerina Houfkova [2], Bohuslava Vankova [5], Jakub Sebek [1], Martin Skala [1], Jakub Fichtl [1], Kristyna Prochazkova [1] and Ondrej Topolcan [6]

1 Department of Surgery, Faculty Hospital Plzen, Faculty of Medicine in Pilsen, Charles University, alej Svobody 80, 304 60 Plzen, Czech Republic; vodicka@fnplzen.cz (J.V.); sebekj@fnplzen.cz (J.S.); skalama@fnplzen.cz (M.S.); fichtlj@fnplzen.cz (J.F.); prochazkovak@fnplzen.cz (K.P.)
2 Department of Biology, Faculty of Medicine in Pilsen, Charles University, alej Svobody 76, 323 00 Plzen, Czech Republic; katerina.houfkova@lfp.cuni.cz
3 Biomedical Center, Faculty of Medicine in Pilsen, Charles University, alej Svobody 76, 323 00 Plzen, Czech Republic
4 Department of Medical Chemistry and Biochemistry, Faculty of Medicine in Pilsen, Charles University, Karlovarska 48, 301 66 Plzen, Czech Republic; vlastimil.kulda@lfp.cuni.cz
5 Department of Pathology, Faculty Hospital Plzen, Faculty of Medicine in Pilsen, Charles University, Edvarda Benese 13, 305 99 Plzen, Czech Republic; kokoskovab@fnplzen.cz
6 Department of Immunochemistry Diagnostics, Faculty Hospital Plzen, Faculty of Medicine in Pilsen, Charles University, Edvarda Benese 13, 305 99 Plzen, Czech Republic; topolcan@fnplzen.cz
* Correspondence: martin.pesta@lfp.cuni.cz; Tel.: +420-377-593-261

Abstract: The aim of the study was to compare the prognostic significance of lymph node status of patients with lung cancer analyzed by three different methods: hematoxylin and eosin (H&E), immunohistochemistry of cytokeratin 19 (IHC CK19), and One-Step Nucleic Acid Amplification (OSNA). The clinical relevance of the results was evaluated based on relation to prognosis; the disease-free interval (DFI) and overall survival (OS) were analyzed. During radical surgical treatment, a total of 1426 lymph nodes were obtained from 100 patients, creating 472 groups of nodes (4–5 groups per patient) and examined by H&E, IHC CK19 and OSNA. The median follow-up was 44 months. Concordant results on the lymph node status of the H&E, IHC CK19 and OSNA examinations were reported in 78% of patients. We recorded shorter OS in patients with positive results provided by both OSNA and H&E. The study demonstrated a higher percentage of detected micrometastases in lymph nodes by the OSNA method. However, the higher sensitivity of the OSNA, with the cut-off value 250 copies of mRNA of CK19/μL, resulted in a lower association of OSNA positivity with progress of the disease compared to H&E. Increasing the cut-off to 615 copies resulted in an increase in concordance between the OSNA and H&E, which means that the higher cut-off is more relevant in the case of lung tumors.

Keywords: lung cancer; lymph nodes; H&E; IHC CK19; OSNA

1. Introduction

Today, the standard detection of tumor cells in hilar and mediastinal lymph nodes (LNs) removed during radical surgical treatment of primary and secondary lung tumors is performed

using histopathological methods, i.e., by the microscopic examination of specimens stained using hematoxylin-eosin (H&E) by pathologists. However, this approach is limited, in particular in the case of micrometastases, clusters (clusters of tumor cells), or isolated tumor cells, where, according to certain studies, false negative results of the examination are produced in up to 20% of cases [1]. One of the available methods for the improved detection of micrometastases in regional LNs can be, based on data provided by recent studies, both the proof of tumor cells by immunohistochemical examination with an antibody against cytokeratin 19 (IHC CK19), and the molecular genetic method OSNA (One-Step Nucleic Acid Amplification), which detects CK19 mRNA [2–4]. Although the IHC CK19 method has been available for a number of years, it has not yet been routinely used for the histopathological examination of LNs. The molecular genetic method OSNA represents a more recent approach to the proof of CK19 in LNs, based on detecting CK19 mRNA copies in a given sample by isothermal amplification (LAMP).

A number of studies comparing the OSNA method with the standard histopathological examination in patients with breast cancer and/or colorectal carcinoma (CRC) have been published. The conclusions of these studies presented comparable results (concordance level of 95–97%, OSNA to H&E sensitivity 86–96%, OSNA to H&E specificity 92–100%) [1,2,4–10]. Recently, there are efforts to implement LN examination by OSNA method in management of patients with other tumors, e.g., endometrial cancer [11], gastric cancer [12] or thyroid carcinoma [13,14].

In the case of lung tumors, the OSNA method has been the subject of several studies, the purpose of which was both to ascertain the presence of CK19 in these tumors and offer a comparison of OSNA to H&E [3,15–17]. Among them, was also our prospective study commenced in 2015, the purpose of which was to refine the pathological TNM (pTNM) lymph node staging (N0, N1, N2) of primary and secondary lung tumors by the more sensitive detection of micrometastases in LNs using the IHC CK19 and the OSNA method compared to the H&E examination, specifically by a thorough analysis of all intra-operatively removed LNs. In 2018, we published the results of the comparison of the OSNA, H&E, and IHC CK19 methods, which were based on a set of 64 patients (885 examined nodes) [18]. The results showed a higher percentage of detected micrometastases in hilar and mediastinal lymph nodes when examined by the OSNA method compared to H&E and IHC CK19 (upstaging by 16%). In addition, we proposed a method for the clinical application of the OSNA method to lung tumors based on the pooling of LNs [18].

The aim of the present study was to analyze, by carefully monitoring patients, the relationship between micrometastases detected in LNs using the OSNA, H&E, and IHC CK19 methods and the progress of the disease (the median follow-up was 44 months) in a group of 100 patients.

2. Materials and Methods

2.1. Patients

The inclusion of patients with operable non-small cell lung carcinoma (NSCLC) and pulmonary metastases of colorectal carcinoma in the prospective study was performed in the period of 2015–2017. The study was approved by the Ethics Committee of the Faculty Hospital in Pilsen (No. 20150604). All patients provided their informed consent for inclusion in the study. The detailed characteristics of the group of 100 patients are provided in Table 1 (80 patients with NSCLC) and Table 2 (20 patients with pulmonary metastases of colorectal carcinoma). In all patients, the primary pulmonary tumor, or pulmonary metastasis, was radically removed and in all cases a systematic nodal dissection was executed according to the well-proven scheme of the International Association for the Study of Lung Cancer (IASLC) of 2009 [19]. The patients' median follow-up was 44 months.

Table 1. Characteristics of 80 patients with non-small cell lung carcinoma (NSCLC).

Variables	Number of Patients	%
Gender		
Male	50	62.5
Female	30	37.5
Type of operation		
Pneumonectomy	6	7.5
Bi-lobectomy	7	8.8
Lobectomy	67	83.7
Histology of NSCLC		
Adenocarcinoma	45	56.3
Squamous cell carcinoma	33	41.2
Adenosquamous carcinoma	2	2.5
Pathological T status of NSCLC [1]		
T1a	20	25.0
T1b	22	27.5
T2a	26	32.5
T2b	6	7.5
T3	5	6.3
T4	1	1.2
Adjuvant chemotherapy		
No	52	65.0
Yes	28	35.0

[1] TNM scores for malignant tumors, the 7th edition [15] (valid at the time of the patients' inclusion in the study, 2015–2017).

Table 2. Characteristics of 20 patients with pulmonary metastases of colorectal carcinoma.

Variables	Number of Patients	%
Gender		
Male	13	65.0
Female	7	35.0
Adjuvant chemotherapy		
no	12	60.0
yes	8	40.0

2.2. Examination of Lymph Nodes

During the surgery of 100 patients, a total of 1426 lymph nodes were removed, with the average value being 14.3 LNs/person (5–32 LNs). Each LN was dissected into four parts, whereby parts one and three were examined using the H&E and IHC CK19 method, and parts two and four were examined using the OSNA assay. For methodological reasons, parts of LNs for OSNA method (Sysmex, Kobe, Japan) were pooled into 3–5 groups of LNs within the framework of one nodal zone based on the IASLC LNs classification developed from the Mountain–Dresler classification [19] creating 472 groups in total. On the basis of the results on groups of nodes, we obtained lymph node staging for a patient (N0, N1, N2).

The removal of lymph nodes, the scheme for dissecting and pooling, as well as the histopathological and immunohistochemical examinations, CK19 detection and the OSNA method, are described in detail in our previous article [18].

Briefly, LNs of one group were homogenized and lysed according to the manufacturer's instructions. Determination was performed using the diagnostic kit LYNOAMP BC OSNA (Sysmex, Kobe, Japan). Determination of the presence of mRNA CK19, as the marker of epithelial cells, was executed using the RD100i instrument (Sysmex, Kobe, Japan). The net time of amplification reaction is 16 minutes, up to four groups of pooled lymph nodes can be analyzed in parallel. The cut-off values for the OSNA method were determined as specified in the LYNOAMP BC OSNA manufacturer's manual

and were used in the previous studies of tumor cells in LNs in patients with lung cancer (absence of tumor cells—cut-off value < 250 copies of mRNA of CK19/μL, presence of a micrometastasis—cut-off value ranging from 250 to 5000 copies of mRNA of CK19/μL, presence of a macrometastasis—cut-off value > 5000 copies of mRNA of CK19/μL) [2,3,15,20,21].

2.3. Statistical Analysis

The statistical analysis was calculated using the SAS software (SAS Institute Inc., Cary, NC, USA). Essential descriptive statistics for all variables of interest were prepared based on the clinical and pathological data of the patients. Categorical variables were reported as absolute and percentage values. Venn diagrams were used for comparing the results of H&E, IHC CK19 and OSNA method. Kaplan–Meier survival curves for overall survival (OS) and disease-free interval (DFI) were generated to compare prognostic significance of results obtained by H&E and OSNA method. The statistical significance of differences in CK19 mRNA copies assessed by OSNA between H&E-positive and H&E-negative samples was calculated using t test for independent samples. The statistical significance level was determined at the alpha limit = 5%.

3. Results

3.1. Concordance among H&E, IHC CK19 and OSNA for Groups of LNs

The concordance of the H&E, IHC CK19 and OSNA examinations was evaluated in 472 groups of lymph nodes. Full concordance of the three methods was recorded in 432 groups of lymph nodes (91.5%), 400 groups of lymph nodes were concordantly negative, and 32 groups of lymph nodes were concordantly positive, see Figure 1a.
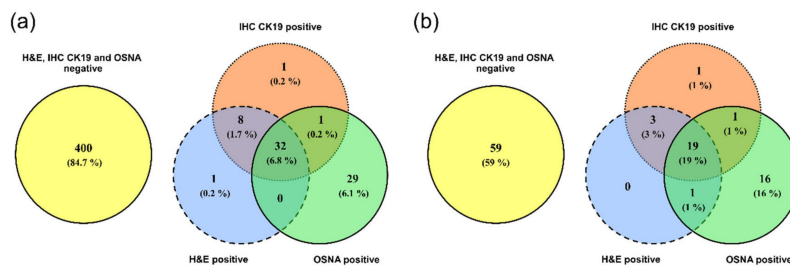

Figure 1. Comparison of examination results for the presence of tumor cells using the H&E, IHC CK19 and OSNA methods by Venn diagrams. (**a**) Groups of lymph nodes; (**b**) patients.

3.2. Concordance among H&E, IHC CK19 and OSNA for Individual Patients

After evaluating the groups of lymph nodes for a given patient (in each patient, 3–5 groups of lymph nodes were evaluated), concordance was recorded in 78 patients (78%), of whom 59 patients had all examined LNs concordantly negative and 19 patients concordantly positive. Micrometastases in the lymph nodes were detected in 16 patients (16%) by the OSNA method, with negative results for the other methods. In three cases (3%), the H&E and IHC CK19 examinations were positive while the OSNA method produced negative results, see Figure 1b.

3.3. Comparison of Prognostic Significance of H&E and OSNA

The clinical significance of the presence of tumor cells in lymph nodes determined by the H&E and OSNA methods was evaluated by analyzing the relation to DFI and OS. The Kaplan-Meier curves comparing NSCLC patients with positive and negative LNs detected concordantly by the H&E and OSNA methods are provided in Figure 2a,b. Survival analysis of patients with pulmonary metastases

concordantly analyzed by both methods is shown in Figure 2e,f. The Kaplan-Meier curves show that patients with positive LNs have a shorter OS.
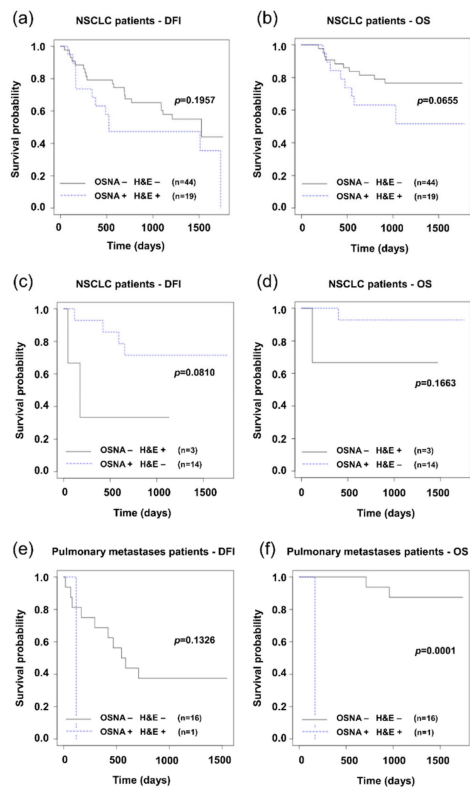

Figure 2. Kaplan-Meier survival distribution functions of patients stratified according to lymph node status (result of method negative: −, result of method positive: +). (**a**) Disease-free survival (DFI) of non-small cell lung carcinoma (NSCLC) patients with concordance of H&E and OSNA (OSNA − H&E − vs. OSNA + H&E +); (**b**) overall survival (OS) of NSCLC patients with concordance of H&E and OSNA; (**c**) disease-free survival (DFI) of NSCLC patients with discordance of H&E and OSNA (OSNA − H&E + vs. OSNA + H&E −); (**d**) overall survival (OS) of NSCLC patients with discordance of H&E and OSNA; (**e**) disease-free survival (DFI) of pulmonary metastases patients with concordance of H&E and OSNA; (**f**) overall survival (OS) of pulmonary metastases patients with concordance of H&E and OSNA.

In patients with discordant results (17 out of 80 NSCLC patients), the relevance to prognosis spoke in favor of the H&E method (see Figure 2c). Patients with lymph node positivity as detected by the H&E method and not detected by the OSNA method had a less favorable prognosis (DFI). Here it needs to be noted that the result may be affected by the low number of discordances between the two methods, apparent in particular in the chart for OS, where another limit is the low number of events.

In the clinical use, the status of lymph nodes itself is just a part of the TNM score, based on which the stage of the disease is classified. Table 3 shows the TNM score and stages of the disease in the patients with discordant results of LN examinations by the H&E and OSNA methods.

Table 3. Changes in the pTNM staging depending on H&E, IHC CK19 and OSNA results.

NSCLC (80 Patients)							
Concordance of H&E, IHC CK19 and OSNA assay						61 patients (76.3%)	
Differences between H&E, IHC CK19 and OSNA assay						19 patients (23.7%)	
H&E		IHC CK19		OSNA		Cases	Commentary
TNM	Stage	TNM	Stage	TNM	Stage		
T2aN0	IB	T2aN1	IIA	T2aN1	IIA	1	higher stage by both OSNA and IHC CK19
T1aN0	IA	T1aN0	IA	T1aN2	IIIA	2	
T1bN0	IA	T1bN0	IA	T1bN1	IIA	4	
T1bN0	IA	T1bN0	IA	T1bN2	IIIA	1	higher stage by OSNA
T2aN0	IB	T2aN0	IB	T2aN1	IIA	2	
T2aN0	IB	T2aN0	IB	T2aN2	IIIA	4	
T1aN1	IIA	T1aN1	IIA	T1aN0	IA	1	
T2aN2	IIIA	T2aN2	IIIA	T2aN0	IB	1	lower stage by OSNA
T1aN2	IIIA	T1aN2	IIIA	T1aN0	IA	1	
T3N2	IIIA	T3N0	IIB	T3N0	IIB	1	lower stage by both OSNA and IHC CK19
T1bN0	IA	T1bN2	IIIA	T1bN0	IA	1	higher stage by IHC CK19
Lung Metastases of Colorectal Carcinoma (20 patients)							
Concordance of H&E, IHC CK19 and OSNA assay						17 patients (85.0%)	
Differences between H&E, IHC CK19 and OSNA assay						3 patients (15.0%)	
H&E N-stage		IHC CK19 N-stage		OSNA N-stage		Cases	Commentary
N0		N0		N1		2	higher N-stage by OSNA
N0		N0		N2		1	

Abbreviations: NSCLC: non-small cell lung carcinoma; H&E: hematoxylin-eosin; IHC CK19: immunohistochemical examination with the anti-cytokeratin 19 antibody; OSNA: One-Step Nucleic Acid Amplification.

The following charts show the relevance between the stage of the disease based on the TNM score to the prognosis for patients with NSCLC, where the status of the lymph nodes was evaluated either by the H&E method or by the OSNA method (Figure 3).

3.4. Proposing a New OSNA Cut-Off Value

The values of the number of copies of mRNA of CK19 determined in the group of lymph nodes concordantly positive according to the OSNA, and H&E methods were statistically significantly higher ($p < 0.0001$) than in the groups of lymph nodes that were positive only according to the OSNA method (Figure 4a). The relevance of this finding is explained in the discussion.

Based on aforementioned results, we decided to propose a new cut-off value for the OSNA method. This value is based on the number of copies in the specimen with the lowest number of copies that was concordantly positive using the OSNA, H&E, and IHC CK19 methods. In this specimen, the measured expression level of mRNA CK19 was 620 copies of mRNA of CK19/µL. Therefore, we propose that the cut-off value be 615 copies of mRNA CK19/µL. After applying this new cut-off value, 16 groups of lymph nodes detected as positive were revaluated as negative by the OSNA method. The result of revaluation was increase in concordance between the H&E and OSNA methods to 95.1%, when evaluating lymph node groups. When evaluating overall lymph node status of a given patient, the number of patients with a discordant result according to the OSNA and H&E methods decreased from 20 to 13. The complete results are provided in the Venn diagram in Figure 4b. Comparing the prognosis (DFI, OS) of these patients could not be performed correctly due to the low number of discordant patients (13 patients).
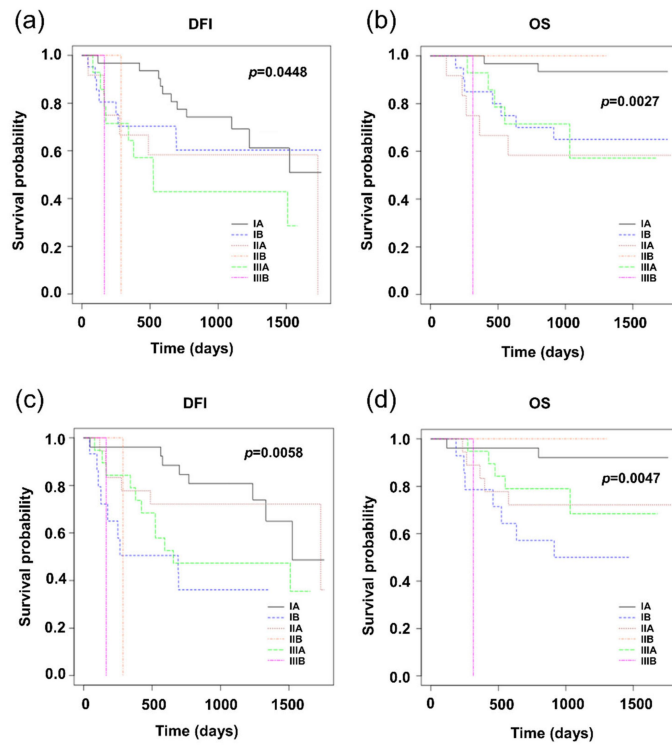
Figure 3. Kaplan–Meier survival distribution functions of NSCLC patients stratified according to stage of disease. (**a**) Disease-free survival (DFI) of patients classified according to the results of H&E; (**b**) overall surviv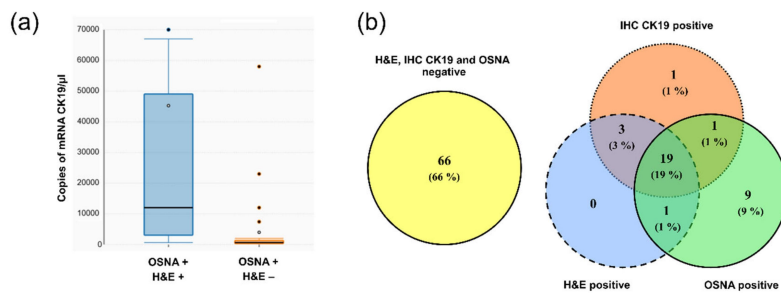al (OS) of patients classified according to the results of H&E; (**c**) disease-free survival (DFI) of patients classified according to the results of OSNA; (**d**) overall survival (OS) of patients classified according to the results of OSNA.

Figure 4. Data supporting new cut-off value. (**a**) Box plots showing copy number of mRNA CK19. Groups of lymph nodes, positive based on both OSNA and H&E methods (OSNA + H&E +), have significantly higher copies of mRNA CK19 than those positive by the OSNA method but negative by H&E (OSNA + H&E −); (**b**) comparison of examination results of patients for the presence of tumor cells using the H&E, IHC CK19 and OSNA methods by Venn diagrams using the new cut-off value of the OSNA method 615 copies of mRNA CK19/μL.

4. Discussion

The purpose of the study was to compare the three methods for detecting the presence of tumor cells in the lymph nodes of patients with NSCLC and CRC metastases, which is a necessary examination for deciding on further oncological treatment. The clinical relevance of individual methods was assessed based on analyzing the examination result related to the further progress of the disease, i.e., to prognosis (DFI, OS). Determination of tumor cells in the lymph nodes was carried out using the standard method employed by pathologists (preparation staining by H&E), IHC CK19, and by the OSNA molecular biology method. Considering the fact that the results of the IHC CK19 method were concordant with those ascertained by the H&E staining method, with only a single exception, the survival charts include only the comparison of the H&E and OSNA methods. The methodological approach is completely different for H&E and OSNA, in terms of both the quantity of analyzed tissue, and the rate of processing. Therefore, each method has its advantages and disadvantages. It is obvious that evaluation of clinical benefits also depends on priorities. The OSNA method allows the entire lymph node to be analyzed, and compared to the H&E method, it requires less experience from the health care professional.

Compared to certain other tumors, examination of LNs in the case of lung tumors is also specific due to the fact that the concept of the first regional (sentinel) node cannot be applied. One of the reasons is a high percentage of so-called skip metastases [22,23]. This means that it is necessary to remove and examine a higher number of lymph nodes to prove dissemination. In our study, the average number was 14.3 examined LNs per patient. Depending on their anatomical localization, these lymph nodes were pooled into groups according to IASLC mapping scheme. The OSNA method allows lymph nodes belonging to the same group to be pooled and analyzed as a whole.

4.1. Concordance of H&E, IHC CK19, and OSNA

Concordance of the H&E and IHC CK19 examinations was ascertained in 99.4% groups of nodes (469 out of 472, see Figure 1), which reflects the similar methodological approach of the two methods. Therefore, in this study, hardly any benefit of IHC CK19 compared to the routine H&E method was observed. This is the reason why we focus below on comparing the OSNA and H&E methods. Out of 472 analyzed groups of LNs, OSNA and H&E provided concordant results in 433 (91.7%) of the groups. OSNA indicated tumor cells in an additional 30 (6.4%) groups of lymph nodes that were H&E-negative.

From the point of view of decisions on treatment, the result specifying the presence of tumor cells in patient LNs is relevant (N-staging). Out of 100 patients, OSNA and H&E were concordant in 80 (80%) of the patients in N-staging; OSNA detected tumor cells in an additional 17 (17%) patients who were H&E-negative. On the other hand, H&E revealed micrometastases in three (3%) patients where the result of the OSNA method was negative. These results are similar to those previously published by other authors. Masai et al. monitored the CK19 expression in primary pulmonary tumors and breast cancer pulmonary metastases. CK19 was detected in 88% of patients with a pulmonary tumor and in nearly 91% of patients with breast cancer metastases [16]. Hayama et al. compared the sensitivity of the OSNA method and H&E examination when examining 40 LNs of 20 patients with primary pulmonary lung cancer (OSNA sensitivity 100%, specificity 92%) [3]. Inoue et al. presented a larger sample when they examined 165 LNs in 49 patients, again with promising results (positive predictive value of the OSNA method 95%, negative predictive value 99%, accuracy 99%) [15]. Nakagawa et al., who examined 410 LNs in 111 patients with NSCLC, found the level of correspondence between the H&E examination and OSNA method to be almost 93%, with sensitivity exceeding 79% [17].

4.2. Comparison of H&E and OSNA Based on Relation to Prognosis

From our point of view, the most relevant criterion for correctly detecting tumor cells (the CK 19 expression) for the purposes of N-staging as a part of TNM classification is correspondence with the progress of the disease, vesting the result with clinical significance. The clinical significance of the

higher sensitivity of OSNA compared to H&E was assessed based on the analysis of the examination result's relevance to disease-free interval (DFI) and overall survival (OS). In patients with concordant results detected by both methods (80% of patients), it was observed that positivity of lymph nodes was associated with worse prognosis for both subgroups of patients (NSCLC, pulmonary metastases of CRC). From the point of view of our research aims, patients for whom discordance between H&E and OSNA was observed, were key for further analysis. There were 20 such patients out of 100, 17 with NSCLC and three with pulmonary metastases of CRC. For each patient, 3–5 groups of lymph nodes were examined with differences detected in only 39 out of 472 groups of lymph nodes. It was observed that the further progress of the disease better correlated with the examination based on the H&E method (Figure 2c,d).

To explain this finding, it is necessary to focus on patients with LN positivity detected by H&E but not by OSNA. An explanation could be offered that tumor cells present in LNs of these patients do not express CK19. CK19 is an intermediate filament of the cytoskeleton, which is present in the cells of epithelial origin, but not in LN tissue. The presence of CK19 in an LN is therefore an indicator of the metastatic involvement by tumor cells of epithelial origin [24]. However, some carcinomas in the process of carcinogenesis lose CK19 expression. Such phenomenon was observed in the case of some squamous cell carcinomas [25]. Two out of three H&E-positive but OSNA-negative NSCLC patients really had squamous cell carcinoma as a histological subtype. However, the part of LN examined by pathologist was IHC-CK19-positive. Therefore, a more likely explanation is that tumor cells were present only in the part of lymph node analyzed by pathologist but not in the part processed for OSNA.

Further progress of the disease is affected not only by the positivity of the lymph nodes themselves, but also other parameters assessed by the TNM score, and/or the stage of the disease. More relevant to the progress of the disease is the stage classification based on the N-staging according to results obtained by the H&E method compared to the OSNA method (Figure 3). In this respect, it is necessary to note that patient management (decisions on the administration of adjuvant chemotherapy) was performed in accordance with the results of the routine H&E method, which could definitely have an effect on the comparison results. Kaplan–Meier graphs in Figure 3 raise a question as to whether the adjuvant treatment of stage IB patients is not underestimated.

4.3. Proposal of the OSNA New Cut-Off Value

In the OSNA molecular genetic method, the key parameter is the cut-off value of the number of copies of mRNA of CK19. This value determines what number of copies will be analyzed as positive, i.e., interpreted as the presence of tumor cells in the LN. When the study was implemented, the kit for the assay of lung cancer LNs was not yet available and that was why published studies, including ours, employed kits for assays of LNs obtained from patients with breast cancer, including the set cut-off value, which was 250 copies of mRNA of CK19/μL.

The instrument RD100i (and currently available RD210) used for the OSNA method to quantify mRNA of CK19 makes it possible to export the numbers of copies for individual assays. We compared the numbers of copies of mRNA of CK19 for the results concordantly positive with those obtained by the H&E method and for the positive results, which were negative if the H&E method was used. The results concordantly positive with the H&E method had statistically significantly more copies of mRNA of CK19 compared to the OSNA-positive results which were H&E-negative. None of the results concordantly positive with the H&E method had a number of copies lower than 620 copies of mRNA of CK19/μL. In the case of results which were OSNA-positive and H&E-negative, 53% of the specimens had a number of copies lower than 620 copies of mRNA of CK19/μL. The increase in the cut-off value to 615 copies of mRNA of CK19/μL proposed by us would increase the theoretical concordance between the OSNA and H&E methods for the analysis of groups of lymph nodes from 91.7% to 95.1%. With these results reflected in the complete evaluation of the patients' lymph nodes (N0 vs. N1 or N2), concordance would increase from 80% to 87%.

Studies aiming to define a new cut-off value for the OSNA method better reflecting clinical outcomes have been already published for sentinel lymph node examination in patients with breast cancer [26,27]. Terrenato et al. suggested a cut-off of 2150 CK19 mRNA copies in sentinel lymph node to be a powerful predictor of non-sentinel lymph node positivity to identify patients who really need axillary lymph node dissection [27].

The high value of sensitivity and the cut-off value of the OSNA method are closely related to the clinical relevance of clusters and/or solitary tumor cells, which may or may not have potential for further progression, and/or may be eliminated by the immune system. The study carried out by Ren et al. has proven that the quantity of residual tumor cells in the lymph nodes of patients with bronchogenic adenocarcinoma is relevant to prognosis. The employed method was IHC anti-CK detection, while micrometastases referred to sets of cells—the largest dimension of which was smaller than 2 mm. The authors described that patients with micrometastases had significantly shorter recurrence-free survival and overall survival compared to N0, but significantly longer than for those with N1 macrometastases [28].

We can conclude that for patients who were OSNA-positive and at the same time H&E-negative, the higher sensitivity of OSNA was not reflected in a less favorable progress of the disease. On the other hand, it must be noted that the OSNA method allows the entire lymph node to be analyzed, and, compared to the H&E method, requires less experience from the health care professional. However, the aforementioned advantage is paid by the lower association of OSNA positivity with the progress of the disease (with the cut-off value 250 copies of mRNA of CK19/μL). The increase in the cut-off value to 615 copies of mRNA of CK19/μL increased concordance between the OSNA and H&E methods.

5. Conclusions

The results of the study demonstrated a higher percentage of detected micrometastases in hilar and mediastinal lymph nodes when the OSNA method was used for examination. However, the higher sensitivity of the OSNA method in our set of patients corresponded less with the progress of the disease (relevance to DFI, OS) when compared to the H&E method. The less time-consuming OSNA method was associated with an 8.3% discordance of results between OSNA and H&E during the analysis of LNs. The study suggests that an increase in the cut-off value of the OSNA method results in significantly higher concordance between the two methods.

References

1. Croner, R.S.; Geppert, C.-I.; Bader, F.G.; Nitsche, U.; Späth, C.; Rosenberg, R.; Zettl, A.; Matias-Guiu, X.; Tarragona, J.; Güller, U.; et al. Molecular staging of lymph node-negative colon carcinomas by one-step nucleic acid amplification (OSNA) results in upstaging of a quarter of patients in a prospective, European, multicentre study. *Br. J. Cancer* **2014**, *110*, 2544–2550. [CrossRef]
2. Osako, T.; Iwase, T.; Kimura, K.; Horii, R.; Akiyama, F. Sentinel node tumour burden quantified based on cytokeratin 19 mRNA copy number predicts non-sentinel node metastases in breast cancer: Molecular whole-node analysis of all removed nodes. *Eur. J. Cancer* **2013**, *49*, 1187–1195. [CrossRef]

3.　Hayama, M.; Chida, M.; Karube, Y.; Tamura, M.; Kobayashi, S.; Oyaizu, T.; Honma, K. One-step nucleic acid amplification for detection of lymph node metastasis in lung cancer. *Ann. Thorac. Cardiovasc. Surg.* **2014**, *20*, 181–184. [CrossRef]

4.　Vogelaar, F.J.; Reimers, M.S.; van der Linden, R.L.A.; van der Linden, J.C.; Smit, V.T.H.B.M.; Lips, D.J.; van de Velde, C.J.H.; Bosscha, K. The Diagnostic Value of One-Step Nucleic acid Amplification (OSNA) for Sentinel Lymph Nodes in Colon Cancer Patients. *Ann. Surg. Oncol.* **2014**, *21*, 3924–3930. [CrossRef]

5.　Chaudhry, A.; Williams, S.; Cook, J.; Jenkins, M.; Sohail, M.; Calder, C.; Winters, Z.E.; Rayter, Z. The real-time intra-operative evaluation of sentinel lymph nodes in breast cancer patients using One Step Nucleic Acid Amplification (OSNA) and implications for clinical decision-making. *Eur. J. Surg. Oncol.* **2014**, *40*, 150–157. [CrossRef]

6.　Le Frère-Belda, M.-A.; Bats, A.-S.; Gillaizeau, F.; Poulet, B.; Clough, K.B.; Nos, C.; Peoc'h, M.; Seffert, P.; Bouteille, C.; Leroux, A.; et al. Diagnostic performance of one-step nucleic acid amplification for intraoperative sentinel node metastasis detection in breast cancer patients. *Int. J. Cancer* **2012**, *130*, 2377–2386. [CrossRef]

7.　Güller, U.; Zettl, A.; Worni, M.; Langer, I.; Cabalzar-Wondberg, D.; Viehl, C.T.; Demartines, N.; Zuber, M. Molecular investigation of lymph nodes in colon cancer patients using one-step nucleic acid amplification (OSNA): A new road to better staging? *Cancer* **2012**, *118*, 6039–6045. [CrossRef]

8.　Osako, T.; Iwase, T.; Kimura, K.; Masumura, K.; Horii, R.; Akiyama, F. Incidence and possible pathogenesis of sentinel node micrometastases in ductal carcinoma in situ of the breast detected using molecular whole lymph node assay. *Br. J. Cancer* **2012**, *106*, 1675–1681. [CrossRef]

9.　Remoundos, D.D.; Ng, V.V.; Wilson, H.A.; Ahmed, F.; Chia, Y.; Cunnick, G.H. The use of one step nucleic-acid amplification (OSNA) in clinical practice: A single-centre study. *Breast* **2013**, *22*, 162–167. [CrossRef]

10.　Yamamoto, N.; Daito, M.; Hiyama, K.; Ding, J.; Nakabayashi, K.; Otomo, Y.; Tsujimoto, M.; Matsuura, N.; Kato, Y. An Optimal mRNA Marker for OSNA (One-step Nucleic Acid Amplification) Based Lymph Node Metastasis Detection in Colorectal Cancer Patients. *Jpn. J. Clin. Oncol.* **2013**, *43*, 264–270. [CrossRef]

11.　Kosťun, J.; Pešta, M.; Sláma, J.; Slunéčko, R.; Vlasák, P.; Bouda, J.; Novotný, Z.; Topolčan, O.; Kučera, R.; Kulda, V.; et al. One-step nucleic acid amplification vs ultrastaging in the detection of sentinel lymph node metastasis in endometrial cancer patients. *J. Surg. Oncol.* **2019**, *119*, 361–369. [CrossRef]

12.　Gęca, K.; Rawicz-Pruszyński, K.; Mielko, J.; Mlak, R.; Sędłak, K.; Polkowski, W.P. Rapid Detection of Free Cancer Cells in Intraoperative Peritoneal Lavage Using One-Step Nucleic Acid Amplification (OSNA) in Gastric Cancer Patients. *Cells* **2020**, *9*, 2168. [CrossRef]

13.　Del Carmen, S.; Gatius, S.; Franch-Arcas, G.; Baena, J.A.; Gonzalez, O.; Zafon, C.; Cuevas, D.; Valls, J.; Pérez, A.; Martinez, M.; et al. Concordance study between one-step nucleic acid amplification and morphologic techniques to detect lymph node metastasis in papillary carcinoma of the thyroid. *Hum. Pathol.* **2016**, *48*, 132–141. [CrossRef]

14.　Medas, F.; Coni, P.; Podda, F.; Salaris, C.; Cappellacci, F.; Faa, G.; Calò, P.G. Evaluation of accuracy of one-step nucleic acid amplification (OSNA) in diagnosis of lymph node metastases of papillary thyroid carcinoma. Diagnostic study. *Ann. Med. Surg. 2012* **2019**, *46*, 17–22. [CrossRef]

15.　Inoue, M.; Hiyama, K.; Nakabayashi, K.; Morii, E.; Minami, M.; Sawabata, N.; Shintani, Y.; Nakagiri, T.; Susaki, Y.; Maeda, J.; et al. An accurate and rapid detection of lymph node metastasis in non-small cell lung cancer patients based on one-step nucleic acid amplification assay. *Lung Cancer* **2012**, *78*, 212–218. [CrossRef]

16.　Masai, K.; Nakagawa, K.; Yoshida, A.; Sakurai, H.; Watanabe, S.; Asamura, H.; Tsuta, K. Cytokeratin 19 expression in primary thoracic tumors and lymph node metastases. *Lung Cancer* **2014**, *86*, 318–323. [CrossRef]

17.　Nakagawa, K.; Asamura, H.; Tsuta, K.; Nagai, K.; Yamada, E.; Ishii, G.; Mitsudomi, T.; Ito, A.; Higashiyama, M.; Tomita, Y.; et al. The novel one-step nucleic acid amplification (OSNA) assay for the diagnosis of lymph node metastasis in patients with non-small cell lung cancer (NSCLC): Results of a multicenter prospective study. *Lung Cancer* **2016**, *97*, 1–7. [CrossRef]

18.　Vodicka, J.; Mukensnabl, P.; Vejvodova, S.; Spidlen, V.; Kulda, V.; Topolcan, O.; Pesta, M. A more sensitive detection of micrometastases of NSCLC in lymph nodes using the one-step nucleic acid amplification (OSNA) method. *J. Surg. Oncol.* **2018**, *117*, 163–170. [CrossRef]

19.　Rusch, V.W.; Asamura, H.; Watanabe, H.; Giroux, D.J.; Rami-Porta, R.; Goldstraw, P. The IASLC Lung Cancer Staging Project: A Proposal for a New International Lymph Node Map in the Forthcoming Seventh Edition of the TNM Classification for Lung Cancer. *J. Thorac. Oncol.* **2009**, *4*, 568–577. [CrossRef]

20.   Tamaki, Y. One-step nucleic acid amplification (OSNA): Where do we go with it? *Int. J. Clin. Oncol.* **2017**, *22*, 3–10. [CrossRef]

21.   Buglioni, S.; Di Filippo, F.; Terrenato, I.; Casini, B.; Gallo, E.; Marandino, F.; Maini, C.L.; Pasqualoni, R.; Botti, C.; Di Filippo, S.; et al. Quantitative molecular analysis of sentinel lymph node may be predictive of axillary node status in breast cancer classified by molecular subtypes. *PLoS ONE* **2013**, *8*, e58823. [CrossRef]

22.   Tateishi, M.; Fukuyama, Y.; Hamatake, M.; Kohdono, S.; Ishida, T.; Sugimachi, K. Skip mediastinal lymph node metastasis in non-small cell lung cancer. *J. Surg. Oncol.* **1994**, *57*, 139–142. [CrossRef]

23.   Wang, L.; Zhan, C.; Gu, J.; Xi, J.; Lin, Z.; Xue, L.; Ge, D.; Wang, Q. Role of Skip Mediastinal Lymph Node Metastasis for Patients With Resectable Non-small-cell Lung Cancer: A Propensity Score Matching Analysis. *Clin. Lung Cancer* **2019**, *20*, e346–e355. [CrossRef]

24.   Mehrpouya, M.; Pourhashem, Z.; Yardehnavi, N.; Oladnabi, M. Evaluation of cytokeratin 19 as a prognostic tumoral and metastatic marker with focus on improved detection methods. *J. Cell. Physiol.* **2019**, *234*, 21425–21435. [CrossRef]

25.   Noorlag, R.; van Es, R.J.J.; de Bree, R.; Willems, S.M. Cytokeratin 19 expression in early oral squamous cell carcinoma and their metastasis: Inadequate biomarker for one-step nucleic acid amplification implementation in sentinel lymph node biopsy procedure: One-step nucleic acid amplification in early oral cancer. *Head Neck* **2017**, *39*, 1864–1868. [CrossRef]

26.   Deambrogio, C.; Castellano, I.; Paganotti, A.; Zorini, E.O.; Corsi, F.; Bussone, R.; Franchini, R.; Antona, J.; Miglio, U.; Sapino, A.; et al. A new clinical cut-off of cytokeratin 19 mRNA copy number in sentinel lymph node better identifies patients eligible for axillary lymph node dissection in breast cancer. *J. Clin. Pathol.* **2014**, *67*, 702–706. [CrossRef]

27.   Terrenato, I.; D'Alicandro, V.; Casini, B.; Perracchio, L.; Rollo, F.; De Salvo, L.; Di Filippo, S.; Di Filippo, F.; Pescarmona, E.; Maugeri-Saccà, M.; et al. A cut-off of 2150 cytokeratin 19 mRNA copy number in sentinel lymph node may be a powerful predictor of non-sentinel lymph node status in breast cancer patients. *PLoS ONE* **2017**, *12*, e0171517. [CrossRef]

28.   Ren, Y.; Zhang, L.; Xie, H.; She, Y.; Su, H.; Xie, D.; Zheng, H.; Zhang, L.; Jiang, G.; Wu, C.; et al. Lymph Node Micrometastasis Prognosticates Survival for Patients with Stage 1 Bronchogenic Adenocarcinoma. *Ann. Surg. Oncol.* **2018**, *25*, 3812–3819. [CrossRef]

PŘÍLOHA 4

RESEARCH ARTICLE

WILEY Journal of SURGICAL ONCOLOGY

One-step nucleic acid amplification vs ultrastaging in the detection of sentinel lymph node metastasis in endometrial cancer patients

Jan Kosťun MD[1] | Martin Pešta MD, PhD[2,3,4] | Jiří Sláma MD, PhD[5] |
Robert Slunéčko MD[6] | Pavel Vlasák MD[1] | Jiří Bouda MD, PhD[1] |
Zdeněk Novotný MD[1] | Ondřej Topolčan MD[4] | Radek Kučera PhD[4] |
Vlastimil Kulda MD[7] | Kateřina Houfková Mgr[2] | Denis Berezovskiy MD[1] |
Alena Bartáková MD, PhD[1] | Jiří Presl MD, PhD[1]

[1]Department of Gynaecology and Obstetrics, University Hospital Pilsen, Charles University, Prague, Czech Republic

[2]Department of Biology, Faculty of Medicine in Pilsen, Charles University, Pilsen, Czech Republic

[3]Biomedical Centre, Faculty of Medicine in Pilsen, Charles University, Pilsen, Czech Republic

[4]Department of Immunochemistry, University Hospital and Faculty of Medicine in Pilsen, Charles University, Pilsen, Czech Republic

[5]Department of Obstetrics and Gynaecology, First Faculty of Medicine, Charles University, General University Hospital, Prague, Czech Republic

[6]Sikl's Department of Pathology, University Hospital Pilsen, Charles University, Prague, Czech Republic

[7]Department of Medical Chemistry and Biochemistry, Faculty of Medicine in Pilsen, Charles University, Prague, Czech Republic

Correspondence
Jiří Presl, MD, PhD, Department of Gynaecology and Obstetrics, University Hospital Pilsen, Charles University Prague, alej Svobody 80, 304 60 Plzeň-Lochotín, Czech Republic.
Email: preslj@fnplzen.cz

Background and Objectives: Utilisation of the one-step nucleic acid amplification (OSNA) molecular biology method for the detection of the metastatic involvement of sentinel lymph nodes (SLNs) in endometrial cancer (EC) patients. A comparison with histopathological ultrastaging and a description of the clinical consequences.

Methods: Surgically treated EC patients underwent detection of SLNs. Nodes greater than 5 mm were cut into sections 2-mm thick parallel to the short axis of the node. Odd sections were examined according to the OSNA method, while even ones according to an appropriate ultrastaging protocol. Nodes less than or equal to 5 mm were cut into halves along the longitudinal axis with one half examined according to the OSNA method and the other half by ultrastaging.

Results: Fifty-eight patients were included and 135 SLNs were acquired. Both ultrastaging and OSNA agreed on 116 results. According to the OSNA method, 20.69% more patients were classified into International Federation of Gynecology and Obstetrics (FIGO) stage III. When comparing the results of the OSNA method to the conclusions of ultrastaging as a reference method, sensitivity of 90.9%, specificity of 85.5% and concordance of 85.9% were attained.

Conclusions: The results of the OSNA method showed a higher frequency of detection of micrometastases and included 20.69% more patients into FIGO stage III.

KEYWORDS
cytokeratin 19, micrometastasis, one-step nucleic acid amplification assay

1 | INTRODUCTION

Endometrial carcinoma (EC) is the fourth most common malignity in the female population in developed countries.[1] Due to the early

clinical symptoms, the disease is detected in a majority of patients in the early stages without the lymphatic system being involved, which means that the 5-year survival rate exceeds 90%.[2] However, with the involvement of the pelvic and paraaortic lymph nodes, the 5-year

survival rate decreases considerably to 57% to 58% and 49% to 52%, respectively.[3]

According to the current recommendations of the National Comprehensive Cancer Network (NCCN), systematic pelvic and paraaortic lymphadenectomy is recommended as standard for the staging of the lymphatic system.[4] This surgical treatment is demanding in terms of technique and time and is associated with an increased risk of perioperative and postoperative morbidity.[5,6] Similarly, as in the case of other gynaecological malignancies, the push to utilise the sentinel lymph node (SLN) concept for EC is on the rise as it allows the radicality of the surgical treatment and its potential complications to be reduced.[7] In 2017, the American Joint Committee on Cancer (AJCC) implemented revisions to the staging system for EC. The new version came into force in January 2018 and became an integral part of the NCCN recommendations.[4] The role of SLN mapping is still under evaluation, but it can be considered for surgical staging of uterine-confined disease. The utilisation of ultrastaging based on published data improves the detection of the metastatic involvement of lymph nodes by approximately 5%.[8]

Finding a sentinel lymph node enables detailed examination – ultrastaging. Examination based on staining by haematoxylin and eosin (H&E) and immunohistochemical examination utilising the cytokeratin 19 antibody (IHC CK19) enable the detection of cancer cells up to the level of micrometastases or isolated tumour cells (ITCs). Unfortunately, such examinations are very time consuming and provide delayed final results. On an intraoperative basis, the frozen section method, the attained reliability of which is only 60% based on available references, can be used.[9]

Our study deals with the possibility to improve the detection of micrometastases and macrometastases in sentinel lymph nodes (SLN) using the one-step nucleic acid amplification (OSNA) molecular biology method based on the detection of CK19 messenger RNA (mRNA) with the complete processing of SLNs in EC patients.

The objective of the study was to describe the sensitivity, specificity and diagnostic concordance of the OSNA method in comparison with an extensive histopathological examination at the ultrastaging level. Another objective was to determine the way in which the detection of lymph node metastases by the OSNA method would influence the patient's staging based on the International Federation of Gynecology and Obstetrics (FIGO) classification.

2 | MATERIALS AND METHODS

2.1 | Study objectives

The main objective of the study was to compare the results of the OSNA-method with a detailed ultrastaging examination as a reference method in the evaluation of the metastatic involvement of SLNs in EC patients.

Another objective was to describe the effect of the SLN evaluation attained by these methods on the patients' FIGO classification.

2.2 | Patient selection

The inclusion criterion was the histologically confirmed EC assessed according to the current histological classification adopted by the WHO in 2014.[10]

For preoperative purposes, all patients underwent an expert ultrasonographic examination of the abdomen and pelvis. The objective was to gain a detailed description of the uterine cavity, endometrium, myometrium, peritoneal surfaces, the presence of free intraperitoneal fluid, pelvic and paraaortic lymph nodes. The examination was always performed by one of two certified expert sonographers and a detailed record of each examination generated in accordance with the standards maintained by our clinic.[11,12] Where necessary, a computerized tomography (CT) examination of the abdomen and pelvis was carried out to eliminate the possibility that the tumour had spread outside the uterus and retroperitoneally. Patients with enlarged lymph nodes or suspected involved lymph nodes were not included in the study.

The study was approved by the Ethics Committee of the Faculty of Medicine in Pilsen of Charles University in Prague and the Teaching Hospital in Pilsen. All the patients signed informed consent forms in conjunction with their voluntary participation in the study. The study is registered at ClinicalTrials.gov under ID No.: NCT02826291.

2.3 | Sentinel lymph node mapping

The detection of SLNs was executed using several procedures. In one group of patients (72.4%), a dose of 2 mL of 1% solution of Bleu Patente and a dose of 8 mL containing 50 MBq of nanocolloid ^{99m}Tc-albumin solution was applied to all four quadrants of the cervix, at first superficially (1-3 mm) and then deeper into the cervix stroma (10-20 mm). The application was executed with a thin 23-gauge needle.

In the remaining patients, either Bleu Patente (15.5%, due to a temporary unavailability of technecium) was applied using the same technique and in the same dosage or a 2.5 mg dose of indocyanine green (10.3%) dissolved in 2 mL of sterile water using the same application technique. In one case (1.7%) mapping was executed only using technecium due to the risks associated with the patient's allergic reaction to Bleu Patente.

Sentinel lymph nodes were detected during operations by direct visualisation (Bleu Patente, ICG) and the use of a γ probe (^{99m}Tc).

2.4 | Sentinel lymph node processing

After excision, the sentinel lymph nodes were mechanically cleaned under sterile conditions. Those sentinel lymph nodes that were greater than 5 mm were cut into sections 2-mm thick parallel to the short axis of the node. Those sentinel lymph nodes that were less than or equal to 5 mm were cut into halves along the longitudinal axis. Sterile conditions were preserved to prevent the node tissue from contacting the epithelium resulting in potential contamination by CK19 and potential false-positive results acquired by the OSNA examination method. The odd sections were submitted for examination according

to the OSNA method, while the even ones were subjected to histopathological and immunohistochemical examination at the level of ultrastaging.

2.5 | Pathological evaluation

The 2 mm sections of the sentinel lymph node intended for histopathological examination were fixed in 10% buffered formalin, then embedded in a paraffin block and examined according to the ultrastaging protocol. Two consecutive sections with a thickness of 2 μm within the interval of 150 μm were acquired. The odd preparations were stained with H&E, while the even preparations were subjected to immunohistochemical examination on the basis of the detection of low molecular cytokeratins (CK MNF 116), including CK19 detection, using the A53-B/A2.26 monoclonal antibody (Ventana automatic instrument protocol; Ventana Medical Systems, Tucson, AZ). The immunohistochemical detection of CK19 was also performed on the primary tumour to confirm its expression. Approximately 40 sections from a single lymph node were examined.

The aforementioned protocol corresponds to the ultrastaging protocol for the processing of sentinel lymph nodes at our clinic and enables detection up to the level of individual ITCs. Metastatic lesions greater than 2 mm were evaluated as macrometastases, lesions less than or equal to 2 mm and greater than 0.2 mm as micrometastases and lesions less than or equal to 0.2 mm were evaluated as ITCs.

2.6 | OSNA evaluation

OSNA is a method for detecting mRNA of CK19 in lymph nodes upon the homogenisation of a whole node (or a part thereof where applicable) sample using the reverse transcription loop-mediated isothermal amplification (RT-LAMP) technique. CK19 is the cytoskeleton filament of epithelial cells and also of the cells of carcinomas and their metastases. Normal lymphoid tissue does not express CK19.

Using isothermal amplification, the OSNA method is able to detect the numbers of CK19 mRNA copies. The whole lymph node is processed, not only several sections thereof. The surgeon has the result at their disposal within 20 to 30 minutes.

Analysis was performed using the OSNA Assay (Sysmex, Kobe, Japan) according to the manufacturer's instructions. Briefly, the 2 mm sections of the lymph nodes intended for OSNA processing were homogenised to form a lysate. The lysate was then centrifuged and inserted into the RD 100i instrument (Sysmex) where the isothermal amplification of CK19 mRNA by the RT-LAMP method was executed.[13,14]

For the purposes of the study, the cut-off values of the OSNA method implemented for the description of micrometastases or macrometastases in lymph nodes in breast cancer patients were utilised. This means that values less than 250 copies of CK19 mRNA/μL were evaluated as negative, from 250 to 4999 copies of CK19 mRNA/μL as micrometastases and 5000 and more copies of

CK19 mRNA/μL as macrometastatic involvement. Those lymph nodes with a value exceeding greater than or equal to 250 copies of CK19 mRNA/μL were therefore evaluated and statistically processed as positive. The expression of CK19 by endometrial carcinoma was always immunohistochemically verified in the primary tumour as well.

2.7 | Statistical analysis

The data characterising the group of patients included in the study are arranged in the form of Table 1 to 4, Venn diagrams (Figures 1 and 2), followed by the statistical evaluation of the data with a description of the percentage representation of specific phenomena

TABLE 1 Patients characteristics, patients N = 58, SLN's N = 135

Age, median (range)	65.5 (31-81)
BMI, median (range)	31.8 (17-44.9)
Number of SLN, n (%)	135 (100%)
Bilateral SLN mapping, n (%)	54 (93.1%)
Number of SLNs per patient, median (range)	2 (1-5)
Histology, n (%)	
Endometrioid	54 (93.1%)
Clear cell	2 (3.4%)
Serous	1 (1.7%)
Carcinosarcoma	1 (1.7%)
Tumour grades, n (%)	
1	33 (56.9%)
2	16 (27.6%)
3	9 (15.5%)
Lymphovascular invasion, n (%)	
No	45 (77.6%)
Yes	13 (22.4%)
FIGO stages, n (%)	
I	45 (77.6%)
II	7 (12.1%)
III	6 (10.3%)

Abbreviations: BMI, body mass index; FIGO, International Federation of Gynecology and Obstetrics; SLNs, sentinel lymph nodes.

TABLE 2 Sentinel lymph nodes – relationship of histopathological ultrastaging vs OSNA

Lymph nodes (n = 135)	Histopathological ultrastaging (combination of H&E and IHC)	
	Positive	Negative
OSNA assay positive	10	18[a]
OSNA assay negative	1	106[b]

Abbreviations: H&E, haematoxylin and eosin; IHC, Immunohistochemistry; OSNA, one-step nucleic acid amplification.
[a]This number includes also one OSNA positive SLN with benign epithelial inclusions in histopathological evaluation (17 + 1).
[b]All the sentinel lymph nodes finally considered negative, this number includes also two nodes with benign epithelial inclusions and one node with ITC (103 + 3).

TABLE 3 Discordant nodes characteristics

Node	Histology	Grades	LVSI	H&E	OSNA	IHC	mRNA CK19 copy/μL	Comments
1.	Endometrioid	1	Yes	++	+	++	1300	
2.	Endometrioid	2	No	−	+	−	1400	
3.	Clear cell	3	Yes	++	+	++	620	
4.	Clear cell	3	Yes	++	+	++	270	
5.	Endometrioid	2	Yes	−	+	−	270	
6.	Endometrioid	2	Yes	−	+	−	620	
7.	Endometrioid	1	No	−	+	−	620	
8.	Endometrioid	1	No	−	+	−	270	
9.	Clear cell	3	Yes	−	+	−	410	
10.	Clear cell	3	Yes	−	+	−	270	
11.	Endometrioid	2	No	−	++	−	35 000	
12.	Endometrioid	2	No	−	+	−	3800	
13.	Endometrioid	1	No	−	++	+	5200	Epithelial inclusions
14.	Endometrioid	1	No	−	−	+	<250	Epithelial inclusions
15.	Endometrioid	1	No	−	+	−	710	
16.	Endometrioid	1	No	−	+	−	470	
17.	Endometrioid	3	Yes	++	+	++	710	
18.	Endometrioid	2	Yes	−	++	−	13 000	
19.	Endometrioid	1	No	+	−	+	<250	
20.	Endometrioid	2	No	−	+	−	260	
21.	Endometrioid	2	No	−	+	−	400	
22.	Endometrioid	1	Yes	−	+	+	920	Isolated tumour cells
23.	Endometrioid	3	Yes	++	+	++	1800	
24.	Endometrioid	1	No	−	−	+	<250	Epithelial inclusions
25.	Endometrioid	3	No	−	+	−	2100	
26.	Serous	3	No	−	+	−	410	

Abbreviations: H&E, haematoxylin and eosin; IHC, Immunohistochemistry; LVSI, lymphovascular space invasion; mRNA, messenger RNA; OSNA, one-step nucleic acid amplification; +, micrometastasis; ++, macrometastasis.

TABLE 4 Changes in TNM and FIGO stage depending on OSNA results in discordant patients

	Ultrastaging		OSNA staging			
Cases	TNM	FIGO	TNM	FIGO	LVSI	Histology
1.	T1aN0M0	IA	T1aN1miM0	IIIC1	No	Endometrioid
2.	T2N0M0	II	T2N1miM0	IIIC1	Yes	Endometrioid
3.	T1aN0M0	IA	T1aN1miM0	IIIC1	No	Endometrioid
4.	T1aN0M0	IA	T1aN1miM0	IIIC1	No	Endometrioid
5.	T2N0M0	II	T2N1miM0	IIIC1	Yes	Clear Cell
6.	T2N0M0	II	T2N1aM0	IIIC1	No	Endometrioid
7.	T1aN0M0	IA	T1aN1aM0	IIIC1	No	Endometrioid
8.	T1aN0M0	IA	T1aN1miM0	IIIC1	No	Endometrioid
9.	T1aN0M0	IA	T1aN1miM0	IIIC1	No	Endometrioid
10.	T1bN0M0	IB	T1bN1miM0	IIIC1	Yes	Endometrioid
11.	T1aN0M0	IA	T1aN1miM0	IIIC1	No	Endometrioid
12.	T1aN0M0	IA	T1aN1miM0	IIIC1	No	Serous
13.	T1bN1mi	IIIC1	T1bN0M0	IB	No	Endometrioid

Abbreviations: FIGO, International Federation of Gynecology and Obstetrics; LVSI, lymphovascular space invasion; OSNA, one-step nucleic acid amplification; TNM, tumour-node-metastasis.
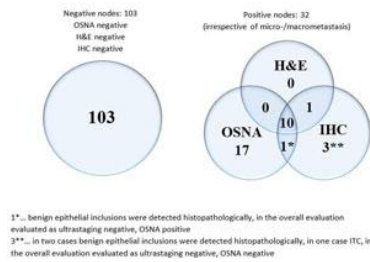
FIGURE 1 Examination of sentinel lymph nodes – relationship of the IHC, H&E and OSNA methods (number of nodes: 135). H&E, haematoxylin and eosin; IHC, Immunohistochemistry; OSNA, one-step nucleic acid amplification [Color figure can be viewed at wileyonlinelibrary.com]
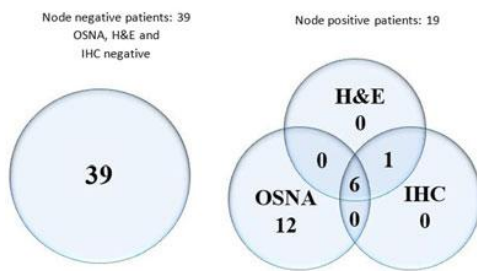

FIGURE 2 Resulting evaluation of the patients on the basis of the results of the examination using the IHC, H&E and OSNA methods (number of patients: 58). H&E, haematoxylin and eosin; IHC, Immunohistochemistry; OSNA, one-step nucleic acid amplification [Color figure can be viewed at wileyonlinelibrary.com]

in the studied population or part thereof. The main objective was to describe the sensitivity, specificity and concordance of the OSNA method compared with a combination of histopathological and immunohistochemical examinations at the ultrastaging level.

The statistical evaluation of the comparison of the frequency of the detection of metastases by the OSNA and ultrastaging method in sentinel lymph nodes was conducted on the basis of the χ^2 method without Yates correction.

3 | RESULTS

3.1 | Patient characteristics

A total of 58 patients operated on between April 2016 and January 2018 were included in the study and a total of 135 SLNs were examined based on the study protocol (Table 1).

During every examination by the pathologist, immunohistochemical verification of the CK19 expression was executed in the

tumorous tissue. In all the patients, the CK19 expression induced by a tumour was ascertained, within the range of 10% to 100%.

3.2 | Sentinel lymph node detection

In the majority of patients (42; 72.4%), the sentinel lymph node was detected by the intracervical application of a combination of the Bleu Patente and ^{99m}Tc tracers before the commencement of the operation. In 54 out of 58 (93.1%) patients included in the study, bilateral mapping was attained, while in four (6.9%) patients sentinel lymph nodes were localised only unilaterally. The most common localisation of the sentinel lymph node was in the position of the external iliac vessels (76.3%), with the second most common site being the obturator fossa (14.8%). All detected sentinel lymph nodes were located in the pelvic region or presacrally; during this study, no sentinel lymph nodes were found in4the paraaortic region.

3.3 | Comparison of OSNA and histopathological diagnosis

A total of 135 lymph nodes were examined for the presence of metastatic involvement. One hundred and six lymph nodes were evaluated as negative by all three methods (H&E, IHC CK19, and OSNA), while the remaining 29 lymph nodes were evaluated as positive by at least one method. The lymph node was evaluated positively only if the presence of a micrometastasis or macrometastasis was proven, while the presence of ITC was evaluated as negative. All three methods agreed on the positivity of 10 (13.5%) of the sentinel lymph nodes.

A total of 11 positive sentinel lymph nodes were detected by the H&E and IHC CK19 methods (ultrastaging). The OSNA method detected positivity in 18 more lymph nodes (more than 250 copies of CK19 mRNA/µL) that were indicated as negative according to the ultrastaging approach. It was only possible in one case to detect the metastatic involvement of the lymph node at the level of micro-metastasis using H&E and IHC CK19, while OSNA indicated the material from the lymph node as negative (Table 2 and Figure 1).

Table 2 summarises the comparison of positivity and negativity produced by the OSNA and ultrastaging methods in the final evaluation of the sentinel lymph nodes. Based on the results, the sensitivity, specificity and concordance of the used methods were calculated.

Detection of the metastatic involvement of sentinel lymph nodes using the OSNA method compared with ultrastaging as a standard reference method attained sensitivity of 90.9%, specificity of 85.5% and concordance of 85.9%. This proves that the OSNA method has a significantly greater proportion of detected positive sentinel lymph nodes ($P = 0.0033$).

3.4 | The ability of the applied methods to detect micrometastases and macrometastases

In addition to the comparison of the ability of the methods to detect the metastatic involvement of lymph nodes, we compared the individual methods (OSNA, H&E and IHC CK 19) from the point of view of their ability to detect micrometastases or macrometastatic involvement.

In the case of 26 discordant SLNs metastatic involvement was described using the OSNA method within the meaning of micrometastasis or macrometastasis. However, the result was not consistent with the results of the H&E or IHC methods. The methods did not bring consistent results both in terms of the detection of metastatic involvement of the node and in terms of the metastatic involvement level – micrometastasis vs macrometastasis.

In one SLN, the OSNA method recorded a negative result although the H&E and IHC CK19 examinations were positive for micrometastatic involvement.

In five SLNs, all methods detected the presence of metastatic involvement but were not consistent as far as the degree of its scope (micrometastasis vs macrometastasis) was concerned.

Out of 17 SLNs that were detected as positive using the OSNA method and as negative using the H&E and IHC CK19 methods, 14 were OSNA positive for micrometastasis, while the other methods produced a negative result. In three SLNs the OSNA method detected macrometastatic involvement, with the H&E and IHC CK19 methods providing a negative result.

In one SLN, the pathologist described ITC, which according to the OSNA method was micrometastasis positive. In two SLNs with IHC positivity vs H&E and OSNA negativity and one SLN with IHC and OSNA positivity vs H&E negativity, ectopic epithelial inclusions were described. The cases with benign epithelial inclusions were evaluated by the pathologist as three false-positive results (Table 3).

3.5 | Evaluation of patients on the basis of SLN condition

The results of the OSNA method and both standard methods (H&E and IHC) in relation to the individual patients are shown in Figure 2.

All three methods were consistent in 39 patients in the absence of metastatic involvement of SLNs. In six patients, all three methods were consistent in terms of the positivity of the examined sentinel lymph nodes. In addition, the OSNA method detected positive SLNs in 12 patients, whereas in one patient, the SLN's positivity detected by the H&E and IHC CK19, which was detected as negative by the OSNA method.

The false-positive lymph nodes due to benign epithelial inclusions detected by IHC CK 19 indicated in Figure 1 did not affect the overall evaluation of the patient.

3.6 | Tumour-node-metastasis (TNM) and FIGO classification of the patients based on the used examination methods

Under the OSNA method, diagnostics classified 12 patients (20.69%) as FIGO stage III, while the examination of the sentinel lymph nodes by ultrastaging resulted in their classification as FIGO stages I and II (Table 4).

One of the patients was classified as FIGO stage III based on the ultrastaging examination, while the examination of the SLNs using the OSNA method classified this patient as FIGO stage I.

In 45 patients, the TNM and FIGO classifications based on the SLN examinations using the OSNA and ultrastaging methods were consistent. These patients are not included in Table 4.

4 | DISCUSSION

Our study represents the largest group of EC patients to be examined so far using the OSNA method for the detection of the metastatic involvement of SLNs. Compared with standard ultrastaging, the OSNA method proved the metastatic involvement of SLNs more frequently and resulted in the upstaging of as many as 20.69% patients. The used methodology allowed every sentinel lymph node to be examined by ultrastaging and the OSNA method at the same time, whereby the results of both procedures could be compared. At all times, one-half of the sections were processed according to the OSNA method, while the other half were subjected to standard histopathological ultrastaging. While ultrastaging evaluated 8.15% (11/135) of the lymph nodes as metastatically involved, the OSNA method detected 20.69% (28/135) as metastatically involved ($P \leq 0.0033$). The concordance of the OSNA method and the ultrastaging of sentinel lymph nodes as a reference method was 85.9%. The false negativity of the OSNA method was only recorded in one case.

The detection of the metastatic involvement of lymph nodes using the OSNA method in the case of EC was used in two smaller published studies. In 2014, a group of Japanese authors used the OSNA method in 35 EC patients for the first time. The examination of 137 sentinel lymph nodes resulted in the detection of 15 (10.95%) positive ones. The 2-mm-interval histopathological method was used as a control standard. The node was cut into sections 2-mm thick. The even sections were processed in a standard manner, while the odd ones using the OSNA method. Although the study utilised a less detailed histopathological examination (2-mm-interval histopathology method) than our study, a greater concordance was achieved. Only four discordant findings were described. Concordance of the OSNA method and the standard histopathological examination was 97.1%.[15] A detailed ultrastaging method of the processing of sentinel lymph node parts would further improve the comparison of both the methods, including the detection of phenomena comprising micrometastases, ITC or benign epithelial inclusion.

In another study, the authors examined a total of 94 sentinel lymph nodes from 34 patients using the OSNA method. The central 1-mm thick section of the lymph node was examined by H&E and IHC CK19, while the remaining lymph node tissue was examined according to the OSNA method. In this study, the OSNA method detected 16 metastatically involved lymph nodes and thus attained 88.3% concordance with the histopathological examination. Within the framework of this study, a total of 11 discordant results were detected: OSNA positive and histopathology negative. In two SLNs, benign epithelial inclusions were detected as a result of the histopathological examination, with the OSNA method providing a positive result in these cases. Regardless of the fact that the use of

the OSNA method proved to be more sensitive to metastases detection, the study was limited by the detailed histopathological examination of only the 1-mm central section of the node, which may not have detected metastatic involvement properly.[16]

Unlike our sample, neither study evaluates the possible impact of the selected detection methods on the management of the patients participating in the study. Considering the high proportion of upstaging in our study, we regard this fact as very important from the clinical point of view. We believe that a more accurate detection of lymph node metastatic involvement using the OSNA method could result in a more precise indication of adjuvant treatment in patients who have so far been included in the low-risk group, thereby reducing the risk of disease recurrence.

The processing of SLNs represents an essential issue. The OSNA method has established itself as a very efficient and comparable method to ultrastaging in that it provides information on the presence of tumour involvement from the entire lymph node and not on the basis of just several sections. However, its nature excludes a feedback check of the sample by the pathologist. Three lymph nodes included in our study, benign ectopic epithelial inclusions were found in the samples. Such inclusions may cause a false positivity of the OSNA method. The incidence of such inclusions in SLNs is very low; the references state about 1.6%. The total incidence, including non-SLNs then fluctuates around 0.1% to 0.2%.[16] In our group of examined SLNs their incidence attained 2.2% and caused one true-false positivity using the OSNA method. However, this result had no effect on the final evaluation of the patient as they also had an ultrastaging positive contralateral SLN with a detected micrometastasis.

In one case, the SLN was evaluated according to the OSNA method as negative, whereas ultrastaging evaluated the same lymph node as positive with a micrometastasis. This can be explained by the method used for cutting the node into sections 2-mm thick. It is possible that the pathologist received the part of the lymph node with micrometastatic involvement, while the instrument for the OSNA examination received the part of the lymph node without metastatic involvement. The same principle could have played a role in the opposite case, that is, the positivity of the OSNA method for a micrometastasis with H&E and IHC negativity. However, the significantly higher statistical incidence of such cases in our group, with a total of 18 positive lymph nodes with negative ultrastaging, is indicative of a higher sensitivity of the OSNA method to metastatic involvement compared to histopathological and IHC examinations (Table 3).

Detection of a sentinel lymph node in EC patients is not a standardised process yet. There are several methods of detection that differ according to the site of application and the combination of tracers.[17,18] In our study, the method of intracervical application was used. In addition, the possibility of the detection of sentinel lymph nodes within the framework of paraaortic localisation is controversial. Based on references, about 10% of sentinel lymph nodes are localised in this region.[19] The incidence of isolated metastases in this region, that is, without the involvement of pelvic lymph nodes, is reported to be about 1% to 3%.[20,21] Unsuccessful detection of an

isolated metastatically involved paraaortic lymph node could lead to the selection of an irrelevant adjuvant treatment. In addition, within the framework of preoperative examination it is possible to reduce this risk by utilising detailed imaging examinations (such as CT, positron emission tomography–computed tomography [PET-CT] or expert ultrasound) to identify clinically suspect lymph nodes in this region. Some of the published studies also point to the benefits of sentinel lymph node mapping (SLNM) in EC patients compared with the execution of systematic pelvic and paraaortic lymphadenectomy. The SLNM strategy shows a higher degree of detection of affected pelvic lymph nodes with a possible lower radicality of surgical treatment.[22] How et al[19] even describes a decrease in the incidence of pelvic recurrence of the disease (pelvic sidewall recurrences) by up to 68%.

Recently published data dealing with the importance of lympho-vascular space invasion (LVSI) in pT1N0 node-negative patients has shown the 5-year disease recurrence rate of 4.8% in lymph node negative and LVSI negative and 14.1% lymph node negative and LVSI-positive patients ($P = 0.006$).[23] The question arises whether these facts are caused by the low sensitivity of the standard tests used for the detection of metastatic involvement of SLNs or not. In our group of patients, the OSNA method detected a statistically significant higher number of positive lymph nodes, which would result in the classification of a statistically significant higher number of patients into higher FIGO stages, which would better correspond to the frequency of patients in whom the recurrence of the disease occurs in the early stage.

In our medical care system, the cost of a sentinel lymph node examination using the OSNA method is about 10 times higher than histopathological ultrastaging. However, it is evident from practice that with the increasing number of OSNA tests, the cost of implementing is decreasing. Moreover, with a higher sensitivity of nodal involvement detection with the OSNA method, a decrease in retreatment costs may also be expected due to adequate first-line adjuvant therapy. A detailed cost-benefit analysis of the OSNA examination for patients with endometrial cancer has not yet been published. However, the cost-benefit analysis for breast cancer patients estimated by the total cost of treatment is in favour of OSNA testing, despite the higher entry cost per lymph node.[24,25]

5 | CONCLUSIONS

In conclusion, the OSNA method offers a quick and accurate alternative to detailed ultrastaging examination. Based on the results of this study, the OSNA method, compared with ultrastaging, shows sensitivity of 90.9%, specificity of 85.5% and concordance of 85.9%. In our study, the OSNA method compared with ultrastaging led to the detection of a higher number of metastatically involved SLNs, with the consequent upstaging of 20.69% more patients. In the case of breast and colorectal cancers, this method proved itself sufficient in the past and is already accepted as a standard method

in routine clinical practice.[26] The utilisation of the OSNA method in combination with SLNM techniques in EC patients holds great promise for the future for the highly sensitive detection of metastatically involved lymph nodes and the relevant application of adjuvant treatment. The next step of the study is to apply this method for examining SLNs in EC patients should focus on the inclusion of the examination of the whole SLN without indirect histological control.

ACKNOWLEDGEMENTS

AUTHOR CONTRIBUTIONS

Surgical team leader, writing, data collection and analysis: KJ. OSNA method team leader, writing: PM. Writing, writing revisions: SJ. OSNA method team member: KH, TO, KR and VK. Histopathological ultrastaging: SR. Surgical team member, data collection: VP, BJ, NZ, BA and BD. Writing revisions, surgical team member: PJ.

CONFLICTS OF INTEREST

The authors declare that there are no conflicts of interest.

ORCID

Jan Kosťun http://orcid.org/0000-0003-4077-9031
Martin Pešta http://orcid.org/0000-0001-8187-0566

REFERENCES

1. Globocan, Northern America, WHO Europe Region (EURO). *Estimated cancer incidence, all ages: female.* 2012. http://globocan.iarc.fr/old/summary_table_pop-html.asp?selection=145905&selection=221994&title=Northern+America%2C+WHO+Europe+region+%28EURO%29&sex=2&type=0&window=1&sort=3&submit=%C2%A0Execute. Accessed May 14, 2017.
2. Creasman W. Revised FIGO staging for carcinoma of the endometrium. *Int J Gynaecol Obstet.* 2009;105(2):109-109.
3. Lewin SN, Wright JD. Comparative performance of the 2009 International Federation Of Gynecology And Obstetrics' Staging System for uterine corpus cancer. *Obstet Gynecol.* 2011;117(5):1226.
4. NCCN. NCCN Clinical Practice Guidelines in Oncology (NCCN Guidelines). 2017 *Uterine Neoplasms. Version I.2018.* https://www.nccn.org/store/login/login.aspx?ReturnURL=https://www.nccn.org/professionals/physician_gls/pdf/uterine.pdf. Accessed March 26, 2017.
5. Kitchener H, Swart AM, Qian Q, Amos C, Parmar MK. Efficacy of systematic pelvic lymphadenectomy in endometrial cancer (MRC ASTEC trial): a randomised study. *Lancet (London, England).* 2009;373(9658):125-136.
6. Daraï E, Dubernard G, Bats AS, et al. Sentinel node biopsy for the management of early stage endometrial cancer: long-term results of the SENTI-ENDO study. *Gynecol Oncol.* 2015;136(1):54-59.
7. Cibula D, Oonk MH, Abu-Rustum NR. Sentinel lymph node biopsy in the management of gynecologic cancer. *Curr Opin Obstet Gynecol.* 2015;27(1):66-72.
8. Cormier B, Rozenholc AT, Gotlieb W, et al. Sentinel lymph node procedure in endometrial cancer: a systematic review and proposal for standardization of future research. *Gynecol Oncol.* 2015;138(2):478-485.
9. Slama J, Dundr P, Dusek L, Cibula D. High false negative rate of frozen section examination of sentinel lymph nodes in patients with cervical cancer. *Gynecol Oncol.* 2013;129(2):384-388.
10. Kurman RJ, Carcangiu ML, Herrington CS, Young RH. *WHO Classification of Tumours of Female Reproductive Organs.* 4th ed., 6. Lyon: IARC; 2014:121-155.
11. Fischerova D. Ultrasound scanning of the pelvis and abdomen for staging of gynecological tumors: a review. *Ultrasound Obstet Gynecol.* 2011;38(3):246-266.
12. Fischerova D, Frühauf F, Zikan M, et al. Factors affecting sonographic preoperative local staging of endometrial cancer. *Ultrasound Obstet Gynecol.* 2014;43(5):575-585.
13. Tsujimoto M, Nakabayashi K, Yoshidome K, et al. One-step nucleic acid amplification for intraoperative detection of lymph node metastasis in breast cancer patients. *Clin Cancer Res.* 2007;13(16):4807-4816.
14. Vodicka J, Mukensnabl P, Vejvodova S, et al. A more sensitive detection of micrometastases of NSCLC in lymph nodes using the one-step nucleic acid amplification (OSNA) method. *J Surg Oncol.* 2018;117(2):163-170.
15. Nagai T, Niikura H, Okamoto S, et al. A new diagnostic method for rapid detection of lymph node metastases using a one-step nucleic acid amplification (OSNA) assay in endometrial cancer. *Ann Surg Oncol.* 2015;22(3):980-986.
16. López-Ruiz ME, Diestro MD, Yébenes L, et al. One-step nucleic acid amplification (OSNA) for the detection of sentinel lymph node metastasis in endometrial cancer. *Gynecol Oncol.* 2016;143(1):54-59.
17. Robova H, Charvat M, Strnad P, et al. Lymphatic mapping in endometrial cancer: comparison of hysteroscopic and subserosal injection and the distribution of sentinel lymph nodes. *Int J Gynecol Cancer.* 2009;19(3):391-394.
18. Holloway RW, Abu-Rustum NR, Backes FJ, et al. Sentinel lymph node mapping and staging in endometrial cancer: a Society of Gynecologic Oncology literature review with consensus recommendations. *Gynecol Oncol.* 2017;146(2):405-415.
19. How J, Gauthier C, Abitbol J, et al. Impact of sentinel lymph node mapping on recurrence patterns in endometrial cancer. *Gynecol Oncol.* 2017;144(3):503-509.
20. Kumar S, Podratz KC, Bakkum-Gamez JN, et al. Prospective assessment of the prevalence of pelvic, paraaortic and high paraaortic lymph node metastasis in endometrial cancer. *Gynecol Oncol.* 2014;132(1):38-43.
21. Rossi EC, Kowalski LD, Scalici J, et al. A comparison of sentinel lymph node biopsy to lymphadenectomy for endometrial cancer staging (FIRES trial): a multicentre, prospective, cohort study. *Lancet Oncol.* 2017;18(3):384-392.
22. Raimond E, Ballester M, Hudry D, et al. Impact of sentinel lymph node biopsy on the therapeutic management of early-stage endometrial cancer: results of a retrospective multicenter study. *Gynecol Oncol.* 2014;133(3):506-511.
23. Cusano E, Myers V, Samant R, et al. Prognostic significance of lymphovascular space invasion in the absence of lymph node metastases in early-stage endometrial cancer. *Int J Gynecol Cancer.* 2018;28(5):890-894.
24. Raia-Barjat T, Trombert B, Khaddage A, et al. OSNA (one-step nucleic acid amplification) sentinel lymph node intraoperative molecular analysis in breast cancer: a cost-benefit analysis. *Med Oncol.* 2014;31(12):322.

25. Guillén-Paredes MP, Carrasco-González L, Cháves-Benito A, Campillo-Soto Á, Carrillo A, Aguayo-Albasini JL. [One-step nucleic acid amplification (OSNA) assay for sentinel lymph node metastases as an alternative to conventional postoperative histology in breast cancer: a cost-benefit analysis]. *Cir Esp.* 2011;89(7): 456-462.

26. Tamaki Y. One-step nucleic acid amplification (OSNA): where do we go with it? *Int J Clin Oncol.* 2017;22(1):3-10.

PŘÍLOHA 5

Plasma microRNA Levels Combined with CEA and CA19-9 in the Follow-Up of Colorectal Cancer Patients

Martin Pesta [1,2], **Radek Kucera** [2,3], **Ondrej Topolcan** [2], **Marie Karlikova** [2], **Katerina Houfkova** [1], **Jiri Polivka** [2,4], **Tereza Macanova** [1], **Iva Machova** [2], **David Slouka** [2] and **Vlastimil Kulda** [3,*]

[1] Department of Biology, Faculty of Medicine in Pilsen, Charles University, alej Svobody 76, 32300 Pilsen, Czech Republic; martin.pesta@lfp.cuni.cz (M.P.); katerina.houfkova@lfp.cuni.cz (K.H.); tereza.macanova@lfp.cuni.cz (T.M.)

[2] Laboratory of Immunoanalysis, University Hospital in Pilsen, E. Benese 13, 30599 Pilsen, Czech Republic; kucerar@fnplzen.cz (R.K.); topolcan@fnplzen.cz (O.T.); karlikovam@fnplzen.cz (M.K.); jiri.polivka@lfp.cuni.cz (J.P.); iva.machova@lfp.cuni.cz (I.M.); slouka@fnplzen.cz (D.S.)

[3] Department of Medical Chemistry and Biochemistry, Faculty of Medicine in Pilsen, Charles University, Karlovarska 48, 30166 Pilsen, Czech Republic

[4] Department of Histology and Embryology, Faculty of Medicine in Pilsen, Charles University, Karlovarska 48, 30166 Pilsen, Czech Republic

* Correspondence: vlastimil.kulda@lfp.cuni.cz; Tel.: +420-377-593-287

Abstract: Colorectal cancer (CRC) ranks among the most common cancers worldwide. Surgical removal remains the best strategy for treatment of resectable tumors. An important part of caring for patients after surgery is monitoring for early detection of a possible relapse of the disease. Efforts are being made to improve the sensitivity and specificity of routinely used carcinoembryonic antigen (CEA) with the use of additional biomarkers such as microRNAs. The aim of our study was to evaluate the prognostic potential of microRNAs and their use as markers of disease recurrence. The quantitative estimation of CEA, CA19-9, and 22 selected microRNAs (TaqMan Advanced miRNA Assays) was performed in 85 paired (preoperative and postoperative) blood plasma samples of CRC patients and in samples taken during the follow-up period. We have revealed a statistically significant decrease in plasma levels for miR-20a, miR-23a, miR-210, and miR-223a ($p = 0.0093$, $p = 0.0013$, $p = 0.0392$, and $p = 0.0214$, respectively) after surgical removal of the tumor tissue. A statistically significant relation to prognosis (overall survival; OS) was recorded for preoperative plasma levels of miR-20a, miR-21, and miR-23a ($p = 0.0236$, $p = 0.0316$, and $p = 0.0271$, respectively) in a subgroup of patients who underwent palliative surgery. The best discrimination between patients with favorable and unfavorable outcomes was achieved by a combination of CEA, CA19-9 with miR-21, miR-20a, and miR-23a ($p < 0.0001$). The use of these microRNAs for early disease recurrence detection was affected by a low specificity in comparison with CEA and CA19-9. CEA and CA19-9 had high specificity but low sensitivity. Our results show the benefit of combining currently used standard biomarkers and microRNAs for precise prognosis estimation.

Keywords: colorectal cancer; biomarkers; recurrence; microRNA; CEA; CA19-9; blood plasma

1. Introduction

Colorectal cancer (CRC) ranks among the most common cancers worldwide [1]. In the last 20 years, we have witnessed the enlargement of the spectrum of available treatment modalities, especially in the fields of chemotherapy, targeted therapy, and immunotherapy [2,3]. Nevertheless, early surgical removal remains the best strategy for the treatment of resectable tumors. In addition to biomarkers

for early disease detection (screening) and prediction of treatment response, there is also a need for efficient biomarkers for early detection of disease recurrence in the follow-up period of patients.

Approximately 20% of surgically treated CRC patients will suffer from disease recurrence within five years after surgery [4]. For the purpose of early detection of recurrence, the preferred examination must be minimally invasive and repeatable over time. Therefore, the most suitable biological material is peripheral venous blood. Carcinoembryonic antigen (CEA) is a well-established marker for this purpose, recommended by both the American Society of Clinical Oncology (ASCO) and the European Group on Tumor Markers (EGTM) [5,6]. There is good evidence that routine CEA monitoring during the postresection follow-up period detects metastatic disease. However, the sensitivity of this marker is not considered to be sufficient [7]. The sensitivity of CEA is compromised by the lack of consistency in the increase in its plasma levels. There are CRC patients with poorly differentiated tumors with CEA only present at low concentrations or even at undetectable levels [8].

There are efforts to improve the sensitivity and specificity by using additional tumor markers like cancer antigen 19-9 (CA19-9) [9], but also using biomarkers reflecting other characteristics of tumor cells. Just such a group of molecules with new and promising features are microRNAs (miRNAs) [10]. MiRNAs are small, non-coding RNA molecules that play a complex role in the post-transcriptional regulation of gene expression, including ceRNA regulatory networks. The human genome encodes over 2500 miRNAs [11], which may target about 60% of mammalian genes [12]. Many studies have described changes in the expression of miRNAs and their involvement in carcinogenesis, tumor progression, development of metastases, and their relation to prognosis and the effects of treatment in many types of cancer [13–15], including CRC [16,17]. Gene expression profiling has revealed patterns of miRNA expression characteristic for these processes [18].

The key role of miRNAs is in the regulation of cellular processes including those involved in tumor growth. MiRNAs lack a direct executive function as enzymes, signaling molecules, or signal transduction molecules that are the targets of current anti-cancer therapy.

MiRNAs are released from cells into body fluids, and it is possible to detect them in blood plasma/serum as cell-free miRNAs or as cargo in exosomes as exosomal miRNAs.

From the point of view of analytical features, miRNA molecules exhibit high stability and can be easily assessed. However, despite the promising results of published studies on circulating miRNAs [19–22] used as biomarkers in CRC, no miRNA has yet proved robust enough to enter routine clinical use [23]. Therefore, the combining of already validated tumor markers (e.g., CEA, CA19-9) with new promising markers could be a way to make prognosis estimation and indication of disease recurrence more accurate.

Based on research of literature in the databases of PubMed and ISI Web of knowledge (published until February 2017) using the keywords "CRC" and "microRNA" and ("plasma" or "serum" or "circulating"), we selected 22 candidate miRNAs that have a potential role in CRC carcinogenesis. These miRNAs and references to studies based on which the selection was made are listed in the section Materials and Methods (Table 4).

The aim of the study was to identify miRNAs with a significant difference between preoperative and postoperative plasma levels, and to evaluate their ability to contribute to early detection of disease recurrence. We also evaluated the relation of these biomarkers to prognosis.

2. Results

First, we describe the changes revealed between the preoperative and postoperative plasma levels of the evaluated markers. We then show the relation of preoperative plasma levels of miRNAs to prognosis and the improvement of prognostic value achieved by an approach based on the combination of miRNAs and well-established, routinely used tumor markers (CEA, CA19-9). Finally, we demonstrate the use of these markers for the detection of disease recurrence.

From a set of 22 estimated miRNAs, we were able to obtain reliable values for only 9 (miR-20a-5p, miR-21-5p, miR-23a-3p, miR-29-3p, miR-92a-3p, miR-155-5p, miR-199a-3p, miR-210-3p, miR-223-3p).

The others were excluded from evaluation due to high Ct values (Ct > 35) resulting in non-reliable quantification or no amplification.

2.1. Changes between Preoperative and Postoperative miRNA Plasma Levels

We have revealed a significant decrease in miR-21, miR-20a, miR-210, miR-23a, and miR-155 plasma levels after the complete removal of tumor mass (radical surgery). There was no significant change in miRNA plasma levels observed in the subgroup of patients who underwent palliative surgery. In the group comprising all patients (radical or palliative surgery), we revealed a statistically significant decrease in miR-20a, miR-23a, miR-210, and miR-223. The results on preoperative and postoperative changes in miRNA levels are summarized in Table 1. A postoperative decrease in plasma levels was also recorded for CEA and CA19-9 (Table 1). The comparison of preoperative and postoperative biomarker values in the group comprising all patients is shown graphically in Figures 1 and 2. A dramatic decrease in postoperative levels of miRNAs is seen especially in patients with high preoperative levels.

Table 1. Differences in preoperative and postoperative levels of microRNAs, CEA, and CA19-9 according to type of surgery (radical or palliative).

Treatment	All (*n* = 85)			Radical (*n* = 57)			Palliative (*n* = 28)		
Marker	[1]Preoperative	[1]Postoperative	*p*-Value	[1]Preoperative	[1]Postoperative	*p*-Value	[1]Preoperative	[1]Postoperative	*p*-Value
miR-20a	0.247	0.200	0.0093	0.261	0.155	0.0004	0.246	0.266	n.s.
miR-21	1.050	1.007	n.s.	1.050	0.973	0.0336	1.094	1.097	n.s.
miR-23a	0.705	0.379	0.0013	0.964	0.559	0.0044	0.367	0.297	n.s.
miR-29	0.005	0.005	n.s.	0.006	0.003	n.s.	0.005	0.009	n.s.
miR-92a	23.264	19.698	n.s.	17.630	19.160	n.s.	38.288	26.715	n.s.
miR-155	0.016	0.012	n.s.	0.017	0.011	0.0375	0.013	0.014	n.s.
miR-199a	0.321	0.490	n.s.	0.334	0.495	0.0537	0.262	0.349	n.s.
miR-210	0.024	0.021	0.0392	0.021	0.013	0.0228	0.032	0.050	n.s.
miR-223	1.275	0.555	0.0214	1.283	0.540	n.s.	0.747	0.600	n.s.
CEA	3.1 ng/mL	2.4 ng/mL	<0.0001	2.0 ng/mL	1.1 ng/mL	<0.0001	18.5 ng/mL	6.8 ng/mL	0.0002
CA19-9	11 U/mL	9 U/mL	0.0007	8 U/mL	7 U/mL	0.0117	39 U/mL	34 U/mL	0.0278

[1] Values shown are medians of plasma levels, microRNA as relative values. CEA—carcinoembryonic antigen.
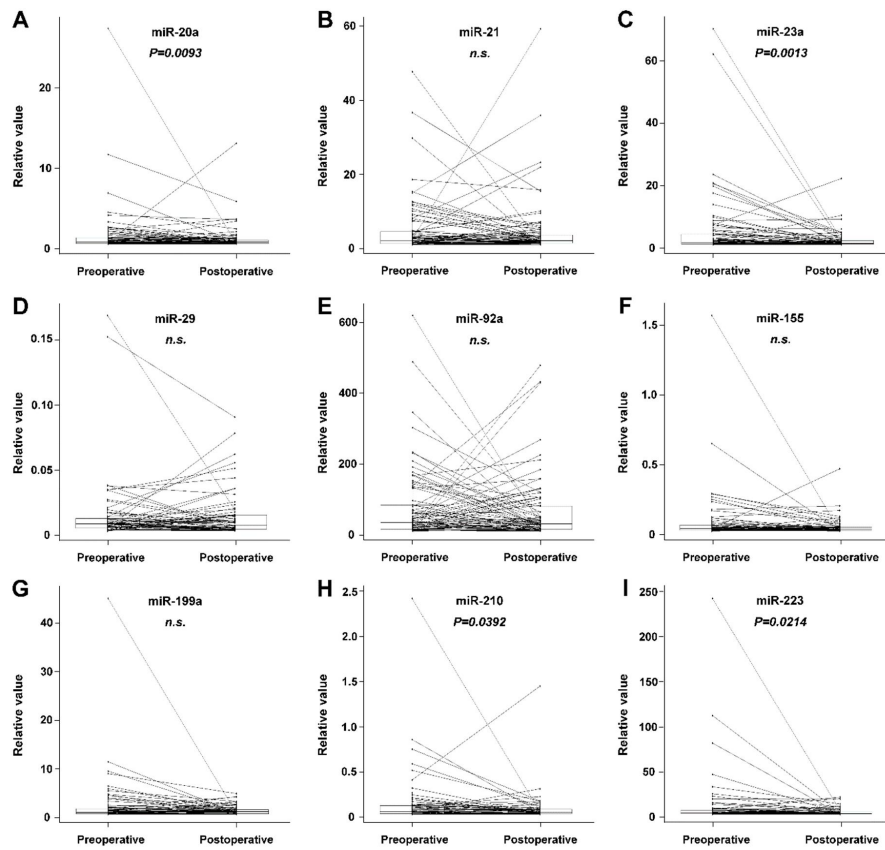
Figure 1. Comparison of paired preoperative and postoperative blood plasma miRNA values in the group comprising all patients. Box-and-whisker plots with outliers shown as separately plotted points. Paired values are connected by a line. A statistically significant decrease was recorded for miR-20a, miR-23a, miR-210, and miR-223. (n.s. = non-significant)
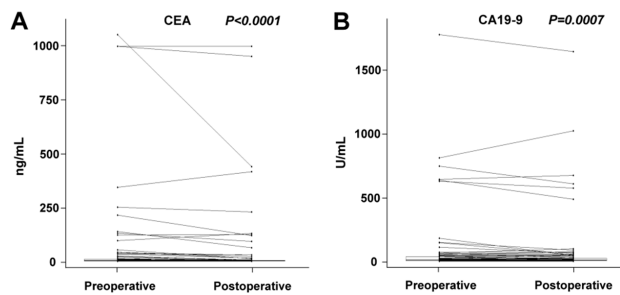

Figure 2. Comparison of paired preoperative and postoperative blood serum CEA (**A**) and CA19-9 (**B**) values in the group comprising all patients. Box-and-whisker plots with outliers shown as separately plotted points. Paired values are connected by a line. A statistically significant decrease was recorded for both CEA and CA19-9.

2.2. The Relation of Preoperative Plasma Levels of miRNAs to Prognosis

The relation to prognosis (OS, overall survival) could only be evaluated in the subgroup of patients who underwent palliative surgery. Within the available follow-up, almost none of the patients who underwent radical surgery died, so no survival data were available. A statistically significant relation to OS was recorded for miR-21, miR-20a, and miR-23a ($p = 0.0316$, $p = 0.0235$, and $p = 0.0270$, respectively). The Kaplan–Meier survival distribution functions are shown in Figure 3.
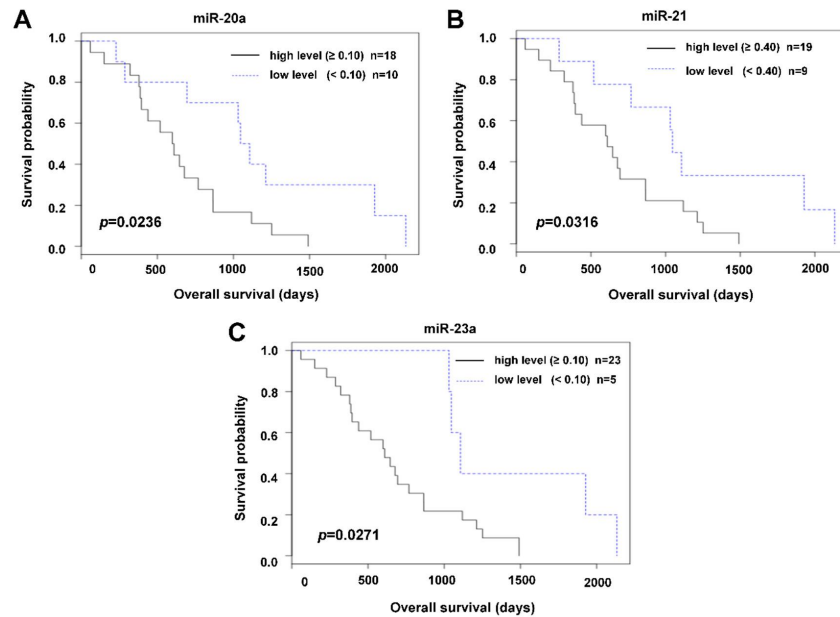

Figure 3. Relation of miR-20a (**A**), miR-21 (**B**), and miR-23a (**C**) preoperative plasma levels to overall survival (OS) in a group of patients who underwent palliative surgery (Kaplan–Meier curves).

Likewise, we observed a statistically significant relation to OS of CEA and CA19-9 ($p = 0.0439$ and $p = 0.0145$, respectively); see Figure 4.
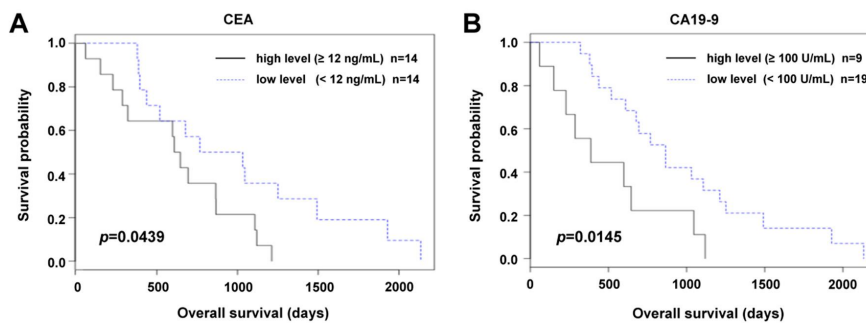

Figure 4. Relation of CEA (**A**) and CA19-9 (**B**) preoperative plasma levels to overall survival (OS) in a group of patients who underwent palliative surgery (Kaplan–Meier curves).

The best discrimination between patients with favorable and unfavorable outcomes was achieved by the combination of estimated tumor markers with miRNAs. Patients with a very high value of any one of CEA, CA19-9, miR-20a, miR-21 or miR-23a, had significantly shorter survival than those who had all the mentioned markers under the cut-off value (Figure 5). It is important to mention that best discrimination between patients with a favorable and unfavorable prognosis is based on the inclusion of all those markers.
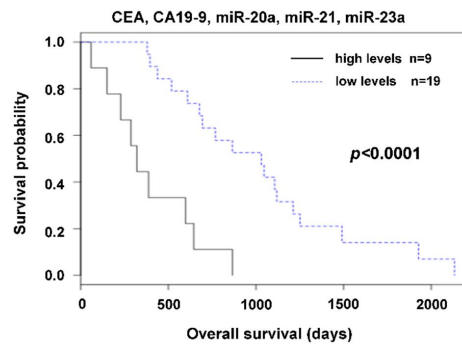

Figure 5. Combining CEA, CA19-9 with miR-20a, miR-21, and miR-23a. Patients with a very high value of any one of CEA, CA19-9, miR-20a, miR-21, or miR-23a had significantly shorter survival than those who had all the mentioned markers under the cut-off value.

2.3. Detection of Disease Recurrence

In the group of patients who underwent radical surgery, it was possible to estimate the sensitivity, specificity, positive predictive value, and negative predictive value of the markers for disease recurrence (Table 2). While CEA and CA19-9 had high specificity and low sensitivity, miRNAs suffered from false positives. Specificity of miRNAs was in the range of 50–60%. However, it is necessary to mention that in the case of follow-up, the data are limited by the small number of patients and the timing of sample collection. Receiver operating characteristic (ROC) curves for miR-20a, miR-21, miR-23a, miR-223, CEA, and CA19-9 are shown in Figure 6.

Table 2. The diagnostic ability of markers in relation to the detection of disease recurrence of patients treated by radical surgery.

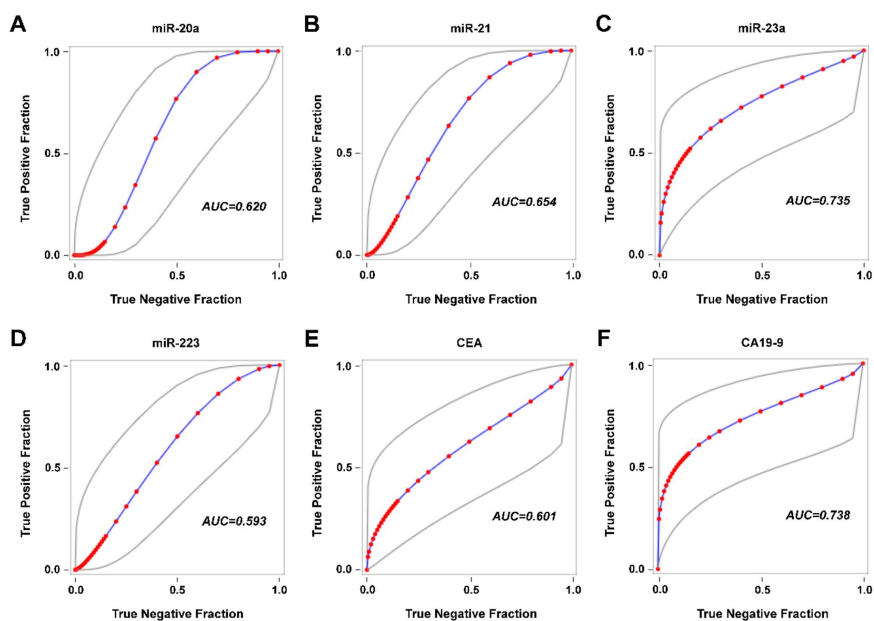| Marker	Recurrence $n = 9$		Remission $n = 22$		Sensitivity	Specificity	Positive Predictive Value	Negative Predictive Value
	True Positive	False Negative	True Negative	False Positive				
miR-20a	6	3	12	10	66.7%	54.6%	37.50%	80.0%
miR-21	7	2	12	10	77.8%	54.6%	41.18%	85.7%
miR-23a	6	3	13	9	66.67%	59.1%	40.00%	81.3%
miR-223	3	6	12	10	33.3%	54.6%	23.1%	66.7%
CEA	3	6	20	2	33.3%	90.9%	60.0%	76.9%
CA19-9	3	6	21	1	33.3%	95.5%	75.0%	77.8%

Figure 6. Receiver operating characteristic (ROC) curves for miR-20a (**A**), miR-21 (**B**), miR-23a (**C**), miR-223 (**D**), CEA (**E**), and CA19-9 (**F**). Abbreviations: AUC—area under the curve.

3. Discussion

Progress in the management of CRC patients has created a need for more accurate biomarkers to guide treatment and for early detection of disease recurrence. The biochemical gold standard for disease recurrence detection is CEA surveillance, and it is most effective when patients have high preoperative serum CEA levels. However, there are some limitations. Sensitivity is far from being sufficient [24]. Plasma concentration of CEA is not consistently elevated in colorectal cancer and may be undetectable or present at only low concentrations with poorly differentiated tumors [8]. There are efforts to improve the sensitivity and specificity using additional tumor markers like CA19-9 [9], but the impact on recurrence detection sensitivity improvement is still limited to those with elevated preoperative serum CA19-9 [25,26].

Progress in understanding the important role of some miRNAs in CRC pathogenesis and the promising features of these molecules from an analytical point of view (stability in body fluids) has led to the possibility of using these molecules for CRC surveillance. miRNAs selected for this study have been previously described as those related to CRC carcinogenesis and could be candidate CRC biomarkers (Table 4). Their plasma levels are expected to be related to the actual process of pathogenesis. This study has revealed miRNAs (miR-20a, miR-210, miR-223, and miR-23a) with a significant difference between preoperative and postoperative plasma levels in a group of surgically treated CRC patients. Detailed data are shown in Table 1 and Figure 1. The study group consisted of two categories of patients: those who underwent radical or palliative surgery. In radically treated patients, it can be assumed that the complete removal of tumor mass will result in a decrease in miRNA levels, while palliative intervention does not lead to the complete removal of tumor mass, so a decrease in miRNA levels may not be significant.

Nevertheless, preoperative plasma values are independent of intervention type, be it radical or palliative. In the case of preoperative values of both radically treated and palliative treated patients, we can expect an association with the actual process of carcinogenesis before treatment and so

preoperative values may have a relationship to prognosis. Due to the favorable outcome of radically treated patients, survival analysis was only computed for the subgroup with palliative intervention. A relation of high preoperative plasma levels of miR-21, miR-20a, and miR-23a to shorter OS was observed. The best discrimination between patients with favorable and unfavorable outcomes was achieved by combining routinely used tumor markers with miRNAs (Figure 5). Our results show the benefit of combining currently used standard biomarkers and miRNAs for precise prognosis estimation.

The use of a combination of biomarkers reflects the current view on carcinogenesis as a multistep process that is individual in number, type, and order of qualitatively and quantitatively aberrantly expressed genes. It would be presumptive to expect that a single biomarker could cover all CRC cases. Similarly, just as there are CRC patients with low or no CEA blood serum levels, there are patients with low levels of particular oncogenic miRNA. In patients with a low preoperative level of such miRNA, we cannot expect a postoperative decrease.

Postoperative decrease is the basic criterion that must be fulfilled by markers, whose plasma levels reflect the course of the disease and could potentially be used for early detection of disease recurrence. We used these candidate molecules in the follow-up period as biomarkers for detection of recurrence. Compared to CEA and CA19-9, miRNAs displayed a higher sensitivity but lower specificity for the detection of disease recurrence. The miRNAs, as biomarkers for detection of recurrence, were compromised by a high number of false positive results. From this point of view, a combination of CEA, CA19-9, and miRNAs (miR-20a, miR-21, miR-223 and miR-23a) seems not to be beneficial. A combination would be beneficial if there were high specificities and non-overlapping low sensitivities.

In 2013, Yong et al. observed, with the use of miRNA microarray profiling and further validation with RT-qPCR, that miR-23a is elevated in both tumor tissue and blood plasma samples of CRC patients [27]. It was later published that miR-23a promotes colorectal cancer cell survival by targeting PDK4 [28], and recently, the participation of miR-23a~27a~24 clusters in CRC progression via reprogramming metabolism to switch from oxidative phosphorylation to glycolysis in a hypoxic tumor environment was reported [29]. The prognostic value of miR-23a has been described for many types of cancer [30], and now we have, for the first time, described a relation between the plasma levels of this miRNA and prognosis in CRC patients.

In 2010, Earle et al. revealed miR-223 to be overexpressed in CRC relative to mucosa [31]. The study of Zekri et al. in 2016 showed that miR-223 is upregulated in blood serum of CRC patients [32]. On the basis of an investigation conducted on colorectal cancer cell line SW620, Ju et al. showed that miR-223 downregulates the FoxO3a/BIM signaling pathway and so promotes proliferation [33]. Li et al. observed that patients with high miR-223 expression in CRC tumor tissue had a poor OS, and miR-223 level correlated with histology grade, metastasis, and tumor-node-metastasis (TNM) stage [34]. We described the relation of miR-223 plasma levels to prognosis.

MiR-21 is the most frequently investigated miRNA with a relation to oncologic diseases. In 2010, we described the prognostic significance of miR-21 expression in CRC tissue and detected its expression in colorectal liver metastases [14]. The diagnostic and prognostic value of tissue miR-21 levels in CRC were evaluated in a meta-analysis by Zhang et al. [35]. A recently published meta-analysis on tissue/serum miR-21 by Guraya [36] concluded that miR-21 may be used as a strong predictor for prognosis of CRC. This meta-analysis contains three studies on circulating miR-21 and four on tissue miR-21 in CRC patients. Our results on circulating miR-21 are in agreement with the conclusion of this meta-analysis.

Yang et al. found serum miR-20a to be downregulated in colorectal neoplasia patients compared to healthy controls [37]. However, Yamada et al. did not find significant differences in serum levels of miR-21 between healthy controls and early colorectal neoplasia patients [38].

As markers for the early detection of recurrence, we have selected from a large number of known miRNAs those previously identified as associated with tumor pathogenesis. For some of these miRNAs, we observed a statistically significant relationship to survival, suggesting their possible use as CRC prognostic markers. However, using these miRNAs during the follow-up period for the

early detection of recurrence, we observed a low specificity. We suggest that these miRNAs also participate in other cellular processes outside tumorigenesis and could also be deregulated due to other pathological situations, e.g., the elevation of circulating miR-21 levels in cardiovascular disease has been described [39].

Therefore, increased levels of miRNA markers in the postoperative period may not be directly related to the recurrence of cancer. For this purpose, it will be necessary to look for miRNAs with exclusive involvement in tumor pathogenesis alone, which will not be easy due to the nature of the miRNA network itself. MiRNAs are involved in competing endogenous RNA crosstalk, where RNA transcripts co-regulate each other by competing for shared miRNAs, thereby titrating miRNA availability (ceRNA hypothesis) [40].

We see the main limit of interpretation of this study in the fact that while preoperative and postoperative specimens collected within a defined period of time were available in all patients, during follow-up specimens were available only in some patients, and in addition to this, they were taken at unequal time intervals. For this reason, we believe that more accurate results have been obtained when comparing preoperative with postoperative values and calculating prognosis (OS).

4. Materials and Methods

4.1. Patients

The study group consisted of 85 patients who underwent surgery for CRC at the Complex Oncology Center of the University Hospital in Pilsen between March 2008 and May 2013. The study was approved by the institutional review board and local ethics committee of the University Hospital in Pilsen. It was a retrospective study. Every patient signed an informed consent form for the use of their blood samples for the assessment of tumor markers. The clinicopathological features are summarized in Table 3.

Table 3. Characteristics of patients in the study.

Variables	Number of Patients	%
Number of Patients	85	100
Gender		
Male	56	65.9
Female	29	34.1
Type of Surgery		
Radical	57	67.1
Palliative	28	32.9
Histology		
Adenocarcinoma	85	100
T Stage		
T2	10	11.8
T3	62	72.9
T4	13	15.3
N Stage		
N0	28	32.9
N1	40	47.1
N2	17	20.0
M Stage		
M0	56	65.9
M1	29	34.1

Table 3. *Cont.*

Variables	Number of Patients	%
Grade		
1	14	16.5
2	60	70.6
3	11	12.9
Clinical Stage		
I	4	4.7
II	17	20.0
III	35	41.2
IV	29	34.1

A total of 57 patients underwent radical surgery and 28 patients a palliative intervention (either partial resection or complete resection of the primary tumor but no removal of liver metastases). Each diagnosis of CRC was verified by a pathologist and all tumors were histologically adenocarcinomas. The stage of disease was determined using the TNM system of the International Union Against Cancer (IUCC, 7th edition) [41]. The median follow-up was 3 years. The evaluation of remission and recurrence was based on response evaluation criteria in solid tumors (RECIST) [42]. The recurrence based on miRNAs (biochemical recurrence) was defined using an individual cut-off value defined as a 1.5-fold increase of the postoperative value or the presence of two consecutive plasma level values higher than the postoperative value.

4.2. Blood Samples

For each patient, preoperative (taken a day before surgery) and postoperative (taken during the period 5–10 days after surgery) peripheral blood samples were analyzed. Peripheral blood samples were also taken during the follow-up period (median follow-up: 27 weeks), however, not for all patients. The number of additional samples collected during the follow-up period was between 0 and 7 per patient. We evaluated 270 samples in total.

Blood samples were taken from the cubital vein. Blood plasma was prepared from 4 mL of whole blood collected into K_3EDTA tubes by centrifugation at $1370\times g$ for 10 min. The blood serum was separated by centrifugation at $1700\times g$ for 10 minutes from 4 mL of blood collected in Vacuette® blood collection tubes (Greiner Bio-One, Kremsmünster, Austria). The samples of plasma and serum were stored at −80 °C until use.

4.3. Quantitative Measurement of microRNAs

Plasma levels of the selected 22 candidate miRNAs were quantified using a reverse transcription real-time polymerase chain reaction (RT real-time PCR). Exogenous cel-miR-39 was used as a spike-in control. Total RNA (including miRNA) was extracted using miRNeasy® Serum/Plasma Kit (Qiagen, Hilden, Germany) from 200 μL of blood plasma with 3.5 μL of a 1.6×10^8 copies/μL working solution of cel-miR-39 (Qiagen, Hilden, Germany). A quantitative estimation of selected miRNAs (Table 4) was performed by an RT real-time PCR method using TaqMan Advanced® miRNA Assays (Thermo Fisher Scientific, Foster City, CA, USA) in technical duplicates on a LightCycler® 96 System (Roche, Basel, Switzerland) according to the manufacturer's protocol (Catalog Number A25576, Publication Number 100027897, Revision C). The assays only target mature miRNAs, not their precursors.

Briefly, cDNA template preparation consisted of the following steps: a poly(A) tailing reaction, an adaptor ligation reaction, and a reverse transcription (RT) reaction using SuperScript III Reverse Transcriptase. Universal forward and reverse primers were then used in a miR-Amp reaction to increase the amount of cDNA. A total of 5 μL of diluted (1:10) cDNA template was mixed with 15 μL of PCR reaction mix containing reverse and forward primers and a TaqMan probe. The primer binding sites depended on

the target miRNA sequence and the TaqMan probe annealed specifically to a complementary sequence between the forward and reverse primer sites. The PCR thermal profile was started by 1 cycle of enzyme activation at a temperature of 90 °C for 20 s followed by 40 cycles at 95 °C for 1 s and 60 °C for 20 s.

Table 4. The analyzed microRNAs with miRBase 22 accession numbers, sequences, catalogue numbers, and references.

Symbol	miRBase 22 Accession Number	5'-3' sequence	Thermo Fisher Scientific Cat. # A25576	References [1]
hsa-miR-17-3p	MIMAT0000071	acugcagugaaggcacuuguag	477932_mir	[43,44]
hsa-miR-18a-5p	MIMAT0000072	uaaggugcaucuagugcagauag	478551_mir	[45,46]
hsa-miR-20a-5p	MIMAT0000075	uaaagugcuuauagugcagguag	478586_mir	[47]
hsa-miR-21-5p	MIMAT0000076	uagcuuaucagacugauguuga	477975_mir	[19,47–49]
hsa-miR-23a-3p	MIMAT0000078	aucacauugccagggauuuccc	478532_mir	[19,50]
hsa-miR-27a-3p	MIMAT0000084	uucacaguggcuaaguuccgc	478384_mir	[19]
hsa-miR-29a-3p	MIMAT0000086	uagcaccaucugaaaucgguua	478587_mir	[43,45]
hsa-miR-92a-3p	MIMAT0000092	uauugcacuugucccggccugu	477827_mir	[46,47,51]
hsa-miR-93-5p	MIMAT0000093	caaagugcuguucgugcagguag	478210_mir	[47]
hsa-miR-96-5p	MIMAT0000095	uuuggcacuagcacauuuuugcu	478215_mir	[52]
hsa-miR-106a-5p	MIMAT0000103	aaaagugcuuacagugcagguag	478225_mir	[44,46]
hsa-miR-141-3p	MIMAT0000432	uaacacugucugguaaagaugg	478501_mir	[48,52,53]
hsa-miR-142-5p	MIMAT0000433	cauaaaguagaaagcacuacu	477911_mir	[19]
hsa-miR-143-3p	MIMAT0000435	ugagaugaagcacuguagcuc	477912_mir	[44,46]
hsa-miR-155-5p	MIMAT0000646	uuaaugcuaaucgugauaggggu	477927_mir	[54,55]
hsa-miR-183-5p	MIMAT0000261	uauggcacugguagaauucacu	477937_mir	[56]
hsa-miR-199a-3p	MIMAT0000232	acaguagucugcacaugguua	477961_mir	[57]
hsa-miR-200b-3p	MIMAT0000318	uaauacugccugguaaugauga	477963_mir	[52]
hsa-miR-200c-3p	MIMAT0000617	uaauacugccggguaaugaugga	478351_mir	[52,55]
hsa-miR-210-3p	MIMAT0000267	cugugcgugugacagcggcuga	477970_mir	[55]
hsa-miR-223-3p	MIMAT0000280	ugucaguugucaaauacccca	477983_mir	[19,46,50,51]
hsa-miR-592	MIMAT0003260	uugugucaauaugcgaugaugu	479075_mir	[58]
cel-miR-39-3p [2]	MIMAT0000010	ucaccggguguaaaucagcuug	478293_mir	[21,59]

[1] Studies showing relation of particular miRNA to carcinogenesis. [2] Exogenous reference (spike-in control).

4.4. Processing of Real-Time PCR Data

Samples were assessed in technical duplicates. In cases where there was disagreement between results obtained from both technical duplicates, the sample assessment was repeated. To avoid plate-to-plate variation, inter-run calibrators (IRCs) were used [60]. Three samples assessed in the first run of the real-time PCR apparatus for assessment of each miRNA were used as IRCs. The samples used as IRCs were selected so that a range of obtained Ct values was covered. To obtain plasma levels of the miRNAs of interest, the ΔCt approach ($2^{-\Delta Ct}$ algorithm) was used. The results are presented as relative values calculated as $2^{-(Ct\ of\ miRNA\ of\ interest\ -\ Ct\ of\ normalizer)}$. From the available approaches for normalization [61], exogenous reference cel-miR-39 was used as a normalizer for circulating miRNAs [21,59].

4.5. Quantitative Measurement of CEA and CA19-9

Serum CEA and CA19-9 levels were determined using the ACCESS CEA and ACCESS CA19-9 chemiluminescent assay with the UniCel DxI 800 Instrument (Beckman Coulter, Brea, CA, USA).

4.6. Statistical Analysis

Statistical analysis was performed using the software SAS 9.3 (SAS Institute Inc., Cary, NC, USA). The statistical results of the comparison of preoperative and postoperative values were calculated by the Wilcoxon signed-rank test. A *p* value of ≤0.05 was considered to be statistically significant.

Prognostic significance was evaluated using the Kaplan–Meier method after finding an "optimal cut off" given by the lowest *p*-value of the logrank test for the examined markers. To evaluate the diagnostic ability of disease recurrence detection, sensitivities, specificities, positive predictive values, and negative predictive values were calculated on the basis of an individual cut-off value (defined in the Section 4.1). Receiver operating characteristic (ROC) curves were generated.

5. Conclusions

We observed prognostic significance of preoperative plasma levels of miR-20a, miR-23a, miR-210, and miR-223 in CRC patients. There was a decrease in plasma levels of these miRNAs after surgical removal of the tumor. The use of these miRNAs for early disease recurrence detection was affected by a low specificity in comparison with CEA and CA19-9. CEA and CA19-9 had high specificity but low sensitivity.

Conflicts of Interest: The authors declare no conflict of interest.

References

1. Bray, F.; Ferlay, J.; Soerjomataram, I.; Siegel, R.L.; Torre, L.A.; Jemal, A. Global cancer statistics 2018: Globocan estimates of incidence and mortality worldwide for 36 cancers in 185 countries. *CA Cancer J. Clin.* **2018**, *68*, 394–424. [CrossRef] [PubMed]

2. Hagan, S.; Orr, M.C.M.; Doyle, B. Targeted therapies in colorectal cancer-an integrative view by PPPM. *EPMA J.* **2013**, *4*, 3. [CrossRef] [PubMed]

3. Kalyan, A.; Kircher, S.; Shah, H.; Mulcahy, M.; Benson, A. Updates on immunotherapy for colorectal cancer. *J. Gastrointest. Oncol.* **2018**, *9*, 160–169. [CrossRef] [PubMed]

4. Wille-Jørgensen, P.; Syk, I.; Smedh, K.; Laurberg, S.; Nielsen, D.T.; Petersen, S.H.; Renehan, A.G.; Horváth-Puhó, E.; Påhlman, L.; Sørensen, H.T.; et al. Effect of more vs. less frequent follow-up testing on overall and colorectal cancer-specific mortality in patients with stage II or III colorectal cancer: The colofol randomized clinical trial. *Jama* **2018**, *319*, 2095–2103. [CrossRef] [PubMed]

5. Duffy, M.J.; van Dalen, A.; Haglund, C.; Hansson, L.; Holinski-Feder, E.; Klapdor, R.; Lamerz, R.; Peltomaki, P.; Sturgeon, C.; Topolcan, O. Tumour markers in colorectal cancer: European Group on Tumour Markers (EGTM) guidelines for clinical use. *Eur. J. Cancer* **2007**, *43*, 1348–1360. [CrossRef] [PubMed]

6. Locker, G.Y.; Hamilton, S.; Harris, J.; Jessup, J.M.; Kemeny, N.; Macdonald, J.S.; Somerfield, M.R.; Hayes, D.F.; Bast, R.C. ASCO 2006 update of recommendations for the use of tumor markers in gastrointestinal cancer. *J. Clin. Oncol.* **2006**, *24*, 5313–5327. [CrossRef]

7. Tan, E.; Gouvas, N.; Nicholls, R.J.; Ziprin, P.; Xynos, E.; Tekkis, P.P. Diagnostic precision of carcinoembryonic antigen in the detection of recurrence of colorectal cancer. *Surg. Oncol.* **2009**, *18*, 15–24. [CrossRef] [PubMed]

8. Park, I.J.; Choi, G.-S.; Lim, K.H.; Kang, B.M.; Jun, S.H. Serum carcinoembryonic antigen monitoring after curative resection for colorectal cancer: Clinical significance of the preoperative level. *Ann. Surg. Oncol.* **2009**, *16*, 3087–3093. [CrossRef]

9. Kawamura, Y.J.; Tokumitsu, A.; Mizokami, K.; Sasaki, J.; Tsujinaka, S.; Konishi, F. First alert for recurrence during follow-up after potentially curative resection for colorectal carcinoma: CA 19-9 should be included in surveillance programs. *Clin. Colorectal Cancer* **2010**, *9*, 48–51. [CrossRef]

10. Pan, C.; Yan, X.; Li, H.; Huang, L.; Yin, M.; Yang, Y.; Gao, R.; Hong, L.; Ma, Y.; Shi, C.; et al. Systematic literature review and clinical validation of circulating microRNAs as diagnostic biomarkers for colorectal cancer. *Oncotarget* **2017**, *8*, 68317–68328. [CrossRef]

11. Kozomara, A.; Birgaoanu, M.; Griffiths-Jones, S. miRBase: From microRNA sequences to function. *Nucleic Acids Res.* **2019**, *47*, D155–D162. [CrossRef] [PubMed]

12. Catalanotto, C.; Cogoni, C.; Zardo, G. MicroRNA in control of gene expression: An overview of nuclear functions. *Int. J. Mol. Sci.* **2016**, *17*, 1712. [CrossRef] [PubMed]

13. Aghdam, S.G.; Ebrazeh, M.; Hemmatzadeh, M.; Seyfizadeh, N.; Shabgah, A.G.; Azizi, G.; Ebrahimi, N.; Babaie, F.; Mohammadi, H. The role of microRNAs in prostate cancer migration, invasion, and metastasis. *J. Cell. Physiol.* **2019**, *234*, 9927–9942. [CrossRef]

14. Smid, D.; Kulda, V.; Srbecka, K.; Kubackova, D.; Dolezal, J.; Daum, O.; Kucera, R.; Topolcan, O.; Treska, V.; Skalicky, T.; et al. Tissue microRNAs as predictive markers for gastric cancer patients undergoing palliative chemotherapy. *Int. J. Oncol.* **2016**, *48*, 2693–2703. [CrossRef] [PubMed]

15. Pratap, P.; Raza, S.T.; Abbas, S.; Mahdi, F. MicroRNA-associated carcinogenesis in lung carcinoma. *J. Cancer Res. Ther.* **2018**, *14*, 249–254. [PubMed]

16. Guo, Y.; Bao, Y.; Yang, W. Regulatory miRNAs in colorectal carcinogenesis and metastasis. *Int. J. Mol. Sci.* **2017**, *18*, 890. [CrossRef] [PubMed]

17. Kulda, V.; Pesta, M.; Topolcan, O.; Liska, V.; Treska, V.; Sutnar, A.; Rupert, K.; Ludvikova, M.; Babuska, V.; Holubec, L.; et al. Relevance of miR-21 and miR-143 expression in tissue samples of colorectal carcinoma and its liver metastases. *Cancer Genet. Cytogenet.* **2010**, *200*, 154–160. [CrossRef]

18. Du, B.; Wu, D.; Yang, X.; Wang, T.; Shi, X.; Lv, Y.; Zhou, Z.; Liu, Q.; Zhang, W. The expression and significance of microRNA in different stages of colorectal cancer. *Medicine* **2018**, *97*, e9635. [CrossRef]

19. Vychytilova-Faltejskova, P.; Radova, L.; Sachlova, M.; Kosarova, Z.; Slaba, K.; Fabian, P.; Grolich, T.; Prochazka, V.; Kala, Z.; Svoboda, M.; et al. Serum-based microRNA signatures in early diagnosis and prognosis prediction of colon cancer. *Carcinogenesis* **2016**, *37*, 941–950. [CrossRef]

20. Fang, Z.; Tang, J.; Bai, Y.; Lin, H.; You, H.; Jin, H.; Lin, L.; You, P.; Li, J.; Dai, Z.; et al. Plasma levels of microRNA-24, microRNA-320a, and microRNA-423-5p are potential biomarkers for colorectal carcinoma. *J. Exp. Clin. Cancer Res.* **2015**, *34*, 86. [CrossRef]

21. Maierthaler, M.; Benner, A.; Hoffmeister, M.; Surowy, H.; Jansen, L.; Knebel, P.; Chang-Claude, J.; Brenner, H.; Burwinkel, B. Plasma miR-122 and miR-200 family are prognostic markers in colorectal cancer. *Int. J. Cancer* **2017**, *140*, 176–187. [CrossRef] [PubMed]

22. Ulivi, P.; Canale, M.; Passardi, A.; Marisi, G.; Valgiusti, M.; Frassineti, G.L.; Calistri, D.; Amadori, D.; Scarpi, E. Circulating plasma levels of miR-20b, miR-29b and miR-155 as predictors of bevacizumab efficacy in patients with metastatic colorectal cancer. *Int. J. Mol. Sci.* **2018**, *19*, 307. [CrossRef] [PubMed]

23. Nikolaou, S.; Qiu, S.; Fiorentino, F.; Rasheed, S.; Tekkis, P.; Kontovounisios, C. Systematic review of blood diagnostic markers in colorectal cancer. *Tech. Coloproctol.* **2018**, *22*, 481–498. [CrossRef] [PubMed]

24. Saito, G.; Sadahiro, S.; Kamata, H.; Miyakita, H.; Okada, K.; Tanaka, A.; Suzuki, T. Monitoring of serum carcinoembryonic antigen levels after curative resection of colon cancer: Cutoff values determined according to preoperative levels enhance the diagnostic accuracy for recurrence. *Oncology* **2017**, *92*, 276–282. [CrossRef] [PubMed]

25. Wang, J.; Wang, X.; Yu, F.; Chen, J.; Zhao, S.; Zhang, D.; Yu, Y.; Liu, X.; Tang, H.; Peng, Z. Combined detection of preoperative serum CEA, CA19-9 and CA242 improve prognostic prediction of surgically treated colorectal cancer patients. *Int. J. Clin. Exp. Pathol.* **2015**, *8*, 14853–14863. [PubMed]

26. Yang, S.-H.; Jiang, J.-K.; Chang, S.-C.; Juang, C.-J.; Lin, J.-K. Clinical significance of CA19-9 in the follow-up of colorectal cancer patients with elevated preoperative serum CA19-9. *Hepatogastroenterology* **2013**, *60*, 1021–1027. [PubMed]

27. Yong, F.L.; Law, C.W.; Wang, C.W. Potentiality of a triple microRNA classifier: miR-193a-3p, miR-23a and miR-338-5p for early detection of colorectal cancer. *BMC Cancer* **2013**, *13*, 280. [CrossRef] [PubMed]

28. Deng, Y.H.; Deng, Z.H.; Hao, H.; Wu, X.L.; Gao, H.; Tang, S.H.; Tang, H. MicroRNA-23a promotes colorectal cancer cell survival by targeting PDK4. *Exp. Cell Res.* **2018**, *373*, 171–179. [CrossRef]

29. Jin, F.; Yang, R.; Wei, Y.; Wang, D.; Zhu, Y.; Wang, X.; Lu, Y.; Wang, Y.; Zen, K.; Li, L. HIF-1α-induced miR-23a~27a~24 cluster promotes colorectal cancer progression via reprogramming metabolism. *Cancer Lett.* **2019**, *440–441*, 211–222. [CrossRef]

30. Wang, N.; Tan, H.-Y.; Feng, Y.-G.; Zhang, C.; Chen, F.; Feng, Y. microRNA-23a in human cancer: Its roles, mechanisms and therapeutic relevance. *Cancers* **2018**, *11*, 7. [CrossRef]

31. Earle, J.S.L.; Luthra, R.; Romans, A.; Abraham, R.; Ensor, J.; Yao, H.; Hamilton, S.R. Association of microRNA expression with microsatellite instability status in colorectal adenocarcinoma. *J. Mol. Diagn.* **2010**, *12*, 433–440. [CrossRef] [PubMed]

32. Zekri, A.-R.N.; Youssef, A.S.E.-D.; Lotfy, M.M.; Gabr, R.; Ahmed, O.S.; Nassar, A.; Hussein, N.; Omran, D.; Medhat, E.; Eid, S.; et al. Circulating serum miRNAs as diagnostic markers for colorectal cancer. *PLoS ONE* **2016**, *11*, e0154130. [CrossRef] [PubMed]

33. Ju, H.; Tan, J.-Y.; Cao, B.; Song, M.-Q.; Tian, Z.-B. Effects of miR-223 on colorectal cancer cell proliferation and apoptosis through regulating FoxO3a/BIM. *Eur. Rev. Med. Pharmacol. Sci.* **2018**, *22*, 3771–3778. [PubMed]

34. Li, Z.; Yang, Y.; Du, L.; Dong, Z.; Wang, L.; Zhang, X.; Zhou, X.; Zheng, G.; Qu, A.; Wang, C. Overexpression of miR-223 correlates with tumor metastasis and poor prognosis in patients with colorectal cancer. *Med. Oncol.* **2014**, *31*, 256. [CrossRef] [PubMed]

35. Zhang, H.; Li, P.; Ju, H.; Pesta, M.; Kulda, V.; Jin, W.; Cai, M.; Liu, C.; Wu, H.; Xu, J.; et al. Diagnostic and prognostic value of microRNA-21 in colorectal cancer: An original study and individual participant data meta-analysis. *Cancer Epidemiol. Biomark. Prev.* **2014**, *23*, 2783–2792. [CrossRef]

36. Guraya, S. Prognostic significance of circulating microRNA-21 expression in esophageal, pancreatic and colorectal cancers; a systematic review and meta-analysis. *Int. J. Surg.* **2018**, *60*, 41–47. [CrossRef] [PubMed]

37. Yang, Q.; Wang, S.; Huang, J.; Xia, C.; Jin, H.; Fan, Y. Serum miR-20a and miR-486 are potential biomarkers for discriminating colorectal neoplasia: A pilot study. *J. Cancer Res. Ther.* **2018**, *14*, 1572–1577.

38. Yamada, A.; Horimatsu, T.; Okugawa, Y.; Nishida, N.; Honjo, H.; Ida, H.; Kou, T.; Kusaka, T.; Sasaki, Y.; Yagi, M.; et al. Serum miR-21, miR-29a, and miR-125b are promising biomarkers for the early detection of colorectal neoplasia. *Clin. Cancer Res.* **2015**, *21*, 4234–4242. [CrossRef]

39. Li, X.; Wei, Y.; Wang, Z. microRNA-21 and hypertension. *Hypertens. Res.* **2018**, *41*, 649–661. [CrossRef]

40. Tay, Y.; Rinn, J.; Pandolfi, P.P. The multilayered complexity of ceRNA crosstalk and competition. *Nature* **2014**, *505*, 344–352. [CrossRef]

41. Sobin, L.; Gospodarowicz, M.; Wittekind, C. *TNM Classification of Malignant Tumours*, 7th ed.; Wiley-Blackwell: New York, NY, USA, 2009.

42. Schwartz, L.H.; Litière, S.; de Vries, E.; Ford, R.; Gwyther, S.; Mandrekar, S.; Shankar, L.; Bogaerts, J.; Chen, A.; Dancey, J.; et al. RECIST 1.1-Update and clarification: From the RECIST committee. *Eur. J. Cancer* **2016**, *62*, 132–137. [CrossRef] [PubMed]

43. Faltejskova, P.; Bocanek, O.; Sachlova, M.; Svoboda, M.; Kiss, I.; Vyzula, R.; Slaby, O. Circulating miR-17-3p, miR-29a, miR-92a and miR-135b in serum: Evidence against their usage as biomarkers in colorectal cancer. *Cancer Biomark. Sect. Dis. Markers* **2012**, *12*, 199–204. [CrossRef] [PubMed]

44. Li, J.; Liu, Y.; Wang, C.; Deng, T.; Liang, H.; Wang, Y.; Huang, D.; Fan, Q.; Wang, X.; Ning, T.; et al. Serum miRNA expression profile as a prognostic biomarker of stage II/III colorectal adenocarcinoma. *Sci. Rep.* **2015**, *5*, 12921. [CrossRef] [PubMed]

45. Brunet Vega, A.; Pericay, C.; Moya, I.; Ferrer, A.; Dotor, E.; Pisa, A.; Casalots, À.; Serra-Aracil, X.; Oliva, J.-C.; Ruiz, A.; et al. microRNA expression profile in stage III colorectal cancer: Circulating miR-18a and miR-29a as promising biomarkers. *Oncol. Rep.* **2013**, *30*, 320–326. [CrossRef] [PubMed]

46. Ristau, J.; Staffa, J.; Schrotz-King, P.; Gigic, B.; Makar, K.W.; Hoffmeister, M.; Brenner, H.; Ulrich, A.; Schneider, M.; Ulrich, C.M.; et al. Suitability of circulating miRNAs as potential prognostic markers in colorectal cancer. *Cancer Epidemiol. Biomark. Prev.* **2014**, *23*, 2632–2637. [CrossRef]

47. Pellatt, D.F.; Stevens, J.R.; Wolff, R.K.; Mullany, L.E.; Herrick, J.S.; Samowitz, W.; Slattery, M.L. Expression profiles of miRNA subsets distinguish human colorectal carcinoma and normal colonic mucosa. *Clin. Transl. Gastroenterol.* **2016**, *7*, e152. [CrossRef] [PubMed]

48. Yin, J.; Bai, Z.; Song, J.; Yang, Y.; Wang, J.; Han, W.; Zhang, J.; Meng, H.; Ma, X.; Yang, Y.; et al. Differential expression of serum miR-126, miR-141 and miR-21 as novel biomarkers for early detection of liver metastasis in colorectal cancer. *Chin. J. Cancer Res.* **2014**, *26*, 95–103.

49. Toiyama, Y.; Takahashi, M.; Hur, K.; Nagasaka, T.; Tanaka, K.; Inoue, Y.; Kusunoki, M.; Boland, C.R.; Goel, A. Serum miR-21 as a diagnostic and prognostic biomarker in colorectal cancer. *J. Natl. Cancer Inst.* **2013**, *105*, 849–859. [CrossRef]

50. Ogata-Kawata, H.; Izumiya, M.; Kurioka, D.; Honma, Y.; Yamada, Y.; Furuta, K.; Gunji, T.; Ohta, H.; Okamoto, H.; Sonoda, H.; et al. Circulating exosomal microRNAs as biomarkers of colon cancer. *PLoS ONE* **2014**, *9*, e92921. [CrossRef]

51. Zheng, G.; Du, L.; Yang, X.; Zhang, X.; Wang, L.; Yang, Y.; Li, J.; Wang, C. Serum microRNA panel as biomarkers for early diagnosis of colorectal adenocarcinoma. *Br. J. Cancer* **2014**, *111*, 1985–1992. [CrossRef]

52. Sun, Y.; Liu, Y.; Cogdell, D.; Calin, G.A.; Sun, B.; Kopetz, S.; Hamilton, S.R.; Zhang, W. Examining plasma microRNA markers for colorectal cancer at different stages. *Oncotarget* **2016**, *7*, 11434–11449. [CrossRef] [PubMed]

53. Yang, I.-P.; Tsai, H.-L.; Miao, Z.-F.; Huang, C.-W.; Kuo, C.-H.; Wu, J.-Y.; Wang, W.-M.; Juo, S.-H.H.; Wang, J.-Y. Development of a deregulating microRNA panel for the detection of early relapse in postoperative colorectal cancer patients. *J. Transl. Med.* **2016**, *14*, 108. [CrossRef] [PubMed]

54. Hongliang, C.; Shaojun, H.; Aihua, L.; Hua, J. Correlation between expression of miR-155 in colon cancer and serum carcinoembryonic antigen level and its contribution to recurrence and metastasis forecast. *Saudi Med. J.* **2014**, *35*, 547–553. [PubMed]

55. Chen, J.; Wang, W.; Zhang, Y.; Chen, Y.; Hu, T. Predicting distant metastasis and chemoresistance using plasma miRNAs. *Med. Oncol.* **2014**, *31*, 799. [CrossRef] [PubMed]

56. Yuan, D.; Li, K.; Zhu, K.; Yan, R.; Dang, C. Plasma miR-183 predicts recurrence and prognosis in patients with colorectal cancer. *Cancer Biol. Ther.* **2015**, *16*, 268–275. [CrossRef]

57. Nonaka, R.; Nishimura, J.; Kagawa, Y.; Osawa, H.; Hasegawa, J.; Murata, K.; Okamura, S.; Ota, H.; Uemura, M.; Hata, T.; et al. Circulating miR-199a-3p as a novel serum biomarker for colorectal cancer. *Oncol. Rep.* **2014**, *32*, 2354–2358. [CrossRef] [PubMed]

58. Liu, M.; Zhi, Q.; Wang, W.; Zhang, Q.; Fang, T.; Ma, Q. Up-regulation of miR-592 correlates with tumor progression and poor prognosis in patients with colorectal cancer. *Biomed. Pharmacother.* **2015**, *69*, 214–220. [CrossRef] [PubMed]

59. Kroh, E.M.; Parkin, R.K.; Mitchell, P.S.; Tewari, M. Analysis of circulating microRNA biomarkers in plasma and serum using quantitative reverse transcription-PCR (qRT-PCR). *Methods* **2010**, *50*, 298–301. [CrossRef] [PubMed]

60. Hellemans, J.; Mortier, G.; De Paepe, A.; Speleman, F.; Vandesompele, J. qBase relative quantification framework and software for management and automated analysis of real-time quantitative PCR data. *Genome Biol.* **2007**, *8*, R19. [CrossRef] [PubMed]

61. Schwarzenbach, H.; da Silva, A.M.; Calin, G.; Pantel, K. Data normalization strategies for MicroRNA quantification. *Clin. Chem.* **2015**, *61*, 1333–1342. [CrossRef]

PŘÍLOHA 6

cancers

Article

The Level of Preoperative Plasma KRAS Mutations and CEA Predict Survival of Patients Undergoing Surgery for Colorectal Cancer Liver Metastases

Jiri Polivka [1,2,†], **Jindra Windrichova** [2,†] , **Martin Pesta** [2,3,*,†], **Katerina Houfkova** [3], **Hana Rezackova** [2], **Tereza Macanova** [3], **Ondrej Vycital** [4], **Radek Kucera** [2] , **David Slouka** [2] and **Ondrej Topolcan** [2]

1   Department of Histology and Embryology and Biomedical Center, Faculty of Medicine in Pilsen, Charles University, Karlovarska 48, 30166 Pilsen, Czech Republic; jiri.polivka2@lfp.cuni.cz
2   Laboratory of Immunoanalysis, University Hospital in Pilsen, E. Benese 13, 30599 Pilsen, Czech Republic; windrichovaj@fnplzen.cz (J.W.); rezackovah@fnplzen.cz (H.R.); kucerar@fnplzen.cz (R.K.); slouka@fnplzen.cz (D.S.); topolcan@fnplzen.cz (O.T.)
3   Department of Biology, Faculty of Medicine in Pilsen, Charles University, alej Svobody 76, 32300 Pilsen, Czech Republic; katerina.houfkova@lfp.cuni.cz (K.H.); tereza.macanova@lfp.cuni.cz (T.M.)
4   Department of Surgery, University Hospital in Pilsen, E. Beneše 13, 30599 Pilsen, Czech Republic; vycitalo@fnplzen.cz
*   Correspondence: martin.pesta@lfp.cuni.cz; Tel.: +420-377-593-261
†   These authors contributed equally to this work.

Abstract: Colorectal cancer (CRC) belongs to the most common cancers. The liver is a predominant site of CRC dissemination. Novel biomarkers for predicting the survival of CRC patients with liver metastases (CLM) undergoing metastasectomy are needed. We examined KRAS mutated circulating cell-free tumor DNA (ctDNA) in CLM patients as a prognostic biomarker, independently or in combination with carcinoembryonic antigen (CEA). Thereby, a total of 71 CLM were retrospectively analyzed. Seven KRAS G12/G13 mutations was analyzed by a ddPCR™ KRAS G12/G13 Screening Kit on QX200 Droplet Digital PCR System (Bio-Rad Laboratories, Hercules, CA, USA) in liver metastasis tissue and preoperative and postoperative plasma samples. CEA were determined by an ACCESS CEA assay with the UniCel DxI 800 Instrument (Beckman Coulter, Brea, CA, USA). Tissue KRAS positive liver metastases was detected in 33 of 69 patients (47.8%). Preoperative plasma samples were available in 30 patients and 11 (36.7%) were KRAS positive. The agreement between plasma- and tissue-based KRAS mutation status was 75.9% (22 in 29; kappa 0.529). Patients with high compared to low levels of preoperative plasma KRAS fractional abundance (cut-off 3.33%) experienced shorter overall survival (OS 647 vs. 1392 days, *p* = 0.003). The combination of high preoperative KRAS fractional abundance and high CEA (cut-off 3.33% and 4.9 µg/L, resp.) best predicted shorter OS (HR 13.638, 95%CI 1.567–118.725) in multivariate analysis also (OS HR 44.877, 95%CI 1.59–1266.479; covariates: extend of liver resection, biological treatment). KRAS mutations are detectable and quantifiable in preoperative plasma cell-free DNA, incompletely overlapping with tissue biopsy. KRAS mutated ctDNA is a prognostic factor for CLM patients undergoing liver metastasectomy. The best prognostic value can be reached by a combination of ctDNA and tumor marker CEA.

Keywords: colorectal cancer; liver metastasis; circulating tumor DNA; cell-free DNA; ctDNA; CEA; liquid biopsy

---

1. Introduction

Colorectal cancer (CRC) belongs to the most common cancers with more than 1.8 million new cases worldwide per year [1]. Moreover CRC accounts for 9% of all cancer-related deaths. Colorectal cancer liver metastases (CLM) are the predominant distant recurrence developing in 25–30% of CRC patients [2,3]. Liver metastasectomy provides potentially curative treatment for those affected by CLM with a five-year survival up to 47–60% [2,4]. However, recurrences occur in 40–75% of patients after liver surgery. Therefore, effective biomarkers predicting patients' survival and disease relapse in this specific clinical scenario are urgently needed. Accurate prognosis assessment will help in deciding on an appropriate treatment or facilitate the possible inclusion of patients in any of the ongoing studies.

Once the presence of circulating acids (circulating cell-free DNA- cfDNA and non-coding RNAs) in body fluids was observed, these molecules attracted interest of cancer research. The benefit of detection of cell-free DNA in plasma or serum of cancer patients is to gain the knowledge about the presence of mutations typical for tumor tissue and so to get minimally invasive diagnostic, prognostic and predictive tool. From a clinical practice perspective, it makes sense to detect the most common mutations (circulating cell-free tumor DNA- ctDNA) for a given oncological disease (diagnostic, prognostic) or mutations that can help in the prediction of treatment.

Carcinogenic Kirsten rat sarcoma viral oncogene homolog (KRAS) is the most frequently mutated proto-oncogene in CRC. Up to 45% of CRC comprise KRAS mutations. KRAS encodes a 21 kDa a membrane-bound small GTPase and is a member of the Ras oncogene family includes also HRAS and NRAS proto-oncogenes. KRAS is located at short arm of chromosome 12 (12p12.1), spans approximately 38 kb and the most frequent mutations in this gene, point substitutions in codons 12 and 13 [5,6]. Oncoprotein KRAS aberrantly activate RAS/MAPK pathway and thus contributes to cell cycle deregulation [7].

Mutated RAS genes were the first tumor specific gene sequences detected in the blood from patients with cancer [8,9]. For the first time the presence of mutated KRAS2 sequences was detected in the blood of patients with pancreatic cancer in 1994 by Sorenson et al. [10]. Since 2000, a number of studies have been published to test the predictive importance of mutations in the KRAS oncogene for low molecular weight inhibitor and biological therapy. Now is established that KRAS mutations together with mutations in another proto-oncogene NRAS (exons 2, 3, and 4) are predicting the lack of treatment efficacy of anti-epidermal growth factor receptor (EGFR) monoclonal antibodies (mAb) cetuximab and panitumumab [11–14]. The US and European clinical practice guidelines involve indications for RAS testing (KRAS and NRAS mutations) before the use of anti-EGFR agents [15,16]. The standard techniques evaluating KRAS mutation status for the decision about anti-EGFR mAb therapy are based on formalin-fixed, paraffin-embedded (FFPE) specimens of tumor tissue obtained during surgery (tissue biopsy). As an alternative, recently developed methods for so-called liquid biopsy analyzing circulating tumor DNA (ctDNA) from peripheral blood can provide a rapid KRAS genotyping that is relatively non-invasive and with a minimal risk of complications compared to tissue biopsy [17,18]. Studies show that blood detected mutated RAS gene bears prognostic value in primary and metastatic colorectal cancer [19–28]. At present, the possibility of identification of mutated KRAS oncogene in ctDNA is extended by determining its exact amount at very low level (for example by the ddPCR technique) and thus the relationship of the mutated KRAS levels to the clinical pathological characteristics of the disease can be examined.

Recent studies have indicated that combining multiple markers may improve the accuracy of diagnostic and assessment of the prognosis [29]. In accordance with this idea, we also combined the plasma ctDNA KRAS marker with routinely used tumor marker in gastrointestinal cancers-carcinoembryonic antigen (CEA). The carcinoembryonic antigen (CEA, CEACAM5, and CD66e) is a 180-kDa N-linked glycoprotein that is not normally produced in significant quantities after birth (<0.49 ng/mL in the blood of healthy adults) but is aberrantly over-expressed by epithelial cancers including cancers of the gastrointestinal tract, breast, lung, ovary and pancreas [30–32]. CEA is the prototypic member of a family of highly related cell surface glycoproteins that includes

12 carcinoembryonic antigen-related cell adhesion molecules (CEACAMs). CEA and CEACAM-1 are integral components of the apical glycocalyx human colonic epithelium [33]. However, a mechanistic role for soluble CEA in tumor progression and metastasis remains to be established [32]. CEA is the biochemical gold standard for early detection of cancer recurrence, recommended by both the American Society of Clinical Oncology (ASCO) and the European Group on Tumor Markers (EGTM) [34]. This marker is also one of the most commonly used prognostic factors for CRC [35]. However, the sensitivity of CEA is not considered to be sufficient [36]. Plasma concentration is not consistently elevated in colorectal cancer and may be undetectable or present at only low levels with poorly differentiated tumors [37]. At the most commonly reported CEA threshold of 5 μg/L shows to detect colorectal cancer recurrence the sensitivity 71% and the specificity 88% [38].

In this study, we evaluated the concordance and prognostic value KRAS mutations in ctDNA-based liquid biopsy compared to FFPE-based tissue biopsy of primary CRC and corresponding CLM assessed by droplet digital PCR methodic (ddPCR). Therefore, to establish the possibility of using plasma levels of mutated KRAS ctDNA as a supplement or replacement for FFPE tissue (biopsies) for prediction of treatment in cases where tissue is not available. We assessed the possibility for the quantification of KRAS mutant alleles in ctDNA to serve as an independent prognostic factor for patients undergoing surgery for liver metastases. The possible synergic prognostic value of combination of KRAS ctDNA-based liquid biopsy with the conventional CRC biomarker-carcinoembryonic antigen (CEA) was also evaluated.

2. Results

2.1. The Presence and the Level of KRAS Mutations in Tissue of Primary Tumor and Liver Metastases

KRAS status in the tumor tissue of primary colorectal cancer (CRC) was available in 63 pts. Tissue KRAS positivity (tKRAS+) was detected in 33 of 63 cases (52.4%). The median tissue KRAS fractional abundance (tFA; proportion of the mutant allele in FFPE total DNA) was 15.66% ranging from minimum 0% up to maximum 49.31%. In colorectal cancer liver metastases (CLM), KRAS status was available in 69 patients. tKRAS+ was found in 33 of 69 cases (47.8%). The median tFA for all patients was 0% ranging from minimum 0% up to maximum 79.95%. The median tFA for 33 KRAS positive patients only was 27.3% (minimum 11.06%, maximum 49.31%).

The overall percentage agreement between primary CRC and CLM tissue KRAS mutation status (i.e., positive or negative) was 93.4% (57/61; kappa, 0.529 ($p = 0.002$)). In contrast, four samples (6.6%) experienced discordant status (Table 1). The KRAS fraction abundance positively correlated between primary tumor tissue and liver metastases samples (R = 0.8, $p < 0.001$, $n = 61$).

Table 1. The concordance between tissue KRAS status (KRAS positive vs. KRAS negative) in primary tumor (CRC) and liver metastases (CLM).

Tissue Origin		CRC	
	KRAS Status	KRAS Negative	KRAS Positive
CLM	KRAS negative	28	3
	KRAS positive	1	29

2.2. The Presence and the Level of KRAS Mutations in Plasma

The plasma samples obtained before primary CRC surgery were available in 7 patients. Plasma KRAS positivity (pKRAS+) was detected in three of seven samples (42.9%). The median plasma KRAS fractional abundance (pFA) was 0% ranging from minimum 0% up to maximum 42.26%. The median pFA for three pKRAS+ patients only was 1.37%. The corresponding plasma samples after CRC surgery were available for four patients. For three of them, negative preoperative pKRAS remained negative after the surgery as well. One patient experienced decrease of pFA following primary tumor

resection (from 42.26% preoperative to 22.85% postoperative, resp.). Both tissue and preoperative plasma samples were available in seven patients. The concordant KRAS status in CRC tissue and plasma samples was found in six of seven patients (85.7%), whereas one patient (14.3%) experienced discordant status.

Before surgery for colorectal cancer liver metastases, preoperative plasma samples were available in 30 patients. Eleven (36.7%) of them were plasma KRAS positive (pKRAS+). The overall percentage agreement of preoperative plasma KRAS status (i.e., positive or negative) between CRC and CLM in the same patient was 80% (4 in 5; kappa, 0.545 (p = 0.171)). The median pFA was 0% ranging from minimum 0% up to maximum 48%. The median pFA for 11 pKRAS+ patients only was 3.33% (min. 1.35%, max. 48%). The KRAS fraction abundance positively correlated between preoperative plasma samples and tissue samples of liver metastases (R = 0.649, p < 0.001, n = 29). Preoperative KRAS fraction abundance did not correlate with a number of liver metastases (R = 0.117, p = 0.536) or the extent of liver metastases (R = −0.17, p = 0.37).

Both pre- and post-operative plasma samples were available in 17 pts. Of them, 12 preoperative pKRAS negative remained negative after surgery, whereas five preoperative pKRAS+ became negative. Therefore, all patients with available plasma samples were pKRAS negative after liver surgery (Figure 1).
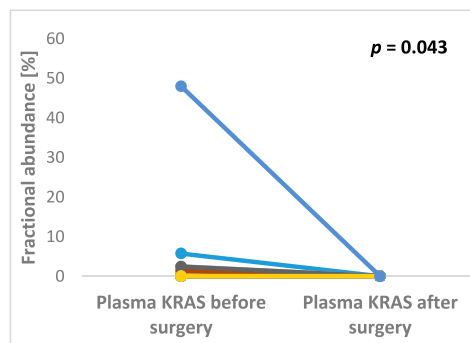

Figure 1. Significant changes in KRAS fractional abundance between pre- and post-operative plasma samples in patients undergoing surgery for colorectal cancer liver metastases (p = 0.043).

Both tissue and plasma samples were available for 29 pts. Of them, pKRAS+ was detected in 10 of 16 tKRAS+ patients (62.5%), whereas 12 of 13 tKRAS negative patients were pKRAS negative (92.3%) (Table 2). The overall percentage agreement between plasma-based and tissue-based KRAS mutation status was 75.9% (22 in 29; kappa, 0.529 (p = 0.002)).

Table 2. The concordance between tissue KRAS status (KRAS positive vs. KRAS negative) in colorectal cancer liver metastases (CLM) and preoperative plasma samples (Plasma).

Tissue vs. Plasma Origin	CLM Tissue		
	KRAS Status	**KRAS Negative**	**KRAS Positive**
Plasma	**KRAS negative**	12	6
	KRAS positive	1	10

2.3. The Preoperative and Postoperative Serum Level of CEA in Patients Undergoing Liver Surgery

The preoperative serum level of CEA was available in 29 patients. The median preoperative CEA level was 11.9 µg/L ranging from minimum 0.8 up to maximum 945.4 µg/L. CEA after liver surgery was available in 17 patients. The median postoperative CEA level was 4.2 µg/L ranging from minimum

0.5 up to maximum 96.5 μg/L. Both pre- and postoperative levels of CEA were available in 16 patients. All of these patients experienced decrease of CEA level after liver surgery with the maximum fold change 43.3 (Figure 2).
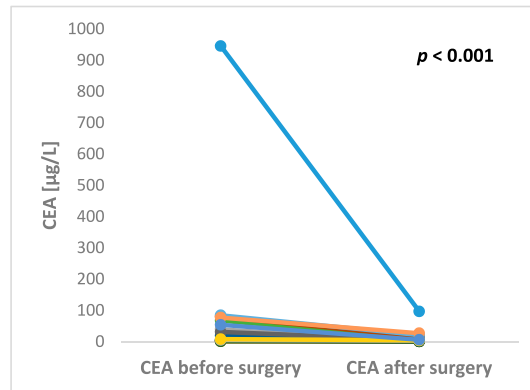

Figure 2. Significant changes in CEA levels between pre- and post-operative blood samples in patients undergoing surgery for colorectal cancer liver metastases ($p < 0.001$).

2.4. Survival Analysis

The median distant metastasis free survival (DMFS) after the surgery of primary tumor was 210 days. The median disease-free survival (DFS) and overall survival (OS) after liver surgery was 423 and 1269 days, respectively. Both the patients with KRAS positive vs. KRAS negative primary tumor tissue experienced similar DMFS (median 210 vs. 186 days, $p = 0.215$). Similarly, there were no differences in DFS (median 475 vs. 357 days, $p = 0.245$) and OS (median 1368 vs. 1230 days, $p = 0.783$) after liver surgery between patients with KRAS positive and negative liver metastasis. The percentage increment of KRAS fractional abundance in primary tumor tissue (tFA) did not influence patients´ DMFS (HR 0.989, $p = 0.185$). Similarly, liver metastasis KRAS tFA did not influence DFS (HR = 1, $p = 0.962$) or OS (HR = 1, $p = 0.968$) after liver surgery. The analysis of the prognostic impact of the other clinicopathological factors showed that patients´ DFS was not affected by tumor grade (grade 2 vs. 1 HR = 1.099, $p = 0.78$; grade 3 vs. 1 HR = 0.737, $p = 0.593$), number of liver metastases (≥2 vs. 1 HR = 1.378, $p = 0.209$), extent of liver metastases (increment in size HR = 0.998, $p = 0.727$), extrahepatic disease (present vs. absent HR = 0.85, $p = 0.756$). Similarly there were no differences in OS in relation to tumor grade (grade 2 vs. 1 HR = 0.602, $p = 0.399$; grade 3 vs. 1 HR = 0.807, $p = 0.703$), number of liver metastases (≥2 vs. 1 HR = 1.184, $p = 0.545$), extent of liver metastases (increment in size HR = 1.004, $p = 0.548$), extrahepatic disease (present vs. absent HR = 1.253, $p = 0.668$).

There was a trend to shorter DFS (median 357 vs. 470 days, $p = 0.074$) (Figure 3) after liver surgery in patients with KRAS positive vs. negative preoperative plasma samples, but not OS (median 1269 vs. 1390 days, $p = 0.234$).
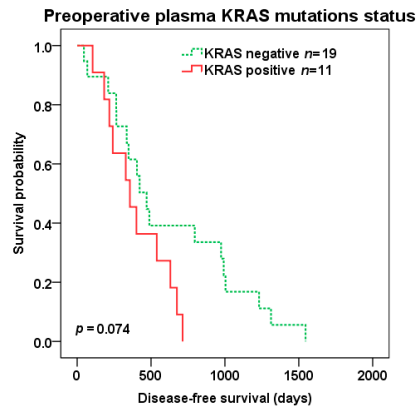
Figure 3. Disease-free survival (DFS) after liver surgery in patients with KRAS positive (red color) vs. negative (green color dotted line) pre-operative plasma samples.

On contrary, percentage increment in preoperative plasma KRAS fractional abundance (pFA) predicted shorter OS (HR 1.04, *p* = 0.049) and trend to shorter DFS (HR 1.037, *p* = 0.073) after liver surgery. Importantly, preoperative pFA were independent predictor for DFS (HR 1.044, *p* = 0.041) and OS (HR 1.05, *p* = 0.021) in multivariate analysis including other covariates (also including parameters: extend of liver resection and presence of biological treatment).

Patients with high compared to low level of preoperative KRAS pFA (cut-off 3.33%) experienced shorter OS (647 vs. 1392 days, *p* = 0.003; HR 4.391, 95%CI 1.529–12.614) (Figure 4), but not DFS (*p* = 0.118). Among 11 pKRAS+ patients, a high level of preoperative pFA (cut-off 3.33%) also predicted shorter OS (647 vs. 1459 days, *p* = 0.009; HR 10.733, 95%CI 1.236–93.24), but not DFS (*p* = 0.3).

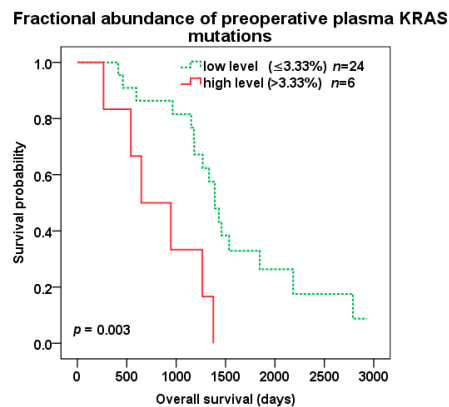**Figure 4.** Overall survival (OS) after liver surgery for all patients with low (green color dotted line) vs. high (red color) KRAS fractional abundance in pre-operative plasma samples (cut-off 3.33%).

In patients treated for CLM, a high level of preoperative KRAS pFA (cut-off 3.33%) remained an independent negative prognostic factor for OS after liver surgery also in multivariate analysis (Table 3).

Table 3. The multivariate analysis of disease free survival (DFS) and overall survival (OS) of patients undergoing liver surgery.

The Multivariate Survival Analysis	DFS		OS	
Status of Biomarkers and Clinical Characteristics	HR (95% Confidence Interval)	Significance	HR (95% Confidence Interval)	Significance
Plasma KRAS fractional abundance [cut-off 3.33%]				
Low level	1.000		1.000	
High level	2.542 (0.823–7.853)	*p* = 0.105	11.732 (2.729–50.432)	***p*= 0.001**
CEA [cut-off 4.9 μg/L]				
Low level	1.000		1.000	
High level	3.264 (1.119–9.521)	***p*= 0.03**	5.409 (1.272–22.998)	***p*= 0.022**
Extend of liver resection				
R0	1.000		1.000	
R1	3.309 (1.09–10.045)	***p*= 0.035**	6.054 (1.499–24.451)	***p*= 0.011**
RFA [1]	2.895 (0.891–9.406)	*p* = 0.077	7.368 (1.479–36.7)	***p*= 0.015**
Biological treatment				
bevacizumab or cetuximab	1.000		1.000	
n.a.	1.546 (0.633–3.774)	*p* = 0.339	0.828 (0.326–2.104)	*p* = 0.692

[1] Radiofrequency ablation.

Patients positive for KRAS mutations in both tissue of liver metastasis and preoperative plasma samples (tKRAS+/pKRAS+, *n* = 10) compared to patients with tissue KRAS positivity only (tKRAS+/pKRAS-, *n* = 6) showed shorter DFS (329 vs. 470 days, *p* = 0.051) (Figure 5), but not OS (*p* = 0.328).
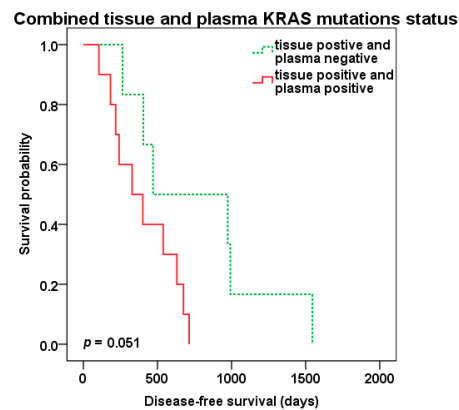
Figure 5. Disease-free survival (DFS) after liver surgery in patients with combined KRAS liver metastasis tissue and preoperative plasma positivity (red color) vs. tissue positivity only (green color dotted line).

Patients with high compared to low preoperative CEA level (cut-off 4.9 μg/L) experienced trend to shorter DFS (401 vs. 796 days, $p = 0.066$) (Figure 6) as well as OS (1265 vs. 1846 days, $p = 0.052$) (Figure 7) after liver surgery.
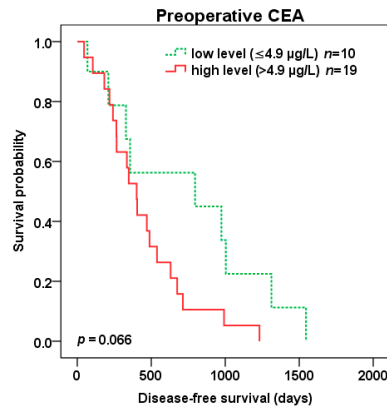

Figure 6. Disease-free survival (DFS) after liver surgery for patients with low (green color dotted line) vs. high (red color) preoperative CEA level (cut-off 4.9 μg/L).

Figure 7. Overall survival (OS) after liver surgery for patients with low (green color dotted line) vs. high (red color) preoperative CEA level (cut-off 4.9 μg/L).

The best predictive value of patient survival after liver surgery was observed with combination of preoperative KRAS pFA and CEA level of CLM patients. Patients with both high pFA and CEA preoperative levels (cut-off 3.33% and 4.9 μg/L, resp.) experienced the worst survival compared to those with combined low pFA and CEA levels and the best OS (647 vs. 1846 days, $p = 0.003$; HR 13.638 95%CI 1.567–118.725) (Figure 8). There was trend to better DFS ($p = 0.079$) for combined low levels of KRAS pFA and CEA as well (Figure 9). Patients with both high levels of preoperative KRAS pFA and CEA showed also the worst OS (HR 44.877 95%CI 1.590–1266.479) in multivariate analysis including other covariates (extend of liver resection, presence of biological treatment).
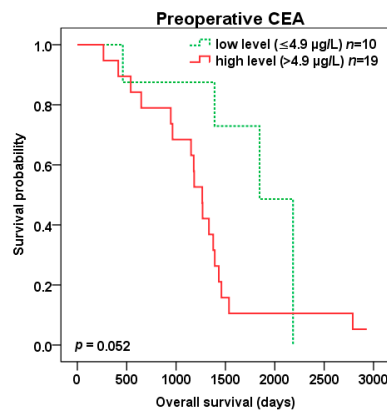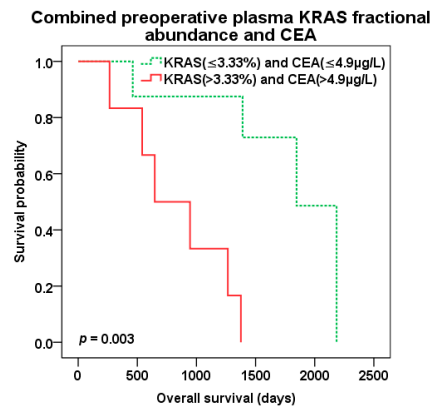
Figure 8. Overall survival (OS) after liver surgery for patients with combined low (green color dotted line) vs. high (red color) preoperative KRAS pFA and CEA levels (cut-off 3.33% and 4.9 µg/L, resp.).
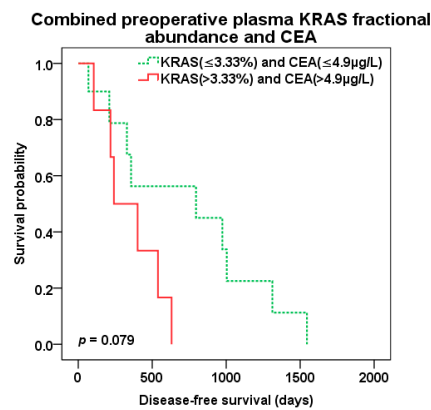

Figure 9. Disease-free survival (DFS) after liver surgery for patients with combined low (green color dotted line) vs. high (red color) preoperative KRAS pFA and CEA levels (cut-off 3.33% and 4.9 µg/L, resp.).

3. Discussion

In the last two decades, we have witnessed an ever-increasing number of modalities of cancer treatment, including a growing spectrum of biological drugs and low molecular weight inhibitor drugs used for targeted treatment of cancer patients. At present, the correct choice of treatment depends also on the determination of prognostic and predictive biomarkers. The ability to respond in the case of recurrence/progression of the disease by changing cancer treatment carries with the need for real-time knowledge of the changes in the genotype of the tumor. This is where the liquid biopsy approach turns out to be very suitable for the patient, compensating in certain cases for the unavailability of the tumor tissue (biopsy, FFPE) and also allowing easy repeated peripheral blood sampling and the analysis of molecules with an assumed origin in the tumor tissue.

Moreover, the liquid biopsy approach overcomes to some extent the problem of tumor heterogeneity that complicates the traditional histopathological examinations. Hand in hand with the development of treatment modalities, more sensitive methods of detection of biomarkers (DNA mutations (ctDNA), oncoproteins and circulating tumor cells (CTC)) are becoming available, on the basis of which it is possible to determine prognosis or decide on an appropriate treatment. The decline in prices for

individual determinations is also favorable, especially in the area of DNA analysis. The ddPCR method provides a sensitive quantitative determination of the genotypes of genes, enabling the determination of mutated DNA on the background of the wild-type majority.

This takes the possibilities of the liquid biopsy approach, specifically of the analysis of the mutated DNA released by the tumor tissue, a step further and allows not only the determination of low ctDNA levels but also the choice of a suitable cut-off for further categorization of cancer patients and a correct assessment of the relationship between the tumor tissue genotype and the phenotype, i.e., the character and extent of the oncological disease. It turns out that different biomarkers, in which a significant relationship to the clinicopathological characteristics of the tumor was found, do not characterize the same properties of the tumor. Therefore a combination of biomarkers based on different processes of the molecular biology of the tumor (protein, miRNA, DNA genotype) may be appropriate, especially for determining the prognosis. In this study, we decided to implement this approach.

The aim of the study was to determining concordance and prognostic significance of level of the KRAS mutations, to establish the possibility of using plasma levels of mutated KRAS ctDNA as a replacement for FFPE tissue for prediction of treatment in cases where FFPE tissue is not available. We used preoperative and postoperative plasma samples of patients treated for primary colorectal carcinoma and then it's liver metastases and the corresponding FFPE tissue samples together with long-term clinical data for determining of the prognostic significance of mutated KRAS level determined by the ddPCR method even in combination with routinely determined tumor marker CEA.

In patients with primary colorectal cancer, we detected KRAS mutation in the tissue in 54% of cases, in liver metastases of these patients it was 47.8% of cases. This corresponds to the upper limit given for larger sample sets [39]. The concordant mutation status between the primary carcinoma and liver metastasis was found in the majority of patients (93.4%). In three patients (9.375%) with primary cancer positivity, no mutation of the KRAS oncogene was observed in the metastasis, the opposite in one patient (7.69%).

It makes sense to discuss the concordance, due to the number of samples, between the presence of a mutation in the KRAS oncogene in liver metastasis tissue and the plasma of a preoperative sample of liver metastases only. The overall percentage agreement between plasma-based and tissue-based KRAS mutation status was 75.9%. Several previous studies evaluated the concordance of KRAS alterations between tissue and ctDNA and found overall concordance to range 67–96% [40]. We also evaluated the relationship between the levels of KRAS mutated fraction of ctDNA and the levels of determined mutations in liver metastasis tissue. The KRAS fraction abundance positively correlated (R = 0.649) between preoperative plasma samples and tissue samples of liver metastases. These results indicate the limits of liquid biopsy as a substitute to tissue biopsy KRAS mutations analysis for treatment prediction. At the same time, this indicate that the results of plasma vs. tissue assays provide different insights into the biology of tumor behavior, discussed below. KRAS mutation in plasma disappeared after removal of metastases in all patients where the assessment was available. It is possible due to relatively short half-life time of DNA in plasma ranging from 15 min to several hours. It also points to the possibility of minimal residual disease detection and non-invasive monitoring if tumor mass was completely removed by surgery in patients with mutated KRAS. Likewise, achieving zero KRAS ctDNA level after liver surgery is important for early detection of potential disease recurrence, where the KRAS ctDNA can increase again.

We also investigated the relationship of KRAS mutated DNA levels to DFS and OS, both tissue and plasma levels. Based on the concordance of the presence of KRAS mutations in the plasma and tissue of patients with liver metastases, we would expect similar results regarding the possible prognostic significance (OS and DFS). However, we recorded prognostic significance only for the determination of mutated DNA of the KRAS gene in plasma. Patients with a fractional abundance value lower than 3.3% had got a significantly better prognosis (OS). Based on the relationship between the level of KRAS mutated ctDNA and prognosis, our results indicate that, in certain cases, it may be more appropriate to determine the presence of a KRAS mutation based on plasma results.

Other studies showed that the quantification of ctDNA is the valuable prognostic factor for CLM patients and support the idea of non-invasive detection of persistent minimal residual disease. In the study by Cassinotti et al. and Frattini et al., the ctDNA concentration significantly decreased after primary tumor resection. However, the ctDNA concentration dramatically increased in patients with a relapse. In "disease-free" patients, the ctDNA level remains in decreasing tendency [41,42]. The preoperative assessment of ctDNA level might be useful for better prognosis estimation and a postoperative assessment could early detect the cancer recurrence. Increased ctDNA level significantly correlated with an unfavorable prognosis in another study as well [43]. In addition, our study showed the benefits of quantifying of copies of KRAS ctDNA by the ddPCR.

In our opinion based on these results, it can be stated that the plasma level of the KRAS mutation does not reflect the same biological properties of oncological disease as the level of the mutated KRAS oncogene DNA determined in the tumor tissue. Plasma assays also include information on the ability to release tumor molecules into the bloodstream. In addition, the result shows that we do not have two groups of patients (KRAS+ and KRAS-), but rather three groups. The group without a mutation in the KRAS oncogene, with a small amount of ctDNA in the bloodstream and a large amount of ctDNA.

There is evidence that ctDNA assessment could be a more preferable biomarker of prognosis than CEA plasma levels. Vymetalkova et al. mentions that, at the time of recurrence, 80% of CRC patients were ctDNA positive, while CEA levels were only elevated in 41% of CRC patients [43]. Reinert et al. [44] and Carpinetti et al. [45] published that ctDNA assessment in follow-up period of CRC patients may show cancer recurrence and therapy response an earlier in comparison with monitoring of CEA or radiological evaluation. We observed the benefit of combining both ctDNA and CEA levels for prognosis.

The limitations of our study must also be mentioned. These are mainly heterogenous treatment protocols applied for oncological patients and also the limited number of plasma samples available for analysis. On the other hand, the strengths are the use of the ddPCR method and detailed long-term patient follow-up with a high maturity of the cohort of patients. The assay for ddPCR used in our study is able to screen spectrum of KRAS mutations (as described in materials and methods) that is very useful in the case of ctDNA analysis and limited amount of isolated DNA. This advantage is limited by the impossibility to discriminate among individual mutations.

4. Materials and Methods

4.1. Patients and Samples

We retrospectively analyzed 71 patients who underwent primary surgery for colorectal carcinoma and after the onset of disease progression into the liver who underwent surgery for CRC liver metastases (Table 4). The study was approved by the institutional review board and local ethics committee of the University Hospital in Pilsen. The ethical code is no.1552016. Every patient signed an informed consent form for the use of their blood samples in clinical research for the assessment of tumor markers. Each FFPE sample of CRC and CLM patients was verified by a pathologist diagnosis. All CRC tumors used in these study were histologically adenocarcinomas. CRC patients were staged base on the TNM system of the International Union Against Cancer (IUCC, 7th edition) [46]. The median patients´ follow-up was 4.1 years. The evaluation of remission and recurrence were classified based on response evaluation criteria in solid tumors (RECIST) [47].

Table 4. Patient characteristics.

Patient Characteristics	Number of Patients (%)
All patients in the study	71 (100%)
Gender	
Female	29 (41%)
Male	42 (59%)
Mean age at liver surgery (min-max)	62.7 (29–77) years
Extent of liver surgery	
R0 resection	38 (54%)
R1 resection	21 (30%)
RFA [1]	11 (16%)
Adjuvant chemotherapy	
Yes	55 (77%)
No	16 (23%)
Adjuvant biological therapy (bevacizumab or cetuximab)	
Yes	15 (21%)
No	56 (79%)
Tumor grade (available in 44 pts.)	
Grade 1	15 (21%)
Grade 2	23 (32%)
Grade 3	6 (9%)
Number of liver metastases	
1	35 (49%)
≥2	36 (51%)
Mean size of metastases (min-max)	38.5 (6–130) mm
Extrahepatic disease	
Yes	4 (6%)
No	67 (94%)

[1] Radiofrequency ablation.

The quantitative estimation of 7 KRAS G12/G13 mutations was performed by ddPCR in 71 colorectal carcinoma tissue samples (FFPE) and paired 71 liver metastasis tissue samples (FFPE). In these patients the quantitative KRAS estimation was also done in 7 preoperative (taken a day before primary CRC surgery) and postoperative (taken a day after primary CRC surgery) plasma samples. Similarly the mutated KRAS was quantified in 30 preoperative and postoperative plasma samples of patients undergoing surgery for CLM.

4.2. Blood Samples

The peripheral blood samples were collected from the cubital vein using K3EDTA Vacutainer tubes (Greiner Bio-One, Kremsmünster, Austria). Plasma was prepared by two-step centrifugation of 6 mL of blood at 950 rcf at 10 min at 4 °C and then at 11,000 rcf at 10 min at 4 °C–to remove any cell debris as a standard procedures used for cell-free DNA assessment.

For CEA detection, the blood serum was separated by centrifugation at 1700 rcf for 10 min from 4 mL of blood collected in Vacuette® blood collection tubes (Greiner Bio-One, Kremsmünster, Austria). Until analysis plasma and serum samples were stored frozen at −80 °C.

4.3. DNA Isolation

Tissue DNA was isolated by AllPrep DNA/RNA FFPE kit (Qiagen, Hilden, Germany). Total circulating DNA was isolated from 1 mL plasma by the QIAamp Circulating Nucleic Acid Kit kit (Qiagen, Hilden, Germany), according to the manufacturer manual.

4.4. ddPCR Assay

Quantitative estimation of 7 KRAS G12/G13 mutations was done by ddPCR™ KRAS G12/G13 Multiplex Screening Kit (catalogue No. 186-350, Bio-Rad Laboratories, Hercules, CA, USA) on QX200 Droplet Digital PCR System (Bio-Rad Laboratories, Hercules, CA USA). This assay enables to screen KRAS variants G12A (dHsaCP2500586), G12C (dHsaCP2500584), G12D (dHsaCP2500596), G12R (dHsaCP2500590), G12S (dHsaCP2500588), G12V (dHsaCP2500592) and G13D (dHsaCP2500598).

For FFPE samples the total DNA load in reaction was 50 ng of isolated DNA per well. To overstep the small amounts of mutated DNA in circulation generally, all plasma samples were analyzed in 3 well simultaneously in each 5 μL of isolated DNA without dilution was added yielded 25–225 ng of DNA per 3 merged wells. Data obtained in 3 wells (same sample) were merged for results as recommended in Bulletin 6628A, Rare mutation detection (Best practices guidelines) by Bio-Rad Laboratories, Hercules, CA, USA.

The analytical procedure was performed according to PrimePCR ddPCR assay manual-Bio-Rad 10,048,179 Rev. A, (Bio-Rad Laboratories, Hercules, CA, USA). No DNA digestion was used for samples, while for FFPE and cell free DNA samples is not required. PCR master mix was prepared by 11 μL 2× ddPCR Supermix for Probe (no dUTP), 1 μL multiplex primers/probes (FAM + HEX) and 7.5 μL nuclease-free water for each FFPE sample. For cell free DNA sample was 33 μL 2× ddPCR Supermix for Probe (no dUTP), 3 μL multiplex primers/probes (FAM + HEX) and 15 μL nuclease-free water for three wells. There was manually transferred 20 μL of final PCR mix into wells of a CG 8 cartridge and added 70 μL Droplet Generation Oil for probes. Cartridge is loaded into QX200TM Droplet Generator (Bio-Rad Laboratories, Hercules, CA, USA) for droplet generation, followed by transfer of 40 μL of sample droplets into the 96-well PCR plate. Plate is heat sealed by foil using PX1 PCR Plate Sealer (Bio-Rad Laboratories, Hercules, CA, USA). Amplification was performed in T100TM Thermal Cycler with 96-Deep Well Reaction Module (thermal cycling protocol: 95 °C for 10 min, 40× cycle of 94 °C for 30 s, 55 °C for 1 min, 98 °C for 10 min (all ramp rate 2 °C/s), and final cooling down to 4 °C, ramp rate 1 °C/s). After thermal cycling, reading analysis was performed on QX200TM Droplet Reader (Bio-Rad Laboratories, Hercules, CA, USA) with setting for FAM/HEX.

In all plates, positive controls for each detected KRAS mutation and negative samples were screened for quality control and "cut-off" set-up. Control samples have checked DNA quality by amplification of control genes: 100–600 bp (BIOMED-2), detection of mutations in positive control samples were performed by PCR and reverse-hybridization accredited according to CSN EN 15189:2013.

Data were analyzed in Biorad-Laboratories software Quantasoft 1.7 and QuantaSoft™ Analysis Pro 1.0. Thresholds were placed manually. Fractional abundance (FA) of targeted mutations in samples, determined as positive, were calculated as percentage FA% = mutated copies/(mutated copies + wildtype copies) × 100. FFPE samples, for which positive droplet count (FAM plus HEX channel) was insufficient, were reanalyzed with DNA load app. 100 ng/well reaction.

According to false positive rate (FPR) 1625 (cumulatively 13 false positive droplets in 8 control samples) in plasma sample plates, the 5 positive droplets were determined as a cut-off for merged plasma sample results.

To avoid any false positive results for FFPE samples, we have chosen relatively high cut-off value: the fractional abundance of 5% for positivity of mutation occurrence, while mean FA% of negative controls was 1.5% and maximum FA% in FFPE negative controls was approximately 3% in FFPE plates.

4.5. Quantitative Measurement of CEA

Serum levels of CEA protein were determined in monoplicates by chemiluminescent assay the ACCESS CEA assay with the UniCel DxI 800 Instrument (Beckman Coulter, Brea, CA, USA). The cut off value of the preoperative serum CEA level was set at 4.9 ng/mL.

4.6. Statistical Analysis

Statistical analysis was performed using the SPSS 22 software package (IBM, Armonk, NY, USA). The statistical significance was considered with a p value of ≤ 0.05. Kaplan–Meier method with an "optimal cut off" found with the lowest p-value of the log rank test was used for survival analysis. Multivariate analysis was performed by the Cox regression model to test independent significance while adjusting for covariates. Data were presented as hazard ratios (HR) and 95% confidence intervals (95%CI). Spearman's rank-order correlation method was used for mutual correlations. The Wilcoxon signed-rank test was used for comparison of differences between pre- and post-operative levels of circulating markers.

5. Conclusions

Published data on liquid biopsy based on ctDNA in colorectal cancer patients with advanced disease provide additional information on the course and prognosis of the disease and may help with the therapy decision making process. The best prognostic value in colorectal cancer patients undergoing surgery for liver metastases was observed based on the detection of the level of KRAS ctDNA in combination with routinely determined tumor marker CEA.

Abbreviations

95% CI	95% Confidence interval
CEA	Carcinoembryonic antigen
CLM	Colorectal cancer liver metastases
CRC	Colorectal cancer
CTC	Circulating tumor cells
cfDNA	Circulating cell-free deoxyribonucleic acid
ctDNA	Circulating cell-free tumor deoxyribonucleic acid
ddPCR	Droplet digital polymerase chain reaction
DFS	Disease-free survival
DMFS	Distant metastasis free survival
DNA	Deoxyribonucleic acid
EGFR	Epidermal growth factor receptor
FFPE	Formalin-fixed, paraffin-embedded
FPR	False positive rate
HR	Hazard ratio
IUCC	International union against cancer
KRAS	Kirsten rat sarcoma viral oncogene homolog
mAb	Monoclonal antibody
miRNA	Micro-ribonucleic acid
NRAS	Neuroblastoma RAS viral oncogene homolog
OS	Overall survival
PCR	Polymerase chain reaction
pFA	Plasma KRAS fractional abundance
pKRAS-	Plasma KRAS negativity
pKRAS+	Plasma KRAS positivity
RECIST	Response evaluation criteria in solid tumors
RFA	Radiofrequency ablation
tFA	Tissue KRAS fractional abundance
tKRAS+	Tissue KRAS positivity
TNM	Tumor, node, metastases

References

1. Bray, F.; Ferlay, J.; Soerjomataram, I.; Siegel, R.L.; Torre, L.A.; Jemal, A. Global cancer statistics 2018: GLOBOCAN estimates of incidence and mortality worldwide for 36 cancers in 185 countries. *CA Cancer J. Clin.* **2018**, *68*, 394–424. [CrossRef] [PubMed]

2. Engstrand, J.; Nilsson, H.; Strömberg, C.; Jonas, E.; Freedman, J. Colorectal cancer liver metastases—A population-based study on incidence, management and survival. *BMC Cancer* **2018**, *18*, 78. [CrossRef] [PubMed]

3. Golubnitschaja, O.; Polivka, J.; Yeghiazaryan, K.; Berliner, L. Liquid biopsy and multiparametric analysis in management of liver malignancies: New concepts of the patient stratification and prognostic approach. *EPMA J.* **2018**, *9*, 271–285. [CrossRef] [PubMed]

4. Kow, A.W.C. Hepatic metastasis from colorectal cancer. *J. Gastrointest. Oncol.* **2019**, *10*, 1274–1298. [CrossRef] [PubMed]

5. Rosty, C.; Young, J.P.; Walsh, M.D.; Clendenning, M.; Walters, R.J.; Pearson, S.; Pavluk, E.; Nagler, B.; Pakenas, D.; Jass, J.R.; et al. Colorectal carcinomas with KRAS mutation are associated with distinctive morphological and molecular features. *Mod. Pathol.* **2013**, *26*, 825–834. [CrossRef]

6. Normanno, N.; Tejpar, S.; Morgillo, F.; De Luca, A.; Van Cutsem, E.; Ciardiello, F. Implications for KRAS status and EGFR-targeted therapies in metastatic CRC. *Nat. Rev. Clin. Oncol.* **2009**, *6*, 519–527. [CrossRef]

7. Malumbres, M.; Barbacid, M. RAS oncogenes: The first 30 years. *Nat. Rev. Cancer* **2003**, *3*, 459–465. [CrossRef]

8.　Vasioukhin, V.; Anker, P.; Maurice, P.; Lyautey, J.; Lederrey, C.; Stroun, M. Point mutations of the N-ras gene in the blood plasma DNA of patients with myelodysplastic syndrome or acute myelogenous leukaemia. *Br. J. Haematol.* **1994**, *86*, 774–779. [CrossRef]

9.　Sorenson, G.D. Detection of mutated KRAS2 sequences as tumor markers in plasma/serum of patients with gastrointestinal cancer. *Clin. Cancer Res.* **2000**, *6*, 2129–2137. [CrossRef]

10.　Sorenson, G.D.; Pribish, D.M.; Valone, F.H.; Memoli, V.A.; Bzik, D.J.; Yao, S.L. Soluble normal and mutated DNA sequences from single-copy genes in human blood. *Cancer Epidemiol. Biomark. Prev.* **1994**, *3*, 67–71.

11.　Karapetis, C.S.; Khambata-Ford, S.; Jonker, D.J.; O'Callaghan, C.J.; Tu, D.; Tebbutt, N.C.; Simes, R.J.; Chalchal, H.; Shapiro, J.D.; Robitaille, S.; et al. K-ras mutations and benefit from cetuximab in advanced colorectal cancer. *N. Engl. J. Med.* **2008**, *359*, 1757–1765. [CrossRef] [PubMed]

12.　Douillard, J.-Y.; Oliner, K.S.; Siena, S.; Tabernero, J.; Burkes, R.; Barugel, M.; Humblet, Y.; Bodoky, G.; Cunningham, D.; Jassem, J.; et al. Panitumumab-FOLFOX4 treatment and RAS mutations in colorectal cancer. *N. Engl. J. Med.* **2013**, *369*, 1023–1034. [CrossRef] [PubMed]

13.　Peeters, M.; Oliner, K.S.; Price, T.J.; Cervantes, A.; Sobrero, A.F.; Ducreux, M.; Hotko, Y.; André, T.; Chan, E.; Lordick, F.; et al. Analysis of KRAS/NRAS Mutations in a Phase III Study of Panitumumab with FOLFIRI Compared with FOLFIRI Alone as Second-line Treatment for Metastatic Colorectal Cancer. *Clin. Cancer Res.* **2015**, *21*, 5469–5479. [CrossRef] [PubMed]

14.　Van Cutsem, E.; Lenz, H.-J.; Köhne, C.-H.; Heinemann, V.; Tejpar, S.; Melezínek, I.; Beier, F.; Stroh, C.; Rougier, P.; van Krieken, J.H.; et al. Fluorouracil, leucovorin, and irinotecan plus cetuximab treatment and RAS mutations in colorectal cancer. *J. Clin. Oncol.* **2015**, *33*, 692–700. [CrossRef] [PubMed]

15.　Allegra, C.J.; Rumble, R.B.; Hamilton, S.R.; Mangu, P.B.; Roach, N.; Hantel, A.; Schilsky, R.L. Extended RAS Gene Mutation Testing in Metastatic Colorectal Carcinoma to Predict Response to Anti-Epidermal Growth Factor Receptor Monoclonal Antibody Therapy: American Society of Clinical Oncology Provisional Clinical Opinion Update 2015. *J. Clin. Oncol.* **2016**, *34*, 179–185. [CrossRef] [PubMed]

16.　Van Cutsem, E.; Cervantes, A.; Adam, R.; Sobrero, A.; Van Krieken, J.H.; Aderka, D.; Aranda Aguilar, E.; Bardelli, A.; Benson, A.; Bodoky, G.; et al. ESMO consensus guidelines for the management of patients with metastatic colorectal cancer. *Ann. Oncol.* **2016**, *27*, 1386–1422. [CrossRef] [PubMed]

17.　Schmiegel, W.; Scott, R.J.; Dooley, S.; Lewis, W.; Meldrum, C.J.; Pockney, P.; Draganic, B.; Smith, S.; Hewitt, C.; Philimore, H.; et al. Blood-based detection of RAS mutations to guide anti-EGFR therapy in colorectal cancer patients: Concordance of results from circulating tumor DNA and tissue-based RAS testing. *Mol. Oncol.* **2017**, *11*, 208–219. [CrossRef]

18.　García-Foncillas, J.; Tabernero, J.; Élez, E.; Aranda, E.; Benavides, M.; Camps, C.; Jantus-Lewintre, E.; López, R.; Muinelo-Romay, L.; Montagut, C.; et al. Prospective multicenter real-world RAS mutation comparison between OncoBEAM-based liquid biopsy and tissue analysis in metastatic colorectal cancer. *Br. J. Cancer* **2018**, *119*, 1464–1470. [CrossRef]

19.　Lecomte, T.; Berger, A.; Zinzindohoué, F.; Micard, S.; Landi, B.; Blons, H.; Beaune, P.; Cugnenc, P.-H.; Laurent-Puig, P. Detection of free-circulating tumor-associated DNA in plasma of colorectal cancer patients and its association with prognosis. *Int. J. Cancer* **2002**, *100*, 542–548. [CrossRef]

20.　Lindforss, U.; Zetterquist, H.; Papadogiannakis, N.; Olivecrona, H. Persistence of K-ras mutations in plasma after colorectal tumor resection. *Anticancer Res.* **2005**, *25*, 657–661.

21.　Trevisiol, C.; Di Fabio, F.; Nascimbeni, R.; Peloso, L.; Salbe, C.; Ferruzzi, E.; Salerni, B.; Gion, M. Prognostic value of circulating KRAS2 gene mutations in colorectal cancer with distant metastases. *Int. J. Biol. Markers* **2006**, *21*, 223–228. [CrossRef] [PubMed]

22.　Spindler, K.-L.G.; Pallisgaard, N.; Vogelius, I.; Jakobsen, A. Quantitative cell-free DNA, KRAS, and BRAF mutations in plasma from patients with metastatic colorectal cancer during treatment with cetuximab and irinotecan. *Clin. Cancer Res.* **2012**, *18*, 1177–1185. [CrossRef] [PubMed]

23.　Bai, Y.; Liu, X.; Wang, Y.; Ge, F.; Zhao, C.; Fu, Y.; Lin, L.; Xu, J. Correlation analysis between abundance of K-ras mutation in plasma free DNA and its correlation with clinical outcome and prognosis in patients with metastatic colorectal cancer. *Zhonghua Zhong Liu Za Zhi* **2013**, *35*, 666–671. [PubMed]

24.　Spindler, K.G.; Appelt, A.L.; Pallisgaard, N.; Andersen, R.F.; Jakobsen, A. KRAS-mutated plasma DNA as predictor of outcome from irinotecan monotherapy in metastatic colorectal cancer. *Br. J. Cancer* **2013**, *109*, 3067–3072. [CrossRef] [PubMed]

25. Xu, J.-M.; Liu, X.-J.; Ge, F.-J.; Lin, L.; Wang, Y.; Sharma, M.R.; Liu, Z.-Y.; Tommasi, S.; Paradiso, A. KRAS mutations in tumor tissue and plasma by different assays predict survival of patients with metastatic colorectal cancer. *J. Exp. Clin. Cancer Res.* **2014**, *33*, 104. [CrossRef]

26. Siravegna, G.; Mussolin, B.; Buscarino, M.; Corti, G.; Cassingena, A.; Crisafulli, G.; Ponzetti, A.; Cremolini, C.; Amatu, A.; Lauricella, C.; et al. Clonal evolution and resistance to EGFR blockade in the blood of colorectal cancer patients. *Nat. Med.* **2015**, *21*, 795–801. [CrossRef] [PubMed]

27. Spindler, K.L.G.; Pallisgaard, N.; Andersen, R.F.; Brandslund, I.; Jakobsen, A. Circulating free DNA as biomarker and source for mutation detection in metastatic colorectal cancer. *PLoS ONE* **2015**, *10*, e0108247. [CrossRef] [PubMed]

28. El Messaoudi, S.; Mouliere, F.; Du Manoir, S.; Bascoul-Mollevi, C.; Gillet, B.; Nouaille, M.; Fiess, C.; Crapez, E.; Bibeau, F.; Theillet, C.; et al. Circulating DNA as a Strong Multimarker Prognostic Tool for Metastatic Colorectal Cancer Patient Management Care. *Clin. Cancer Res.* **2016**, *22*, 3067–3077. [CrossRef]

29. Luo, H.; Shen, K.; Li, B.; Li, R.; Wang, Z.; Xie, Z. Clinical significance and diagnostic value of serum NSE, CEA, CA19-9, CA125 and CA242 levels in colorectal cancer. *Oncol. Lett.* **2020**, *20*, 742–750. [CrossRef]

30. Kang, H.Y.; Choe, E.K.; Park, K.J.; Lee, Y. Factors Requiring Adjustment in the Interpretation of Serum Carcinoembryonic Antigen: A Cross-Sectional Study of 18,131 Healthy Nonsmokers. *Gastroenterol. Res. Pract.* **2017**, *2017*, 9858931. [CrossRef]

31. Hall, C.; Clarke, L.; Pal, A.; Buchwald, P.; Eglinton, T.; Wakeman, C.; Frizelle, F. A Review of the Role of Carcinoembryonic Antigen in Clinical Practice. *Ann. Coloproctol.* **2019**, *35*, 294–305. [CrossRef] [PubMed]

32. Abdul-Wahid, A.; Cydzik, M.; Fischer, N.W.; Prodeus, A.; Shively, J.E.; Martel, A.; Alminawi, S.; Ghorab, Z.; Berinstein, N.L.; Gariépy, J. Serum-derived carcinoembryonic antigen (CEA) activates fibroblasts to induce a local re-modeling of the extracellular matrix that favors the engraftment of CEA-expressing tumor cells. *Int. J. Cancer* **2018**, *143*, 1963–1977. [CrossRef] [PubMed]

33. Calinescu, A.; Turcu, G.; Nedelcu, R.I.; Brinzea, A.; Hodorogea, A.; Antohe, M.; Diaconu, C.; Bleotu, C.; Pirici, D.; Jilaveanu, L.B.; et al. On the Dual Role of Carcinoembryonic Antigen-Related Cell Adhesion Molecule 1 (CEACAM1) in Human Malignancies. *J Immunol. Res.* **2018**, *2018*, 7169081. [CrossRef] [PubMed]

34. Pesta, M.; Kucera, R.; Topolcan, O.; Karlikova, M.; Houfkova, K.; Polivka, J.; Macanova, T.; Machova, I.; Slouka, D.; Kulda, V. Plasma microRNA Levels Combined with CEA and CA19-9 in the Follow-Up of Colorectal Cancer Patients. *Cancers* **2019**, *11*, 864. [CrossRef]

35. Xie, H.-L.; Gong, Y.-Z.; Kuang, J.-A.; Gao, F.; Tang, S.-Y.; Gan, J.-L. The prognostic value of the postoperative serum CEA levels/preoperative serum CEA levels ratio in colorectal cancer patients with high preoperative serum CEA levels. *Cancer Manag. Res.* **2019**, *11*, 7499–7511. [CrossRef]

36. Tan, E.; Gouvas, N.; Nicholls, R.J.; Ziprin, P.; Xynos, E.; Tekkis, P.P. Diagnostic precision of carcinoembryonic antigen in the detection of recurrence of colorectal cancer. *Surg. Oncol.* **2009**, *18*, 15–24. [CrossRef]

37. Park, I.J.; Choi, G.-S.; Lim, K.H.; Kang, B.M.; Jun, S.H. Serum carcinoembryonic antigen monitoring after curative resection for colorectal cancer: Clinical significance of the preoperative level. *Ann. Surg. Oncol.* **2009**, *16*, 3087–3093. [CrossRef]

38. Nicholson, B.D.; Shinkins, B.; Pathiraja, I.; Roberts, N.W.; James, T.J.; Mallett, S.; Perera, R.; Primrose, J.N.; Mant, D. Blood CEA levels for detecting recurrent colorectal cancer. *Cochrane. Database. Syst. Rev.* **2015**, CD011134. [CrossRef]

39. Knijn, N.; Mekenkamp, L.J.M.; Klomp, M.; Vink-Börger, M.E.; Tol, J.; Teerenstra, S.; Meijer, J.W.R.; Tebar, M.; Riemersma, S.; van Krieken, J.H.J.M.; et al. KRAS mutation analysis: A comparison between primary tumours and matched liver metastases in 305 colorectal cancer patients. *Br. J. Cancer* **2011**, *104*, 1020–1026. [CrossRef]

40. Mardinian, K.; Okamura, R.; Kato, S.; Kurzrock, R. Temporal and spatial effects and survival outcomes associated with concordance between tissue and blood KRAS alterations in the pan-cancer setting. *Int. J. Cancer* **2020**, *146*, 566–576. [CrossRef]

41. Cassinotti, E.; Boni, L.; Segato, S.; Rausei, S.; Marzorati, A.; Rovera, F.; Dionigi, G.; David, G.; Mangano, A.; Sambucci, D.; et al. Free circulating DNA as a biomarker of colorectal cancer. *Int. J. Surg.* **2013**, *11* (Suppl. 1), S54–S57. [CrossRef]

42. Frattini, M.; Gallino, G.; Signoroni, S.; Balestra, D.; Battaglia, L.; Sozzi, G.; Leo, E.; Pilotti, S.; Pierotti, M.A. Quantitative analysis of plasma DNA in colorectal cancer patients: A novel prognostic tool. *Ann. N. Y. Acad. Sci.* **2006**, *1075*, 185–190. [CrossRef] [PubMed]

43. Vymetalkova, V.; Cervena, K.; Bartu, L.; Vodicka, P. Circulating Cell-Free DNA and Colorectal Cancer: A Systematic Review. *Int. J. Mol. Sci.* **2018**, *19*. [CrossRef]

44. Reinert, T.; Schøler, L.V.; Thomsen, R.; Tobiasen, H.; Vang, S.; Nordentoft, I.; Lamy, P.; Kannerup, A.-S.; Mortensen, F.V.; Stribolt, K.; et al. Analysis of circulating tumour DNA to monitor disease burden following colorectal cancer surgery. *Gut* **2016**, *65*, 625–634. [CrossRef]

45. Carpinetti, P.; Donnard, E.; Bettoni, F.; Asprino, P.; Koyama, F.; Rozanski, A.; Sabbaga, J.; Habr-Gama, A.; Parmigiani, R.B.; Galante, P.A.F.; et al. The use of personalized biomarkers and liquid biopsies to monitor treatment response and disease recurrence in locally advanced rectal cancer after neoadjuvant chemoradiation. *Oncotarget* **2015**, *6*, 38360–38371. [CrossRef] [PubMed]

46. Sobin, L.H.; Gospodarowicz, M.K.; Wittekind, C. (Eds.) *TNM Classification of Malignant Tumours*, 7th ed.; Wiley-Blackwell: Chichester/West Sussex, UK; Hoboken, NJ, USA, 2011; ISBN 978-1-4443-3241-4.

47. Schwartz, L.H.; Litière, S.; de Vries, E.; Ford, R.; Gwyther, S.; Mandrekar, S.; Shankar, L.; Bogaerts, J.; Chen, A.; Dancey, J.; et al. RECIST 1.1-Update and clarification: From the RECIST committee. *Eur. J. Cancer* **2016**, *62*, 132–137. [CrossRef] [PubMed]

PŘÍLOHA 7

BAI1 as a prognostic marker of clear cell renal cell carcinoma (ccRCC)

Martin Pesta, Ph.D.[a,b], Ivan Travnicek, M.D., Ph.D.[c], Vlastimil Kulda, M.D., Ph.D.[d,*], Jindra Windrichova, Ph.D.[b,d], Hana Rezackova, Ing.[b], Katerina Houfkova, Dr.[a], Tereza Macanova[a], Barbora Bendova, M.D.[c], Andrea Nestorova, M.D.[d], Ondrej Hes, M.D., Ph.D.[e], Milan Hora, M.D., Ph.D.[c], Ondrej Topolcan, M.D., Ph.D.[b] and Jiri Polivka, Ph.D.[b,f]

[a]Department of Biology, Charles University, Faculty of Medicine in Pilsen, alej Svobody 76, 32300 Pilsen, Czech Republic

[b]Laboratory of Immunoanalysis, University Hospital in Pilsen, E. Benese 13, 30599 Pilsen, Czech Republic

[c]Department of Urology, University Hospital in Pilsen, E. Benese 13, 30599 Pilsen, Czech Republic

[d]Department of Medical Chemistry and Biochemistry, Charles University, Faculty of Medicine in Pilsen, Karlovarska 48, 30166 Pilsen, Czech Republic

[e]Department of Pathology, Faculty Hospital Plzen, Faculty of Medicine in Pilsen, Charles University, Edvarda Benese 13, 305 99 Plzen, Czech Republic

[f]Department of Histology and Embryology, Charles University, Faculty of Medicine in Pilsen, Karlovarska 48, 30166 Pilsen, Czech Republic

* Corresponding author: Phone: +420-377-593-287

E-mail address: vlastimil.kulda@lfp.cuni.cz (Vlastimil Kulda)

Department of Medical Chemistry and Biochemistry

Faculty of Medicine in Pilsen, Charles University

Karlovarska 48, 301 66, Plzen, Czech Republic

Abstract

Objectives: Clear cell renal cell carcinoma (ccRCC) belongs to the most common urological malignancies across the world. Patients with advanced ccRCC are stratified into groups of favorable, intermediate, and poor prognosis for the purpose of decision on treatment. Recently, there are efforts being made to improve prognostication of patients by including new molecular biomarkers. The aim of the study was to find prognostic biomarker for patients with ccRCC from the group of 97 genes involved in angiogenesis.

Methods: The study was done on a set of matched (primary tumor, metastasis) FFPE tissue samples (n=20). Quantitative estimation of mRNA of selected genes (TaqMan human Angiogenesis Array, 97 genes including 3 reference genes) was performed by a real-time RT-PCR method with TaqMan® array card block. Expression data of additional 606 patients were obtained from TCGA Kidney Clear Cell Carcinoma (KIRC) database.

Results: Using the Cox regression model 4 genes (PDGFB, FGF4, EPHB2 and BAI1) were identified whose expression was related to progression free interval (PFI). Further analysis using Kaplan Meier method revealed the relationship of BAI1 expression to prognosis. Patients with higher BAI1 expression had significantly shorter overall survival (OS) and PFI.

Conclusions: The identification of BAI1 as prognostic marker in ccRCC is the first step to involve this gene in prognostic panels which could improve scoring systems on which the management of metastatic ccRCC patients is based. Gene expression panels are a tool how to individualize patients' treatment as a part of personalized medicine approach.

Keywords: clear cell renal cell carcinoma; biomarkers; prognostic; BAI1; FFPE

1. Introduction

Clear cell renal cell carcinoma (ccRCC) is the most common histological subtype of renal cancer and belongs the most frequent urological malignancies worldwide. About one third of cases is diagnosed in advanced stages with 5-year survival rate of 12% [1]. The Czech Republic belong to countries with the highest incidence (29.0 per 100 000 in 2017) and mortality (9.7 per 100 000 in 2017) rate of renal cell carcinoma across the world [2].

ccRCC can be one of the clinical manifestations of von Hippel-Lindau (VHL) disease resulting from changes of the von Hippel Lindau (VHL) tumor suppressor gene. Metastatic ccRCC is a highly angiogenic tumor with mutations, deletion or methylation of VHL, the most frequent genetic hallmark of ccRCC. The second most common mutated gene in ccRCC after VHL is PBRM1, a component of the chromatin remodeling complex [3]. Additional to genetics, many lifestyle, dietary and environmental factors have also been associated with ccRCC. The major established risk factors include hypertension, cigarette smoking and obesity [4]. Genetic alterations result in overexpression of VEGF. Therefore, oncologic treatment is based on targeting the angiogenesis vascular endothelial growth factor (VEGF/VEGFR) pathway by monoclonal antibodies or tyrosine kinase inhibitors (TKIs) and immunotherapies aiming to block immune checkpoints [5].

Patients with ccRCC are stratified into groups of favorable, intermediate, and poor prognosis based on the Memorial Sloan Kettering Cancer Center (MSKCC) risk stratification model. Risk scores are obtained from 5 clinical and laboratory parameters as performance status, time from diagnosis to start of therapy, hemoglobin level, serum lactate dehydrogenase and calcium concentration [6,7]. Recently, there are efforts being made to improve prognostication of patients by including specific molecular biomarkers. Voss et al. from Memorial Sloan Kettering Cancer Center proposed to involve the mutation status of three genes (BAP1, PBRM1, and TP53) as genomic biomarkers of ccRCC [8].

Precise patient stratification should help personalize the treatment algorithms to match individual patient profile according to the current approach of preventive, predictive, personalized (3P)

medicine [9]. For most prevalent solid tumors as colorectal cancer and breast cancer, there already are clinically used multigene panels for predicting clinical outcome and treatment response (ColoPrint, MammaPrint and Oncotype DX) based on assessment of expression of certain genes on mRNA level [10,11]. Regarding ccRCC, currently there is no clinically used multigene mRNA expression panel for predicting outcome and treatment response, however, there are promising results on identification genes which could be a part of such panel [12,13].

The aim of our study was to evaluate the prognostic potential of mRNA expression of 97 genes involved in angiogenesis (TaqMan human Angiogenesis Array) in patients with metastatic ccRCC to improve decision about the treatment. The study was done on a set of matched (primary tumor, metastasis) formalin-fixed, paraffin-embedded (FFPE) tissue samples (n=20) and using the The Cancer Genome Atlas (TCGA) [14] dataset (n = 606) to confirm the findings.

2. Materials and Methods

2.1. Patients

The study was approved by the Ethics Committee of the Faculty Hospital in Pilsen (approval from the date 2016/01/06). It was a retrospective study. All patients signed an informed consent for the use of their biological samples for the assessment of tumor markers. The study group consisted of 20 patients who underwent surgery for ccRCC at the Department of Urology of the University Hospital in Pilsen between December 2007 and October 2017.

Each diagnosis of ccRCC was verified by a pathologist. The stage of disease was determined using the TNM system of the Union for International Cancer Control (UICC, 7th edition) [15]. Metastases sites were located in lungs (7 cases), suprarenal glands (5 cases), vertebrae (4 cases), colon (2 cases), brain (2 cases), spleen (2 cases) and retroperitoneal adipose tissue (1 case).

Treatment of 17 out of 20 metastatic ccRCC patients was based on sunitinib (Sutent) administered in cycles consisting of 4 weeks at a dose of 50 mg daily followed by a 2-week rest period

(schedule 4/2), continuing until progression. Two patients were treated by sorafenib (Nexavar) administered at a total daily dose of 800 mg continuously until progression. One patient received pazopanib (Votrient) at a dose of 600 mg daily continuously until progression. The evaluation of treatment response was based on Response Evaluation Criteria in Solid Tumors (RECIST) [16]. The detailed characteristics of patients is provided in Table 1.

Table 1

Characteristics of patients in the study (at the time of ccRCC diagnosis)

Variables	Number of patients	%
Number of patients	20	100
Gender		
Male	16	80
Female	4	20
Type of surgery		
Laparoscopic	8	40
Transperitoneal	12	60
Histologic grade		
G1	3	15
G2	6	30
G3	4	20
G4	2	10
Gx	5	25
T stage		
T1	6	30
T2	5	25
T3	8	40
T4	1	5
N stage		
N0	9	45
N1	4	20
Nx	7	35
M stage		
M0	10	50
M1	8	40
Mx	2	10

We validated gene expression results obtained on our group of patients in additional datasets from TCGA public database available on https://www.cancer.gov/tcga. Characteristic of 606 patients from TCGA Kidney Clear Cell Carcinoma (KIRC) dataset is shown in Table 2. The patients underwent the treatment based on the surgery, pharmaceutical therapy or radiation therapy.

After identification of BAI1 as a prognostic marker in ccRCC patients, due to comparison of prognostic significance of BAI1 expression in ccRCC and other tumor types, where the involvement of BAI1 in pathogenesis is more understood, we performed survival analysis based on BAI1 expression also for glioblastoma and lung cancer adenocarcinoma patients. As a cohort of patients we used TCGA Glioblastoma (GBM) dataset (166 patients) and TCGA Lung Adenocarcinoma (LUAD) dataset (567 patients).

Table 2

Characteristics of patients of TCGA Kidney Clear Cell Carcinoma (KIRC) dataset

Variables	Number of patients	%
Number of patients	606	100
Gender		
Male	398	65.7
Female	208	34.3
Histologic grade		
G1	15	2.5
G2	257	42.4
G3	235	38.8
G4	91	15.0
Gx	8	1.3
T stage		
T1	301	49.7
T2	83	13.7
T3	209	34.5
T4	13	2.1
N stage		
N0	278	45.9
N1	18	2.9
Nx	310	51.2
M stage		
M0	475	78.4
M1	98	16.2
Mx	33	5.4

2.2. Assessment of mRNA expression

2.2.1. Tissue samples

Biopsy tissue samples were processed by standard laboratory techniques at Department of Pathology of the University Hospital in Pilsen. FFPE tissue samples were stored at room temperature until use. Paraffin sections (4-μm thick) were stained with hematoxylin and eosin (H&E),

microscopically verified by pathologists and examined in order to identify sites with primary cancer cells, metastasis and sites of adjacent non-cancerous epithelial tissue suitable for dissection. Areas selected for expression analysis were highlighted manually. Matched samples of primary tumor, adjacent normal tissue and metastasis were analyzed.

2.2.2. RNA isolation

Total RNA was extracted from FFPE sections following macrodissection of tissue of interest using the RNeasy FFPE Kit (Qiagen, Hilden, Germany) as described previously [17]. The 15-μm sections corresponded to H&E representatives, on which the areas for macrodissection were highlighted.

2.2.3. RT Real time PCR

Quantitative estimation of mRNA of selected genes (TaqMan human Angiogenesis Array, 97 genes including 3 reference genes) was performed by a real-time RT-PCR method with TaqMan® array card block on QuantStudio™ 7 Flex Real-Time PCR System (Thermo Fisher Scientific, Foster City, CA, USA) according to manufacturer's protocol. Briefly, reverse transcription was performed on 50 ng of total RNA with SuperScript IV VILO Master Mix (Thermo Fisher Scientific, Foster City, CA, USA) and random hexamers as primers. The qPCR reactions started with incubation at 50˚C for 2 min and followed by 10 min at 92˚C. The amplification was carried out in 40 two-step cycles (95 ˚C for 1 s and 60˚C for 20 s. ROX passive reference dye was used for normalization of interwell variations.

GAPDH, HPRT and β-actin were used as reference genes. Gene expression of particular sample was only evaluated if the expression of all three housekeeping genes was present. The results are presented as normalized values ($2^{-\Delta\Delta Ct}$ algorithm) using the geometric mean of quantifications (Ct) of the three reference genes [18].

2.2.4. Statistical analysis

The statistical analysis was performed using the R software package. The TCGA datasets were browsed using the Xena tool [19]. Downloaded raw data were also analyzed using R. Essential descriptive statistics for all variables of interest were prepared based on the clinical and pathological data of the patients. Cox regression model was applied for the evaluation of prognostic significance. Kaplan–Meier survival curves for progression-free interval (PFI) and overall survival (OS) were generated.

3. Results

We performed a search for prognostic biomarkers of ccRCC patients treated with antiangiogenic targeted therapy by evaluating the relationship of tissue expression of genes involved in angiogenesis. We evaluated the relationship of primary tumor and metastasis tissue expression of 94 genes to PFI. The evaluation of PFI was based on the length of the time period of treatment administration, which continued if the patient responded to treatment, i.e. the patient was in the condition of complete response (CR), partial response (PR), stable disease (SD) according to RECIST criteria. Based on this analysis, we identified 4 genes (BAI1, PDGFB, FGF4 and EPHB2) whose expression was related to PFI (Table 3) using the Cox regression model. For all these genes we observed that higher level of expression was associated with shorter PFI.

Table 3

Relation of gene expression to progression-free interval (PFI) by Cox regression model

Gene	Primary tumor p-value	Metastasis p-value
BAI1	0.0758	0.0291
PDGFB	0.0329	0.4846
FGF4	0.0848	0.0412
EPHB2	0.2276	0.0581

For more detail analysis, Kaplan-Meier survival curves were generated for these genes. There was a statistically significant difference in time to progression between the patients with low and high

BAI1 expression in ccRCC metastatic tissue (Fig. 1A). The patients with low BAI1 expression had better prognosis. Similarly in the case of primary tumor, but statistical significance was not recorded (Fig. 1B).

We validated the relationship of BAI1 ccRCC primary tumor tissue expression to prognosis in a group of 606 ccRCC patients whose data were available in the public TCGA Kidney Clear Cell Carcinoma (KIRC) database. Patients with higher BAI1 expression have significantly shorter OS and PFI (Fig. 2). The data on gene expression in metastatic tissue were not available.

As BAI1 is proposed tumor suppressor in many types of cancer and our results in ccRCC patients presented above are contradictory to this proposed function, we explored the relationship of BAI1 expression to prognosis also in other types of cancer (in detail commented in the Discussion section). Here we present data for glioblastoma and lung adenocarcinoma. Using the Xena tool we found no relation of BAI1 expression to patients' outcome in glioblastoma (TCGA Glioblastoma (GBM) database). In lung adenocarcinoma (TCGA Lung Adenocarcinoma (LUAD) database) it was recorded that patients with lower BAI1 expression had significantly shorter overall survival (OS) and progression free interval (PFI), Fig. 3.
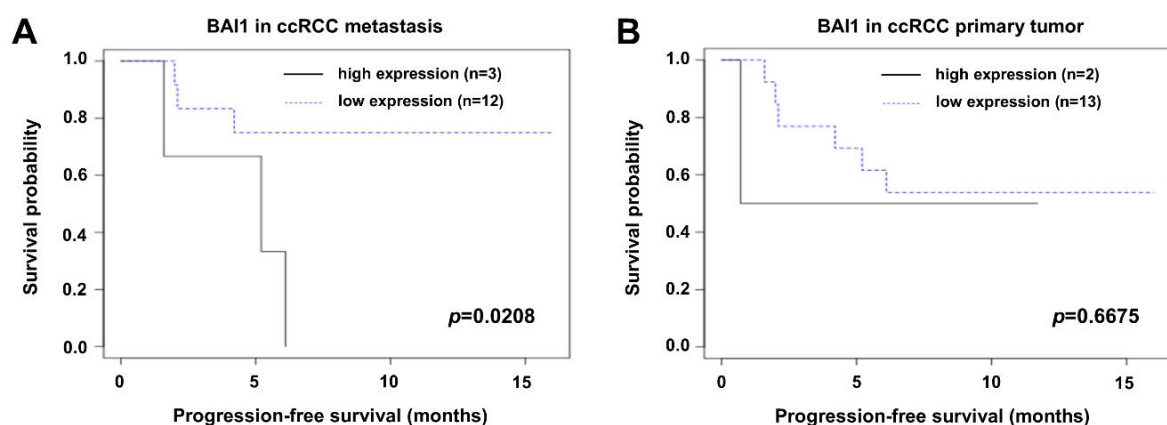
Fig. 1. Kaplan-Meier curves showing relation of BAI1 metastasis (A) and primary tumor (B) tissue expression level to progression-free survival in clear cell renal cell carcinoma (ccRCC) patients. Patients with high BAI1 expression had worse outcome.

Fig. 2. Relation of BAI1 expression to overall survival (A) and to progression-free survival (B) in TCGA Kidney Clear Cell Carcinoma (KIRC) group of patients (Kaplan-Meier curves). Patients with high BAI1 expression had significantly shorter both overall survival and progression free interval.

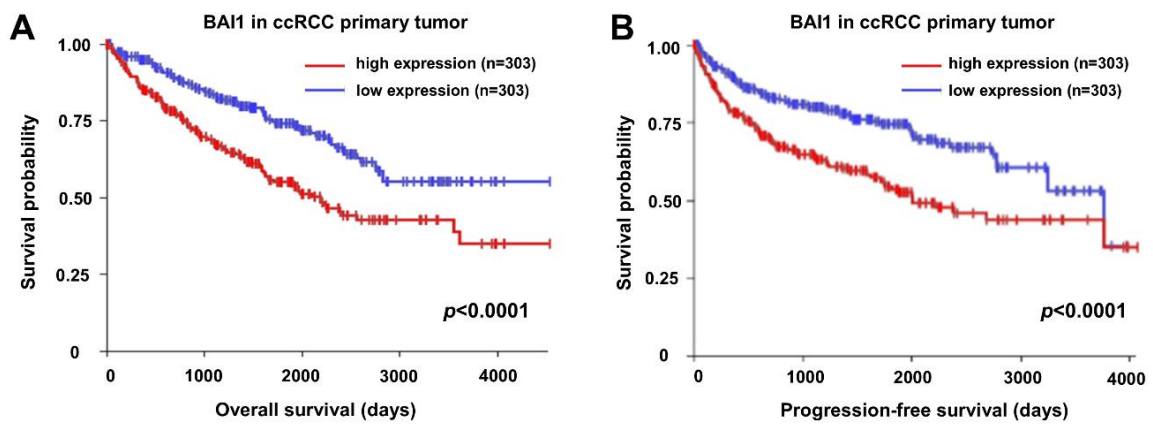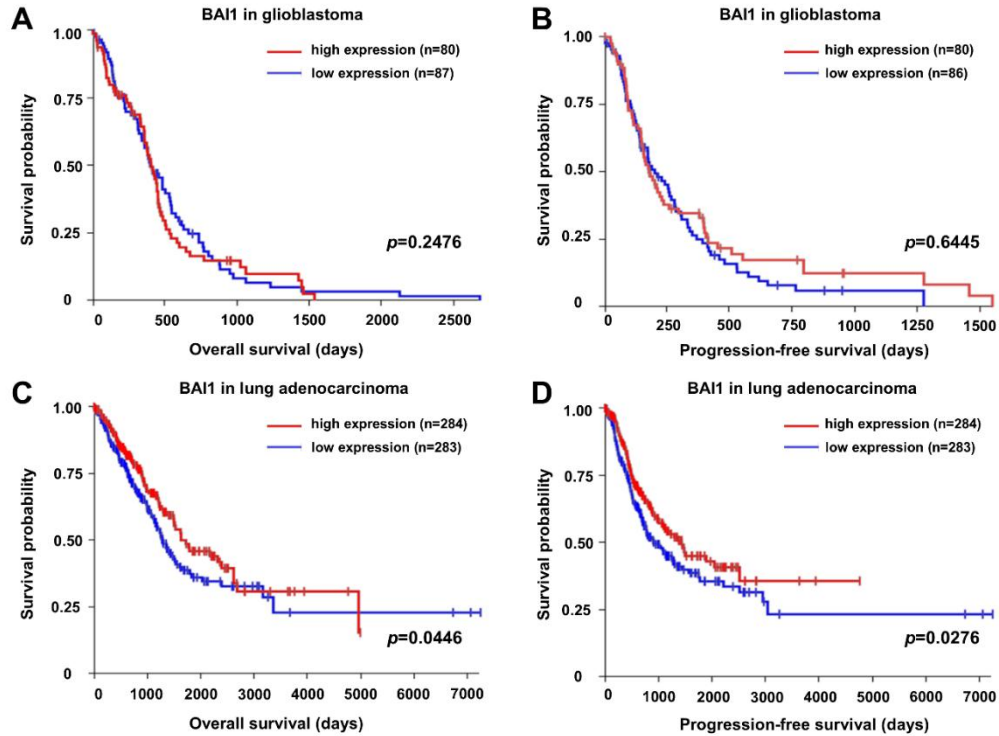Fig. 3. Kaplan-Meier curves showing relation of BAI1 expression to overall survival (OS) and to progression-free survival (PFI) in TCGA Glioblastoma (GBM) group of patients (A,B) and in TCGA Lung Adenocarcinoma (LUAD) group of patients (C,D). There is no relation of BAI1 expression to patients' outcome in glioblastoma. In lung adenocarcinoma it was recorded that patients with lower BAI1 expression had significantly shorter both OS and PFI.

4. Discussion

In management of ccRCC patients, precise patient stratification on the basis of prognostic algorithm helps personalize the treatment algorithms to match patient profiles (personalized medicine). According to American Society of Clinical Oncology (ASCO) and European Society for Medical Oncology (ESMO) guidelines [20,21], stratification of patients with advanced ccRCC into groups of favorable, intermediate, and poor prognosis is important for the selecting appropriate treatment regimen. There are efforts to find new molecular prognostic biomarkers to improve the currently used Memorial Sloan Kettering Cancer Center (MSKCC) scoring system. It can be achieved by employing advanced molecular technologies [7].

Based on the tissue expression of 97 genes involved in angiogenesis (TaqMan human Angiogenesis Array), applying Cox regression model, we identified 4 genes (PDGF-B, FGF4, EPHB2 and BAI1) in relation to PFI. In our set of tissue samples we recorded that high expression levels of BAI1, PDGF-B, FGF4, and EPHB2 were associated with shorter PFI.

Platelet-derived growth factor-B (PDGF-B) is responsible for proliferation and migration of cells during vascular maturation. Wang et al. in 2015 showed that high expression of PDGF-B was associated with significantly decreased risk of ccRCC mortality [22]. An-other study which included PDGF-B expression in ccRCC did not observe any relation to prognosis [23]. Taken together with our data, the results on PDGF-B are inconclusive. Fibroblast growth factor 4 (FGF4) has been reported to induce epithelial-mesenchymal transition (EMT) in lung adenocarcinoma [24]. According to our knowledge, there are no published data showing relation of FGF4 to prognosis ccRCC. EphB2 is a member of large

family of receptor tyrosine kinases with roles in cell motility, EMT and angiogenesis. It appears prognostic in multiple malignancies, especially colorectal cancers [25]. Ghatalia et al. showed differential expression of EphB2 between primary tumor and metastasis of ccRCC with higher expression in metastases [26].

Using Kaplan Meier analysis applied on genes identified by Cox regression model and external validation on publically available expression data (TCGA KIRC database), we identified the BAI1 as a promising prognostic marker in ccRCC patients with the potential to be incorporated in the scoring system.

Brain-specific angiogenesis inhibitor 1 (BAI1) also known as adhesion G protein-coupled receptor B1 (ADGRB1) was isolated and characterized for the first time as a target gene transactivated by P53 [27]. Today we know it belongs to the adhesion G-protein coupled receptors (aGPCRs) subfamily of seven transmembrane spanning receptors (7TMRs) [28,29].

There is a high expression of BAI1 in the brain, however it is expressed also in other tissues like kidney or lungs. It has been described that BAI1 is involved in neuronal synaptogenesis and process of phagocytosis (ref). It was found BAI1 plays a role of tumor suppressor in glioblastoma (ref). BAI1 was named for the ability of its inhibiting angiogenesis in glioblastomas. Liu et al. observed its tumor suppressor effect in lung cancer cells [ref]. These results indicating tumor suppressor function of BAI suggest that high levels of BAI1 have to be associated with better patients' outcome. This corresponds to the results we obtained from the public databases on lung adenocarcinoma patients, where a high level of BAI1 expression meant a better prognosis (Figure 3 C,D). In the case of glioblastoma, we revealed no relationship of BAI1 expression to prognosis (Figure 3 A,B).

In renal cancer, in 2007 Kudo et al. published a work on transgenic mice concluding that the transfer of the BAI1 gene can suppress the tumor growth via the inhibition of angiogenesis [30]. Another study on renal cancer and BAI1 by Izutsu et al. was published in 2011. The authors observed significant decrease in BAI1 mRNA in renal cell carcinoma tissue compared with normal kidney tissue

in a group of 47 renal cell carcinoma patients. Additional to that they detected lower expression in advanced renal cell carcinoma than in localized renal cell carcinoma [31].

However, in our study on ccRCC patients both data obtained from our group (20 patients) and data from TCGA database (606 patients) independently showed that the patients with high BAI1 expression in ccRCC tumor tissue had worse outcome in terms of both shorter OS and PFI. It suggests more complex involvement of BAI1 in cancerogenesis. At this point it is necessary to mention that majority of patients with ccRCC undergoes treatment based on antiangiogenic therapeutics. Of course, there is a question how much BAI1 involved in angiogenesis and probably also in other processes is in relation to the effect of antiangiogenic treatment.

Until now, there were a couple of gene expression panels for the assessment of prognosis of ccRCC patients proposed (none of them included BAI1). Liu et al. constructed a panel containing a cluster of 10 metabolism related genes (ALDH6A1, FBP1, HAO2, TYMP, PSAT1, IL4I1, P4HA3, HK3, CPT1B, and CYP26A1) [32]. Pan et al. identified differentially expressed genes involved in the metastasis of ccRCC and proposed a 5-gene (OTX1, MATN4, PI3, ERVV-2, and NFE4) panel predicting progression and prognosis [13].

5. Conclusions

The identification of BAI1 as prognostic marker in ccRCC is the first step to involve this gene in expression prognostic panels which could improve scoring systems as MSKCC on which the management of metastatic ccRCC patients is based. Gene expression panels are a promising tool how to individualize patients' treatment as a part of personalized medicine.

Conflicts of Interest: The authors declare no conflict of interest.

References

[1]   Padala SA, Barsouk A, Thandra KC, Saginala K, Mohammed A, Vakiti A, et al. Epidemiology of Renal Cell Carcinoma. World J Oncol 2020;11:79–87. https://doi.org/10.14740/wjon1279.

[2]   Wong MCS, Goggins WB, Yip BHK, Fung FDH, Leung C, Fang Y, et al. Incidence and mortality of kidney cancer: temporal patterns and global trends in 39 countries. Sci Rep 2017;7. https://doi.org/10.1038/s41598-017-15922-4.

[3]   Carril-Ajuria L, Santos M, Roldán-Romero JM, Rodriguez-Antona C, de Velasco G. Prognostic and Predictive Value of PBRM1 in Clear Cell Renal Cell Carcinoma. Cancers 2019;12. https://doi.org/10.3390/cancers12010016.

[4]   Wang Q, Tu H, Zhu M, Liang D, Ye Y, Chang DW, et al. Circulating obesity-driven biomarkers are associated with risk of clear cell renal cell carcinoma: a two-stage, case-control study. Carcinogenesis 2019;40:1191–7. https://doi.org/10.1093/carcin/bgz074.

[5]   Angulo JC, Shapiro O. The Changing Therapeutic Landscape of Metastatic Renal Cancer. Cancers 2019;11:1227. https://doi.org/10.3390/cancers11091227.

[6]   Motzer RJ, Mazumdar M, Bacik J, Berg W, Amsterdam A, Ferrara J. Survival and Prognostic Stratification of 670 Patients With Advanced Renal Cell Carcinoma. J Clin Oncol 1999;17:2530–2530. https://doi.org/10.1200/JCO.1999.17.8.2530.

[7]   Kotecha RR, Motzer RJ, Voss MH. Towards individualized therapy for metastatic renal cell carcinoma. Nat Rev Clin Oncol 2019;16:621–33. https://doi.org/10.1038/s41571-019-0209-1.

[8]   Voss MH, Reising A, Cheng Y, Patel P, Marker M, Kuo F, et al. Genomically annotated risk model for advanced renal-cell carcinoma: a retrospective cohort study. Lancet Oncol 2018;19:1688–98. https://doi.org/10.1016/S1470-2045(18)30648-X.

[9]   Golubnitschaja O, Baban B, Boniolo G, Wang W, Bubnov R, Kapalla M, et al. Medicine in the early twenty-first century: paradigm and anticipation - EPMA position paper 2016. EPMA J 2016;7:23. https://doi.org/10.1186/s13167-016-0072-4.

[10]   Lin H-H, Wei N-C, Chou T-Y, Lin C-C, Lan Y-T, Chang S-C, et al. Building personalized treatment plans for early-stage colorectal cancer patients. Oncotarget 2017;8:13805–17. https://doi.org/10.18632/oncotarget.14638.

[11]   Xin L, Liu Y-H, Martin TA, Jiang WG. The Era of Multigene Panels Comes? The Clinical Utility of Oncotype DX and MammaPrint. World J Oncol 2017;8:34–40. https://doi.org/10.14740/wjon1019w.

[12]   Lin X, Kapoor A, Gu Y, Chow MJ, Peng J, Major P, et al. Construction of a Novel Multigene Panel Potently Predicting Poor Prognosis in Patients with Clear Cell Renal Cell Carcinoma. Cancers 2020;12. https://doi.org/10.3390/cancers12113471.

[13]   Pan Q, Wang L, Zhang H, Liang C, Li B. Identification of a 5-Gene Signature Predicting Progression and Prognosis of Clear Cell Renal Cell Carcinoma. Med Sci Monit Int Med J Exp Clin Res 2019;25:4401–13. https://doi.org/10.12659/MSM.917399.

[14]   Cancer Genome Atlas Research Network, Weinstein JN, Collisson EA, Mills GB, Shaw KRM, Ozenberger BA, et al. The Cancer Genome Atlas Pan-Cancer analysis project. Nat Genet 2013;45:1113–20. https://doi.org/10.1038/ng.2764.

[15]   Sobin LH, Gospodarowicz MK, Wittekind C. TNM Classification of Malignant Tumours. Somerset: Wiley; 2011.

[16]   Eisenhauer EA, Therasse P, Bogaerts J, Schwartz LH, Sargent D, Ford R, et al. New response evaluation criteria in solid tumours: revised RECIST guideline (version 1.1). Eur J Cancer Oxf Engl 1990 2009;45:228–47. https://doi.org/10.1016/j.ejca.2008.10.026.

[17]   Smid D, Kulda V, Srbecka K, Kubackova D, Dolezal J, Daum O, et al. Tissue microRNAs as predictive markers for gastric cancer patients undergoing palliative chemotherapy. Int J Oncol 2016;48:2693–703. https://doi.org/10.3892/ijo.2016.3484.

[18]   Pesta M, Cedikova M, Dvorak P, Dvorakova J, Kulda V, Srbecka K, et al. Trends in gene expression changes during adipogenesis in human adipose derived mesenchymal stem cells under dichlorodiphenyldichloroethylene exposure. Mol Cell Toxicol 2018;14:369–79. https://doi.org/10.1007/s13273-018-0041-1.

[19]   Goldman MJ, Craft B, Hastie M, Repečka K, McDade F, Kamath A, et al. Visualizing and interpreting cancer genomics data via the Xena platform. Nat Biotechnol 2020;38:675–8. https://doi.org/10.1038/s41587-020-0546-8.

[20]   Graham J, Heng DYC, Brugarolas J, Vaishampayan U. Personalized Management of Advanced Kidney Cancer. Am Soc Clin Oncol Educ Book 2018:330–41. https://doi.org/10.1200/EDBK_201215.

[21]   Escudier B, Porta C, Schmidinger M, Rioux-Leclercq N, Bex A, Khoo V, et al. Renal cell carcinoma: ESMO Clinical Practice Guidelines for diagnosis, treatment and follow-up. Ann Oncol 2019;30:706–20. https://doi.org/10.1093/annonc/mdz056.

[22]   Wang W, Qi L, Tan M, Zhang Z, Du J, Wei X, et al. Effect of platelet-derived growth factor-B on renal cell carcinoma growth and progression. Urol Oncol Semin Orig Investig 2015;33:168.e17–168.e27. https://doi.org/10.1016/j.urolonc.2014.12.015.

[23]   Shim M, Song C, Park S, Choi S-K, Cho YM, Kim C-S, et al. Prognostic significance of platelet-derived growth factor receptor-β expression in localized clear cell renal cell carcinoma. J Cancer Res Clin Oncol 2015;141:2213–20. https://doi.org/10.1007/s00432-015-2019-x.

[24]   Qi L, Song W, Li L, Cao L, Yu Y, Song C, et al. FGF4 induces epithelial-mesenchymal transition by inducing store-operated calcium entry in lung adenocarcinoma. Oncotarget 2016;7:74015–30. https://doi.org/10.18632/oncotarget.12187.

[25]   Jang BG, Kim HS, Chang WY, Bae JM, Kang GH. Prognostic Significance of EPHB2 Expression in Colorectal Cancer Progression. J Pathol Transl Med 2018;52:298–306. https://doi.org/10.4132/jptm.2018.06.29.

[26]   Ghatalia P, Yang ES, Lasseigne BN, Ramaker RC, Cooper SJ, Chen D, et al. Kinase Gene Expression Profiling of Metastatic Clear Cell Renal Cell Carcinoma Tissue Identifies Potential New Therapeutic Targets. PLOS ONE 2016;11:e0160924. https://doi.org/10.1371/journal.pone.0160924.

[27]   Van Meir EG, Polverini PJ, Chazin VR, Su Huang HJ, de Tribolet N, Cavenee WK. Release of an inhibitor of angiogenesis upon induction of wild type p53 expression in glioblastoma cells. Nat Genet 1994;8:171–6. https://doi.org/10.1038/ng1094-171.

[28]   Nieto Gutierrez A, McDonald PH. GPCRs: Emerging anti-cancer drug targets. Cell Signal 2018;41:65–74. https://doi.org/10.1016/j.cellsig.2017.09.005.

[29]   Stephenson JR, Purcell RH, Hall RA. The BAI subfamily of adhesion GPCRs: synaptic regulation and beyond. Trends Pharmacol Sci 2014;35:208–15. https://doi.org/10.1016/j.tips.2014.02.002.

[30]   Kudo S, Konda R, Obara W, Kudo D, Tani K, Nakamura Y, et al. Inhibition of tumor growth through suppression of angiogenesis by brain-specific angiogenesis inhibitor 1 gene transfer in murine renal cell carcinoma. Oncol Rep 2007;18:785–91.

[31]   Izutsu T, Konda R, Sugimura J, Iwasaki K, Fujioka T. Brain-Specific Angiogenesis Inhibitor 1 is a Putative Factor for Inhibition of Neovascular Formation in Renal Cell Carcinoma. J Urol 2011;185:2353–8. https://doi.org/10.1016/j.juro.2011.02.019.

[32]   Liu M, Pan Q, Xiao R, Yu Y, Lu W, Wang L. A cluster of metabolism-related genes predict prognosis and progression of clear cell renal cell carcinoma. Sci Rep 2020;10:12949. https://doi.org/10.1038/s41598-020-67760-6.

PŘÍLOHA 8

Novinky z genetiky, molekulární biologie a klinické onkologie sarkomů

Novel Aspects of Genetics, Molecular Biology and Clinical Oncology of Sarcomas

Houfková K., Hatina J.

Ústav biologie, LF UK v Plzni

Souhrn

Ve dnech 14.–17. listopadu 2018 se v Římě uskutečnila velká mezinárodní konference Connective Tissue Oncology Group Annual Meeting 2018 (CTOS 2018), která svedla dohromady naprostou většinu nejvýznamnějších specialistů jak na molekulární biologii, tak i klinickou onkologii sarkomů, především sarkomů měkkých tkání. Ve dnech 8.–10. května 2019 se potom v Bergenu konala regionální konference The 39th Plenary Meeting of the Scandinavian Sarcoma Group (SSGM 2019). Soubory otázek, které byly na obou konferencích diskutovány formou přednáškových či posterových sdělení, lze rozdělit do několika zastřešujících okruhů. Byl představen velký projekt zaměřený na objasnění germinální genetiky sarkomů; dosavadní výsledky ukazují na překvapivě velký význam genů kódujících proteiny, které zajišťují integritu telomer, jakož i existenci komplexních mechanizmů genetické predispozice zahrnující polygenní dědičnost či modifikační geny. Problematice somatické genetiky sarkomů dominuje analýza vzniku a mechanizmu účinku fúzních onkogenů odpovídajících za iniciaci značné části především pediatrických sarkomů. U karyotypicky komplexních sarkomů je evidentní snaha po patobiologické specifikaci do subtypů, ať už na základě specifické klinické charakterizace (uterinní leiomyosarkom vs. leiomyosarkom měkkých tkání), či specifických expresních profilů genů (molekulární subtypy nediferencovaného pleiomorfního sarkomu). Molekulární charakterizace může být vodítkem pro koncipování subtypově specifických terapeutických protokolů, jak je tomu v různém měřítku u obou shora zmíněných příkladů. Mezi další prominentní typy sarkomů, u nichž se podařilo transformovat základní molekulárně biologické poznatky do podoby úspěšné cílené terapie, patří např. gastrointestinální stromální tumor, infantilní fibrosarkom či inflamatorní myofibroblastický tumor, a rovněž u světlobuněčného sarkomu a dediferencovaného liposarkomu byly obdobné koncepty prezentovány, byť jejich dosavadní účinnost zůstává za očekáváním, a podobná situace zatím přetrvává u osteosarkomu. Z hlediska molekulárních struktur, na které lze zaměřit cílenou terapii, zaujímá v oblasti sarkomů měkkých tkání zcela zásadní postavení signální systém destičkového růstového faktoru, a to jak u vzácných typů založených na přímé iniciační mutační aktivaci (relativně malá část gastrointestinálních stromálních tumorů, infantilní hereditární myofibromatóza, dermatofibrosarcoma protuberans), u kterých cílená terapie využívá především nízkomolekulárních tyrozinkinázových inhibitorů, tak rovněž u širokého spektra obvyklých typů sarkomů, kde se součástí kombinační chemoterapie stává specifická blokující anti-PDGFRα-protilátka olaratumab. V oblasti klinické prognózy byl pozoruhodný vývoj zaznamenán zejména u tzv. prognostických nomogramů. Zajímavé výsledky byly rovněž prezentovány v oblasti odvození nových experimentálních modelů vzniku a progrese sarkomů.

Klíčová slova

sarkomy měkkých tkání – osteosarkom – genetická predispozice – molekulární subtypy – cílená terapie – prognostické nomogramy – experimentální modely sarkomatogeneze

Summary

The Connective Tissue Oncology Group Annual Meeting 2018 (CTOS 2018) took place in Rome from 4 to 17 November 2018, and the 39th Plenary Meeting of the Scandinavian Sarcoma Group (SSGM 2019) was held in Bergen from 8 to 10 May 2019. These two large international conferences brought together an overwhelming majority of molecular and clinical specialists in the sarcoma field, especially those working on soft tissue sarcoma. Topics discussed on the conferences included, among others, sarcoma genetics, clinical and molecular subclassification, targeted therapy, clinical prognostication, and new experimental sarcoma models. A large ongoing international study on germinal sarcoma genetics was presented, the interim results of which revealed the extremely complex nature of genetic disposition to sarcoma, and, surprisingly, a rather prominent place among predisposing genes for those coding for structural telomere constituents. Fusion oncogenes dominate somatic sarcoma genetics, especially because of their origin and impact on sarcoma clinical behaviour, and are especially relevant for karyotypically simple paediatric sarcomas. A crucial issue in karyotypically complex sarcomas are the efforts being made to obtain a subclassification of sarcoma, other than those based on pathology, using either the clinical characteristics of sarcomas (uterine leiomyosarcoma vs. soft tissue leiomyosarcoma) or specific gene expression profiles (molecular subtypes in undifferentiated pleiomorphic sarcoma), which showed that molecular characterization can open the way for subtype specific therapies. Other examples of where this type of strategy can be applied include gastrointestinal stromal tumours, infantile fibrosarcoma, and inflammatory myofibroblastic tumours, where targeted therapy could be conceived based on the actionable mutations identified. Attempts in this direction have been made also for clear cell sarcoma and dedifferentiated liposarcoma, albeit the effectiveness of molecular-targeted treatments for these sarcomas is still poor, and progress in the treatment of osteosarcoma is still rather slow. Actually, the platelet-derived growth factor signalling system holds a prominent position in searches for targeted therapies, not only against rare sarcoma types, where are activated by mutations (some gastrointestinal stromal tumours, infantile hereditary myofibromatosis, and dermatofibrosarcoma protuberans), but also against other more usual sarcoma types, where the blocking anti-PDGFRα-antibody olaratumab has been successfully integrated into combinatorial chemotherapeutic regimens. In the field of clinical prognostication, remarkable progress in sarcoma nomograms was reported. Interesting results were also presented in the area of new experimental sarcoma models.

Key words

soft tissue sarcomas – osteosarcoma – chondrosarcoma – genetic predisposition – molecular subtypes – targeted therapy – prognostic nomograms – experimental sarcoma models

Genetika sarkomu

Germinální genetika sarkomů, tj. dědičná nádorová predispozice k sarkomu, představuje neobyčejně komplexní problematiku, a to nejen vzhledem k šíři různých konkrétních diagnóz, které lze v současnosti uvnitř rodiny mezenchymálních nádorů rozlišit (více než 70 různých typů [1]). Nejnovější vývoj v rámci projektu zaměřeného na zmapování genů zodpovědných za dědičnou nádorovou predispozici k sarkomu na konferencích Connective Tissue Oncology Group Annual Meeting 2018 (CTOS 2018) a The 39th Plenary Meeting of the Scandinavian Sarcoma Group (SSGM 2019) představila dr. M. Ballinger. Tento projekt nese označení International Sarcoma Kindred Study (ISKS) a ve své aktuální podobě zahrnuje 2 933 probandů postižených různými typy sarkomů, 2 623 jejich příbuzných 1. stupně, od nichž je k dispozici celkem 4 328 vzorků DNA a cca 600 histologických vzorků nádorové tkáně, a rovněž rodokmenovou informaci zhruba 105 000 příslušníků těchto rodin. Od 1 109 probandů již byla získána úplná genetická informace metodikou celogenomového sekvenování nové generace. Tyto impozantní rozměry studie si vynutila řada komplikujících faktorů genetiky sarkomu. Především, až na jednu výjimku, o které se zmíníme později, nebyl dosud popsán žádný mendelisticky dědičný syndrom nádorové predispozice, který by se týkal výlučně či převážně sarkomu (ani jakožto široké skupiny mezenchymálních nádorů, ani žádného z jednotlivých konkrétních typů), jinými slovy neexistuje prakticky žádná sarkomová obdoba např. syndromu dědičné nádorové predispozice k nádorům prsu a vaječníku, familiární adenomatózní polypózy nebo rodinného melanomu. Na druhé straně jsou ovšem různé sarkomy stabilní součástí řady různých syndromů dědičné nádorové predispozice, vč. tří výše zmíněných, a rovněž např. Lynchova syndromu, Li-Fraumeniho syndromu či rodinného retinoblastomu. Jedním z průběžných výsledků projektu ISKS je stanovení relativních rizik pro vývoj sarkomu podmíněných evidentními či pravděpodobnými mutantními alelami (označovanými jako C3, C4 a C5 alelické varianty Mezinárodní agenturou pro výzkum rakoviny (International Agency for Research on Cancer)) celé řady známých „nádorových" genů (tab. 1).

Jeden aspekt se v uvedené studii ukázal jako docela specifický pro různé typy sarkomů, a to velmi významné postavení genů kódujících proteiny zodpovědné za integritu telomery (POT1, TIN2, TRF1). Tyto proteiny spolu navzájem interagují a spolu s dalšími proteiny (TRF2, TPP1 a RAP1) tvoří tzv. „shelterin complex", který chrání terminální části telomery. POT1 má klíčové postavení, protože přímo interaguje jednak s telomerovou jednořetězcovou DNA, jednak prostřednictvím TPP1 i s celým ochranným komplexem. POT1 blokuje přístup telomerázy, a je-li tato funkce porušena, dochází k aberantnímu prodloužení telomer, což má za následek jejich destabilizaci, která může být důležitou součástí, či dokonce iniciátorem destabilizace karyotypu. Samotný POT1 byl nezávisle identifikován jakožto kauzální mutovaný gen u čtyř španělských rodin segregujících celé spektrum nádorů vč. četných sarkomů, i velmi vzácných, jako je angiosarkom srdce či prsu [2]. Identifikovaná mutace (R117C) vede ke ztrátě afinity jak vůči telomeře, tak vůči TPP1 a u nositelů mutace skutečně dochází jak k signifikantnímu prodloužení telomery, tak k nárůstu ohnisek poškozené DNA v oblasti telomery. Dosavadní výsledky projektu ISKS tento předchozí raritní nález potvrzují a rozšiřují, zejména se ukazuje,

že mutace v *POT1* genu predisponují obzvláště ke vzniku častých karyotypicky komplexních sarkomů, jako je osteosarkom nebo leiomyosarkom. V této souvislosti stojí ovšem za to poukázat na výsledky, které prokázaly, že např. u liposarkomu dochází naopak ke stabilizaci telomer aktivací telomerázy, a to buď bodovou mutací v promotoru genu pro katalytickou podjednotku telomerázy hTERT, jako je tomu u myxoidního liposarkomu [3], nebo v důsledku chromozomální translokace a zvýšení exprese *hTERT* genu, která byla prokázána u dediferencovaného liposarkomu [4]. Tato oblast tedy ještě zřejmě přinese řadu překvapivých výsledků.

Jinou komplikací dědičné nádorové predispozice k sarkomu je existence polygenní dědičné složky. Již předchozí publikované dílčí výsledky projektu ISKS ukázaly, že C3 varianty mají výraznou tendenci chovat se aditivně, tj. současné zdědění několika C3 variant v různých genech proporcionálně zvyšuje riziko vzniku sarkomu [5]. Přechodem mezi monogenním a polygenním způsobem dědičnosti je uplatnění tzv. genů modifikátorů, jejichž patologické alely samy nemusejí nutně vést ke zvýšenému riziku, popř. mohou mít svůj specifický fenotypový dopad, ale v kombinaci s patologickou variantou tumorového supresoru či onkogenu výrazně modifikují jejich fenotypový projev, penetranci a expresivitu. Také v tomto ohledu mohou sarkomy nabídnout výborný příklad – mutace v genech *EXT1* a *EXT2* predisponují ke vzniku mnohočetného benigního osteochondromu (mnohočetné hereditární exostózy), v kombinaci s pa-

tologickými variantami celé řady jiných genů (*PMS2, WRN, RECQ4, MLH3, FANCA, FANCL, BUB1B, XPC, TP53, BRCA1, BRCA2, ERC, WT1*) ovšem signifikantně zvyšují riziko vzniku osteosarkomu a chondrosarkomu [5].

Somatické genetice sarkomů dominuje především téma fúzních onkogenů; současné představy o molekulární biologii a patologii sarkomů založených na fúzních onkogenech prezentovala na konferenci CTOS 2018 prof. Cristina R. Antonescu. Onkogeny aktivované genovou fúzí se pokládají za typickou vlastnost celé jedné skupiny sarkomů, které se vyznačují relativně stabilním karyotypem a relativně nízkým

věkem nástupu, který ovšem vykazuje značné rozpětí u různých konkrétních sarkomů, od novorozeneckých až po sarkomy vyskytující se v časné dospělosti. Biologickým důsledkem genové fúze je vznik chimérických onkoproteinů, které typicky kombinují specifické domény dvou různých proteinů; v této formě nejsou genové fúze nikterak specifické pro sarkomy, tento mutační mechanizmus je velmi obvyklý i u značné části leukemií a lymfomů a rovněž u některých karcinomů (např. karcinomu prostaty). Dlouhou dobu se myslelo, že hlavním mechanizmem vzniku fúzních onkogenů jsou reciproké translokace, u nichž dochází k translokačním zlomům uvnitř

Tab. 1. Přehled hlavních predisponujících lokusů ke vzniku sarkomu ze studie International Sarcoma Kindred Study.

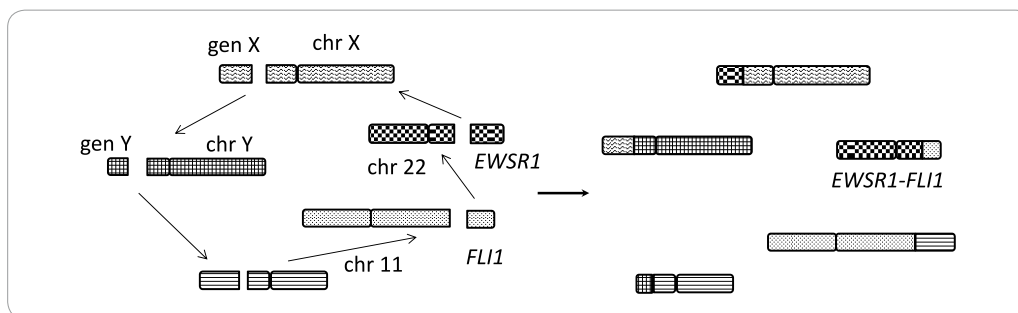| Gen	Všechny případy (n = 1109)	Kontrola (n = 2571)	Celková odezva (interval spolehlivosti)	p-hodnota
TP53	18	0	∞ (8,4–∞)	< 0,0001
POT1	8	0	∞ (3,5–∞)	< 0,0001
ATRIP	6	0	∞ (2,5–∞)	0,001
BRCA1	4	1	9,3 (1,0–218,8)	0,031
NF1	10	3	7,8 (2,0–35,7)	0,001
ERCC2	10	5	4,7 (1,5–15,7)	0,004
BRCA2	16	10	3,8 (1,6–8,9)	0,001
APC	10	7	3,3 (1,2–9,7)	0,015
ATM	12	10	2,8 (1,1–7,0)	0,018
TINF2	5	0	∞ (2,0–∞)	0,002
TERF1	2	0	∞ (0,6–∞)	NS

NS – není signifikantní

Schéma 1. Fúzní onkogeny jakožto výsledek komplexní chromozomální přestavby – chromoplexie. Upraveno podle [6].

Tab. 2. Sarkomy založené na fúzních onkogenech zahrnujících *EWSR1* gen.

EWSR1 – ETS (FLI1, ERG)	Ewingův sarkom / primitivní neuroektodermální tumor
EWSR1 – WT1	desmoplastický kulatobuněčný tumor
EWSR1 – NR4A3	extraskeletální myxoidní chondrosarkom
EWSR1 – DDIT3	myxoidní / kulatobuněčný liposarkom
EWSR1 – ATF1	světlobuněčný sarkom
EWSR1 – CREB1	angiomatoidní fibrózní histiocytom
EWSR1 – POUS5F1/ PBX1/3ZNF444/KLF17	myoepiteliální tumory
EWSR1 – TFCP2	rhabdomyosarkom

zúčastněných onkogenů, popř. méně často inverze či intersticiální delece. V době velmi nedávné byl objeven rozsáhlejší mechanizmus strukturální přestavby karyotypů vedoucí k tvorbě fúzních onkogenů, tzv. chromoplexe, představující soubor chromozomálních přestaveb zahrnujících několik chromozomů, které jsou translokovány v jakési uzavřené "translokační smyčce", tj. první chromozom s druhým, druhý s třetím, třetí se čtvrtým a čtvrtý zase s prvním (schéma 1) [6]. Zdá se, že se jedná o široce používaný mechanizmus, jenž byl zatím prokázán u Ewingova sarkomu, který tvoří historicky, biologicky i klinicky jakýsi prototyp sarkomu závislého na fúzním onkogenu, a dále u synoviálního sarkomu, chondromyxoidního fibromu a fosfaturického mezenchymálního tumoru a již dříve také v komplexnější podobě u karcinomu prostaty. Odhaduje se, že o něco méně než polovina případů Ewingova sarkomu připadá na vrub chromoplexii, zbytek připadá na reciproké translokace, přičemž první skupina vykazovala skoro dvojnásobnou četnost relapsu – komplexní způsob chromozomálních přestaveb v podobě chromoplexického translokačního cyklu lze tudíž považovat za jeden ze znaků agresivity nádoru [6].

Ewingův sarkom představuje paradigmatický typ sarkomu závislého na fúzním onkogenu ještě z několika hledisek. Hlavními dvěma charakteristikami této skupiny sarkomů a genů zúčastněných na tvorbě fúzních onkogenů jsou promiskuita a heterogenita. Podkladem klasického Ewingova sarkomu je genová fúze mezi genem *EWSR1* a jedním z genů kódujících transkripční faktory Ets-rodiny, nejčastěji *FLI1* (90 %), méně často *ERG* (5–8 %) a výjimečně *ETV1, FEV* či *E1AF* (souhrnně 1–2 %). *EWSR1* kóduje RNA-vazebný protein s kryptickou transkripčně aktivační doménou, která je mnohem silnější než přirozené transkripčně aktivační domény Ets-faktorů, fúzní onkogen tedy kombinuje tuto silnou transkripčně aktivační doménu původem *EWSR1* s DNA-vazebnou doménou Ets-faktorů a tento aberantní transkripční faktor vede k rozsáhlé deregulaci transkripce v buňce, která je podkladem maligní transformace.

Jedním z možných vysvětlení těchto dramaticky různých četností vzniku různých fúzních onkogenů jsou vzájemné orientace transkripce zúčastněných genů; zatímco *EWSR1* a *FLI1* jsou transkribovány v témže směru (oba od centromery k telomeře), *ERG* je transkribován v opačném směru. Výsledkem chromozomální přestavby musí být kontinuální biologicky smysluplná kódující sekvence. Jsou-li oba zúčastněné geny orientovány na svých chromozomech opačně, je složitější tuto souvislou "správnou" kódující sekvenci v důsledku chromozomální přestavby získat, a skutečně zatímco *EWSR1-FLI1* může být výsledkem jak reciproké translokace, tak chromoplexie, *EWSR1-ERG* vzniká výhradně na podkladě chromoplexie [6,7].

Řada dalších typů sarkomů na podkladě fúzních onkogenů vykazuje tuto molekulární heterogenitu, přičemž jeden z konkrétních fúzních onkogenů obvykle vysoce převažuje. Například inflamatorní myofibroblastický tumor zahrnuje více než deset alternativních fúzních onkogenů obsahujících gen pro tyrozinovou kinázu ALK, synoviální sarkom je iniciován fúzí genu *SS18* a jednoho z genů *SSX* lokalizovaných na X chromozomu (*SSX1, SSX2* nebo *SSX4*; je zajímavé, že *SSX3*, který je jako jediný transkribován v opačném směru, zatím jakožto součást fúzního onkogenu identifikován nebyl [7]) a u alveolárního rhabdomyosarkomu existuje heterogenita v obou genech (*PAX3/PAX7* a *FOXO1/ NCOA1* [7]). Na druhou stranu *EWSR1* se účastní tvorby fúzních onkogenů u podstatně širšího souboru sarkomů než je Ewingův sarkom (tab. 2) a současně Ewingův sarkom vykazuje nápadné morfologické i klinické podobnosti se sarkomy, jejichž podkladem jsou jiné fúzní onkogeny, např. *CIC-DUX4* (ve srovnání s klasickým Ewingovým sarkomem prognosticky horší a s výraznou preferencí pro měkké tkáně) či *BCOR-CCNB3* (prognosticky srovnatelný s klasickým Ewingovým sarkomem, s výraznou tkáňovou preferencí pro kost); všechny tyto tři typy jsou v současnosti řazeny do rodiny Ewingova sarkomu (Ewing- and Ewing--like tumours [8]).

V některých případech může dokonce prakticky jeden a tentýž fúzní onkogen tvořit podklad různých typů sarkomů, např. *EWSR1* fúzovaný s geny pro transkripční faktory *ATF/CREB* (tab. 3). Jak je možné vysvětlit tuto fenotypovou variabilitu? Hlavním možným vysvětlením jsou odlišné sekundární mutace typické pro každý jednotlivý typ nebo rozdíly v buněčných typech, u nichž dochází k prvotní chromozomální přestavbě a iniciaci sarkomageneze.

Je zajímavé, že použití celogenomového sekvenování nové generace umožnilo detekovat fúzní onkogeny i u typů sarkomů s komplexním karyotypem, jako leiomyosarkom, dediferencovaný liposarkom [4] nebo nediferencovaný pleiomorfní sarkom, není ovšem dosud jasné, jaká je jejich patobiologická funkce v iniciaci sarkomageneze těchto komplexních sarkomů, na rozdíl od předešle diskutované skupiny převážně pediatrických sarkomů se stabilním karyotypem, kde všechno hovoří pro to, že fúzní onkogeny hrají naprosto klíčovou

úlohu, představují tzv. „driver-mutace". Rovněž vzhledem ke značné nestabilitě karyotypicky komplexních sarkomů není jasné, jestli fúzní onkogeny přetrvávají např. v jistém klonu sarkomových buněk, nebo jestli jsou kontinuálně vytvářeny a ztráceny.

Molekulární subtypy sarkomů

Odhlédneme-li od zajímavých molekulárně genetických aspektů zmíněných výše, je nepochybné, že stanovení kauzální mutace, např. ve formě kritického fúzního onkogenu, je klíčové pro stanovení diagnózy. Se stále se prohlubujícím porozuměním molekulární biologii i klinickému chování sarkomů přitom pozorujeme stále jemnější a podrobnější diagnostické členění, kdy se dříve jednotná diagnostická skupina ukazuje jako heterogenní a rozpadá se do jemnějších, homogennějších a molekulárně i klinicky lépe definovaných podskupin. Zajímavý vývoj v tomto směru byl pozorován např. u embryonálního rhabdomyosarkomu (prof. C. R. Antonescu, CTOS 2018). Na rozdíl od alveolárního rhabdomyosarkomu s jeho dobře definovanými fúzními onkogeny *PAX3/PAX7-FOXO1/NCOA1* u embryonálního rhabdomyosarkomu doposud žádné molekulárně či patologicky definované podskupiny známy nebyly, obecnou genetickou charakteristikou byla absence chromozomálních přestaveb a zásadní onkogenní funkce bodových mutací v klíčových onkogenech a tumorových supresorových genech. V poslední době byla definována nová patologická skupina označená jako vřetenobuněčný/sklerozující rhabdomyosarkom, jejíž molekulární charakteristika opět prozradila značnou úroveň heterogenity. Jedna část těchto převážně pediatrických nádorů je opět iniciována fúzními onkogeny mezi geny kódujícími transkripční faktory podílející se významně na diferenciaci kosterního svalu (*SRF, TEAD1, VGLL2*) a transkripčními korepresory *CITED* a *NCOA2* – výsledkem je transkripční represe genů, které by normálně měly být v průběhu diferenciace kosterního svalu aktivovány, tedy dediferenciace a sarkomageneze. Druhá skupina vřetenobuněčného/sklerozujícího rhabdomyosarkomu má svůj molekulární podklad v inaktivujících bodových mutacích v genu kódujícím klíčový a hierarchicky nadřazený transkripční faktor diferenciace kosterního svalu MyoD1 (nejčastější je bodová mutace změny smyslu L122R v DNA-vazebné doméně). Podstatné je, že se tyto dva typy vřetenobuněčného/sklerozujícího rhabdomyosarkomu podstatně liší prognózou – zatímco subtyp založený na fúzních onkogenech je prognosticky příznivý, u MyoD1-mutovaných nádorů se jedná o velice agresivní typ spojený s vysokou a časnou mortalitou.

Z nádorů s komplexním karyotypem se už dlouhou dobu spekuluje o jisté molekulární dichotomii u leiomyosarkomu, přesněji opakovaně se objevují názory, že uterinní leiomyosarkom není biologicky ani klinicky totožný s leiomyosarkomem měkkých tkání. V době velmi nedávné byla provedena komplexní transkriptomická a genomická analýza v rámci projektu The Cancer Genome Anatomy (TCGA), která poskytla těmto hypotézám částečnou oporu [9]. Přestože uterinní leiomyosarkom a leiomyosarkom měkkých tkání si jsou svým expresním profilem a mutačním vzorem navzájem bližší než každý z nich vůči jakémukoliv jinému typu sarkomu, přece se v segregační analýze řadí do odlišných skupin, a bylo možné identifikovat molekulární dráhy, které jsou typické pro každý z nich. U uterinního leiomyosarkomu tak byla významně aktivnější dráha aktivovaná poškozenou DNA (DNA damage response pathway), zatímco leiomyosakrom měkkých tkání měl signifikantně aktivnější signální dráhu aktivovanou hypoxií a transkripčním faktorem HIF1α. Je také už delší dobu známá rozdílná aktivita steroidních receptorů; výše uvedená studie TCGA prokázala specifickou hypometylaci cílových genů pro estrogenový receptor (ERα) specificky u uterinního leiomyosarkomu a zvýšená exprese a aktivita samotného estrogenového, jakož i progesteronového receptoru u uterinního leiomyosarkomu vedla již k několika malým klinickým studiím testujícím prospěšnost integrace inhibitorů aromatáz do různých léčebných protokolů [10]. Tyto výsledky byly na konferenci CTOS 2018 rozšířeny o imunohistochemickou analýzu velkého souboru nádorů shromážděných v podobě „tissue microarrays" (TMA) (přednáška dr. I. M. Schaefer) (tab. 4), která potvrdila signifikantní rozdíly v četnosti mutací klíčových tumorových supresorových genů a v expresi steroidních receptorů mezi oběma subtypy leiomyosarkomu. Za povšimnutí stojí jeden rozpor mezi uváděnou studií TCGA a výsledky imunohistochemické analýzy TMA – zatímco první z nich identifikovala značnou frekvenci delecí *TP53* genu, v imunohistochemické studii TMA prezentované na konferenci byl naopak nalezen ve velké většině případů aberantně exprimovaný p53 prozrazující jeho stabilizaci specifickými bodovými mutacemi. Zatím není jasné, co by mohlo být příčinou tohoto rozdílu, jedná se ovšem o otázku, která je svými důsledky, zejména s ohledem na možnou perspektivní terapii, docela

Tab. 3. Sarkomy založené na fúzních onkogenech mezi *EWSR1* genem a geny pro transkripční faktory ATF-CREB rodiny.

EWSR1 – ATF1	světlobuněčný sarkom / angiomatoidní fibrózní histiocytom
	hyalinizující světlobuněčný sarkom
	pediatrický mezoteliom
	myxoidní intrakraniální mezenchymální tumor
EWSR – CREB1	světlobuněčný sarkom
	angiomatoidní fibrózní histiocytom
	primární plicní myxoidní mezenchymální tumor
EWSR1 – CREM	myxoidní intrakraniální mezenchymální tumor
	světlobuněčný sarkom

Tab. 4. Výsledky imunohistochemické analýzy leiomysarkomů měkkých tkání a uterinních leiomyosarkomů.

	Všechny případy	Leiomyosarkom měkkých tkání	Uterinní leiomyosarkom	Primární tumor	Recidiva[#]
Imunoprofilace	100 % (n = 712)	52 % (n = 358)	50 % (n = 354)	44 % (n = 312)	56 % (n = 400)
Inaktivní forma					
p16	16 %	13 % *	19 % *	18 %	14 %
RB1	89 %	93 % *	84 % *	87 %	90 %
p16 (w/ponechaný RB1)	5 %	4 %	7 %	7 %	4 %
TP53	87 %	90 %	84 %	84 %	89 %
PTEN	41 %	48 %	32 % *	46 % *	39 % *
PTEN + TP53	35 %	44 %	25 % *	38 %	33 %
PTEN + p16 (W/ponechaný RB1)	1 %	2 %	0 %	1 %	1 %
Středně vysoká/vysoká exprese					
ER/PR	34 %	15 % *	54 % *	28 % *	39 % *
ER/PR (w/inaktivní PTEN)	9 %	6 % *	13 % *	12 % *	1 % *

* p < 0,05; [#] zahrnuje lokální recidivy a vzdálené recidivy
ER – estrogenový receptor, PR – progesteronový receptor

důležitá, poněvadž stabilizovaný bodově mutovaný p53 může být přístupný navrácení do nativní konformace specifickými malými molekulami [11] (autoři výše uvedené přednášky dokonce spekulovali o budoucí možnosti této léčby), což samozřejmě u deletovaného p53 nepřichází v úvahu.

Není asi nikterak překvapující, že jednou ze sarkomových diagnóz, která přímo volala po identifikaci molekulárních subtypů, je nediferencovaný pleiomorfní sarkom (undifferentiated pleomorphic sarcoma – UPS), diagnóza, která je často přijímána vylučovacím způsobem a je tudíž ze své podstaty heterogenní. Ostatně už výše citovaná komplexní studie TCGA prokázala kontinuum mezi nediferencovaným pleiomorfním sarkomem a myxofibrosarkomem. Problematiku heterogenity UPS objasnila ve své přednášce na konferenci CTOS 2018 dr. M. Toulmondé, která podrobila sérii 26 primárních nádorových vzorků diagnostikovaných s tímto typem sarkomu komplexní expresní (RNA sekvenování) i genomové (celoexomové sekvenování) a proteomické analýze. Vzorky nediferencovaného pleiomorfního sarkomu se na základě zejména expresní

analýzy rozpadly do tří skupin, dvou vyhraněně odlišných a mezi nimi jedné intermediární. Jedna ze skupin v sobě nesla část expresního profilu prozrazujícího aktivní zánětlivou reakci (pojmenovaná jako „hot-nádory"). Tato skupina měla signifikantně vyšší hladinu bodových mutací; není vyloučeno, že zde existuje oboustranná příčinná souvislost s aktivní zánětlivou reakcí – kyslíkové a dusíkové radikály vylučované zánětlivými buňkami mají prokazatelnou mutagenní aktivitu, současně vysoká úroveň bodových mutací a z toho vyplývající prezentace nádorových antigenů může přilákat do prostředí nádoru imunokompetentní buňky. Druhá, vyhraněně odlišná skupina nádorů, nazvaná případně „cold", vykazovala výrazně vyšší strukturální chromozomální nestabilitu (copy number alteration, tj. rozsáhlejší delece a amplifikace) a byla prognosticky signifikantně méně příznivá. Jednou ze signálních molekul specificky aktivovaných v této skupině je FGFR2, receptorová tyrozinová kináza, pro niž jsou k dispozici specifické nízkomolekulární inhibitory v pokročilé fázi vývoje, a skutečně jeden z těchto inhibitorů (JNJ-42756493) významně inhi-

boval proliferaci „cold-UPS" buněčných linií i primárního xenotransplantačního modelu; tento efekt byl vysoce specifický, u „hot-UPS" experimentálních modelů jej nebylo možné detekovat. Naopak signální dráhy typické pro „hot" podskupinu zahrnovaly transkripční faktor Myc a dále faktory asociované s epiteliálně-mezenchymální tranzicí. Vzhledem k vysoké imunitní infiltraci by se v tomto případě nabízel imunoterapeutický postup, např. formou protilátek proti klíčovým inhibitorům T lymfocytů (tzv. checkpoint inhibitory – CTLA-4, PD-1 či PD-1L [12]), o nichž se dnes diskutuje v souvislosti s většinou nádorů, vč. sarkomů (např. právě probíhající studie IMMUNOSARC [13] či možné uplatnění imunomodulátoru mifamutridu, které se pozvolna začíná stále více prosazovat u osteosarkomu – viz dále).

Molekulární biologie sarkomů jakožto cesta k identifikaci racionální personalizované terapie

Příklad molekulárních subtypů nediferencovaného pleiomorfního sarkomu ukazuje možnou hlavní aplikaci molekulární biologie sarkomageneze, totiž mož-

nou identifikaci optimální protinádorové terapie, která by byla přesně přizpůsobena molekulárním změnám v nádorových buňkách a přesně na tyto změny zacílena [14]. Bohužel už výše uvedené příklady sarkomů založených na fúzních onkogenech naznačily, že pro většinu z nich je podobná strategie zatím nedostupná, poněvadž hlavní funkční kategorií proteinů, kterých se vznik fúzních onkogenů týká, jsou aberantní transkripční faktory a v současné době není k dispozici žádná klinicky zralá strategie jejich inhibice. Již současné použití cílené terapie u karcinomů a hematologických malignit prozrazuje, že naopak v zásadě dobře zvládnutá je farmakologická inhibice různých onkogenních kináz. Bohužel jen nemnoho sarkomů je molekulárně založeno právě na aberantní kinázové aktivitě. Nicméně takové příklady také existují a u některých z nich byl na konferenci prezentován pozoruhodný terapeutický pokrok.

Poměrně velká pozornost byla na konferenci CTOS 2018 věnována infantilnímu fibrosarkomu (satelitní sympozium vedené dr. G. S. Demetrim, dr. S. DuBoisem a prof. J. Y. Blayem, přednáška pronesená dr. N. Federmanem). Jedná se o vzácný novorozenecký až dětský nádor, jehož metastatická kapacita je sice omezená, který ale roste rychle a lokálně invazivně, což při radikálním operativním zásahu s sebou často nese trvalou invalidizaci dítěte, a pro nějž nebyl k dispozici spolehlivý chemoterapeutický režim, nehledě na obecnou problematičnost klasické chemoterapie u dětí takto nízkého věku. Již koncem 90. let 20. století byla u infantilního fibrosarkomu odhalena fúze genu pro transkripční faktor *ETV6* a genu *NTRK3* kódujícího tyrozinovou kinázu TRKC [15]; v tomto případě, přestože se genové fúze účastní gen pro transkripční faktor, je její dopad odlišný než u příkladů citovaných výše, poněvadž *ETV6* přispívá do výsledného fúzního onkogenu, resp. onkoproteinu toliko svým promotorem a dimerizační doménou, a NTRK3 dodává intracelulární doménu vč. katalytické domény receptorové tyrozinkinázy *TRKC*. Výsledkem fúze tedy není globální deregulace transkripce, ale konstitutivně aktivní kináza. TRKC je jednou z trojice receptorových

kináz pro neurotrofní růstové faktory, zbylé dvě jsou TRKA a TRKB, kódované geny *NTRK1* a *NTRK2* [16], jejichž genové fúze byly v nádorech rovněž identifikovány, vč. infantilního fibrosarkomu (např. *TMP3-NTRK1, PDE4DPI-NTRK1, SQSTM1--NTRK1* nebo *LMNA-NTRK1* [17,18]; 5'-fúzní partner vždy musí dodávat promotor aktivní v mezenchymálních buňkách, jelikož uvedené kinázy sloužící jako receptory pro neurotrofní růstové faktory jsou fyziologicky exprimovány v nervové tkáni, a nějakou formu dimerizační či oligomerizační domény – dimerizace jakékoliv receptorové kinázy ligandem je nezbytnou součástí jejich fyziologické aktivace [16]. Fúzní onkoproteiny zahrnující TRK-receptorové kinázy jsou nalézány v celém spektru nádorů, vč. velmi obvyklých karcinomů (např. plic, prsu, kolorekta, pankreatu aj.), melanomu či akutní lymfoblastické a myeloidní leukemie či gastrointestinálního stromálního tumoru (GIST), vždy ovšem tvoří pouze výraznou menšinu případů, typicky kolem 5 %. Naproti tomu u infantilního fibrosarkomu a několika dalších dětských nádorů (jako dětský sekretující karcinom prsu či mezoblastický nefrom) jsou *NTRK*-fúzní onkogeny prakticky definiční a vyskytují se ve více než 90 % případů [16]. Podstatné je rovněž, že máme k dispozici velmi dobré nízkomolekulární inhibitory entrectinib a larotrectinib. U infantilního fibrosarkomu znamenalo nasazení těchto inhibitorů opravdový průlom v léčbě, především v neoadjuvantním a částečně i adjuvantním režimu ve spojení se šetrnou a neinvalidizující chirurgickou léčbou, při velice příznivém profilu vedlejších účinků.

Existuje několik dalších typů mezenchymálních nádorů, u kterých léčba zahrnuje či je přímo postavena na využití cílených kinázových inhibitorů. Příkladem, který není možné opomínout, je samozřejmě GIST, jeden z paradigmatických příkladů cílené protinádorové terapie [14]. Přestože GIST lze rovněž zařadit ke spektru nádorů, u nichž je malá část případů způsobena shora uvedenými *NTRK*-fúzními onkogeny, a tudíž i citlivá vůči entrectinibu nebo larotrectinibu, v naprosté většině případů je mutační mechanizmus odlišný a spočívá v bodových aktivačních mutacích

genů pro receptorové tyrozinkinázy c-Kit (80–85 % případů) a PDGFRα (10 % případů), a bylo šťastnou shodou okolností, že se velice záhy zjistilo, že většina těchto nádorů je citlivá vůči jednomu z prvních dostupných kinázových inhibitorů imatinibu. V současné době existují s touto léčbou již bohaté zkušenosti a do popředí se tak dostává otázka terapeutické rezistence a jejího adekvátního řešení, ať se už jedná o primárně rezistentní nádory (např. nádory nesoucí specifickou mutaci PDGFRα D842V), nebo pokud se týče vývoje sekundární rezistence v důsledku selekce klonů nesoucích specifické mutace v ATP-vazebné doméně nebo aktivační smyčce c-Kit nebo PDGFRα. Novou nadějí pro tyto pacienty jsou kinázové inhibitory nové generace, jednak avapritinib (BLU-285 – přednáška na konferenci CTOS 2018, dr. M. Heinrich), jednak DCC-2618 (přednáška na konferenci CTOS 2018, dr. S. George). Obě přednášky prezentovaly výsledky klinických studií fáze I zahrnující pacienty s pokročilým GIST s historií několika linií předchozí standardní terapie a obě prokázaly akceptovatelný profil toxicity a velmi povzbudivou klinickou účinnost.

V léčbě sarkomů nachází uplatnění rovněž crizotinib, duální inhibitor kináz ALK a MET. V případě ALK je zjevnou aplikací inflamatorní myofibroblastický tumor (viz výše) a v případě MET je to světlobuněčný sarkom. Ten je sice založen na translokacích t(12;22)(q13;q12) či t(2;22)(q32.3;q12), které vedou k vytvoření fúzních onkogenů *EWSR1-ATF*, resp. *EWSR1-CREB1* (tab. 3), nedochází tedy k přímé ligand-nezávislé aktivaci kinázy jako např. u infantilního fibrosarkomu, nicméně tento aberantní transkripční faktor aktivuje, pravděpodobně s výrazným přispěním jiného transkripčního faktoru MITF, gen kódující tyrozinovou kinázu MET. Výsledky prezentované malé klinické studie (přednáška na konferenci CTOS 2018, dr. P. Schöffski) jsou ovšem dosti skromné, jen u necelých 4 % pacientů došlo k objektivní částečné klinické odpovědi, nicméně u značné části (60 %) došlo ke stabilizaci onemocnění. Tato studie ovšem trpěla některými koncepčními nedostatky, jednak u pacientů nebyla analyzována a pou-

žita jako vstupní kritérium exprese/aktivita MET, jednak jsou dnes již k dispozici účinnější inhibitory MET-kinázy než crizotinib, takže definitivní závěr ještě není možné učinit. Poslední ze skupiny kinázových inhibitorů, které byly na konferenci diskutovány, jsou inhibitory CDK4 (abemaciclib a ribociclib) u dediferencovaného liposarkomu; podkladem je zde notorická amplifikace části chromozomu 12 (12q13-q15), která zahrnuje *CDK4* gen a rovněž gen pro inhibitor p53 *MDM2*, vůči němuž jsou také k dispozici specifické farmakologické inhibitory (např. nutliny nebo SAR405838). Obě dvě skupiny inhibitorů byly nezávisle samostatně testovány (přednášky na konferenci CTOS 2018, dr. M. Gounder a dr. M. A. Dickson) a výsledky obou studií prezentovaných na konferenci jsou opět relativně střízlivé, s nejčastější odpovědí ve formě stabilizace onemocnění. Vyvstává proto myšlenka kombinace obou inhibitorů, otázkou ovšem je, jestli taková terapie nebude zatížena příliš vysokou toxicitou.

Systém destičkového růstového faktoru jakožto terapeutický cíl sarkomů měkkých tkání

Zcela specifické a do jisté míry výjimečné postavení v sarkomagenezi má signální systém destičkového růstového faktoru (platelet-derived growth factor – PDGF). Lidský genom nese celkem čtyři *PDGF* geny, označované jako *A, B, C* a *D*. Signálně aktivní ligand je dimer, a to buď homodimer, nebo heterodimer *PDGFAB*. K dispozici jsou dva geny pro receptory, *PDGFRA* a *PDGFRB* (receptory samotné se označují jako α a β), přičemž tak jako u všech tyrozinkinázových receptorů prvním krokem transdukce signálu je vazba ligandu a ligandem zprostředkovaná dimerizace receptoru, jejímž výsledkem tedy mohou být tři formy aktivovaného receptoru (αα, αβ a ββ). Existují přitom dosti komplexní preference mezi dostupnými pěti ligandy a třemi receptorovými komplexy [19].

PDGF je jedním z nejsilnějších mitogenů pro mezenchymální buňky a má klíčové kauzální postavení u několika typů karyotypicky jednoduchých sarkomů. Již byla řeč o aktivačních somatických mutacích *PDGFRA* u asi 10 % GIST.

Germinální aktivační mutace u *PDGFRB* jsou podkladem vzácného syndromu dědičné nádorové predispozice (zřejmě jediného, který se manifestuje výlučně ve formě sarkomu – viz výše) – hereditární infantilní myofibromatózy [20,21]. Jedná se o nádory tvořené aktivovanými fibroblasty, které mohou vznikat v jakémkoli věku, ovšem často jsou pediatrické, a jejichž klinické chování velmi závisí na výchozí tkáni. Pokud vznikají v kůži, podkoží, svalu či kosti, je jejich chování často indolentní a dochází u nich často dokonce ke spontánní regresi, pokud se vyvíjejí ve vnitřních orgánech, jsou často agresivní a spojené s vysokou mortalitou. Žádná standardní terapie nebyla pro tyto nádory formulována, na konferenci CTOS 2018 byly prezentovány výsledky izraelské skupiny s klasickou chemoterapeutickou léčbou (poster dr. M. Manisterski) spočívající v kombinaci nízkodávkovaného metotrexátu a vinblastinu, přičemž ze čtyř pediatrických pacientů s postižením vnitřních orgánů tři přežili (jeden ovšem zaznamenal relaps onemocnění po vysazení chemoterapie) a jeden zemřel. Možná je rovněž také cílená léčba kinázovými inhibitory imatinibem nebo sunitinibem, s nímž byla u pozoruhodné kazuistiky úspěšná brněnská skupina [22].

Samotný ligand PDGFB má kauzální postavení v případě dermatofibrosarcoma protuberans, kožního sarkomu iniciovaného translokací t(17;22)(q22;q13), jejímž výsledkem je fúzní gen mezi genem pro kolagen 1A1 a právě *PDGFB* genem. Translokační zlom je u kolagenového genu velmi variabilní, podstatné je, že jeho promotor řídí transkripci fúzního onkogenu. U *PDGFB* je naproti tomu translokační zlom lokalizován vždy v prvním intronu. Kolagenový promotor je samozřejmě v mezenchymálních buňkách velmi aktivní, výsledkem je tedy masivní nadprodukce PDGFB-faktoru. Také v tomto případě je u lokálně pokročilých nebo metastatických nádorů, které se ovšem vyskytují velmi vzácně, indikován imatinib [23].

Zatímco výše uvedené příklady se vždy týkají jen zcela specifické, geneticky přesně definované a početně zpravidla malé skupiny pacientů, signální

systém PDGF se v nedávné době stal cílovou strukturou terapie sarkomů měkkých tkání v této široké specifikaci, tj. napříč různými typy a vč. obvyklých karyotypicky komplexních typů. Stalo se tak v podobě zavedení terapeutické protilátky proti PDGFRα olaratumabu. Jedná se o lidskou monoklonální protilátku třídy IgG1, která specificky a s vysokou afinitou rozeznává extracelulární ligand-vazebnou doménu PDGFRα, čímž zabraňuje vazbě ligandu a aktivaci receptoru. V *in vitro* a *in vivo* podmínkách olaratumab signifikantně inhiboval růst řady sarkomových buněčných linií [24] a překvapivě dobrého výsledku bylo dosaženo v kombinované klinické studii fáze I/II (studie JGDG), u které kombinace olaratumabu a doxorubicinu prakticky zdvojnásobila celkovou dobu přežití oproti monoterapii doxorubicinem u souboru pacientů s pokročilými sarkomy měkkých tkání [25]. Na konferenci CTOS 2018 byla představena návazná studie (přednáška dr. S. Bauer), u které byl kombinován olaratumab s kombinační chemoterapií doxorubicinem a ifosfamidem. Studie fáze I, která byla předmětem přednášky, zahrnovala 15 pacientů (3 se synoviálním sarkomem, 3 s maligními tumory z pochvy periferního nervu (malignant peripheral nerve sheath tumours – MPNST), 3 s liposarkomem, 2 s leiomyosarkomem, 2 se světlobuněčným sarkomem a 2 s nediferencovaným pleomorfním sarkomem). Plánovaná kombinační chemoterapie zahrnovala šest cyklů s podáním olaratumabu (15 mg/kg) 1. a 8. den, doxorubicinu (75 mg/m^2) 1., 2. a 3. den a ifosfamidu (20 g/m^2) 1., 2., 3. a 4. den, následovanými monoterapií olaratumabem až do progrese. V rámci výsledků studie fáze I nebyla přídavkem olaratumabu zaznamenána zvýšená toxicita oproti publikované toxicitě kombinační chemoterapie samotné [26]. Z pacientů, kteří dokončili plánovaný režim, zaznamenal pouze 1 progresi, u 5 došlo k částečné odpovědi (z čehož ovšem 1 progredoval při monoterapii olaratumabem), u 6 došlo ke stabilizaci onemocnění (klinická odpověď 25 %, kontrola onemocnění 69 %). U 3 pacientů umožnila dosažená klinická odpověď následnou operaci.

Bude nepochybně zajímavé sledovat tuto studii v delším časovém horizontu,

aby bylo možné vyhodnotit důsledky pro celkové přežití. Lze rovněž doufat, že tato nová kombinace pomůže osvětlit některé z ne zcela jednoznačně interpretovatelných závěrů studie JGDG, např. ne zcela snadno vysvětlitelný nesoulad mezi jen poměrně skromným zvýšením doby do progrese a poměrně razantním zvýšením celkového přežití, jakož i nemožnost prokázat jakýkoliv vztah mezi expresí PDGFRα v nádoru a léčebnou odpovědí [25].

Otevře molekulární biologie osteosarkomu dveře k nové terapii?

Jedním z častých typů sarkomů, u kterých by zavedení nových terapeutických postupů bylo skutečně na místě, je osteosarkom. Pro tyto pacienty zůstává základní léčebný protokol prakticky nezměněn od 70. let, kdy byla formulována základní kombinační chemoterapie metotrexátem, doxorubicinem a cisplatinou a u refrakterních a relapsujících nádorů gemcitabinem a docetaxelem. Jedinou inovací, která ovšem stále zůstává pojímána jako experimentální léčba, je doplnění této polychemoterapie imunomodulační látkou mifamurtidem, který pravděpodobně stimuluje tumoricidní aktivitu alveolárních makrofágů a snižuje tak pravděpodobnost růstu a progrese plicních metastáz [26]; přestože se jedná o experimentální léčbu, většina na osteosarkom specializovaných účastníků konference SSGM 2019 se spíše přiklání k názoru, že je tato imunomodulační léčba klinicky přínosná.

Neblahou vlastností osteosarkomu je náhlý explozivní růst a poměrně rychlá progrese, takže naprostá většina nádorů je diagnostikována jakožto „high grade" a u většiny pravděpodobně již v době diagnózy byly založeny mikrometastázy. Jedná se rovněž o sarkom s vyhraněně nestabilními karyotypy s desítkami, možná stovkami numerických a strukturálních chromozomových aberací a polyklonálním vývojem [27]. Svými vlastnostmi osteosarkom docela překvapivě připomíná serózní „high grade" ovariální karcinom, a možná právě to bylo impulzem k tomu, že v nedávné době byl osteosarkom podrobně geneticky

analyzován na aktivitu enzymatických komplexů DNA-reparační dráhy homologní rekombinací (tzv. BRCAness, podle *BRCA-1* a *BRCA-2* genů) a skutečně se zjistilo, že tato reparační dráha je porušena u značné části osteosarkomů, což samozřejmě hned vyvolalo naději na možné léčebné uplatnění PARP-inhibitorů [28]. Přestože se zprvu zdálo, že se jedná o skoro univerzální vlastnost osteosarkomu, situace asi bude o mnoho složitější a zejména heterogennější. Na konferenci SSGM 2019 prezentoval poměrně rozsáhlou experimentální studii citlivosti etablovaných osteosarkomových buněčných linií vůči PARP-inhibitoru BMN 673 prof. O. Myklebost a zjistil jednak značnou heterogenitu, jednak, aspoň prozatím, nemožnost předpovědět citlivost na základě jakékoli molekulárně biologické charakteristiky. Studie právě publikovaná na primárních osteosarkomových liniích udržovaných ve formě xenotransplantátů (patient derived xenografts – PDX), viz dále, tento nález potvrdila [29]. Bez identifikace spolehlivého prediktivního markeru lze tudíž o této terapii uvažovat jen obtížně.

Prognostické nomogramy sarkomů měkkých tkání

Viděli jsme již, že jak v případě Ewingova sarkomu, rhabdomyosarkomu i nediferencovaného pleomorfního sarkomu nese v sobě molekulárně genetická charakterizace, ať už v jakékoliv podobě (mutační mechanizmus, konkrétní „driver" mutace, molekulární subtyp charakterizovaný specifickým expresním profilem), také významnou prognostickou informaci. Stanovení prognózy onemocnění na základě takové molekulárně genetické informace je v oblasti sarkomu měkkých tkání ovšem přinejlepším záležitostí klinických studií a pro standardní odhad prognózy onemocnění jsou určující klinické a patologické charakteristiky. Ty je možné kombinovat v podobě tzv. prognostických nomogramů. Klasický prognostický nomogram představuje grafický prognostický nástroj, kdy je každá nezávislá prognosticky významná charakteristika vynesena na své podélné ose a její přímá či konvertovaná kvantitativní hodnota je převedena

do podoby bodového skóre [30]. Pravděpodobnost, že k definované klinické události (celkové přežití, sarkom-specifické přežití, přežití bez metastatického rozsevu apod.) dojde v předem stanoveném časovém okamžiku, je odvozena od celkového bodového součtu po sečtení bodového příspěvku všech zohledněných klinických charakteristik [31,32]. Některé z klinických ukazatelů vstupují do prognostických nomogramů jakožto kvantitativní veličiny (typicky např. věk pacienta), některé kvantitativní proměnné mohou být někdy naopak dichotomizovány (např. velikost nádorů může do prognostických nomogramů vstupovat jako kvantitativní veličina nebo nádory mohou být např. diferencovány a odlišně bodově ohodnoceny podle toho, jestli nedosahují určité arbitrárně stanovené hodnoty, např. 15 cm, nebo ji naopak přesahují [33]). Některé ze vstupních proměnných mají duální charakter samy o sobě (např. fokalita – unifokální vs. multifokální nádory), některé jsou ze své podstaty kvalitativní a bodové ohodnocení je jim přiděleno specificky v rámci daného nomogramu (u sarkomů typicky histopatologický typ). Rovněž záleží na tom, jestli je konstruován obecný nomogram, nebo nomogram specializovaný pouze na určitou podskupinu. První sarkomový nomogram [34] měl obecný charakter, novější nomogramy jsou už specializované. K této specializaci může u sarkomů docházet ve dvou ohledech – jednak jsou k dispozici nomogramy omezené jen na specifický histopatologický typ (např. synoviální sarkom [35] či uterinní leiomyosarkom [36]) či histopatologickou rodinu (liposarkom [37]), jednak byly konstruovány nomogramy specializované na určité anatomické místo prezentace nádoru (retroperitoneální sarkomy [38] a končetinové sarkomy [39]). Důsledkem této specializace je možnost vzít při konstrukci nomogramu v úvahu specifické proměnné, které mají dominantní postavení jen u určité skupiny sarkomů. Např. u retroperitoneálního liposarkomu byly při konstrukci specializovaného liposarkomového nomogramu rozlišeny případy, kdy chirurgická resekce mohla být zaměřena jen na nádor jako takový, od případů, kdy předmětem resekce musel

být také nějaký vnitřní orgán, s vyšším bodovým ohodnocením druhé z možností [37]. Někdy se dokonce může jednat o odlišnou formu distribuce společné kvantitativní proměnné. Například u současného nomogramu zaměřeného na končetinové sarkomy je velikost nádoru zohledněna jakožto kvantitativní proměnná s lineární distribucí [40], zatímco současný nomogram konstruovaný pro retroperitoneální sarkomy nahlíží na velikost nádoru jako na kvantitativní proměnnou s nelineární distribucí – extrémně velké nádory dosahují nižšího bodového ohodnocení než nádory s velikostí 30 cm, což je hraniční hodnota, do které je distribuce lineární [41]. Příčinou je skutečnost, že obzvláště velké retroperitoneální sarkomy jsou z velké většiny dobře diferencované liposarkomy s příznivějším klinickým průběhem než jiné typy sarkomů, jako např. dediferencovaný liposarkom či leiomyosarkom [42]. Tento poslední příklad rovněž ilustruje interakci různých proměnných, které, ač *a priori* stanovené jako nezávislé, se navzájem podmiňují. Konstrukce nomogramů je statisticky poměrně komplexní problém, kvalita každého nomogramu je určena především dvěma ukazateli – kalibrací a diskriminací [40,42]. Kalibrace je grafický výraz validace prognostické hodnoty nomogramu, kdy na jedné ose vynášíme vypočítanou předpokládanou hodnotu veličiny (např. celkové přežití), na druhé ose hodnotu reálnou – u ideálního nomogramu bychom tak měli získat přímku se směrnicí 45°. Diskriminace je pravděpodobnost, že z náhodně vybrané dvojice pacientů se předpokládaná událost, jejíž pravděpodobnost nomogram stanovuje (smrt, rekurence, metastáza apod.) objeví dříve u pacienta s vyšším bodovým součtem, a tudíž vyšší vypočítanou pravděpodobností. Ideální diskriminace dosahuje hodnoty 1 (tj. 100 %), diskriminace 0,5 (50 %) znamená nulovou prognostickou hodnotu nomogramu. Spolehlivost nomogramu je zejména dána jeho externí validací, tj. spolehlivý nomogram dosahuje podobné kalibrace a diskriminace u etnicky a geograficky různých populací pacientů ošetřovaných v různých specializovaných centrech [43].

Příspěvky na konferenci CTOS 2018 se týkaly tří aspektů vývoje prognostických nomogramů sarkomů měkkých tkání. Nevyhnutelná interakce různých proměnných byla zohledněna ve specifické modifikaci nomogramu pro končetinové sarkomy, tzv. dynamickém prognostickém nomogramu (přednáška prof. D. Callegaro). Jak toto označení již nechává tušit, tou hlavní proměnnou, jejíž interakce s ostatními je předmětem této modifikace, je čas; zatímco klasické nomogramy, o nichž jsme diskutovali výše, umožňují jednorázový odhad úmrtí, rekurence či metastatického rozsevu na základě hodnot jednotlivých proměnných zjištěných v okamžiku operace, tento dynamický nomogram umožňuje opakovanou kalkulaci po 12, 24 a 36 měsících, a to na základě jak vstupních klinických dat v okamžiku operace, tak i klinického vývoje od okamžiku operace po provedení opakované kalkulace. Druhým aspektem je integrace molekulárně genetické informace; v našem dosavadním textu jsme prognostické nomogramy dávali do jakéhosi protikladu k molekulárně genetickým a molekulárně biologickým faktorům odhadu prognózy, a to čistě z důvodu logického členění textu. Lze ovšem téměř s jistotou předpovědět, že tato hranice se bude v budoucnosti čím dále tím více stírat a molekulárně geneticky či biologicky založené charakteristiky individuálních nádorů se stanou jedněmi z proměnných prognostických nomogramů. Jakousi předzvěstí tohoto vývoje byla přednáška dr. I. Wei, která ukázala možnosti integrace konkrétní mutační informace (tři nejčastější mutace *CTNNB1* genu či wt-alela či jiná mutace) do prognostického nomogramu rekurence desmoidní fibromatózy; podstatné přitom je, že začleněním této molekulární proměnné došlo ke zvýšení diskriminace z hodnoty 0,707, dosažené pouze s klinickými proměnnými, na 0,729 u všech pacientů a 0,744 u pacientů s primárně diagnostikovanou desmoidní fibromatózou. Konečně, třetí oblastí, ve které prognostické nomogramy sarkomů doznaly v poslední době významného rozvoje, je jejich aplikační forma. Cílem je co nejvíce rozšířit a usnadnit jejich praktické použití v každodenní klinické praxi. Sar-

kulátor je jedna z takových aplikačních inovací (www.sarculator.com). Jedná se o volně dostupnou aplikaci vyvinutou pro smartphony a tablety, která je určena dospělým pacientům po resekci retroperitoneálního a končetinového sarkomu. Poskytuje odhad onkologických výsledků na základě věku pacienta, stadia onemocnění a velikosti a histologie nádoru. Po vložení těchto specifických kovariátů do aplikace je uživateli vykalkulována pravděpodobnost celkového přežití, bezpříznakového přežití nebo výskytu vzdálených metastáz po resekci primárního sarkomu. Koncepčně podobná, i když v detailech odlišná, a nikoliv široce dostupná aplikační forma byla vyvinuta také specificky pro myxoidní liposarkom (poster dr. D. D. McMillan). Jedním z příkladů uplatnění Sarkulátoru je studie prezentovaná v přednášce dr. S. Pasqualiho, jejímž cílem bylo pokusit se redefinovat postavení adjuvantní chemoterapie v léčbě končetinových sarkomů měkkých tkání. Dosavadní klinické studie poskytly velmi rozporuplné výsledky; poslední velká randomizovaná klinická studie [41] neprokázala klinický benefit kombinační adjuvantní chemoterapie doxorubicinem a ifosfamidem. Jestliže ovšem totožní pacienti byli *ex post* stratifikováni na základě Sarkulátorem kalkulovaného odhadu pravděpodobnosti 8letého celkového přežití (jako hraniční hodnota bylo zvoleno 60 %), pak u vysoce rizikových pacientů (tzn. s kalkulovanou pravděpodobností celkového 8letého přežití pod 60 %) byl efekt adjuvantní terapie statisticky významný.

Nové experimentální modely sarkomu měkkých tkání

Jedním z problémů experimentální onkologie sarkomů obecně je nedostatek vhodných experimentálních modelů; ostatně to bylo také téma našich příspěvků. Na konferenci CTOS 2018 jsme posterovou formou prezentovali naše dosavadní výsledky získané analýzou progresivní série fibrosarkomových buněčných linií odvozených z fibrosarkomu indukovaného hlubokým poraněním u v-jun transgenní myši [42,43], zejména výsledky transkriptomické analýzy. Tento experimentální systém zahrnuje relativně málo transformovanou

sarkomovou linii JUN-2 s nízkou úrovní proliferace, motility a invazivity, z ní odvozenou dceřinou linii JUN-2fos3, která si zachovává nízkou úroveň proliferace, ale došlo u ní k výrazné manifestaci buněčné motility a invazivity, a vysoce transformovanou sarkomovou linii JUN-3 s vysokou úrovní proliferace, motility i invazivity. Tato unikátní sestava sarkomových buněčných linií nám umožnila identifikovat v jediné transkriptomické analýze jak geny zodpovědné za proliferaci (kontrastní expresní profil u JUN-3 oproti JUN-2 a JUN-2fos3), tak geny zodpovědné za motilitu a invazivitu (kontrastní expresní profil u JUN-3 a JUN-2fos3 oproti JUN-2). Ukázalo se tak, že JUN-3 sarkomové buňky disponují značnou autokrinní aktivací jak buněčné proliferace, tak motility; jeden z těchto autokrinních motilitních faktorů, chemokin Ccl8, může být farmakologicky inhibován, a skutečně tato inhibice signifikantně snižuje motilitu této sarkomové buněčné linie. Autokrinní regulace buněčné proliferace má zřejmě komplexnější charakter; JUN-3 buňky skutečně specificky nadměrně exprimují řadu růstových faktorů (amfiregulin, epiregulin, fibroblastové růstové faktory 10 a 13, hepatocytární růstový faktor) či receptorů (rovněž výše diskutovaný PDGFRα) a jejich proliferace není závislá na obsahu séra v médiu, na druhou stranu jimi kondiciované médium specificky inhibuje růst JUN-2 sarkomových buněk. To by mohlo otevřít cestu k objasnění interakce nezávislých nádorových klonů v komplexních nádorech vč. klasického fenoménu klonální dominance. Na konferenci SSGM 2019 jsme potom formou komentovaného posteru tento model rozšířili o další progresivní sarkomovou sérii založenou na velice obvyklé preadipocytární buněčné linii 3T3L1. Francouzská skupina publikovala spontánní transformaci této preadipocytární buněčné linie *in vivo* do dediferencovaného liposarkomu, ze kterého byla odvozena příslušná buněčné linie LM3D [44]. Opět jsme postupovali cestou celogenomové transkriptomické analýzy, která nám poskytla vhled do možných základních mechanizmů vzniku a progrese nádorů tukové tkáně. Obecnější význam by mohl mít bioinformaticky identifi-

kovaný průnik transkriptomických profilů obou agresivních sarkomových linií, tj. JUN-3 a LM3D, který jsme označili jako „sarcoma progression signature". Celkem se nám podařilo identifikovat 95 souhlasně transkripčně aktivovaných genů a 78 souhlasně transkripčně reprimovaných genů, které by mohly ukrývat obecnější informaci o biologických mechanizmech progrese sarkomu. Prvotní analýza aktivovaných genů odhalila přítomnost překvapivě různorodé skupiny genů, které byly v různém kontextu publikovány jakožto inhibitory klasické, tzv. konvenční Wnt/β-kateninové signální dráhy (Dickkopf-2 a -3, Apcdd1, Meg3, Fibulin-5, Ints6, Msx1), a současně též aktivaci exprese genu kódujícího receptor tyrosine kinase-like orphan receptor 2 (Ror-2); to by napovídalo, že během progrese sarkomů (na rozdíl od mnohých karcinomů) dochází k utlumení klasické Wnt/β-kateninové signální dráhy a k jejímu nahrazení tzv. nekonvenční Wnt5a/Ror-2 signální dráhou [45]. To by potvrzovala i přítomnost některých genů, které byly publikovány jakožto aktivované právě touto nekonvenční Wnt5a/Ror-2 signální dráhou, mezi aktivovanými geny našeho „sarcoma progression signature", jako je gen pro onkoprotein c-jun anebo geny pro metaloproteinázy matrix, konkrétně MMP-16. Podle stejné logiky by farmakologické aktivátory konvenční Wnt/β-kateninové dráhy mohly představovat slibné kandidáty pro novou chemoterapii pokročilých sarkomů; za zmínku v tomto ohledu stojí např. bortezomib [46].

Obecným problémem klasických buněčných kultur jsou arteficiální podmínky růstu nádorových buněk, které nemohou napodobit komplexní mikroprostředí nádoru [47]. Jednou z možností, jak zmírnit tento problém, jsou xenotransplantační modely, kdy se nativní fragmenty nádorů přímo implantují přísně imunodeficientní myši, tzv. PDX (patient-derived xenografts). Tuto techniku využila i skupina, která popsala molekulární subtypy nediferencovaného pleomorfního sarkomu pro analýzu účinnosti FGFR2 – specifických inhibitorů u tzv. „cold-UPS" nádorů, nebo nedávná studie hledající nové te-

rapeutické možnosti u osteosarkomu (viz výše) [29]. Skupina z belgické univerzity v Leuvenu (projekt XenoSarc – poster na konferenci CTOS 2018, dr. A. Wozniak) se takto zaměřila na celou škálu sarkomů měkkých tkání zahrnující myxofibrosarkom, dediferencovaný liposarkom, synoviální sarkom, MPNST, leiomyosarkom, epitelioidní hemangioendoteliom, mezenchymální chondrosarkom, rhabdomyosarkom a nediferencovaný pleomorfní sarkom. Celkem se v současnosti jedná o 30 xenotransplantačních modelů, a současně s nimi je připravována i odpovídající tissue microarray, takže by mělo být možné současně analyzovat jednotlivé sarkomy imunohistochemicky i funkčním testem. Samozřejmě že metodika PDX je o mnoho komplikovanější a zejména experimentálně méně přístupná než klasické buněčné kultury. Skupina z milánského Istituto Nazionale dei Tumori (poster na konferenci CTOS 2018, dr. C. Colombo) se pokusila tento problém zmírnit současným odvozením xenotransplantátů i klasických buněčných linií ze vzorků získaných po chirurgickém odstranění retroperitoneálně lokalizovaných dediferencovaných liposarkomů a podle prezentovaných výsledků se zdá, že úspěšně; ze tří dediferencovaných liposarkomů se podařilo odvodit paralelně oba modely a využít je pro zatím základní screening chemosenzitivity. Jinou možností, jak zachovat komplexní nádorové interakce a současně získat experimentálně přístupnější model, než jsou xenotransplantáty, je použít trojrozměrné buněčné kultivace. Skupina z německé kliniky Helios (poster na konferenci CTOS 2018, dr. M. Gaebler) se zaměřila právě tímto směrem. Jedná se o tzv. sarkomové organoidy, tedy trojrozměrné mikronádory kultivované v komplexní extracelulární matrix (tzv. Matrigel); tento systém se označuje PD3D (patient-derived 3D-culture). Smyslem je získat experimentálně schůdný systém, který bude např. přístupný dlouhodobé kultivaci s cílem identifikovat potenciálně terapeuticky využitelné mutace každého individuálního sarkomového pacienta a na základě toho formulovat individualizovanou terapii, nebo použít tento systém jakožto screeningovou platformu pro identifikaci nových farmakologicky zajímavých molekul.

Primární buněčné kultury klinických sarkomů představují metodicky poměrně nelehký úkol; vzhledem k histopatologické variabilitě je obtížné definovat kultivační podmínky tak, aby se podařilo ustanovit primární buněčné kultury s rozumnou úspěšností u různých pacientů se sarkomy. Pozoruhodného úspěchu, prezentovaného formou přednášky a komentovaného posteru na konferenci SSGM 2019, dosáhla v tomto ohledu švédská skupina z Karolinska Institutet [48], která s více než 50% úspěšností kultivovala primární nádorové kultury odvozené z aspirátů získaných tenkou jehlou nebo z chirurgicky získaných vzorků několika typů sarkomů (Ewingova sarkomu, embryonálního rhabdomyosarkomu, alveolárního sarkomu měkkých tkání, angiosarkomu). Primární buněčné kultury byly následně podrobeny expresní analýze a současně testovány na citlivost vůči farmakologické knihovně zahrnující 525 farmakologicky aktivních látek a následně konfrontovány s pozorovanou odpovědí pacientů na empiricky podanou chemoterapii. Dosavadní výsledky (rozsah studie je zatím malý – 14 primárních buněčných kultur) ukazují na velmi dobrou schopnost předpovědět klinickou rezistenci a v jednom případě rovněž senzitivitu. Prezentovaným cílem projektu je tento kultivační a screeningový systém v blízké budoucnosti použít jakožto platformu pro *in vitro* test chemosenzitivity a podle něj modifikovat, či dokonce formulovat individualizovanou terapii.

Literatura

1. Fletcher CD, Unni KK, Mertens F (eds). WHO classification of tumours of soft tissue and bone. 4th ed. Lyon: IARC Press 2013.
2. Calvete O, Martinez P, Garcia-Pavia P et al. A mutation in the POT1 gene is responsible for cardiac angiosarcoma in TP53-negative Li–Fraumeni-like families. Nat Commun 2015; 6: 8383. doi: 10.1038/ncomms9383.
3. Koelsche C, Renner M, Hartmann W et al. TERT promoter hotspot mutations are recurrent in myxoid liposarcomas but rare in other soft tissue sarcoma entities. J Exp Clin Cancer Res 2014; 33(1): 33. doi: 10.1186/1756-9966-33-33.
4. Delespaul L, Lesluyes T, Pérot G et al. Recurrent TRIO fusion in nontranslocation–related sarcomas. Clin Cancer Res 2017; 23(3): 857–867. doi: 10.1158/1078-0432.CCR-16-0290.
5. Ballinger ML, Goode DL, Ray-Coquard I et al. Monogenic and polygenic determinants of sarcoma risk: an international genetic study. Lancet Oncol 2016; 17(9): 1261–1271. doi: 10.1016/S1470-2045(16)30147-4.
6. Anderson ND, de Borja R, Young MD et al. Rearrangement bursts generate canonical gene fusions in bone

and soft tissue tumors. Science 2018; 361(6405): 8419. doi: 10.1126/science.aam8419.
7. Mertens F, Antonescu CR, Mitelman F. Gene fusions in soft tissue tumors: recurrent and overlapping pathogenetic themes. Genes Chromosomes Cancer 2016; 55(4): 291–310. doi: 10.1002/gcc.22335.
8. Specht K, Hartmann W. Ewing-Sarkome und Ewingartige Sarkome. Pathologe 2018; 39(2): 154–163. doi: 10.1007/s00292-018-0421-2.
9. Cancer Genome Atlas Research Network. Comprehensive and integrated genomic characterization of adult soft tissue sarcomas. Cell 2017; 171(4): 950–965. doi: 10.1016/j.cell.2017.10.014.
10. George S, Serrano C, Hensley ML et al. Soft tissue and uterine leiomyosarcoma. J Clin Oncol 2017; 36(2): 144–150. doi: 10.1200/JCO.2017.75.9845.
11. Synnott NC, Bauer MR, Madden S et al. Mutant p53 as a therapeutic target for the treatment of triple-negative breast cancer: preclinical investigation with the anti-p53 drug, PK11007. Cancer Lett 2018; 414: 99–106. doi: 10.1016/j.canlet.2017.09.053.
12. Darvin P, Toor SM, Sasidharan Nair V et al. Immune checkpoint inhibitors: recent progress and potential biomarkers. Exp Mol Med 2018; 50(12): 165. doi: 10.1038/s12276-018-0191-1.
13. Broto JM, Hindi N, Redondo A et al. IMMUNOSARC: A collaborative Spanish (GEIS) and Italian (ISG) Sarcoma Groups phase I/II trial of sunitinib plus nivolumab in selected bone and soft tissue sarcoma subtypes – results of the phase I part. Ann Oncol 2019; 30 (Suppl 5): v683-v709. doi: 10.1093/annonc/mdz283.
14. Dufresne A, Brahmi M, Karanian M et al. Using biology to guide the treatment of sarcomas and aggressive connective-tissue tumours. Nat Rev Clin Oncol 2018; 15(7): 443–458. doi: 10.1038/s41571-018-0012-4.
15. Knezevich SR, McFadden DE, Tao W et al. A novel ETV6-NTRK3 gene fusion in congenital fibrosarcoma. Nat Genet 1998; 18(2): 184–187. doi: 10.1038/ng0298-184.
16. Cocco E, Scaltriti M, Drilon A. NTRK fusion-positive cancers and TRK inhibitor therapy. Nat Rev Clin Oncol 2018; 15(12): 731–747. doi: 10.1038/s41571-018-0113-0.
17. DuBois SG, Laetsch TW, Federman N et al. The use of neoadjuvant larotrectinib in the management of children with locally advanced TRK fusion sarcomas. Cancer 2018; 124(21): 4241–4247. doi: 10.1002/cncr.31701.
18. Davis JL, Lockwood CM, Albert CM et al. Infantile NTRK-associated mesenchymal tumors. Pediatr Dev Pathol 2018; 21(1): 68–78. doi: 10.1177/1093526617712639.
19. Papadopoulos N, Lennartsson J. The PDGF/PDGFR pathway as a drug target. Mol Aspects Med 2018; 62: 75–88. doi: 10.1016/j.mam.2017.11.007.
20. Cheung YH, Gayden T, Campeau PM et al. A recurrent PDGFRB mutation causes familial infantile myofibromatosis. Am J Hum Genet 2013; 92(6): 996–1000. doi: 10.1016/j.ajhg.2013.04.026.
21. Martignetti JA, Tian L, Li D et al. Mutations in PDGFRB cause autosomal-dominant infantile myofibromatosis. Am J Hum Genet 2013; 92(6): 1001–1007. doi: 10.1016/j.ajhg.2013.04.024.
22. Mudry P, Slaby O, Neradil J et al. Case report: rapid and durable response to PDGFR targeted therapy in a child with refractory multiple infantile myofibromatosis and a heterozygous germline mutation of the PDGFRB gene. BMC Cancer 2017; 17(1): 119. doi: 10.1186/s12885-017-3115-x.
23. Noujaim J, Thway K, Fisher C et al. Dermatofibrosarcoma protuberans: from translocation to targeted therapy. Cancer Biol Med 2015; 12(4): 375–384. doi: 10.7497/j.issn.2095-3941.2015.0067.
24. Lowery CD, Blosser W, Dowless M et al. Olaratumab exerts antitumor activity in preclinical models of pediatric bone and soft tissue tumors through inhibition of platelet-derived growth factor receptor α. Clin Cancer

Res 2018; 24(4): 847–857. doi: 10.1158/1078-0432.CCR-17-1258.
25. Antoniou G, Lee AT, Huang PH et al. Olaratumab in soft tissue sarcoma – current status and future perspectives. Eur J Cancer 2018; 92: 33–39. doi: 10.1016/j.ejca.2017.12.026.
26. Meyers PA, Chou AJ. Muramyl tripeptide-phosphatidyl ethanolamine encapsulated in liposomes (L-MTP-PE) in the treatment of osteosarcoma. Adv Exp Med Biol 2014; 804: 307–321. doi: 10.1007/978-3-319-04843-7_17.
27. Baumhoer D. Die klonale Evolution des Osteosarkoms. Pathologe 2016; 37 (Suppl 2): 163–168. doi: 10.1007/s00292-016-0200-x.
28. Kovac M, Blattmann C, Ribi S et al. Exome sequencing of osteosarcoma reveals mutation signatures reminiscent of BRCA deficiency. Nat Commun 2015; 6: 8940. doi: 10.1038/ncomms9940.
29. Loh AH, Stewart E, Bradley CL. Combinatorial screening using orthotopic patient derived xenograft-expanded early phase cultures of osteosarcoma identify novel therapeutic drug combinations. Cancer Letters 2019; 442: 262–270. doi: 10.1016/j.canlet.2018.10.033.
30. Balachandran VP, Gonen M, Smith JJ et al. Nomograms in oncology: more than meets the eye. Lancet Oncol 2015; 16(4): 173–180. doi: 10.1016/S1470-2045(14)71116-7.
31. Eilber FC, Kattan MW. Sarcoma nomogram: validation and a model to evaluate impact of therapy. J Am Coll Surg 2007; 205 (Suppl 4): S90–S95. doi: 10.1016/j.jamcollsurg.2007.06.325.
32. Tattersall HL, Callegaro D, Ford SJ et al. Staging, nomograms and other predictive tools in retroperitoneal soft tissue sarcoma. Chin Clin Oncol 2018; 7(4): 36. doi: 10.21037/cco.2018.08.01.
33. Anaya DA, Lahat G, Wang X et al. Postoperative nomogram for survival of patients with retroperitoneal sarcoma treated with curative intent. Ann Oncol 2009; 21(2): 397–402. doi: 10.1093/annonc/mdp298.
34. Kattan MW, Leung DH, Brennan MF. Postoperative nomogram for 12-year sarcoma-specific death. J Clin Oncol 2002; 20(3): 791–796. doi: 10.1200/JCO.2002.20.3.791.
35. Canter RJ, Qin LX, Maki RG et al. A synovial sarcoma-specific preoperative nomogram supports a survival benefit to ifosfamide-based chemotherapy and improves risk stratification for patients. Clin Cancer Res 2008; 14(24): 8191–8197. doi: 10.1158/1078-0432.CCR-08-0843.
36. Zivanovic O, Jacks LM, Iasonos A. et al. A nomogram to predict postresection 5-year overall survival for patients with uterine leiomyosarcoma. Cancer 2012; 118(3): 660–669. doi: 10.1002/cncr.26333.
37. Dalal KM, Kattan MW, Antonescu CR et al. Subtype specific prognostic nomogram for patients with primary liposarcoma of the retroperitoneum, extremity, or trunk. Ann Surg 2006; 244(3): 381–391. doi: 10.1097/01.sla.0000234795.98607.00.
38. Gronchi A, Miceli R, Shurell E et al. Outcome prediction in primary resected retroperitoneal soft tissue sarcoma: histology-specific overall survival and disease-free survival nomograms built on major sarcoma center data sets. J Clin Oncol 2013; 31(13): 1649–1655. doi: 10.1200/JCO.2012.44.3747.
39. Callegaro D, Miceli R, Bonvalot S et al. Development and external validation of two nomograms to predict overall survival and occurrence of distant metastases in adults after surgical resection of localised soft-tissue sarcomas of the extremities: a retrospective analysis. Lancet Oncol 2016; 17(5): 671–680. doi: 10.1016/S1470-2045(16)00010-3.
40. Raut CP, Miceli R, Strauss DC et al. External validation of a multi-institutional retroperitoneal sarcoma nomogram. Cancer 2016; 122(9): 1417–1424. doi: 10.1002/cncr.29931.
41. Woll PJ, Reichardt P, Le Cesne A et al. Adjuvant chemotherapy with doxorubicin, ifosfamide, and lenograstim for resected soft-tissue sarcoma (EORTC

62931): a multicentre randomised controlled trial. Lancet Oncol 2012; 13(10): 1045–1054. doi: 10.1016/S1470-2045(12)70346-7.

42. Hatina J, Hájková L, Peychl J et al. Establishment and characterization of clonal cell lines derived from a fibrosarcoma of the H2-K/v-jun transgenic mouse. Tumour Biol 2003; 24(4): 176–184. doi: 10.1159/000074427.

43. Peychl J, Hatina J, Reischig J et al. Vztah motility a invazivity transformovaných buněk-model H2-K/V-JUN fibrosarkomových buněčných linií. Klin Onkol 2003; 16(5): 223–226.

44. Mariani O, Brennetot C, Coindre JM et al. JUN oncogene amplification and overexpression block adipocytic differentiation in highly aggressive sarcomas. Cancer Cell 2007; 11(4): 361–374. doi: 10.1016/j.ccr.2007. 02.007.

45. Endo M, Nishita M, Fujii M et al. Insight into the role of Wnt5a-induced signaling in normal and cancer cells. Int Rev Cell Mol Biol 2015; 314: 117–148. doi: 10.1016/bs.ircmb.2014.10.003.

46. Qiang YW, Hu B, Chen Y et al. Bortezomib induces osteoblast differentiation via Wnt-independent activation of beta-catenin/TCF signaling. Blood 2009; 113(18): 4319–4330. doi: 10.1182/blood-2008-08-174300.

47. Witz IP. Tumor–microenvironment interactions: dangerous liaisons. Adv Cancer Res 2008; 100: 203–229. doi: 10.1016/S0065-230X(08)00007-9.

48. Brodin BA, Wennerberg K, Lidbrink E et al. Drug sensitivity testing on patient-derived sarcoma cells predicts patient response to treatment and identifies c-Sarc inhibitors as active drugs for translocation sarcomas. Br J Cancer 2019; 120(4): 435–443. doi: 10.1038/s41416-018-0359-4.

PERSONALIA

Vzpomínka na prof. MUDr. Vítězslava Kolka, DrSc.

V lidském životě přicházejí chvíle, které nás bolestně zaskočí a kterým nemůžeme porozumět. K takové patřil i den (30. 1. 2020), v němž se uzavřel neopakovatelný životní příběh profesora Vítězslava Kolka. Nečekaně zemřel a zarmoutil tím všechny své blízké.

V profesoru Vítězslavu Kolkovi odešel dobrý člověk, zanícený pneumolog, který se neustále pokoušel pro obor vybojovat důstojné postavení, vynikající lékař, pedagog, vědec, kolega a přítel.

Českou pneumologii díky hlubokým znalostem, jazykové vybavenosti, pohotovosti a osobnímu charizmatu dostal do povědomí nejen v ČR, ale i v evropském a světovém měřítku. Mladým lékařům důsledně vštěpoval kvalitní lidskou medicínu a učil je i vědecké práci. Dokázal lidi motivovat a inspirovat. Jeho odborný záběr byl velmi široký. Věnoval se problematice sarkoidózy, intervenční bronchologii, pneumoniím, pneumoon-

kologii a dalším. Byl autorem a spoluautorem celé řady knih, vědeckých publikací a přednášek v ČR i v zahraničí.

Od roku 1999 byl přednostou Kliniky nemocí plicních a tuberkulózy Lékařské fakulty Univerzity Palackého a Fakultní nemocnice Olomouc. Dvě volební období byl předsedou České pneumologické a ftizeologické společnosti České lékařské společnosti Jana Evangelisty Purkyně a řadu let jejím místopředsedou. Byl také předsedou České aliance proti chronickým respiračním nemocem. Určité období pracoval jako proděkan a měl na starosti výuku zahraničních studentů.

Zanechal tu všechno, co ho těšilo a co měl rád – rodinu, domov, přátele, kliniku se svými kolegy a žáky a také své pacienty. Zanechal tu také kolegy a přátele z ČR a dalších zemí. Žádnými slovy se nedá vyjádřit ztráta, kterou znamená jeho smrt.

Nedokončené dílo profesora Kolka zůstane inspirací pro ty, kteří v něm budou pokračovat. Nutí nás vážit si života a využít ho do posledních chvil, jak se to podařilo jemu.

prof. MUDr. Jana Skřičková, CSc.
Klinika nemocí plicních a tuberkulózy
LF MU a FN Brno

PŘÍLOHA 9

Article

Complex Interplay of Genes Underlies Invasiveness in Fibrosarcoma Progression Model

Michaela Kripnerová [1], Hamendra Singh Parmar [1,†], Jiří Šána [2,3], Alena Kopková [2,4], Lenka Radová [2], Sieghart Sopper [5,6], Krzysztof Biernacki [7], Jan Jedlička [8], Michaela Kohoutová [8], Jitka Kuncová [8], Jan Peychl [9,‡], Emil Rudolf [9], Miroslav Červinka [9], Zbyněk Houdek [1], Pavel Dvořák [1], Kateřina Houfková [1], Martin Pešta [1], Zdeněk Tůma [10], Martina Dolejšová [10], Filip Tichánek [11], Václav Babuška [12], Martin Leba [13], Ondřej Slabý [2,14,*] and Jiří Hatina [1,*]

[1] Institute of Biology, Faculty of Medicine in Pilsen, Charles University, 323 00 Plzen, Czech Republic; Michaela.Kripnerova@lfp.cuni.cz (M.K.); hamendrasingh999@yahoo.co.in (H.S.P.); Zbynek.Houdek@lfp.cuni.cz (Z.H.); Pavel.Dvorak@lfp.cuni.cz (P.D.); Katerina.Houfkova@lfp.cuni.cz (K.H.); Martin.Pesta@lfp.cuni.cz (M.P.)

[2] Central European Institute of Technology (CEITEC), Masaryk University, 625 00 Brno, Czech Republic; jiri.sana@ceitec.muni.cz (J.Š.); alena.kopkova@ceitec.muni.cz (A.K.); avodar@gmail.com (L.R.)

[3] Department of Comprehensive Cancer Care, Masaryk Memorial Cancer Institute, 602 00 Brno, Czech Republic

[4] Department of Pathology, University Hospital Brno, 625 00 Brno, Czech Republic

[5] Internal Medicine V, Medical University of Innsbruck, 6020 Innsbruck, Austria; sieghart.sopper@i-med.ac.at

[6] Tyrolean Cancer Research Institute, 6020 Innsbruck, Austria

[7] Department of Medical and Molecular Biology, Faculty of Medical Sciences in Zabrze, Medical University of Silesia in Katowice, 41-808 Zabrze, Poland; kbiernacki@sum.edu.pl

[8] Institute of Physiology, Faculty of Medicine in Pilsen, Charles University, 323 00 Plzen, Czech Republic; Jan.Jedlicka@lfp.cuni.cz (J.J.); Michaela.Markova@lfp.cuni.cz (M.K.); Jitka.Kuncova@lfp.cuni.cz (J.K.)

[9] Department of Medical Biology and Genetics, Faculty of Medicine in Hradec Kralove, Charles University, 500 03 Hradec Kralove, Czech Republic; peychl@mpi-cbg.de (J.P.); Rudolf@lfhk.cuni.cz (E.R.); cervinka@lfhk.cuni.cz (M.Č.)

[10] Biomedical Center, Faculty of Medicine in Pilsen, Charles University, 323 00 Plzen, Czech Republic; zdenek.tuma@lfp.cuni.cz (Z.T.); martina.dolejsova@lfp.cuni.cz (M.D.)

[11] Institute of Pathological Physiology, Faculty of Medicine in Pilsen, Charles University, 323 00 Plzen, Czech Republic; tichanef@lfp.cuni.cz

[12] Institute of Medical Chemistry and Biochemistry, Faculty of Medicine in Pilsen, Charles University, 301 66 Plzen, Czech Republic; vaclav.babuska@lfp.cuni.cz

[13] Department of Cybernetics, Faculty of Applied Sciences, University of West Bohemia in Pilsen, 301 00 Plzen, Czech Republic; lebam@students.zcu.cz

[14] Department of Biology, Faculty of Medicine, Masaryk University, 625 00 Brno, Czech Republic

[*] Correspondence: oslaby@med.muni.cz (O.S.); Jiri.Hatina@lfp.cuni.cz (J.H.)

[†] School of Biotechnology, Devi Ahilya University, Takshashila Campus, Khandwa Road, Indore 452001, MP, India.

[‡] Light Microscopy Facility, Max Planck Institute of Molecular Cell Biology and Genetics, 01307 Dresden, Germany.

Abstract: Sarcomas are a heterogeneous group of mesenchymal tumours, with a great variability in their clinical behaviour. While our knowledge of sarcoma initiation has advanced rapidly in recent years, relatively little is known about mechanisms of sarcoma progression. JUN-murine fibrosarcoma progression series consists of four sarcoma cell lines, JUN-1, JUN-2, JUN-2fos-3, and JUN-3. JUN-1 and -2 were established from a single tumour initiated in a *H2K/v-jun* transgenic mouse, JUN-3 originates from a different tumour in the same animal, and JUN-2fos-3 results from a targeted in vitro transformation of the JUN-2 cell line. The JUN-1, -2, and -3 cell lines represent a linear progression from the least transformed JUN-2 to the most transformed JUN-3, with regard to all the transformation characteristics studied, while the JUN-2fos-3 cell line exhibits a unique transformation mode, with little deregulation of cell growth and proliferation, but pronounced motility and invasiveness. The invasive sarcoma sublines JUN-2fos-3 and JUN-3 show complex metabolic profiles, with activation of both mitochondrial oxidative phosphorylation and glycolysis and a significant increase in spared respiratory capacity. The specific transcriptomic profile of invasive sublines features very complex biological relationships across the identified genes and proteins, with accentuated autocrine control of

motility and angiogenesis. Pharmacologic inhibition of one of the autocrine motility factors identified, Ccl8, significantly diminished both motility and invasiveness of the highly transformed fibrosarcoma cell. This progression series could be greatly valuable for deciphering crucial aspects of sarcoma progression and defining new prognostic markers and potential therapeutic targets.

1. Introduction

Sarcomas represent a very heterogeneous group of tumours of mesenchymal origin, accounting for ~1% of human malignancies, affecting about 200,000 people per year across the globe. At the genomic level, sarcomas can be classified into two broad categories. The first group, especially prevailing among paediatric cases, involves tumours of near diploid karyotypes, featuring well-defined focused mutational changes, like specific translocations, amplifications, or activating point mutations in crucial driver oncogenes or inactivating mutations in key tumour suppressor genes. The second group comprises adult-type sarcomas including adult fibrosarcoma, osteosarcoma, chondrosarcoma, most liposarcomas, angiosarcoma, leiomyosarcoma, and undifferentiated pleomorphic sarcoma, with complex and unbalanced karyotypes and extensive genomic instability [1–5]. The clinical behaviour of sarcomas can be highly variable, ranging from indolent to highly aggressive invasive and metastatic tumours. Whereas localised tumours can frequently be successfully treated by surgery alone or in combination with radiotherapy, the prognosis of advanced stage metastatic sarcomas is poor, with a median overall survival of only 8–12 months [2,6]. While the issue of sarcoma initiation has experienced substantial progress in recent years, both regarding the identification of a plethora of driver fusion oncogenes in translocation-dependent sarcomas [3,7] and concerning mesenchymal stem cells as a probable cell of origin for most sarcomas [8], relatively little progress has been achieved in deciphering the mechanisms of sarcoma progression. This issue is of utmost importance, nevertheless, the metastatic dissemination is the principal cause of sarcoma-related death according to all the available evidence [9]; interestingly, a similar prognostic impact on patient survival as the metastatic dissemination seems to be the already existent presence of histologic invasion, suggesting that invasiveness might be a rate-limiting step of the entire metastatic cascade [10]. Moreover, a survey of recent soft tissue sarcoma phase III clinical trials revealed that up to 50% of enrolled patients experience rapid progression, which might obscure any effect of an investigational agent if it is not dramatic enough. Such rapid progressors are seen across histopathological subtypes, suggesting that a yet to be identified general aspect of disease biology might underlie them [11]. The CINSARC gene expression signature has been identified with the implicit assumption that metastatic ability is intimately connected to genome destabilisation, and there is convincing evidence that it can significantly outperform available clinical parameters in forecasting sarcoma cases with propensity to metastasise [12]. However, all the CINSARC-genes function primarily within the context of cell division, mitotic regulation, and chromosome integrity, and while some of the genes identified might have additional functions in classical progression-coupled traits like motility and invasiveness [13], the CINSARC signature as such probably reflects the mere proclivity to progress that is greatly facilitated by genome destabilisation in order to accumulate further mutations, rather than revealing the very biological mechanisms of progression. Indeed, the CINSARC signature is able to predict progression in tumour types that are as biologically different as sarcomas, carcinomas, lymphomas, and leukaemias [14]. Important insights into the mechanistic basis of sarcoma progression could be achieved by analysing several experimental model systems. A remarkable rat fibrosarcoma progression series has been instrumental in unravelling an important mechanistic basis of motility, invasiveness, and metastatic competence in terms of cytoskeletal dynamics [15,16]. Another interesting animal sarcoma progression series

A single clone expressing the highest level of the *c-fos* transcript (clone 3, Figure S1) was designated as JUN-2fos-3 and used for all other analyses.

2.3. Expression of Fos and Jun Genes in Fibrosarcoma Cell Lines

Total RNA was isolated from cell lines using the RNeasy mini kit (Qiagen, Hilden, Germany). Then, 250 ng of total RNA were reverse transcribed using SuperScriptIII reverse transcriptase (Invitrogen), with random hexamer primers in a reaction volume of 20 μL. The *c-fos* transcript was amplified by the pair of primers with the following sequences: C-FOS forward 5′-GAC TCC TTC TCC AGC ATG GGC TC-3′; C-FOS reverse, 5′-GCT CTG GTC TGC GAT GGG GCC ACG-3′; the primer sequences are conserved between the murine (i.e., endogenous) and human (i.e., transfected) *c-fos* gene and the PCR amplicon was of 173 bp in length. The *jun* transcript was amplified by the pair of primers with the following sequences: JUN forward 5′-CAT CCA CGG CCA ACA TGC-3′; JUN reverse, 5′-TCA AAA CGT TTG CAA CTG-3′; the primer sequences are conserved between the murine *c-jun* and the *v-jun* genes [25] and the PCR amplicon was of 113 bp in length. The analysis was performed in technical duplicates on the Stratagene M×3005P apparatus (Agilent Technologies, Santa Clara, CA, USA) according to the manufacturer's protocol. The amplification included initial denaturation at 95 °C for 10 min, followed by 40 cycles of 95 °C (10 s), 95 °C (30 s), 55 °C (1 min), and 72 °C (1 min). The qualitative PCR was performed by iTaq Universal SYBR® Green SuperMix (Bio-Rad, Hercules, CA, USA). The 2 ΔΔCq method was used for the quantification of qPCR data; the expression was normalised to GAPDH gene with the following sequences: GAPDH forward 5′-AGG TCG GTG TGA ACG GAT TTG-3′; GAPDH reverse, 5′-TGT AGA CCA TGT AGT TGA GGT CA-3′.

2.4. Indirect Immunofluorescence

Cells were sparsely seeded on a coverslip and grown to 70% confluence, fixed with 100% ice-cold methanol for 30 min, permeabilised in 0.1% saponin-TBS solution, and blocked in 2% normal goat serum in PBS for 60 min. Cells were then sequentially incubated with the primary polyclonal rabbit anti-v-Jun antibody (Antibodies–online ABIN1109458, cross reactivity for avian and mammalian c-Jun) or primary polyclonal rabbit anti-human c-Fos antibody (Sigma F7799, cross reactivity for mouse, rat, and pig c-Fos, Sigma, Prague, CZ) (1% in PBS for 90 min at room temperature) and Atto 488–labelled goat anti-rabbit IgG secondary antibody (Sigma 18772—0.5% in PBS, 60 min at room temperature in dark, Sigma, Prague, CZ), with extensive washing after each incubation. The negative control staining wascarried out by omitting the respective primary antibody (Figure S2). The coverslips were mounted in Vectashield mounting medium (Vector Laboratories, Burlingame, CA, USA) and analysed using the Olympus AX70 fluorescent microscope equipped with the Olympus DP71 camera system.

2.5. Analysis of Cell Morphology

Basic morphological evaluation was carried out by routine phase contrast microscopic observation. The cell size analysis was described by a published procedure [26]. Briefly, phase contrast photographs of growing cells were taken at a 10× magnification by the Hamamatsu Orca-ER camera mounted on the Olympus IX 70 inverted microscope (Olympus, Tokyo, Japan). The QuickPHOTO Industrial 2.3 (Promicra Ltd., Prague, Czech Republic) software was used for the photo evaluations. The area of the cells in each clone (n = 15) was calculated based on the polygon surface created by tracing the contour of cells.

2.6. Evaluation of Growth Characteristics

The characteristics related to deregulated proliferation were analysed with the aid of the xCELLigence system (Roche, Basel, Switzerland) [27]. The xCELLigence system monitors the cellular events in real time by measuring electrical impedance using micro-electrodes at the bottom of each cell culture plate well. The RTCA software calculates

the cell index (CI) as a relative change in measured impedance. Two major parameters were assessed—the slope of the linear phase of the growth curve describing the steepness incline, and the doubling time (DT), i.e., the period of time required for a given quantity to double in size or value; assuming an exponential growth, the relationship between these parameters is: slope = log2/DT. The procedure was performed according to the instructions provided by the manufacturer. Briefly, 5000 cells in 100 μL DMEM per well were seeded in triplicate (E plate 16), in the final volume of 200 μL of growth medium and maintained in a culture under standard conditions. Dynamic cell proliferation and growth were monitored every 15 min for 77 h. Each cell line produced a distinct profile with the RTCA HT Instrument, corresponding to differences in growth rate, cell morphology or doubling time, and the values of the cell index were calculated and plotted on the graph. Experiments were performed in triplicates and repeated at least twice with similar results.

2.7. Anchorage-Independent Growth

The ability of anchorage-independent growth was quantified as clonogenicity in 15% methylcellulose-containing full growth medium [28]. Cells were harvested by routine trypsinisation, dissolved in 15% methylcellulose-containing full growth medium and partitioned in triplicates onto ultra-low attachment surface 6-well plates (Corning); 20,000 cells per well were used. Colonies were counted after four weeks of culture, with supplementation with the normal growth medium every week. Photographic documentation was taken by the Olympus IX 70 inverted microscope equipped with the Hamamatsu Orca-ER camera. Experiments were performed in triplicates and repeated four times with similar results.

2.8. Sphere Formation Assay and Side Population Assay

The ability to grow in sarcospheres was assessed as described [29,30]. Briefly, cells were harvested by routine trypsinisation at ~80% confluence. Then, 100,000 cells were seeded per one well in ultra-low attachment surface 6-well plates (Corning, NY, USA) in serum-free DMEM/1% methylcellulose medium supplemented with the recombinant mouse FGF2 (Sigma SRP4038–10 ng/mL, Sigma, Prague, CZ) EGF from murine submaxillary gland (Sigma E4127–10 ng/mL, Sigma, Prague, CZ) and 1× N2 supplement (Gibco/Invitrogen), with regular addition of FGF-2 and EGF every other day. Following 10–14 days in culture, colonies that contained >10 cells were quantitated by inverted phase contrast microscopy. Experiments were performed in triplicates and repeated a minimum of twice with similar results. The side population was analysed as DyeCycle™ Violet (ThermoFischer Scientific, Carslbad, CA, USA) dim cells, as described previously [31].

2.9. Motility Assay

The motility assay was performed as the in vitro wound-healing assay as described previously [20]. Briefly, cells were plated onto plastic Petri dishes (60 mm diameter) and grown to confluence. The confluent monolayers were wounded using white plastic micropipette tips, washed with culture medium, and returned to the incubator. The course of the healing was followed for 48 h in Olympus IX70 phase-contrast microscope, and photo-documented at several time points using the Olympus C-35AD-4 camera.

2.10. Assessment of Invasive Ability

Two independent approaches were applied to assess the invasiveness of JUN- sarcoma cell lines. First, the BD BioCoatTM MatrigelTM Invasion Chamber (Becton Dickinson, Franklin Lakes, NJ, USA) was used, following the instructions of the manufacturer, with minor modifications, as described previously [20]. Briefly, after trypsinisation and harvesting, 50,000 cells were seeded onto 8 μm pore Matrigel-coated invasion chambers. The invasion test was left for 24 h, with complete, serum-supplemented culture medium in both the lower and upper compartments of the chamber. At the conclusion of the incubation time, cells attached to the upper surface of the membrane (i.e., non-invading) were mechanically removed. The invading cells were fixed using the Carnoy fixative and Giemsa

(Sigma, Prague, CZ)-stained. Cell invasion was evaluated in triplicate and repeated twice and expressed as an absolute average number of invading cells from five randomly chosen fields using an Olympus IX 70 inverted microscope.

Second, we adopted a recently described method of three-dimensional invasion assay [32]. Multicell tumour spheroids were generated by a liquid overlay technique [33] by placing 200,000 cells into agarose-covered 6-well plates; spheroids were harvested after 10 days. The spheroids were embedded into type I collagen (Sigma, Prague, CZ); stock solution was made by diluting type I collagen in 0.02 M acetic acid to the final concentration of 8.5 mg/mL at 4 °C overnight. The experimental collagen type I solution was made by quickly mixing equal volumes of the stock solution and sterile neutralizing buffer (100 mM HEPES in 2× PBS). Next, 200 μL of the experimental collagen solution was quickly pipetted per well into a 24-well plate and allowed to solidify for 2 h in a standard CO_2 incubator at 37 °C, 95% humidity, and 5% CO_2. Afterwards, the single spheroids were carefully transferred onto the top of the gels and overlaid by 100 μL of experimental collagen solution and again incubated at 37 °C, 95% humidity, and 5% CO_2 for an additional 2 h to allow for the solidification of the upper collagen layer. Finally, 50 μL of full growth medium was added to the top of the sandwich and the plate was returned into the CO_2 incubator. After embedding, changes in the spheroids' shape reflecting the active movement and invasion of tumour cells out of an embedded spheroid into the surrounding collagen matrix were monitored by phase contrast microscopy over a period of two weeks and photo-documented as described above. This experiment was repeated twice.

2.11. Analysis of Cellular Energy Metabolism

Oxygen consumption by JUN-1 ($n = 8$), JUN-2 ($n = 8$), JUN-3 ($n = 11$), and JUN-2fos3 ($n = 9$) cells was analysed by high-resolution respirometry in 2 mL glass chambers of oxygraph Oroboros at 37 °C using DatLab software for data acquisition and analysis (Oroboros, Innsbruck, Austria). The oxygen flux was calculated online as a negative time derivative of the oxygen concentration and its values were corrected for instrumental background measured in separate experiments performed in the same medium without cells. After equilibration, the cells were injected into the chambers, mixed, and counted. Respiratory activity of cells was assessed as routine respiration (ROUT; R). State LEAK (L) reflecting intrinsic mitochondrial uncoupling due to the proton leak, proton and electron slip, and cation cycling [34] was measured after inhibition of ATP synthesis by oligomycin (2 μg/mL). Uncoupler trifluorocarbonylcyanide phenylhydrazone (FCCP; 0.05 μmol/L titration steps) was used to induce the state ETS (E), i.e., the maximum capacity of the electron-transporting system. The residual oxygen consumption (ROX) remaining after the inhibition of ETS was determined by antimycin A injection (2.5 μmol/L). In the results, oxygen fluxes recorded in the individual titration steps were corrected for ROX. The results were expressed per IU of citrate synthase (CS) activity reflecting mitochondrial content in cells, assayed in the samples aspirated from each oxygraph chamber [35,36]. The assay medium consisted of 0.1 mmol/L 5,5-dithio-bis-(2-nitrobenzoic) acid, 0.25% Triton-X, 0.5 mmol/L oxalacetate, 0.31 mmol/L acetyl coenzyme A, 5 μmo/L EDTA, 5 mmol/L triethanolamine hydrochloride, and 0.1 mol/L Tris-HCl, pH 8.1 [35]. Then, 200 μL of the mixed and homogenised chamber content was added to 800 μL of the medium. The enzyme activity was measured spectrophotometrically at 412 nm and 30 °C for 200 s and expressed in mIU per 10^6 cells.

The cell culture medium glucose measurement was performed according to method using a glucose assay kit (GAHK-20, Sigma, Prague, CZ) [37]. Briefly, with this method, glucose is phosphorylated by hexokinase (HK) in the presence of adenosine triphosphate (ATP) to produce glucose-6-phosphate (G-6-P) and adenosine diphosphate (ADP). Glucose-6-phosphate dehydrogenase (G-6-PDH) specifically oxidises G-6-P to 6-phosphogluconate with the concurrent reduction of nicotinamide adenine dinucleotide (NAD) to nicotinamide adenine dinucleotide reduced (NADH). The NADH absorbs light at 340 nm and can be detected spectrophotometrically as an increased absorbance.

Lactate secretory activity was determined using the enzymatic colourimetric assay of conditioned culture media. Medium from each treatment was collected and tested for lactate concentration using an L-lactate Assay Kit (#1200012002, Eton Biosciences Inc., San Diego, CA, USA) [38]. Briefly, L-lactate is oxidised to pyruvate by the specific enzyme lactate oxidase (LOD) and hydrogen peroxide (H_2O_2). In the next reaction, enzyme peroxidase (POD) is used to generate a colour dye using the hydrogen peroxide created in the first reaction. The intensity of the colour formed is directly proportional to the L-lactate concentration. It is determined by measuring the increase in absorbance at 552 nm wavelength. Experiments were performed in triplicates and repeated a minimum of two times with similar results.

2.12. Transcriptomic Profiling

Total cellular RNA were extracted from dry pellets of JUN-2, JUN-2fos-3, and JUN-3 cells (each cell line in biological triplicates; Figure S3) by mirVana™ miRNA Isolation Kit (Invitrogen™; ThermoFisher Scientific, Carslbad, CA, USA) according to manufacturer protocol. DNase treatment of extracted RNA was performed by DNA-free™ DNA Removal Kit (Invitrogen™; ThermoFisher Scientific, Carslbad, CA, USA) to remove possible genomic contaminations. Quality and integrity of purified RNA was determined by NanoDrop 2000c (ThermoFisher Scientific, Carslbad, CA, USA) and TapeStation RNA ScreenTape (Agilent Technologies, Santa Clara, CA, USA) to select appropriate RNA samples for analysis. The subsequent synthesis of labelled and fragmented cRNA was performed by GeneChip™ 3′ IVT PLUS Reagent Kit (Applied Biosystems™; ThermoFisher Scientific, Carslbad, CA, USA) according to the manufacturer protocol. Subsequent high-throughput gene expression analyses were performed using the hybridisation technology GeneChip Mouse Genome 430 2.0 Array (ThermoFisher Scientific, Carslbad, CA, USA) according to the manufacturer protocol; intensity values for each probe cell (.cel file) were calculated using Affymetrix GeneChip Command Console (AGCC) software. These arrays cover over 39,000 mouse transcripts. All data were pre-processed and further analysed by the software packages included in the R/Bioconductor, and pre-processing was performed by the RMA method [39]. Complete linkage clustering (farthest neighbour clustering) with Euclidean distance measurements were applied for the visualisation of sample similarities and clusters. As it was impossible to visualise the heatmap structure of all the genes included in the full data matrix of expression data consisting of 22,690 genes, the heatmap was based on expression data of 2000 randomly selected genes. To identify differentially expressed transcripts, the LIMMA approach was applied with additional Benjamini–Hochberg correction of *p* values. Gene set over-representation analysis on upregulated and downregulated gene groups was performed using ConsensusPathDB-mouse (Max Planck Institute for Molecular Genetics in Berlin, Germany, Retrieved from http://cpdb.molgen.mpg.de/MCPDB, (Accessed date on 24 July 2020)) using default settings to detect pathways across various databases (KEGG, MouseCyc, Reactome, and Wikipathways) connected to our gene groups. If the same pathway was detected in various databases, the one with the lowest *p*-value was used. All pathways were sorted in ascending order according to their *p*-value.

2.13. Pharmacologic Inhibition of CCL8 Activity

JUN-3 cells were used to test consequences of pharmacologic inhibition of both the ligand CCL8 by Bindarit [40,41] (Abcam ab143292) and of its major receptor CCR5 by Maraviroc [42,43] (Sigma, Prague, CZ), either individually or in combination. The drugs were dissolved in DMSO (Sigma, Prague, CZ) with 50 mM stock solutions. The effects of CCL8–CCR5 inhibition on cell motility was analysed using special migration plate with 8 μm pore membranes (CIM-Plate®; used with the xCELLigence® RTCA DP system from ACEA Biosciences, USA; contains electronically integrated Boyden chambers) [44]. Briefly, 20,000 cells in 90 μL of serum-free medium were seeded to each well of the upper chamber, then 10 μL of drug solutions was added (final concentration of inhibitors: 10 μM Maraviroc and 250 μM Bindarit). The wells of the bottom chamber were filled with 160 mL of 10%

serum-containing media. The DP instrument with CIM-Plate 16 was placed in a standard CO_2 incubator. The xCELLigence software was set to collect impendence data (reported as cell index—CI) at every 15 min for 30 h. Finally, we analysed the cell index curves and determined the cell migration activity. Experiments were performed in triplicates and repeated a minimum of two times with similar results. The consequences of either inhibitor on cell invasiveness were evaluated by 3D collagen invasion assay as described above, with the addition of either inhibitor directly into the type I collagen gel (final concentration of inhibitors: 10 μM Maraviroc and 250 μM Bindarit), and monitoring of the invasiveness of JUN-3 spheroids by phase contrast microscopy over a period of two weeks. This experiment was repeated twice.

2.14. Additional Statistical Analysis

Statistical analyses and data visualisations were performed in R statistical software [45]. Parametric statistical analyses were extended by permutational (hypothesis testing) or bias-corrected and accelerated bootstrap [46] (estimation of 95% confidence intervals) techniques (10,000–21,000 permutations/resamplings), which do not rely on assumptions of parametric methods and give reliable results even for small sample sizes. Comparisons between groups were performed by permutational ANOVA followed by permutational t-test (exact if N < 11, Monte-Carlo otherwise) with false discovery rate correction for multiple comparisons [47] as a post hoc, both using predictmeans' R package [48] and our previously used and published R scripts [49,50]. Heteroscedastic residuals were stabilised by appropriate data transformation. Plots were created using 'beeswarm' [51] and 'vioplot' [52] R packages.

3. Results

3.1. Extension of JUN-Sarcoma Progression Series for the JUN-2fos-3 Cell Line

The JUN-fibrosarcoma progression series described previously [20] featured a linear gradation of all the transformation-related traits from relatively non-transformed JUN-2 cells, through JUN-1 with an intermediate transformation status to the highly transformed JUN-3 cells. We also noticed an inverse relationship between the *v-jun* oncogene expression and the transformation grade. This relatively high and ubiquitous *v-jun* expression in JUN-2 cells presenting a low transformation status encouraged us to address the possibility of their targeted in vitro transformation by virtue of overexpressing the cooperating oncogene *c-fos*; indeed, we were able to establish a derivative cell line, JUN-2fos-3, with a high level of *c-fos* expression (Figure S1, Table S1). We could verify that both JUN-2 and its new daughter cell line expressed a high level of *jun* oncogenes (*v-jun* and *c-jun*) (Figure 1). As both *jun* and *fos* oncogenes code for nuclear transcription factors, we were also interested in subcellular localisation of the respective oncoproteins. Both JUN-2 and its derivative daughter JUN-2fos-3 displayed prominent high nuclear expression of both fos and jun oncoproteins. Remarkably, we could not see any nuclear c-fos signal in JUN-1 cells, and we saw very unusual subcellular localisation of the c-fos protein in JUN-3 cells, with a very prominent perinuclear localisation, as opposed to the diffuse pan-nuclear staining in JUN-2, and especially in JUN-2fos-3 cells. With regard to the jun expression, our immunofluorescence analysis showed, in addition to the high nuclear expression in both JUN-2 and JUN-2fos-3 cell lines, a low but evident expression in JUN-1 cells, and minimal expression in the bulk of the JUN-3 cells; interestingly, we noticed individual scattered JUN-1 as well as JUN-3 cells showing appreciably high nuclear jun oncoprotein expression, whose identity remains to be established (Figure 2, cells are marked with arrows; Figure S2).
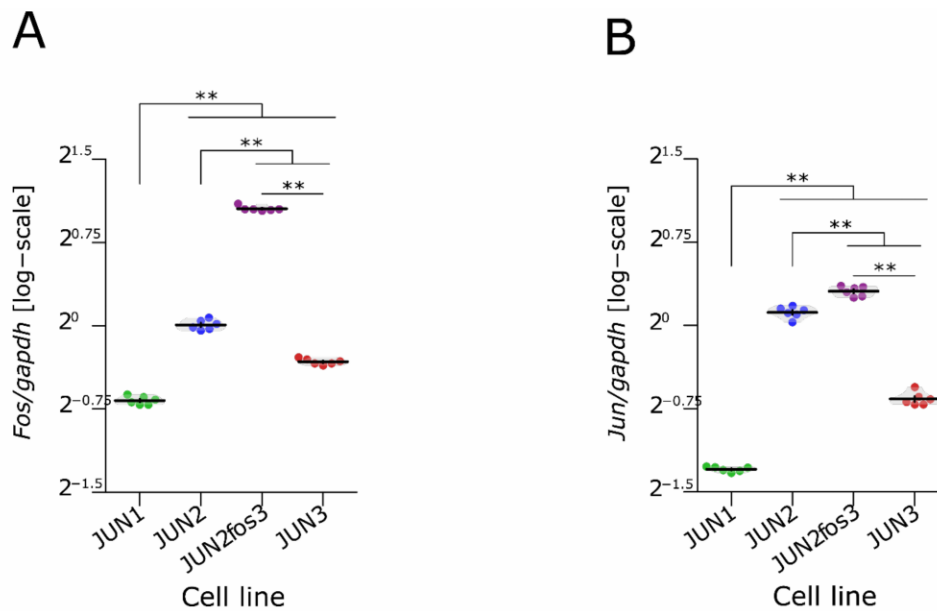
Figure 1. *Fos* and *Jun* expression in fibrosarcoma cell lines. (**A**,**B**) Comparison of *jun* and *fos* expression in different JUN-sarcoma cell lines. Results of permutational ANOVA: $F_{3,20}$ = 1531, ** $p < 0.01$ (*jun* expression) and $F_{3,20}$ = 2948, ** $p < 0.01$ (*fos* expression). See Table S1 for results of contrasts between pairs of lines, their confidence intervals, and exact *p*-values. Each point represents an individual experiment (*n* = 6). Violin plots with means ± SEM are shown.

Morphologically, isolated JUN-2fos-3 cells presented with prominent lamellipodia and the largest cell size, whereas the JUN-3 cells represented the opposite size phenotype, being the smallest of the series (Figures 2 and 3A–C, Table S2).

3.2. Proliferation Characteristics

We applied two assays to evaluate the proliferative activity of the cells. Proliferation in a two-dimensional culture setting was quantified with the aid of two variables—the doubling time and the slope of the exponential growth phase. The results of this analysis are shown in Figure 4A,B, Table 1 and Table S3. We verified the previous results obtained with simpler methodology for JUN-1, -2, and -3 cell lines [20], with JUN-3 being the fastest growing cell line and JUN-1 and JUN-2 showing an intermediary growth intensity. The proliferative activity of the newly established derivative JUN-2fos-3 was inferior to all the other sarcoma cell lines of the series, even below the proliferative activity of its parental cell line JUN-2.

Proliferation in three-dimensional culture was analysed as anchorage-independent growth by evaluating clonogenicity in methylcellulose-containing medium. We evaluated two characteristics—the total number of colonies and their size. We saw the same distribution of sarcoma cell lines as in the two-dimensional culture. JUN-3 was by far the most active cell line in both the total colony number and their size (Figure 4C,D, Table S3), whereas JUN-2fos-3 showed the weakest proliferation activity in the methylcellulose clonogenicity assay. JUN-1 and JUN-2 reached practically identical colony numbers, with distinctly larger colonies produced by the JUN-1 cell line.

3.3. Sarcosphere Formation and Clonogenic Activity Is Not Associated with Apparent Side Population

The results of the anchorage-independent growth can be interpreted in two ways. Apparently, the clonogenicity in a semisolid medium may reflect a combination of the proliferative activity and evasion from anoikis, and the overall excellent correlation between the steepness of growth curves in a classical two-dimensional culture and the clonogenicity in methylcellulose suggests that the general proliferative activity could indeed be essential for the anchorage-independent growth of the JUN-sarcoma cell lines. On the other hand, clonogenicity in semisolid media is also increasingly viewed as an assay for cancer stem cells [53,54], and in this case, differences in the clonogenicity in methylcellulose among the JUN-sarcoma cell lines could be more indicative of differences in a relative frequencies of sarcoma stem cells. To resolve this question, we performed the sarcosphere assay (Figure 4E,F, Table S3). Remarkably, the JUN-2fos-3 cell line showed the second highest sarcosphere formation efficiency, indicating that its poor clonogenicity in methylcellulose could be rather attributed to its overall low proliferation activity. The significantly highest sarcosphere formation efficiency was observed in the JUN-3 cell line, which thus couples a high proliferation intensity with the relatively highest frequency of sarcoma stem cells (Figure 4E, Table S3).

On the other hand, we were unable to evidence any appreciable side population in JUN-3 cell line (data not shown); the biological underpinnings of clonogenic and sarcosphere-founding cells thus remains to be further characterised.

3.4. JUN-2fos-3 and JUN-3 Cell Lines Are Highly Motile and Invasive

Besides the growth characteristics, we were also interested in the progression characteristics of JUN-sarcoma cell lines; as noted above, our initial characterisation of JUN-1, -2, and -3 cell lines revealed a perfect correlation between growth and progression-related transformation characteristics [20]. A surprising finding was that the newly established JUN-2fos-3 cell line was highly motile in the in vitro wound-healing assay (Figure 5A,B). Although the invasiveness expressed as the total number of cells invading the Matrigel-coated insert and adhering on its bottom in the Matrigel invasion assay were 3.92 times lower than for the highly invasive JUN-3 cell line (Figure 5C,D, Table S4), we noticed that for both the JUN-2fos-3 and JUN-3, the bottom of the Matrigel insert was covered by a confluent cell layer, and indeed, this coefficient was practically identical to the size relation between the JUN-2fos-3 and JUN-3 cells (adherent cell area of JUN-2fos-3 is 3.85 times larger than that of JUN-3 cells). Therefore, we hypothesised that the observed difference in the Matrigel invasion was due to the difference in the cell size of JUN-3 and JUN-2fos-3. To corroborate this notion, we performed an independent invasion assay that could not be influenced by differences in the cell size, namely the three-dimensional invasion assay of spheroids embedded in type I collagen. Both the JUN-2fos-3 and the JUN-3 cell lines showed comparatively intensive invasion in this assay (Figure 5C). The JUN-1 cell line displayed an intermediate invasion in the Matrigel invasion assay and minimal invasiveness in spheroids embedded in type I collagen, whereas the JUN-2 cell line was completely non-invasive in both the invasion assays.

3.5. Invasive Cell Lines Have Different Metabolic Profiles

Figure 6A,C and Table S5 depict the values of respiratory states of all cells under investigation. Interestingly, JUN-2fos-3 cells displayed significantly higher oxygen consumption in the states R, L, and E compared to the least transformed non-invasive, non-motile JUN-2 cells. Accordingly, their respiration related to mitochondrial ATP production calculated as a difference between routine and leak respiration (R-L; free routine activity) did not differ from that measured in the most transformed JUN-3 cells. In addition, the spare respiratory capacity (excess E-R capacity), i.e., the difference between the fully uncoupled and routine cellular oxygen consumption, was higher in invasive and motile cell lines (JUN-3 and JUN-2fos-3) than in cells with limited motility and invasiveness (JUN-1 and JUN-2).
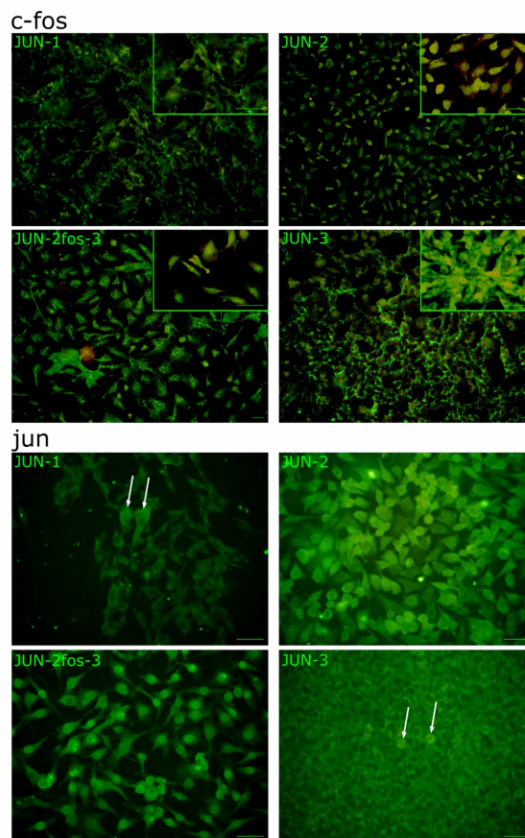
Figure 2. Fos and Jun oncoproteins expression in fibrosarcoma cell lines. Indirect immunofluorescence analysis. Notice the high nuclear expression of both oncoproteins in JUN-2 as well as JUN-2fos-3 cells and their low expression levels in JUN-1 cells. Fos seems to be quite highly expressed in JUN-3 cells as well, with an unusual perinuclear localisation. Both JUN-1 and JUN-3 seem to be generally devoid of appreciable nuclear Jun, except some individual scattered cells (arrows). Pictures were taken by Olympus IX70 fluorescent microscope equipped with the Olympus DP71 camera system (Bar: 100 μm) Negative controls are shown in Figure S2.

Table 1. Growth characteristics of the JUN-sarcoma cell lines.

Cell Line	Doubling Time (h)	Slope of the Exponential Growth Phase
JUN-1	9.5	0.032
JUN-2	10.4	0.029
JUN-2fos-3	30.9	0.010
JUN-3	7.4	0.041
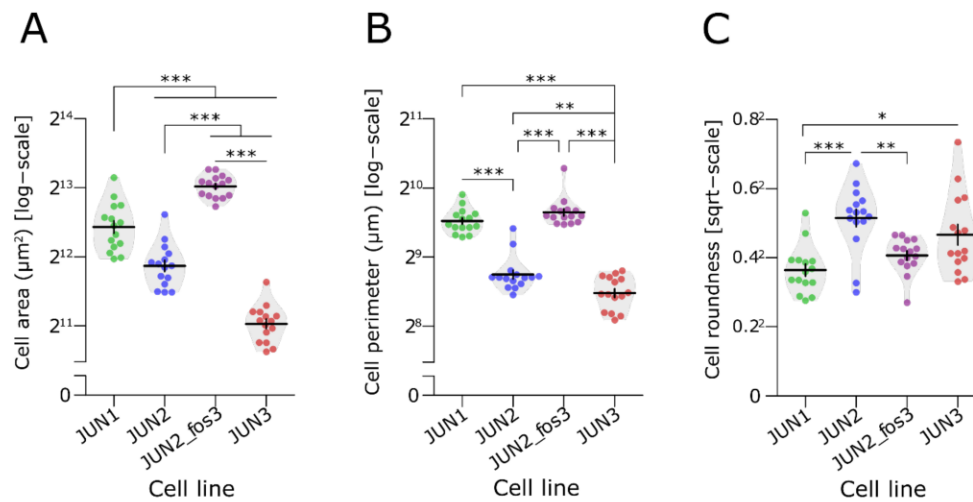
Figure 3. Morphological characteristics of JUN-sarcoma cell lines. (**A–C**) Size analysis of single adherent cells of JUN-sarcoma cell lines. Three parameters were evaluated—the total cell area of an adherent cell (μm^2; permutational ANOVA: $F_{3,34} = 3.4$, $p = 0.021$), the cell perimeter (μm; permutational ANOVA: $F_{3,34} = 45$, $p < 0.001$), and the cell roundness (permutational ANOVA: $F_{3,34} = 3.8$, $p = 0.018$). The JUN-2-fos-3 cell line presented the largest cell size with prominent lamellipodia. $* p < 0.05$, $** p < 0.01$, $*** p < 0.001$. The statistical significances are based on permutational t-test with FDR correction. See Table S2 for effect sizes, their confidence intervals, and exact *p*-values. Each point represents an individual cell ($n = 15$). Violin plots with means $\pm$ SEM are shown.

If expressed per 10^6 cells, the JUN-2 cell line had a relatively high capacity of oxidative phosphorylation and the lowest production of lactate (Figure 6B, Table S5), suggesting that ATP is generated, especially aerobically, through the respiratory chain. In contrast, JUN-2fos-3 cell line displayed high oxphos and electron-transporting capacities and a high production of lactate in parallel. The most transformed JUN-3 cell line combined relatively high oxphos parameters with the highest production of lactate and consumption of glucose, taking advantage of both pathways of energy production. Accordingly, the glucose consumption rate was also significantly higher in both invasive sarcoma sublines (Figure 6D, Table S5).

Citrate synthase activity was the highest in JUN-2fos-3 cell line (77.2 ± 10.9 mIU/10^6 cells), comparable in JUN-2 and JUN-3 cells (62.1 ± 25.2 and 51.3 ± 20.6 mIU/10^6 cells, respectively), and the lowest in JUN-1 cells (27.4 ± 16.7 mIU/10^6) with intermediary proliferation, motility, and invasiveness characteristics.

3.6. Distribution of Transformation Traits among JUN Fibrosarcoma Cell Lines Allows for the Straightforward Identification of Genes Potentially Responsible for Sarcoma Cell Proliferation and Motility/Invasiveness

These unique combinations of transformation-related traits made it possible for us to identify two separate groups of genes tentatively involved in sarcoma progression in a single transcriptomic analysis—on the one hand, proliferation-related genes could be identified by their differential expression in JUN-3 compared to both JUN-2 and JUN-2fos3, and, on the other hand, motility and invasiveness-related genes could be identified by their common expression pattern in JUN-2fos3 and JUN-3 cells compared to JUN-2 (Table 2). The former will be addressed in a separate article, and for the remainder of this article, we focus on genes potentially underlying the invasive character of JUN-2fos3 and JUN-3 cell lines. Starting with individual comparisons of each of the invasive sarcoma cell lines with the reference cell line JUN-2 (Tables S9 and S10), we finally arrived at a common transcriptomic

profile in both the invasive cell lines. In total, we identified 126 genes that were significantly upregulated and 249 genes that were significantly downregulated in the motile/invasive fibrosarcoma cell lines JUN-2fos3 and JUN-3 compared to JUN-2 (Table S6). The gene set enrichment analysis (Figure 7 and Table S7) revealed that the downregulated genes are dominated by extracellular matrix and cell adhesion, as well as antigen presentation, whereas upregulated pathways, surprisingly, involve an unexpected number of molecular pathways related to cell cycle regulation and DNA replication.

Table 2. Overall strategy of transcriptomic analysis. The distribution of transformation traits among JUN-2, JUN-2fos-3 and JUN-3 fibrosarcoma cell lines made us possible to identify separate sets of genes responsible for motility/invasiveness and proliferation, respectively, in a single transcriptomic analysis *.

Motility and invasiveness-related genes	JUN3↑ JUN2f3↑ JUN2↓ and JUN3↓ JUN2f3↓ JUN2↑ (activators of motility) (suppressors of motility)
Proliferation-related genes	JUN3↑ JUN2f3↓ JUN2↓ and JUN3↓ JUN2f3↑ JUN2↑ (activators of proliferation) (suppressors of proliferation)

* Arrows indicate expression change of a hypothetical gene from the two biological groups in individual sarcoma cell lines.

3.7. CCL8 Represents a Druggable Target to Curtail Motility and Invasion

As an initial proof of conceptual correctness and usefulness of our transcriptomic screen, we chose CCL8 to test for pharmacological targeting of motility and invasiveness. We were lead in our choice mainly by the availability of clinically applicable pharmacologic inhibitors for both the ligand by Bindarit [55], and its major receptor CCR5 by Maraviroc [56]. Both inhibitors were able to substantially decrease both the motility of JUN-3 cells in the real-time xCELLigence® RTCA DP system assay (Figure 8A, Table S8) and the invasion of JUN-3-derived multicellular spheroids into type I collagen gels (Figure 8B), with an indication for their additive effects upon drug combination.
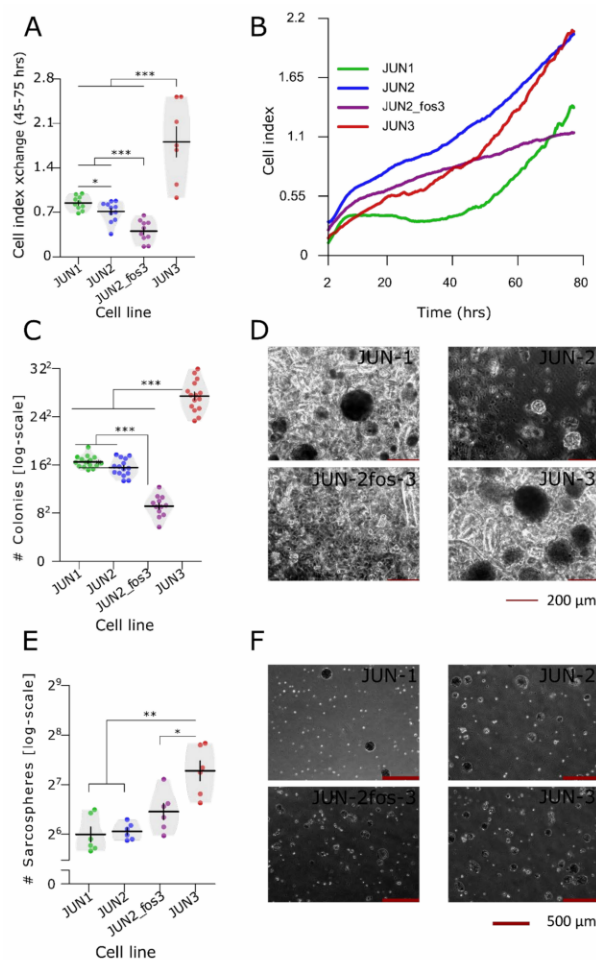
Figure 4. Proliferation and stemness-related characteristics of JUN-sarcoma cell line. (**A**) Proliferation of JUN-sarcoma cell lines. The doubling time and slope analysis (Table 1) were performed on linear growth phase, set arbitrarily as growth curve interval between 45 and 75 h (permutational ANOVA: $F_{3,34} = 33$, $p < 0.001$). The JUN-3 cell line showed the fastest growth. The proliferative activity of the newly established derivative JUN-2fos-3 was inferior to all the other sarcoma cell lines of the series, even below the proliferative activity of its parental cell line JUN-2. (**B**) Growth curve of the JUN-sarcoma cell lines. The proliferative activity of the newly established derivative JUN-2fos-3 was inferior to all the other sarcoma cell lines of the series, even below the proliferative activity of its parental cell line JUN-2. (**C**) Clonogenicity in semisolid media differ among JUN-sarcoma cell lines (permutational ANOVA: $F_{3,53} = 252$, $p < 0.001$). JUN-3 was the most active cell line, whereas the JUN-2fos-3 showed the weakest clonogenicity. Representative pictures of colonies formed in 15% methylcellulose are shown in (**D**). The pictures were taken by the Olympus IX 70 inverted microscope equipped with the Hamamatsu Orca-ER camera at $100\times$ magnification. (**E**) Sarcosphere formation capacity differed among JUN-sarcoma cell lines (permutational ANOVA: $F_{3,20} = 14.8$, $p < 0.001$).

Both JUN-2fos-3 and JUN-3 presented rather high sarcosphere formation activity. Representative pictures of spheres are shown in (**F**). The pictures were taken by the Olympus IX 70 inverted microscope equipped with the Hamamatsu Orca-ER camera at 40× magnification. * $p < 0.05$, ** $p < 0.01$, *** $p < 0.001$ (A,C,E, respectively). The statistical significances are based on a permutational *t*-test with FDR correction. See Table S3 for effect sizes, their confidence intervals, and exact *p*-values. Each point represents an individual well. Violin plots with means ± SEM are shown.
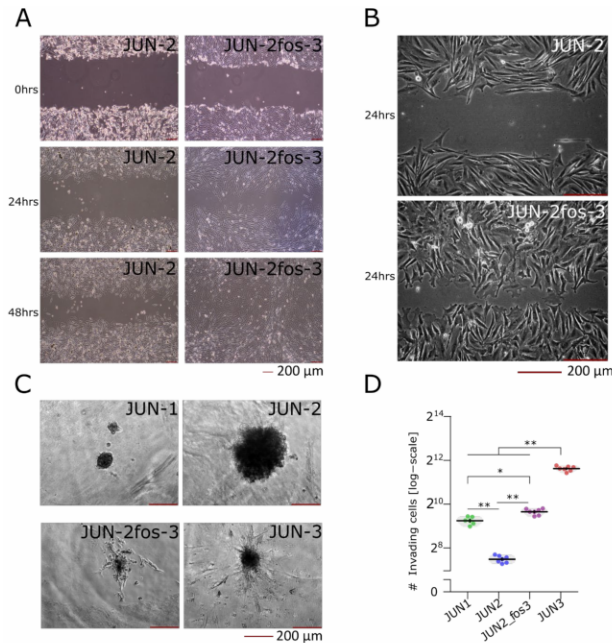
Figure 5. Invasion-related characteristics of JUN-sarcoma cell line. (**A–D**) JUN-2fos-3 cells are highly motile and invasive. (**A**) Cell motility after 24 and 48 h in vitro wound-healing test. The newly established JUN-2fos-3 cell line was highly motile in the in vitro wound-healing assay compared to its mother cell line JUN-2. Representative pictures were taken by the Olympus IX 70 inverted microscope at 40× magnification (at 100× magnification in detail (**B**)). (**C**) Invasion of multicell tumour spheroids of JUN-sarcoma cell lines embedded into type I collagen at 100× magnification. JUN-3 and JUN-2fos-3 cell lines showed comparatively intensive invasion, whereas the JUN-2 cell line was completely non-invasive. JUN-1 cell line displayed minimal invasiveness in type I collagen. (**D**) Matrigel in vitro invasion assay differed among JUN-sarcoma cell lines (permutational ANOVA: $F_{3,23} = 910$, $p < 0.001$). Both the JUN-2fos-3 and the JUN-3 cell lines showed comparatively intensive invasion in this assay. * $p < 0.05$, ** $p < 0.01$ The statistical significances are based on permutational *t*-test with FDR correction. See Table S4 for effect sizes, their confidence intervals, and exact *p*-values. Each point represents an individual well. Violin plots with means ± SEM are shown.
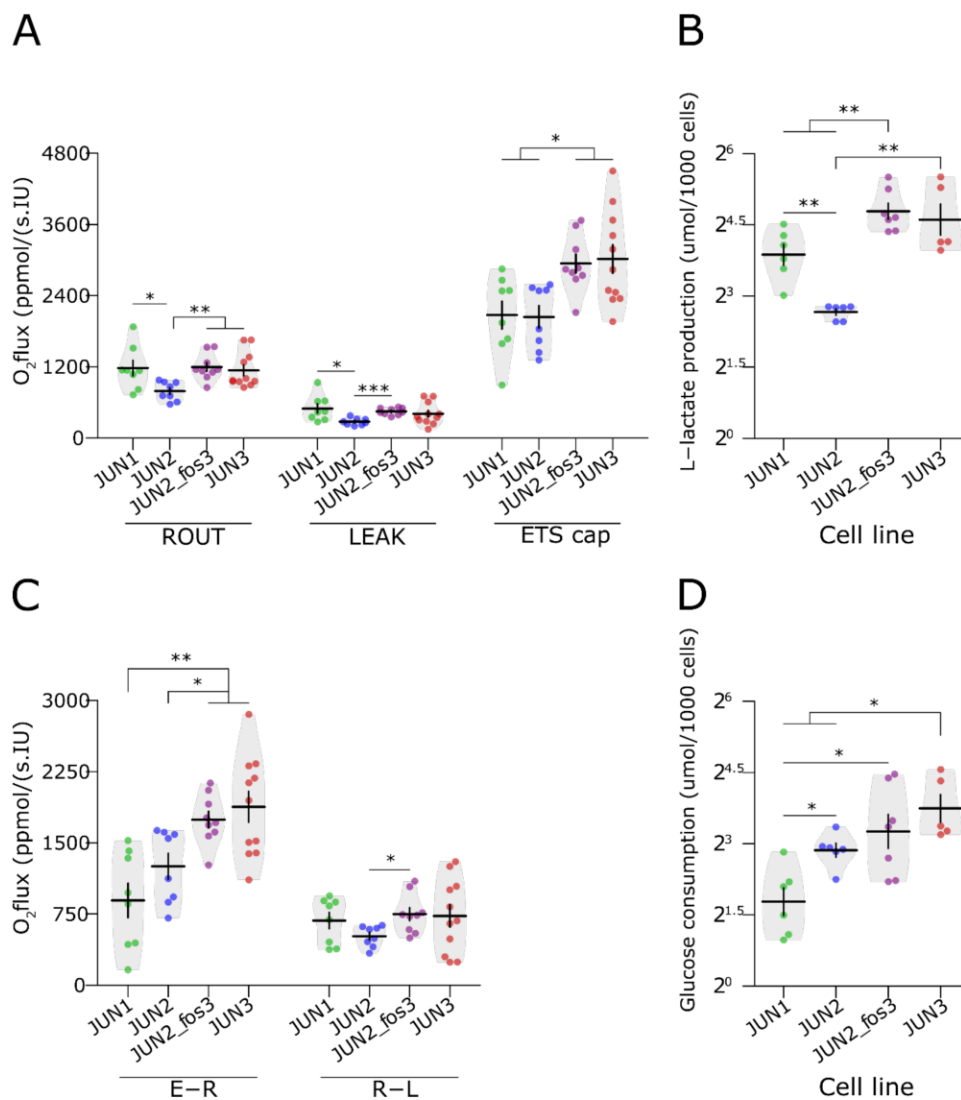
Figure 6. Metabolic analysis of JUN-sarcoma cell lines. (**A**,**C**) Mitochondrial oxygen consumption in JUN-sarcoma cell lines. Cell lines differed in oxygen consumptions in state R (permutational ANOVA: $F_{3,32} = 4$, $p = 0.015$), L (permutational ANOVA: $F_{3,32} = 3.2$, $p < 0.032$), and E (permutational ANOVA: $F_{3,32} = 6$, $p = 0.0021$), and also differed in E-R capacity (permutational ANOVA: $F_{3,32} = 9.5$, $p < 0.001$) but not R-L capacity (permutational ANOVA: $F_{3,32} = 1.3$, $p = 0.3$). The JUN-2fos-3 cell line displayed significantly higher oxygen consumption in the states R, L, and E compared to the least transformed non-invasive, non-motile JUN-2 cells. The spare respiratory capacity (excess E-R capacity) was higher in both invasive and motile cell lines, JUN-3 and JUN-2fos-3, than in cells with limited motility and invasiveness, JUN-1 and JUN-2. (**B**) The production of L-lactate differed among JUN-sarcoma cell lines (µmol/1000 cells; (permutational ANOVA: $F_{3,20} = 25$, $p < 0.001$). The JUN-2 cell line had a relatively high capacity of oxidative phosphorylation and the lowest production of lactate, suggesting

that ATP is generated especially aerobically through the respiratory chain. (**D**) The consumption of glucose differed among JUN-sarcoma cell lines (μmol/1000 cells; (permutational ANOVA: $F_{3,23} = 9.9$, $p < 0.001$). Both the invasive cell lines JUN-2fos-3 and JUN-3 combined relatively high oxphos parameters with the highest production of lactate and consumption of glucose, taking advantage of both pathways of energy production. * $p < 0.05$, ** $p < 0.01$, *** $p < 0.001$. The statistical significances are based on permutational t-test with FDR correction. See Table S5 for effect sizes, their confidence intervals, and exact p-values. Each point represents an individual experiment. Violin plots with means $\pm$ SEM are shown. (ROUT: (R)—resting respiration of intact cells, LEAK (L)—oxygen consumption essential for compensation for the proton leakage, ETS cap (E)—uncoupled respiration, i.e., maximum capacity of the electron-transporting system. R-L—ATP-linked oxygen consumption, E-R—spare respiratory capacity).

Figure 7. The gene set enrichment analysis of JUN-sarcoma cell lines. Median log (fold change) with 95% confidence interval in pathways sorted by fold change. Downregulated pathways are shown in blue, whereas upregulated pathways are shown in red colours. Analysis revealed that the downregulated genes are dominated by extracellular matrix and cell adhesion, as well as antigen presentation, whereas among upregulated pathways, those related to cell cycle regulation and DNA replication are particularly frequent (see Table S7 The gene set enrichment analysis for complete list of genes in each pathway).
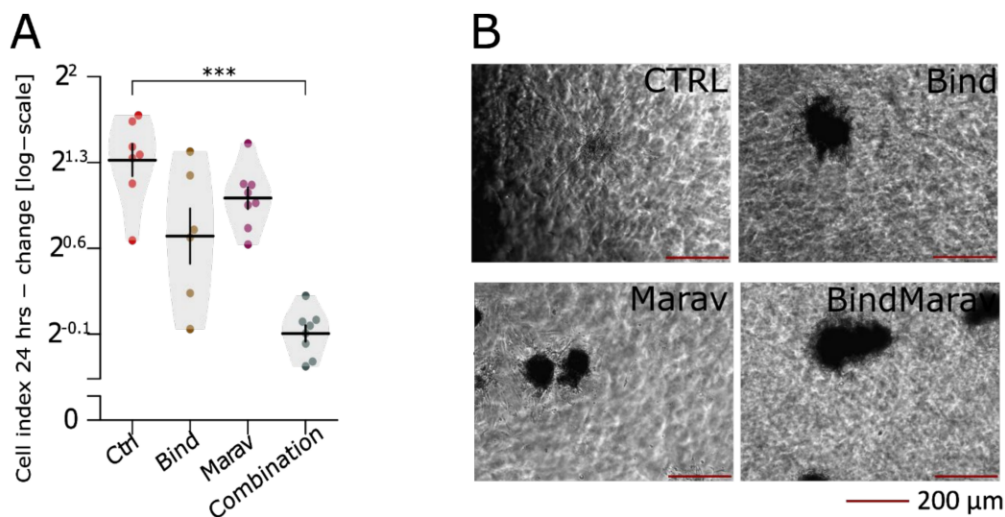
Figure 8. Pharmacological inhibition of Ccl8 - Ccr5 signalling entails a significant decline in invasive capacity. Cells were treated with Bindarit (Ccl8 inhibitor, 250 μM), Maraviroc (Ccr5 inhibitor, 10 μM), or their combination and their invasiveness was analysed by xCelligence motility assay (**A**) and by the invasion of multicell tumour spheroids of JUN-sarcoma cell lines embedded into type I collagen identically to or. (**B**) Linear model revealed that both Bindarit (SS = −0.89 (95% CI: −1.15, −0.69), $p < 0.001$) and Maraviroc (SS = −0.54 (−0.82, −0.26), $p < 0.001$) significantly decreased the motility of JUN-3 cells, but we were not able to detect significant effect of their interaction (SS = −0.48 (−1.04, 0.08), $p = 0.072$). *** $p < 0.001$. The statistical significances are based on permutational *t*-test with FDR correction. See Table S8 for effect sizes, their confidence intervals, and exact *p*-values. Each point represents an individual well. Violin plots with means ± SEM are shown.

4. Discussion

In the previous report [20], we established three sarcoma cell lines from two consecutive sarcomas initiated in a single female *H2-K/v-jun* transgenic mouse. These cell lines—JUN-1, -2, and -3—exhibited a gradual level of transformation, with JUN-2 being the least transformed cell line, JUN-3 being highly transformed, and JUN-1 presenting with an intermediate transformation status; strikingly, both proliferation and progression (motility, invasiveness) characteristics followed this distribution in each cell line. The expression of the *v-jun* oncogene displayed an inverse relationship to the transformation, which prompted us to speculate that the *v-jun* transgene expression merely provided an initial trigger for sarcoma development in this transgenic model system.

In an attempt to further develop this progression series, we reasoned that the least transformed cell line JUN-2 could be, by virtue of its high *v-jun* expression [20], an excellent candidate for a further in vitro transformation by the *c-fos* oncogene. Oncoproteins of the jun and fos families, together forming the oncogenic transcription factor AP-1, have a particular relevance in sarcoma biology [57,58]. Both oncogene families were founded by viral oncogenes of acutely transforming retroviral strains, and both of them initiated sarcomagenesis in susceptible animal hosts (chicken fibrosarcoma in the case of *v-jun* and murine osteosarcoma for *v-fos*). This predilection for transformation of mesenchymal lineage was preserved in the respective transgenic mice; transgenic *c-fos* overexpression resulted in osteosarcomas [59], whereas *v-jun* overexpressing transgenic mice developed fibrosarcomas secondary to deep wounding [21]. The *c-jun* has been indeed verified as a bona fide human oncogene, by discovering its amplification in a non-negligible proportion of aggressive dedifferentiated liposarcomas [60,61].

Indeed, we were able to establish a derivative cell line, JUN-2fos-3, with a high level of c-fos oncoprotein expression. Overall, we could see a very good correlation between respective quantitative mRNA expression level and a more qualitatively conceived immunofluorescence analysis (Figures 1 and 2), indicating that transcription is the primary regulatory level for both oncogenes. Nevertheless, we also found indications for the existence of additional regulatory mechanisms. Especially conspicuous is the observation of the prominent perinuclear localisation of c-fos in JUN-3 cells. Strikingly in this respect, c-fos has been described as a lamin A-interaction protein, leading to its affinity towards nuclear lamina [62], which can be modulated by mitogenic signalling [62,63]; whether this can explain our immunofluorescence finding and inasmuch as this could impact the high transformation status of JUN-3 sarcoma cells awaits further analyses. Another point deserving a short discussion is the heterogeneity within the sarcoma cell population, especially remarkable for the jun oncoprotein in JUN-1 and JUN-3 cells. As for the latter, we have preliminary evidence that the frequency of nuclear jun-positive cells significantly increases in cells treated with the leukaemia inhibitory factor and connective tissue growth factor, respectively, in both cases accompanied by marked increase in anchorage-independent clonogenicity. This suggests that the JUN-3 cells featuring high nuclear jun expression could correspond to clonogenic stem-like cells.

The newly derived JUN-2fos-3 sarcoma cell subline is especially remarkable by its uncoupling of proliferation on the one hand, and its motility/invasiveness on the other hand, which was essential to our aim to unravel a complex molecular basis of sarcoma motility/invasiveness, as a crucial and rate-limiting step in sarcoma progression and metastatic dissemination. Two specific aspects stand out in this respect—the specific metabolic adaptation and a specific signalling context as revealed by the specific transcriptomic profile.

As for the former, the targeted overexpression of c-fos in JUN-2fos-3 cells resulted in a markedly affected pattern of the cellular energy metabolism compared to the relatively non-transformed JUN-2 cells. Besides enhanced mitochondrial oxygen consumption, the cells also featured increased dependence on glycolytic energy production. The combination of the two ATP-generating pathways approached the metabolic profile of JUN-2fos-3 cells to the most transformed JUN-3 cell line. The deregulation of cellular energetics with changing patterns of glycolytic and mitochondrial contributions in relation to the degree of transformation is not a new finding, although the precise role of these alterations in the chemoresistance, metastasis, and cancer aggressiveness is yet not fully understood [64].

In any case, the JUN progression series is somewhat reminiscent of a previously analysed entirely in vitro-based fibroblastic progression, where an increase in tumourigenic potential was initially associated with the increasing levels of markers of mitochondrial biogenesis and citric-acid cycle metabolites to switch over to increased dependency on glycolysis for energy production in highly transformed sarcoma cells [19]. Analysis of an analogical transformation series of human mesenchymal stem cells (MSCs) suggested that during transformation, not only did MSCs not undergo a similar metabolic reprogramming, but their dependency on oxidative phosphorylation was even increased, and glycolysis served only as a backup energy supply in case of hypoxia [18]. Our data obtained from largely genuine sarcoma cell lines draw a more complex picture, with concurrent activation of both the glycolytic pathway and mitochondrial respiratory chain in highly invasive sarcoma cells.

The most remarkable metabolic commonality of both the invasive sarcoma cell lines JUN-2fos-3 and JUN-3 is the increased spare respiratory capacity. There are just a few reports, and none in the sarcoma field, connecting increased spare respiratory capacity and invasiveness. Such observations have been reported in invasive and metastatic ovarian cancer cell lines [65], as well as a specific aspect of Krüpel-like factor 4-induced invasiveness of glioblastoma cells [66,67]. There is still a vivid debate about the exact physiological interpretation of the spare respiratory capacity [68]. It may reflect an ability to increase energy production in response to a sudden need, such as stress, and it can also be interpreted as a synthetic expression of the bioenergetics fitness of the cell. Indeed, active cell locomotion

is unthinkable without an immediate supply of energy, and this correlation between enhanced spare respiratory capacity and motility and/or invasiveness could be biologically meaningful. As is the case in other experimental systems, it is rather difficult to relate this complex metabolic phenotype with particular genes, as revealed in our transcriptomic analysis. On the one hand, the transcriptomic profile of invasive sarcoma cells revealed increased expression of both hexokinase-1 (*Hk-1*) and phosphofructokinase-P (*Pfk-p*), two important enzymes of glycolytic pathway, in good agreement with their extra glycolytic proficiency. On the other hand, the downregulation of *Nupr1*, *Psph,* and *Tgfb* genes was observed in their transcriptome; these genes are part of a specific 10 gene signature of defect mitochondria that has been recently reported in hepatocellular carcinoma [69], which could be interpreted as a reflexion of greater mitochondrial fitness exhibited by invasive sarcoma cell lines. Together with the pyruvate supplied by the activated glycolytic pathway, this provides a plausible mechanistic explanation for their enhanced spare respiratory capacity. Even less clear is their regulatory context. Taking a lesson from the glioblastoma experimental system cited above, as well as from the largely complementing and overlapping metabolic impact of all the pluripotency transcription factors [70], we can hypothesise that the increased expression of *Sox-2* found in our invasive sarcoma cell lines could be the crucial regulatory factor. On the other hand, our pathway analysis (Figure 6 and Table S6) disclosed a downregulation of pluripotency stemness along with a concomitant upregulation of Hippo-pathway stemness, and indeed, *Sox-2* can be viewed as a crucial factor in both these stemness circuits [71,72]. Supporting this notion, both *Hk-1* and *Pfk-p* have also been described as Yap-downstream genes [73].

Indeed, the transcriptomic profile of fibrosarcoma cell invasiveness that emerged from our analysis of the JUN-progression series indicates a far more complex interplay involving a plethora of factors, as opposed to a great part of previous studies aimed at deciphering the molecular framework of cancer (especially sarcoma) cell invasiveness, which concentrated each on a small number of "strong" factors, either taken a priori by a candidate gene approach, or extracted from genomic profiling analyses. Interestingly, we have little evidence for an essential role of any proteolytic enzymatic activity, in concert with findings reported independently on a rat sarcoma progression series [16] that strongly argued that it is the cell motility that constitutes a rate-limiting ability of the invasive phenotype in sarcoma; in fact, the gene most profoundly downregulated in the invasive sarcoma sublines codes for the matrix metalloproteinase 13, and *Mmp-3* expression is diminished as well. Among the genes overexpressed in our invasive transcriptomic profile, we can find several known activators of cell motility/invasiveness and/or genes independently associated with progression in soft tissue sarcoma (*BIRC5* coding for surviving [74], *RHAMM* [75]) or other cancer types, such as *CCL8* (breast carcinoma [76], melanoma [77]), *Tetraspanin 2* (lung carcinoma [78]), Protein Phosphatase and Actin Regulator 1 (breast carcinoma [79]), *Semaphorin 3A* (glioblastoma [80]), or *FOXD1* (osteosarcoma [81], lung carcinoma [82], melanoma [83]); importantly, in the context of the overall strategy of our transcriptomic screen, at least for melanoma, FOXD1 was described as a pure motility/invasiveness factor, with little impact on cell proliferation [83].

With regard to the CCL8, the major difference in our results and the results from the other studies cited above is that, whereas in both breast carcinoma [76] and melanoma [77] this activating chemokine is provided by activated cancer stroma, this paracrine motility regulation switched to autocrine in our invasive sarcoma cells. Indeed, the tumour microenvironment can be both the source of the inflammatory chemokines including CCL8, as well as the major recipient of their signals, as revealed by analysis of a chemically induced fibrosarcoma model, where increased chemokine expression could be correlated with the recruitment of regulatory T-cells and local immunosuppression [84]. Likewise, effects of the pharmacologic inhibition of the CCL8-CCR5 signalling pathway in various cancer models, either with the CCL8 inhibitor Bindarit [85,86], or by inhibiting its major receptor CCR5 by Maraviroc [42,87,88], has been thus far, for the most part, attributed to their complex effects on the tumour microenvironment, e.g., by diminution of cancer-related

inflammation and myeloid or suppressor T-cell cell infiltration, or by limiting accumulation of cancer-associated fibroblasts. Both the inflammatory chemokines and the CCR5 receptor have recently been attributed to cancer cell-autonomous effects, nevertheless, they are notable as activators of cell motility and invasiveness, and, accordingly, both Bindarit and Maraviroc exert direct effects on these transformation traits [89–92]. Our results are, to our knowledge, the first showing similar cell-autonomous effects of both drugs in sarcoma and, thus, warrant further experimental and translational research effort in this direction.

Semaphorin 3A is another autocrine motility factor, as already described in glioblastoma [80]; it is worth noting that the initial identification of the Semaphorin 3A–Neuropilin-1 (a canonical constituent of the Semaphorin 3A receptor) signalling system as an activator of cell motility in glioblastoma resulted initially from a systematic proteomic screen performed in the HT1080 human fibrosarcoma cells [80], providing an independent confirmation of our results. In fact, the Semaphorin 3A has been described as a motility factor even for normal mesenchymal cells, like vascular smooth muscle cells [93].

On the other hand, signalling consequences of the Semaphorin 3A are remarkably pleiotropic, and one of its strongest effects is a pronounced angiogenesis inhibition [93]. It would seem to be counterintuitive that any cancer cell line progression series would activate a strong antiangiogenic program, and indeed, we can find in our invasive transcriptomic profile at least two established angiogenic activators—*Angiopoietin-2* [94] and *c-fos*–induced growth factor coding for vascular endothelial growth factor D [95]. The latter has been traditionally regarded as an activator of lymphangiogenesis, which is presumed to have a marginal impact (albeit significant within a small fraction of cases [96]) in sarcoma biology, as sarcomas preferentially disseminate via blood vasculature. Recent findings have somewhat questioned this traditional view, nevertheless, they have shown that VEGFD is also involved in vascular angiogenesis and, moreover, one of the VEGFD receptors, VEGFR3, has been found to be expressed on the very tumour cells in a fraction of soft tissue sarcomas, with a significant negative prognostic relevance [97]. Indeed, VEGFD has been repeatedly described as a direct motility factor for both activated fibroblasts [98] and various sarcoma cells, like chondrosarcoma [99] or Kaposi sarcoma [95].

Intriguingly, the same dual role, i.e., angiogenic activator counterbalancing the Sema 3A-induced antiangiogenic action and being a direct motility/invasiveness activator, has been ascribed to the Angiopoietin-2 as well. Ang-2, by engaging the specific receptor tyrosine kinase Tie-2, is crucial for vascular remodelling at sites of active vessel sprouting; this activity relies on simultaneous presence of VEGFs and its specific therapeutic inhibition is actually actively pursued and clinically tested [100]. At the same time, nevertheless, Ang-2 can directly stimulate motility/invasiveness of both monocytes/macrophages [101] and tumour cells [102], by serving as an adhesion ligand to various integrins. Ang-2-activated macrophage motility/invasion is directed towards fibrin clots that may result from the vascular sprouting itself, and it generates a specific fibrin degradation product, D-dimer, whose negative prognostic relevance has been described for many cancer types, including sarcomas [103,104]. The Ang-2 receptor mediating this fibrinolytic activity of macrophages is Integrin β_2, which is traditionally viewed as a specialised leukocyte integrin. Quite unexpectedly in this respect, and not without interest, the Integrin β_2 is a part of our sarcoma invasiveness transcriptomic profile as well.

All in all, this suggests a remarkable network of cooperating, antagonizing, and compensating biological activities, co-opted from various normal as well as transformed cell types, which collectively underlie sarcoma cell motility and invasion in our model, and which call for a similar paradigmatic change in viewing this process, from individual "strong" factors regarded in isolation to such molecular networks.

Interestingly, among the genes downregulated in invasive sarcoma cells, the gene showing the second highest fold diminution of expression was *Xist*, coding for a long non-coding RNA, which is crucial for X-chromosome inactivation in female mammals. The role for long non-coding RNAs in tumourigenesis is increasingly appreciated [105], and as for Xist, strikingly conflicting results have been reported, even within the context of a

single tumour type like osteosarcoma [106,107]. Importantly, Xist-targeted deletion in foetal haematopoietic stem cells is dramatically protumourigenic [108], resulting in fully penetrant, female-specific carcinogenic transformation encompassing chronic myelomonocytic leukaemia, myeloproliferative disease, and a rare haematologically derived sarcoma—histiocytic sarcoma. It is tempting to speculate that we witness a milder version of a similar protumourigenic effect in our sarcoma model resulting from a diminished expression rather than a hard mutation; it should be noticed in this regard that the entire JUN-fibrosarcoma progression series originated from a single female mouse [20]. On the other hand, we did not see a widespread activation of X-linked oncogenes in our model, a mechanism proposed for the leukaemogenic mouse model cited above; in fact, from the overexpressed genes discussed above, only the gene coding for VEGFD is X-linked, suggesting another molecular mechanism. Another interesting point is the mechanism of *Xist* downregulation. It has been reported that pluripotency transcription factors are major *Xist* repressors in embryonic stem cells [109]; our transcriptomic screen revealed Sox-2 among the activated genes in invasive sarcoma cell lines and, possibly, a similar role of a stemness factor could also be ascribed to FOXD1, at least in the context of induced pluripotent stem cells [110]. On the other hand, as noted above, the pathway analysis suggested a general downregulation of the pluripotency stemness pathway; thus, the biological relevance of the mechanism suggested above remains uncertain.

5. Conclusions

In conclusion, we believe that our fibrosarcoma progression model and the differentially expressed genes identified by its transcriptomic analysis can provide important new information on biology of soft tissue sarcoma progression. We showed that motility/invasiveness is a druggable target, fitting into the current concept of migrastatics as a new class of pharmacological weapons to combat metastasizing cancer [111,112]. Importantly, in addition to CCL8 inhibitors used paradigmatically here, there are pharmacologic inhibitors available for several other molecules identified in our transcriptomic screen, like Sema3A [113], Ang-2 [100], or survivin [114]. Moreover, our results strongly suggest that any pharmacological intervention must take into account the complex relationship between the different signalling molecules; the Sema3A inhibition would thus probably only be thinkable if combined with an antiangiogenic therapy. In any case, we believe that the presently studied series of sarcoma progression cell lines will be an elegant model to explore novel therapeutic targets, potential drug candidates, and prognostic markers in the near future. On the other hand, the current analysis is based entirely on in vitro experimental approaches, and an extension to the in vivo system would be desirable and is intended in future research. As mentioned above, this article focuses exclusively on exploiting the JUN-fibrosarcoma progression series for the identification of potential invasiveness markers and therapeutic targets, and we have good indications that the complementary part of our transcriptomic analysis resulting in the identification of proliferation-related genes (Table 2) bears a great potential for improving our understanding of complex sarcoma biology as well.

different lines of sarcoma cells. Table S6. Genes with significantly changed expression in invasive sarcoma cell lines JUN-3 and JUN-2fos-3 compared to JUN-2 (available in xls.). Table S7. The gene set enrichment analysis (available in xls.). Table S8. Table of contrasts (post hoc tests) from comparison of invasiveness of JUN-3 sarcoma cells treated with Bindarit (Bind), Maraviroc (Marav), or their combination (comb) compared to untreated control. Table S9. Genes with significantly changed expression in JUN-2 compared to JUN-3 (available in xls.). Table S10. Genes with significantly changed expression in JUN-2fos3 compared to JUN-2 (available in xls.). Supplementary Tables of genes (Tables S6, S7, S9 and S10 in xls.)

References

1. Oda, Y.; Yamamoto, H.; Kohashi, K.; Yamada, Y.; Iura, K.; Ishii, T.; Maekawa, A.; Bekki, H. Soft Tissue Sarcomas: From a Morphological to a Molecular Biological Approach. *Pathol. Internat.* **2017**, *67*, 435–446. [CrossRef] [PubMed]
2. Quesada, J.; Amato, R. The Molecular Biology of Soft-Tissue Sarcomas and Current Trends in Therapy. *Sarcoma* **2012**, *2012*, 849456. [CrossRef]
3. Sbaraglia, M.; Dei Tos, A.P. The Pathology of Soft Tissue Sarcomas. *Radiol. Med.* **2019**, *124*, 266–281. [CrossRef] [PubMed]
4. Skubitz, K.M.; D'Adamo, D.R. Sarcoma. *Mayo Clin. Proc.* **2007**, *82*, 1409–1432. [CrossRef] [PubMed]
5. Taylor, B.S.; Barretina, J.; Maki, R.G.; Antonescu, C.R.; Singer, S.; Ladanyi, M. Advances in Sarcoma Genomics and New Therapeutic Targets. *Nat. Rev. Cancer* **2011**, *11*, 541–557. [CrossRef]
6. Riedel, R.F. Systemic Therapy for Advanced Soft Tissue Sarcomas. *Cancer* **2012**, *118*, 1474–1485. [CrossRef]
7. Mertens, F.; Antonescu, C.R.; Mitelman, F. Gene Fusions in Soft Tissue Tumors: Recurrent and Overlapping Pathogenetic Themes. *Genes Chromosomes Cancer* **2016**, *55*, 291–310. [CrossRef]
8. Hatina, J.; Kripnerova, M.; Houfkova, K.; Pesta, M.; Kuncova, J.; Sana, J.; Slaby, O.; Rodríguez, R. Sarcoma Stem Cell Heterogeneity. *Adv. Exp. Med. Biol.* **2019**, *1123*, 95–118. [CrossRef]
9. Pennacchioli, E.; Tosti, G.; Barberis, M.; De Pas, T.M.; Verrecchia, F.; Menicanti, C.; Testori, A.; Mazzarol, G. Sarcoma Spreads Primarily through the Vascular System: Are There Biomarkers Associated with Vascular Spread? *Clin. Exp. Metastasis* **2012**, *29*, 757–773. [CrossRef]
10. Tsukushi, S.; Nishida, Y.; Urakawa, H.; Kozawa, E.; Ishiguro, N. Prognostic Significance of Histological Invasion in High Grade Soft Tissue Sarcomas. *SpringerPlus* **2014**, *3*, 544. [CrossRef]
11. Lee, A.T.J.; Pollack, S.M.; Huang, P.; Jones, R.L. Phase III Soft Tissue Sarcoma Trials: Success or Failure? *Curr. Treat. Options Oncol.* **2017**, *18*, 19. [CrossRef] [PubMed]
12. Chibon, F.; Lagarde, P.; Salas, S.; Pérot, G.; Brouste, V.; Tirode, F.; Lucchesi, C.; de Reynies, A.; Kauffmann, A.; Bui, B.; et al. Validated Prediction of Clinical Outcome in Sarcomas and Multiple Types of Cancer on the Basis of a Gene Expression Signature Related to Genome Complexity. *Nat. Med.* **2010**, *16*, 781–787. [CrossRef] [PubMed]

13. Jemaà, M.; Abdallah, S.; Lledo, G.; Perrot, G.; Lesluyes, T.; Teyssier, C.; Roux, P.; van Dijk, J.; Chibon, F.; Abrieu, A.; et al. Heterogeneity in Sarcoma Cell Lines Reveals Enhanced Motility of Tetraploid versus Diploid Cells. *Oncotarget* **2016**, *8*, 16669–16689. [CrossRef] [PubMed]

14. Chibon, F.; Lesluyes, T.; Valentin, T.; Guellec, S.L. CINSARC Signature as a Prognostic Marker for Clinical Outcome in Sarcomas and Beyond. *Genes Chromosomes Cancer* **2019**, *58*, 124–129. [CrossRef] [PubMed]

15. Cavanna, T.; Pokorna, E.; Vesely, P.; Gray, C.; Zicha, D. Evidence for Protein 4.1B Acting as a Metastasis Suppressor. *J. Cell Sci.* **2007**, *120*, 606–616. [CrossRef] [PubMed]

16. Rosel, D.; Brabek, J.; Tolde, O.; Mierke, C.T.; Zitterbart, D.P.; Raupach, C.; Bicanova, K.; Kollmannsberger, P.; Pankova, D.; Vesely, P.; et al. Up-Regulation of Rho/ROCK Signaling in Sarcoma Cells Drives Invasion and Increased Generation of Protrusive Forces. *Mol. Cancer Res.* **2008**, *6*, 1410–1420. [CrossRef]

17. Kainov, Y.; Favorskaya, I.; Delektorskaya, V.; Chemeris, G.; Komelkov, A.; Zhuravskaya, A.; Trukhanova, L.; Zueva, E.; Tavitian, B.; Dyakova, N.; et al. CRABP1 Provides High Malignancy of Transformed Mesenchymal Cells and Contributes to the Pathogenesis of Mesenchymal and Neuroendocrine Tumors. *Cell Cycle* **2014**, *13*, 1530–1539. [CrossRef]

18. Funes, J.M.; Quintero, M.; Henderson, S.; Martinez, D.; Qureshi, U.; Westwood, C.; Clements, M.O.; Bourboulia, D.; Pedley, R.B.; Moncada, S.; et al. Transformation of Human Mesenchymal Stem Cells Increases Their Dependency on Oxidative Phosphorylation for Energy Production. *Proc. Natl. Acad. Sci. USA* **2007**, *104*, 6223–6228. [CrossRef]

19. Ramanathan, A.; Wang, C.; Schreiber, S.L. Perturbational Profiling of a Cell-Line Model of Tumorigenesis by Using Metabolic Measurements. *Proc. Natl. Acad. Sci. USA* **2005**, *102*, 5992–5997. [CrossRef]

20. Hatina, J.; Hajkova, L.; Peychl, J.; Rudolf, E.; Finek, J.; Cervinka, M.; Reischig, J. Establishment and Characterization of Clonal Cell Lines Derived from a Fibrosarcoma of the *H2-K/v-Jun* Transgenic Mouse. *Tumor Biol.* **2003**, *24*, 176–184. [CrossRef]

21. Schuh, A.C.; Keating, S.J.; Monteclaro, F.S.; Vogt, P.K.; Breitman, M.L. Obligatory Wounding Requirement for Tumorigenesis in V-Jun Transgenic Mice. *Nature* **1990**, *346*, 756–760. [CrossRef] [PubMed]

22. Katoh, K.; Takahashi, Y.; Hayashi, S.; Kondoh, H. Improved Mammalian Vectors for High Expression of G418 Resistance. *Cell Struct. Funct.* **1987**, *12*, 575–580. [CrossRef]

23. Chomczynski, P.; Sacchi, N. The Single-Step Method of RNA Isolation by Acid Guanidinium Thiocyanate-Phenol-Chloroform Extraction: Twenty-Something Years On. *Nat. Protoc.* **2006**, *1*, 581–585. [CrossRef] [PubMed]

24. Ausubel, F.M.; Brent, R.; Kingston, R.E.; Moore, D.D.; Seidman, J.G.; Smith, J.A.; Struhl, K. *Current Protocols in Molecular Biology*; John Wiley & Sons: Brooklyn, NY, USA, 1995; ISBN 978-0-471-50338-5.

25. Maki, Y.; Bos, T.J.; Davis, C.; Starbuck, M.; Vogt, P.K. Avian Sarcoma Virus 17 Carries the Jun Oncogene. *Proc. Natl. Acad. Sci. USA* **1987**, *84*, 2848–2852. [CrossRef] [PubMed]

26. Holubova, M.; Leba, M.; Sedmikova, M.; Vannucci, L.; Horak, V. Characterization of Three Newly Established Rat Sarcoma Cell Clones. *In Vitro Cell Dev. Biol. Anim.* **2012**, *48*, 610–618. [CrossRef] [PubMed]

27. Ke, N.; Wang, X.; Xu, X.; Abassi, Y.A. The XCELLigence System for Real-Time and Label-Free Monitoring of Cell Viability. *Methods Mol. Biol.* **2011**, *740*, 33–43. [CrossRef] [PubMed]

28. Mori, S.; Chang, J.T.; Andrechek, E.R.; Matsumura, N.; Baba, T.; Yao, G.; Kim, J.W.; Gatza, M.; Murphy, S.; Nevins, J.R. Anchorage-Independent Cell Growth Signature Identifies Tumors with Metastatic Potential. *Oncogene* **2009**, *28*, 2796–2805. [CrossRef]

29. Fujii, H.; Honoki, K.; Tsujiuchi, T.; Kido, A.; Yoshitani, K.; Takakura, Y. Sphere-Forming Stem-like Cell Populations with Drug Resistance in Human Sarcoma Cell Lines. *Int. J. Oncol.* **2009**, *34*, 1381–1386.

30. Liu, W.-D.; Zhang, T.; Wang, C.-L.; Meng, H.-M.; Song, Y.-W.; Zhao, Z.; Li, Z.-M.; Liu, J.-K.; Pan, S.-H.; Wang, W.-B. Sphere-Forming Tumor Cells Possess Stem-like Properties in Human Fibrosarcoma Primary Tumors and Cell Lines. *Oncol. Lett.* **2012**, *4*, 1315–1320. [CrossRef]

31. Boesch, M.; Reimer, D.; Rumpold, H.; Zeimet, A.G.; Sopper, S.; Wolf, D. DyeCycle Violet Used for Side Population Detection Is a Substrate of P-Glycoprotein. *Cytometry A* **2012**, *81*, 517–522. [CrossRef]

32. Quail, D.F.; Maciel, T.J.; Rogers, K.; Postovit, L.M. A Unique 3D in Vitro Cellular Invasion Assay. *J. Biomol. Screen.* **2012**, *17*, 1088–1095. [CrossRef]

33. Santini, M.T.; Rainaldi, G.; Indovina, P.L. Multicellular Tumour Spheroids in Radiation Biology. *Int. J. Radiat. Biol.* **1999**, *75*, 787–799. [CrossRef]

34. Pesta, D.; Gnaiger, E. High-Resolution Respirometry: OXPHOS Protocols for Human Cells and Permeabilized Fibers from Small Biopsies of Human Muscle. *Methods Mol. Biol.* **2012**, *810*, 25–58. [CrossRef] [PubMed]

35. Kuznetsov, A.V.; Strobl, D.; Ruttmann, E.; Königsrainer, A.; Margreiter, R.; Gnaiger, E. Evaluation of Mitochondrial Respiratory Function in Small Biopsies of Liver. *Anal. Biochem.* **2002**, *305*, 186–194. [CrossRef] [PubMed]

36. Larsen, S.; Nielsen, J.; Hansen, C.N.; Nielsen, L.B.; Wibrand, F.; Stride, N.; Schroder, H.D.; Boushel, R.; Helge, J.W.; Dela, F.; et al. Biomarkers of Mitochondrial Content in Skeletal Muscle of Healthy Young Human Subjects. *J. Physiol.* **2012**, *590*, 3349–3360. [CrossRef]

37. Chen, J.-R.; Lazarenko, O.P.; Blackburn, M.L.; Rose, S.; Frye, R.E.; Badger, T.M.; Andres, A.; Shankar, K. Maternal Obesity Programs Senescence Signaling and Glucose Metabolism in Osteo-Progenitors From Rat and Human. *Endocrinology* **2016**, *157*, 4172–4183. [CrossRef] [PubMed]

38. Zhuang, Y.; Chan, D.K.; Haugrud, A.B.; Miskimins, W.K. Mechanisms by Which Low Glucose Enhances the Cytotoxicity of Metformin to Cancer Cells Both in Vitro and in Vivo. *PLoS ONE* **2014**, *9*, e108444. [CrossRef]

39. Huber, W.; Carey, V.J.; Gentleman, R.; Anders, S.; Carlson, M.; Carvalho, B.S.; Bravo, H.C.; Davis, S.; Gatto, L.; Girke, T.; et al. Orchestrating High-Throughput Genomic Analysis with Bioconductor. *Nat. Methods* **2015**, *12*, 115–121. [CrossRef]

40. Mirolo, M.; Fabbri, M.; Sironi, M.; Vecchi, A.; Guglielmotti, A.; Mangano, G.; Biondi, G.; Locati, M.; Mantovani, A. Impact of the Anti-Inflammatory Agent Bindarit on the Chemokinome: Selective Inhibition of the Monocyte Chemotactic Proteins. *Eur. Cytokine Netw.* **2008**, *19*, 119–122. [CrossRef] [PubMed]

41. Paccosi, S.; Giachi, M.; Di Gennaro, P.; Guglielmotti, A.; Parenti, A. The Chemokine (C-C Motif) Ligand Protein Synthesis Inhibitor Bindarit Prevents Cytoskeletal Rearrangement and Contraction of Human Mesangial Cells. *Cytokine* **2016**, *85*, 92–100. [CrossRef]

42. Halvorsen, E.C.; Hamilton, M.J.; Young, A.; Wadsworth, B.J.; LePard, N.E.; Lee, H.N.; Firmino, N.; Collier, J.L.; Bennewith, K.L. Maraviroc Decreases CCL8-Mediated Migration of CCR5 + Regulatory T Cells and Reduces Metastatic Tumor Growth in the Lungs. *OncoImmunology* **2016**, *5*, e1150398. [CrossRef] [PubMed]

43. Sicoli, D.; Jiao, X.; Ju, X.; Velasco-Velazquez, M.; Ertel, A.; Addya, S.; Li, Z.; Ando, S.; Fatatis, A.; Paudyal, B.; et al. CCR5 Receptor Antagonists Block Metastasis to Bone of V-Src Oncogene-Transformed Metastatic Prostate Cancer Cell Lines. *Cancer Res.* **2014**, *74*, 7103–7114. [CrossRef] [PubMed]

44. Scrace, S.; O'Neill, E.; Hammond, E.M.; Pires, I.M. Use of the xCELLigence System for Real-Time Analysis of Changes in Cellular Motility and Adhesion in Physiological Conditions. In *Adhesion Protein Protocols*; Coutts, A.S., Ed.; Methods in Molecular Biology; Humana Press: Totowa, NJ, USA, 2013; pp. 295–306. ISBN 978-1-62703-538-5.

45. R Core Team (2020)—European Environment Agency. Available online: https://www.eea.europa.eu/data-and-maps/indicators/oxygen-consuming-substances-in-rivers/r-development-core-team-2006 (accessed on 9 November 2020).

46. DiCiccio, T.J.; Efron, B. Bootstrap Confidence Intervals. *Statist. Sci.* **1996**, *11*, 189–228. [CrossRef]

47. Benjamini, Y.; Hochberg, Y. Controlling the False Discovery Rate: A Practical and Powerful Approach to Multiple Testing. *J. R. Stat. Soc. Series B Stat. Methodol.* **1995**, *57*, 289–300. [CrossRef]

48. Luo, D.; Koolaard, S.G.J. Predictmeans: Calculate Predicted Means for Linear Models. Available online: https://cran.r-project.org/web/packages/predictmeans/predictmeans.pdf (accessed on 20 November 2020).

49. Tichanek, F.; Salomova, M.; Jedlicka, J.; Kuncova, J.; Pitule, P.; Macanova, T.; Petrankova, Z.; Tuma, Z.; Cendelin, J. Hippocampal Mitochondrial Dysfunction and Psychiatric-Relevant Behavioral Deficits in Spinocerebellar Ataxia 1 Mouse Model. *Sci. Rep.* **2020**, *10*, 5418. [CrossRef] [PubMed]

50. Cendelin, J.; Tichanek, F. Cerebellar Degeneration Averts Blindness-Induced Despaired Behavior during Spatial Task in Mice. *Neurosci. Lett.* **2020**, *722*, 134854. [CrossRef]

51. Eklund, A. Beeswarm: The Bee Swarm Plot, an Alternative to Stripchart. Available online: https://rdrr.io/cran/beeswarm/ (accessed on 25 November 2020).

52. Kelly, T. TomKellyGenetics/Vioplot. Available online: https://cran.r-project.org/web/packages/vioplot/vioplot.pdf (accessed on 11 November 2020).

53. Hatina, J.; Fernandes, M.I.; Hoffmann, M.J.; Zeimet, A.G. Cancer Stem Cells—Basic Biological Properties and Experimental Approaches. In *eLS*; John Wiley & Sons: Chichester, UK, 2013. [CrossRef]

54. Trucco, M.; Loeb, D. Sarcoma Stem Cells: Do We Know What We Are Looking For? *Sarcoma* **2012**, 291702. [CrossRef] [PubMed]

55. Colombo, A.; Basavarajaiah, S.; Limbruno, U.; Picchi, A.; Lettieri Valgimigli, M.; Sciahbasi, A.; Prati, F.; Calabresi, M.; Pierucci, D.; Guglielmotti, A. A Double-Blind Randomised Study to Evaluate the Efficacy and Safety of Bindarit in Preventing Coronary Stent Restenosis. *EuroIntervention* **2015**, *11*, 20140918-01. [CrossRef] [PubMed]

56. Parra, J.; Portilla, J.; Pulido, F.; Sánchez-de la Rosa, R.; Alonso-Villaverde, C.; Berenguer, J.; Blanco, J.L.; Domingo, P.; Dronda, F.; Galera, C.; et al. Clinical Utility of Maraviroc. *Clin. Drug Investig.* **2011**, *31*, 527–542. [CrossRef]

57. Ozanne, B.W.; McGarry, L.; Spence, H.J.; Johnston, I.; Winnie, J.; Meagher, L.; Stapleton, G. Transcriptional Regulation of Cell Invasion: AP-1 Regulation of a Multigenic Invasion Programme. *Eur. J. Cancer* **2000**, *36*, 1640–1648. [CrossRef]

58. Ozanne, B.W.; Spence, H.J.; McGarry, L.C.; Hennigan, R.F. Transcription Factors Control Invasion: AP-1 the First among Equals. *Oncogene* **2007**, *26*, 1–10. [CrossRef]

59. Wang, Z.-Q.; Liang, J.; Schellander, K.; Wagner, E.F.; Grigoriadis, A.E. C-Fos-Induced Osteosarcoma Formation in Transgenic Mice: Cooperativity with c-Jun and the Role of Endogenous c-Fos. *Cancer Res.* **1995**, *55*, 6244–6251. [PubMed]

60. Mariani, O.; Brennetot, C.; Coindre, J.-M.; Gruel, N.; Ganem, C.; Delattre, O.; Stern, M.-H.; Aurias, A. JUN Oncogene Amplification and Overexpression Block Adipocytic Differentiation in Highly Aggressive Sarcomas. *Cancer Cell* **2007**, *11*, 361–374. [CrossRef]

61. Snyder, E.L.; Sandstrom, D.J.; Law, K.; Fiore, C.; Sicinska, E.; Brito, J.; Bailey, D.; Fletcher, J.A.; Loda, M.; Rodig, S.J.; et al. C-Jun Amplification and Overexpression Are Oncogenic in Liposarcoma but Not Always Sufficient to Inhibit the Adipocytic Differentiation Programme. *J. Pathol.* **2009**, *218*, 292–300. [CrossRef] [PubMed]

62. Ivorra, C.; Kubicek, M.; González, J.M.; Sanz-González, S.M.; Alvarez-Barrientos, A.; O'Connor, J.-E.; Burke, B.; Andrés, V. A Mechanism of AP-1 Suppression through Interaction of c-Fos with Lamin A/C. *Genes Dev.* **2006**, *20*, 307–320. [CrossRef] [PubMed]

63. Mohamood, A.S.; Gyles, P.; Balan, K.V.; Hollis, V.W.; Eckberg, W.R.; Asseffa, A.; Han, Z.; Wyche, J.H.; Anderson, W.A. Estrogen Receptor, Growth Factor Receptor and Protooncogene Protein Activities and Possible Signal Transduction Crosstalk in Estrogen Dependent and Independent Breast Cancer Cell Lines. *J. Submicrosc. Cytol. Pathol.* **1997**, *29*, 1–17. [PubMed]

64. La Vecchia, S.; Sebastián, C. Metabolic Pathways Regulating Colorectal Cancer Initiation and Progression. *Semin. Cell Dev. Biol.* **2020**, *98*, 63–70. [CrossRef]

65. Caneba, C.A.; Bellance, N.; Yang, L.; Pabst, L.; Nagrath, D. Pyruvate Uptake Is Increased in Highly Invasive Ovarian Cancer Cells under Anoikis Conditions for Anaplerosis, Mitochondrial Function, and Migration. *Am. J. Physiol. Endocrinol. Metab.* **2012**, *303*, E1036–E1052. [CrossRef]

66. Wan, J.; Su, Y.; Song, Q.; Tung, B.; Oyinlade, O.; Liu, S.; Ying, M.; Ming, G.; Song, H.; Qian, J.; et al. Methylated Cis-Regulatory Elements Mediate KLF4-Dependent Gene Transactivation and Cell Migration. *eLife* **2017**, *6*, e20068. [CrossRef]

67. Wang, S.; Shi, X.; Wei, S.; Ma, D.; Oyinlade, O.; Lv, S.-Q.; Ying, M.; Zhang, Y.A.; Claypool, S.M.; Watkins, P.; et al. Krüppel-like Factor 4 (KLF4) Induces Mitochondrial Fusion and Increases Spare Respiratory Capacity of Human Glioblastoma Cells. *J. Biol. Chem.* **2018**, *293*, 6544–6555. [CrossRef]

68. Marchetti, P.; Fovez, Q.; Germain, N.; Khamari, R.; Kluza, J. Mitochondrial Spare Respiratory Capacity: Mechanisms, Regulation, and Significance in Non-Transformed and Cancer Cells. *FASEB J.* **2020**. [CrossRef] [PubMed]

69. Lee, Y.-K.; Jee, B.A.; Kwon, S.M.; Yoon, Y.-S.; Xu, W.G.; Wang, H.-J.; Wang, X.W.; Thorgeirsson, S.S.; Lee, J.-S.; Woo, H.G.; et al. Identification of a Mitochondrial Defect Gene Signature Reveals NUPR1 as a Key Regulator of Liver Cancer Progression. *Hepatology* **2015**, *62*, 1174–1189. [CrossRef] [PubMed]

70. Machida, K. Pluripotency Transcription Factors and Metabolic Reprogramming of Mitochondria in Tumor-Initiating Stem-like Cells. *Antioxid. Redox Signal.* **2018**, *28*, 1080–1089. [CrossRef] [PubMed]

71. Basu-Roy, U.; Bayin, N.S.; Rattanakorn, K.; Han, E.; Placantonakis, D.G.; Mansukhani, A.; Basilico, C. Sox2 Antagonizes the Hippo Pathway to Maintain Stemness in Cancer Cells. *Nat. Commun.* **2015**, *6*, 6411. [CrossRef] [PubMed]

72. Maurizi, G.; Verma, N.; Gadi, A.; Mansukhani, A.; Basilico, C. Sox2 Is Required for Tumor Development and Cancer Cell Proliferation in Osteosarcoma. *Oncogene* **2018**, *37*, 4626–4632. [CrossRef]

73. Yamaguchi, H.; Taouk, G.M. A Potential Role of YAP/TAZ in the Interplay Between Metastasis and Metabolic Alterations. *Front. Oncol.* **2020**, *10*. [CrossRef]

74. Würl, P.; Kappler, M.; Meye, A.; Bartel, F.; Köhler, T.; Lautenschläger, C.; Bache, M.; Schmidt, H.; Taubert, H. Co-Expression of Survivin and TERT and Risk of Tumour-Related Death in Patients with Soft-Tissue Sarcoma. *Lancet* **2002**, *359*, 943–945. [CrossRef]

75. Nikitovic, D.; Kouvidi, K.; Karamanos, N.K.; Tzanakakis, G.N. The Roles of Hyaluronan/RHAMM/CD44 and Their Respective Interactions along the Insidious Pathways of Fibrosarcoma Progression. *BioMed Res. Int.* **2013**, *2013*, 929531. [CrossRef] [PubMed]

76. Farmaki, E.; Chatzistamou, I.; Kaza, V.; Kiaris, H. A CCL8 Gradient Drives Breast Cancer Cell Dissemination. *Oncogene* **2016**, *35*, 6309–6318. [CrossRef]

77. Barbai, T.; Fejős, Z.; Puskas, L.G.; Tímár, J.; Rásó, E. The Importance of Microenvironment: The Role of CCL8 in Metastasis Formation of Melanoma. *Oncotarget* **2015**, *6*, 29111–29128. [CrossRef]

78. Otsubo, C.; Otomo, R.; Miyazaki, M.; Matsushima-Hibiya, Y.; Kohno, T.; Iwakawa, R.; Takeshita, F.; Okayama, H.; Ichikawa, H.; Saya, H.; et al. TSPAN2 Is Involved in Cell Invasion and Motility during Lung Cancer Progression. *Cell Rep.* **2014**, *7*, 527–538. [CrossRef] [PubMed]

79. Fils-Aimé, N.; Dai, M.; Guo, J.; El-Mousawi, M.; Kahramangil, B.; Neel, J.-C.; Lebrun, J.-J. MicroRNA-584 and the Protein Phosphatase and Actin Regulator 1 (PHACTR1), a New Signaling Route through Which Transforming Growth Factor-β Mediates the Migration and Actin Dynamics of Breast Cancer Cells. *J. Biol. Chem.* **2013**, *288*, 11807–11823. [CrossRef] [PubMed]

80. Bagci, T.; Wu, J.K.; Pfannl, R.; Ilag, L.L.; Jay, D.G. Autocrine Semaphorin 3A Signaling Promotes Glioblastoma Dispersal. *Oncogene* **2009**, *28*, 3537–3550. [CrossRef] [PubMed]

81. Tao, J.; Cong, H.; Wang, H.; Zhang, D.; Liu, C.; Chu, H.; Qing, Q.; Wang, K. MiR-30a-5p Inhibits Osteosarcoma Cell Proliferation and Migration by Targeting FOXD1. *Biochem. Biophys. Res. Commun.* **2018**, *503*, 1092–1097. [CrossRef]

82. Li, D.; Fan, S.; Yu, F.; Zhu, X.; Song, Y.; Ye, M.; Fan, L.; Lv, Z. FOXD1 Promotes Cell Growth and Metastasis by Activation of Vimentin in NSCLC. *Cell Physiol. Biochem.* **2018**, *51*, 2716–2731. [CrossRef] [PubMed]

83. Wu, H.; Larribère, L.; Sun, Q.; Novak, D.; Sachindra, S.; Granados, K.; Umansky, V.; Utikal, J. Loss of Neural Crest-Associated Gene FOXD1 Impairs Melanoma Invasion and Migration via RAC1B Downregulation. *Int. J. Cancer* **2018**, *143*, 2962–2972. [CrossRef]

84. Ondondo, B.; Colbeck, E.; Jones, E.; Smart, K.; Lauder, S.N.; Hindley, J.; Godkin, A.; Moser, B.; Ager, A.; Gallimore, A. A Distinct Chemokine Axis Does Not Account for Enrichment of Foxp3(+) CD4(+) T Cells in Carcinogen-Induced Fibrosarcomas. *Immunology* **2015**, *145*, 94–104. [CrossRef]

85. Gazzaniga, S.; Bravo, A.I.; Guglielmotti, A.; van Rooijen, N.; Maschi, F.; Vecchi, A.; Mantovani, A.; Mordoh, J.; Wainstok, R. Targeting Tumor-Associated Macrophages and Inhibition of MCP-1 Reduce Angiogenesis and Tumor Growth in a Human Melanoma Xenograft. *J. Investig. Dermatol.* **2007**, *127*, 2031–2041. [CrossRef]

86. Liu, S.; Gao, H.; Gao, C.; Liu, W.; Xing, D. Bindarit Attenuates Pain and Cancer-Related Inflammation by Influencing Myeloid Cells in a Model of Bone Cancer. *Arch. Immunol. Ther. Exp.* **2018**, *66*, 221–229. [CrossRef] [PubMed]

87. Ward, S.T.; Li, K.K.; Hepburn, E.; Weston, C.J.; Curbishley, S.M.; Reynolds, G.M.; Hejmadi, R.K.; Bicknell, R.; Eksteen, B.; Ismail, T.; et al. The Effects of CCR5 Inhibition on Regulatory T-Cell Recruitment to Colorectal Cancer. *Br. J. Cancer.* **2015**, *112*, 319–328. [CrossRef]

88. Tanabe, Y.; Sasaki, S.; Mukaida, N.; Baba, T. Blockade of the Chemokine Receptor, CCR5, Reduces the Growth of Orthotopically Injected Colon Cancer Cells via Limiting Cancer-Associated Fibroblast Accumulation. *Oncotarget* **2016**, *7*, 48335–48345. [CrossRef] [PubMed]

89. Zollo, M.; Di Dato, V.; Spano, D.; De Martino, D.; Liguori, L.; Marino, N.; Vastolo, V.; Navas, L.; Garrone, B.; Mangano, G.; et al. Targeting Monocyte Chemotactic Protein-1 Synthesis with Bindarit Induces Tumor Regression in Prostate and Breast Cancer Animal Models. *Clin. Exp. Metastasis* **2012**, *29*, 585–601. [CrossRef] [PubMed]

90. Singh, S.K.; Mishra, M.K.; Eltoum, I.-E.A.; Bae, S.; Lillard, J.W.; Singh, R. CCR5/CCL5 Axis Interaction Promotes Migratory and Invasiveness of Pancreatic Cancer Cells. *Sci. Rep.* **2018**, *8*, 1323. [CrossRef] [PubMed]

91. Pervaiz, A.; Zepp, M.; Mahmood, S.; Ali, D.M.; Berger, M.R.; Adwan, H. CCR5 Blockage by Maraviroc: A Potential Therapeutic Option for Metastatic Breast Cancer. *Cell. Oncol.* **2019**, *42*, 93–106. [CrossRef] [PubMed]

92. Yang, J.; Sontag, D.; Gong, Y.; Minuk, G.Y. Alterations in Chemokine Receptor CCR5 Activity Influence Tumor Cell Biology in Human Cholangiocarcinoma Cell Lines. *Ann. Hepatol.* **2021**, *21*, 100265. [CrossRef]

93. Maione, F.; Molla, F.; Meda, C.; Latini, R.; Zentilin, L.; Giacca, M.; Seano, G.; Serini, G.; Bussolino, F.; Giraudo, E. Semaphorin 3A Is an Endogenous Angiogenesis Inhibitor That Blocks Tumor Growth and Normalizes Tumor Vasculature in Transgenic Mouse Models. *J. Clin. Investig.* **2009**, *119*, 3356–3372. [CrossRef] [PubMed]

94. Hu, B.; Cheng, S.-Y. Angiopoietin-2: Development of Inhibitors for Cancer Therapy. *Curr. Oncol. Rep.* **2009**, *11*, 111–116. [CrossRef]

95. Marconcini, L.; Marchio, S.; Morbidelli, L.; Cartocci, E.; Albini, A.; Ziche, M.; Bussolino, F.; Oliviero, S. C-Fos-Induced Growth Factor/Vascular Endothelial Growth Factor D Induces Angiogenesis in Vivo and in Vitro. *Proc. Natl. Acad. Sci. USA* **1999**, *96*, 9671–9676. [CrossRef]

96. Yanagawa, T.; Shinozaki, T.; Watanabe, H.; Saito, K.; Raz, A.; Takagishi, K. Vascular Endothelial Growth Factor-D Is a Key Molecule That Enhances Lymphatic Metastasis of Soft Tissue Sarcomas. *Exp. Cell Res.* **2012**, *318*, 800–808. [CrossRef]

97. Kilvaer, T.K.; Valkov, A.; Sorbye, S.; Smeland, E.; Bremnes, R.M.; Busund, L.-T.; Donnem, T. Profiling of VEGFs and VEGFRs as Prognostic Factors in Soft Tissue Sarcoma: VEGFR-3 Is an Independent Predictor of Poor Prognosis. *PLoS ONE* **2010**, *5*, e15368. [CrossRef]

98. Zhao, T.; Zhao, W.; Meng, W.; Liu, C.; Chen, Y.; Bhattacharya, S.K.; Sun, Y. Vascular Endothelial Growth Factor-D Mediates Fibrogenic Response in Myofibroblasts. *Mol. Cell Biochem.* **2016**, *413*, 127–135. [CrossRef] [PubMed]

99. Wang, P.; Chen, S.-H.; Hung, W.-C.; Paul, C.; Zhu, F.; Guan, P.-P.; Huso, D.L.; Kontrogianni-Konstantopoulos, A.; Konstantopoulos, K. Fluid Shear Promotes Chondrosarcoma Cell Invasion by Activating Matrix Metalloproteinase 12 via IGF-2 and VEGF Signaling Pathways. *Oncogene* **2015**, *34*, 4558–4569. [CrossRef] [PubMed]

100. Siemann, N.M.; Siemann, D.W. Angiopoietin-2 Axis Inhibitors: Current Status and Future Considerations for Cancer Therapy. Available online: https://www.eurekaselect.com/115040/article (accessed on 2 November 2020).

101. Bezuidenhout, L.; Zilla, P.; Davies, N. Association of Ang-2 with Integrin Beta 2 Controls Ang-2/PDGF-BB-Dependent Upregulation of Human Peripheral Blood Monocyte Fibrinolysis. *Inflammation* **2009**, *32*, 393–401. [CrossRef] [PubMed]

102. Hu, B.; Jarzynka, M.J.; Guo, P.; Imanishi, Y.; Schlaepfer, D.D.; Cheng, S.-Y. Angiopoietin 2 Induces Glioma Cell Invasion by Stimulating Matrix Metalloprotease 2 Expression through the Alphavbeta1 Integrin and Focal Adhesion Kinase Signaling Pathway. *Cancer Res.* **2006**, *66*, 775–783. [CrossRef]

103. Morii, T.; Mochizuki, K.; Tajima, T.; Ichimura, S.; Satomi, K. D-Dimer Levels as a Prognostic Factor for Determining Oncological Outcomes in Musculoskeletal Sarcoma. *BMC Musculoskelet. Disord.* **2011**, *12*, 250. [CrossRef] [PubMed]

104. Raj, S.D.; Zhou, X.; Bueso-Ramos, C.E.; Ravi, V.; Patel, S.; Benjamin, R.S.; Vadhan-Raj, S. Prognostic Significance of Elevated D-Dimer for Survival in Patients with Sarcoma. *Am. J. Clin. Oncol.* **2012**, *35*, 462–467. [CrossRef] [PubMed]

105. Bure, I.V.; Kuznetsova, E.B.; Zaletaev, D.V. Long Noncoding RNAs and Their Role in Oncogenesis. *Mol. Biol.* **2018**, *52*, 907–920. [CrossRef]

106. Zhang, R.; Xia, T. Long Non-Coding RNA XIST Regulates PDCD4 Expression by Interacting with MiR-21-5p and Inhibits Osteosarcoma Cell Growth and Metastasis. *Int. J. Oncol.* **2017**, *51*, 1460–1470. [CrossRef] [PubMed]

107. Lv, G.-Y.; Miao, J.; Zhang, X.-L. Long Noncoding RNA XIST Promotes Osteosarcoma Progression by Targeting Ras-Related Protein RAP2B via MiR-320b. *Oncol. Res.* **2018**, *26*, 837–846. [CrossRef] [PubMed]

108. Yildirim, E.; Kirby, J.E.; Brown, D.E.; Mercier, F.E.; Sadreyev, R.I.; Scadden, D.T.; Lee, J.T. Xist RNA Is a Potent Suppressor of Hematologic Cancer in Mice. *Cell* **2013**, *152*, 727–742. [CrossRef]

109. Navarro, P.; Chambers, I.; Karwacki-Neisius, V.; Chureau, C.; Morey, C.; Rougeulle, C.; Avner, P. Molecular Coupling of Xist Regulation and Pluripotency. *Science* **2008**, *321*, 1693–1695. [CrossRef] [PubMed]

110. Koga, M.; Matsuda, M.; Kawamura, T.; Sogo, T.; Shigeno, A.; Nishida, E.; Ebisuya, M. Foxd1 Is a Mediator and Indicator of the Cell Reprogramming Process. *Nat. Commun.* **2014**, *5*, 3197. [CrossRef] [PubMed]

111. Gandalovičová, A.; Rosel, D.; Fernandes, M.; Veselý, P.; Heneberg, P.; Čermák, V.; Petruželka, L.; Kumar, S.; Sanz-Moreno, V.; Brábek, J. Migrastatics-Anti-Metastatic and Anti-Invasion Drugs: Promises and Challenges. *Trends Cancer* **2017**, *3*, 391–406. [CrossRef] [PubMed]

112. Rosel, D.; Fernandes, M.; Sanz-Moreno, V.; Brábek, J. Migrastatics: Redirecting R&D in Solid Cancer Towards Metastasis? *Trends Cancer* **2019**, *5*, 755–756. [CrossRef] [PubMed]

113. Kikuchi, K.; Kishino, A.; Konishi, O.; Kumagai, K.; Hosotani, N.; Saji, I.; Nakayama, C.; Kimura, T. In Vitro and in Vivo Characterization of a Novel Semaphorin 3A Inhibitor, SM-216289 or Xanthofulvin. *J. Biol. Chem.* **2003**, *278*, 42985–42991. [CrossRef]

114. Martínez-García, D.; Manero-Rupérez, N.; Quesada, R.; Korrodi-Gregório, L.; Soto-Cerrato, V. Therapeutic Strategies Involving Survivin Inhibition in Cancer. *Med. Res. Rev.* **2019**, *39*, 887–909. [CrossRef]

PŘÍLOHA 10

Chapter 7
Sarcoma Stem Cell Heterogeneity

Jiri Hatina, Michaela Kripnerova, Katerina Houfkova, Martin Pesta, Jitka Kuncova, Jiri Sana, Ondrej Slaby, and René Rodríguez

Abstract Sarcomas represent an extensive group of divergent malignant diseases, with the only common characteristic of being derived from mesenchymal cells. As such, sarcomas are by definition very heterogeneous, and this heterogeneity does not manifest only upon intertumoral comparison on a bulk tumor level but can be extended to intratumoral level. Whereas part of this intratumoral heterogeneity could be understood in terms of clonal genetic evolution, an essential part includes a hierarchical relationship between sarcoma cells, governed by both genetic and epigenetic influences, signals that sarcoma cells are exposed to, and intrinsic developmental programs derived from sarcoma cells of origin. The notion of this functional hierarchy operating within each tumor implies the existence of sarcoma stem cells, which may originate from mesenchymal stem cells, and indeed, mesenchymal stem cells have been used to establish several crucial experimental sarcoma models and to trace down their respective stem cell populations. Mesenchymal stem cells themselves are heterogeneous, and, moreover, there are alternative possibilities for sarcoma cells of origin, like neural crest-derived stem cells, or mesenchymal committed precursor cells, or – in rhabdomyosarcoma – muscle satellite cells. These various origins result in substantial heterogeneity in possible sarcoma initiation. Genetic and epigenetic changes associated with sarcomagenesis profoundly impact

J. Hatina (✉) · M. Kripnerova · K. Houfkova · M. Pesta
Faculty of Medicine in Pilsen, Charles University, Institute of Biology, Plzen, Czech Republic
e-mail: jiri.hatina@lfp.cuni.cz

J. Kuncova
Faculty of Medicine in Pilsen, Charles University, Institute of Physiology, Plzen, Czech Republic

J. Sana · O. Slaby
Central European Institute of Technology, Molecular Oncology II—Solid Cancer, Brno, Czech Republic

R. Rodríguez
Central University Hospital of Asturias—Health Research Institute of Asturias, Oviedo, Spain

CIBERONC, Madrid, Spain

the biology of sarcoma stem cells. For pediatric sarcomas featuring discrete reciprocal translocations and largely stable karyotypes, the translocation-activated oncogenes could be crucial factors that confer stemness, principally by modifying transcriptome and interfering with normal epigenetic regulation; the most extensively studied examples of this process are myxoid/round cell liposarcoma, Ewing sarcoma, and synovial sarcoma. For adult sarcomas, which have typically complex and unstable karyotypes, stemness might be defined more operationally, as a reflection of actual assembly of genetically and epigenetically conditioned stemness factors, with dedifferentiated liposarcoma providing a most thoroughly studied example. Alternatively, stemness can be imposed by tumor microenvironment, as extensively documented in osteosarcoma. In spite of this heterogeneity in both sarcoma initiation and underlying stemness biology, some of the molecular mechanisms of stemness might be remarkably similar in diverse sarcoma types, like abrogation of classical tumor suppressors pRb and p53, activation of Sox-2, or inhibition of canonical Wnt/β-catenin signaling. Moreover, even some stem cell markers initially characterized for their stem cell enrichment capacity in various carcinomas or leukemias seem to function quite similarly in various sarcomas. Understanding the biology of sarcoma stem cells could significantly improve sarcoma patient clinical care, leading to both better patient stratification and, hopefully, development of more effective therapeutic options.

Keywords Sarcoma · Liposarcoma · Ewing sarcoma · Chondrosarcoma · Synovial sarcoma · Osteosarcoma · Mesenchymal stem cells · Sarcoma stem cells · Sarcoma cells of origin · Genetic and epigenetic plasticity · In vitro sarcoma progression models · Sox-2 · p53 · pRb · Wnt/β-catenin pathway · Dickkopf

Sarcomas represent an unusually wide, extensive, and heterogeneous group of tumors, whose sole common denominator is that they originate from mesenchymal cells. They could be divided according to various criteria. The most traditional histopathologic classification divides sarcomas into two large groups according to the type of tissue of primary manifestation, namely bone sarcomas, including osteosarcoma and chondrosarcoma, and soft tissue sarcomas, including liposarcoma, fibrosarcoma, undifferentiated pleomorphic sarcoma, leiomyosarcoma, rhabdomyosarcoma, and a large group of other pediatric sarcomas [1]. Besides, we can classify sarcomas according to genetic criteria, and, again, we can distinguish two large groups: sarcomas with largely normal karyotypes and discrete structural chromosomal changes and sarcomas with complex karyotypes and pronounced karyotypic instability. The first group includes especially pediatric sarcomas, which rely for the most part on reciprocal translocations to activate specific oncogenes (Table 7.1). The adult sarcomas – including osteosarcoma, chondrosarcoma, most liposarcomas, fibrosarcoma, angiosarcoma, leiomyosarcoma, and undifferentiated pleomorphic sarcoma – carry usually very complex karyotypes with numerous structural and numerical alterations [2, 4]. Researchers have only begun to understand the complex mechanisms behind this karyotypic instability. Especially dedifferentiated

Table 7.1 Most frequent structural chromosomal aberrations found in sarcomas[a]

Tumors	Cytogenetic events	Genes involved/fusion
Fibrosarcoma, infantile	t(12;15)(p13;q26)	*ETV6-NTRK3*
Synovial sarcoma	t(X;18)(p11.2;q11.2)	*SS18-SSX1, SSX2*
Clear cell sarcoma	t(12;22)(q13;q12)	*EWSR1-ATF1*
	t(2;22)(q32.3;q12)	*EWSR1-CREB1*
Alveolar rhabdomyosarcoma	t(2;13)(q35;q14)	*PAX3-FOXO1*
	t(1;13)(q36;q14)	*PAX7-FOXO1*
Mesenchymal chondrosarcoma	del(8)(q13;3q21.1)	*HEY1-NCOA2*
Alveolar soft-part sarcoma	t(X;17)(p11;q25)	*ASPSCR1-TFE3*
Lipoma	12q15 rearrangement	*HMGA2* rearrangement
Ewing sarcoma	t(11;22)(q24;q12)	*EWSR1-FLI1*
	t(21;22)(q22,q12)	*EWSR1-ERG*
	t(7;22)(p22;q12)	*EWSR1-ETV1*
	t(17;22)(q12;q12)	*EWSR1-E1AF*
	t(2;22)(q33;q12)	*EWSR1-FEV*
	t(16;21)(p11;q22)	*TLS(FUS)-ERG*
	Inversion of 22q	*EWSR1-ZSG*
Myxoid/round cell liposarcoma	t(12;16)(q13;p11)	*FUS-DDIT3*
	t(12;22)(q13;q12)	*EWSR1-DDIT3*
Extraskeletal myxoid chondrosarcoma	t(9;22)(q22;q12)	*EWSR1-NR4A3*
	t(9;17)(q22;q12)	*TAF15-NR4A3*
Dermatofibrosarcoma protuberans/ giant cell fibrosarcoma	t(17;22)(q22;q13), supernumerary ring chromosomes encompassing chr 17 and 22	*COL1A1-PFGFB*
Inflammatory myofibroblastic tumor	t(2;19)(p23;p13)	*TPM4-ALK*
	t(2;17)(p23;q23)	*CLTC-ALK*
	inv(2)(p23;q13)	*RANBP2-ALK*
Angiomatoid fibrous histiocytoma	t(2;22)(q32.3;q12)	*EWSR1-CREB1*
	t(12;22)(q13;q12)	*EWSR1-ATF1*
	t(12;16)(q13;q11)	*TLS(FUS)-ATF1*
Low-grade fibromyxoid sarcoma	t(7;213)(q34;p11)	*FUS-CREB3L2*
Sclerosing epithelioid fibrosarcoma	t(11;16)(p11;p11)	*FUS-CREB3L1*
Hemosiderotic fibrolipomatous tumor	t(1;10)(p11;q24)	*MGEA5-TGFBR3*
Epithelioid hemangioendothelioma	t(1;3)(p36;q25)	*WWTR1-CAMTA1*
Soft tissue myoepithelioma	t(1;22)(q23;q12)	*EWSR1-PBX1*
GCT of tendon sheath	t(1;2)(p13;q37)	*COL6A3-CSF1*
Solitary fibrous tumor	inv(12)(q13;q13)	*NAB2-STAT6*
Nodular fasciitis	t(17;22)(p13;q13)	*MYH9-USP6*
Pseudomyogenic hemangioendothelioma	t(7;19)(q22;q13)	*SERPINE1-FOSB*
Soft tissue angiofibroma	t(5;8)(q15;q13)	*AHRR-NCOA2*
CIC-DUX4 sarcoma	t(4;19)(q35;q13)	*CIC-DUX4*

(continued)

Table 7.1 (continued)

Tumors	Cytogenetic events	Genes involved/fusion
	t(10;19)(q26;q13)	*CIC-DUX4L10*
BCOR-CCNB3 sarcoma	inv(X)(p11.4;p11.22)	*BCOR-CCNB3*
Phosphaturic mesenchymal tumor	t(2;8)(q35;q11)	*FN1-FGFR1*
Leiomyoma (uterine)	t(12;14)(q15;q24) or deletion of 7q	*HMGA1 (HMGIC)* rearrangement
Synovial sarcoma	t(X;18)(p11;p11)	*SS18-SSX1 or SS18-SSX2, SS18-SSX4*
Desmoplastic small round cell tumor	t(11;22)(p13;q12)	*EWSR1-WT1*
Endometrial stromal tumor	t(7;17)(p15;q21)	*JAZF1-SUZ12*
Extraskeletal myxoid chondrosarcoma	t(9;22)(q22;q12)	*EWSR1-NR4A3*
	t(9;17)(q22;q11)	*TAF15-NR4A3*
	t(9;15)(q22;q21)	*TCF12-CHN*

[a]Source: References [1–3]

liposarcoma (one of four major liposarcoma groups [5]) features a constantly changing karyotype involving the so-called neochromosomes – giant, sometimes ring-shaped, chromosomal structures that accumulate most of the amplified onco-gene loci originating from different chromosomes and result from multiple complex mechanisms, such as chromothripsis and breakage-fusion-bridge cycles [6].

Mesenchymal Stem Cells

Many of the mesenchymal tissues that can be affected by sarcomas undergo continuous remodeling and renewal much like epithelia, and it comes as little surprise that there is a similar hierarchical cellular organization. Supposedly sitting on the top of this cell hierarchy are mesenchymal stem cells (MSCs), which behave much like other adult stem cells, i.e., they can self-renew and differentiate into the respective downstream cell types. For MSCs, trilineage differentiation potential in vitro is considered a sort of a definition criterion. Upon appropriate stimulation, MSCs can enter osteogenic, adipogenic, and chondrogenic differentiation [7, 8]. The true differentiation potential of MSCs is broader, however. At least in vitro, they are able to enter the neurogenic differentiation pathway as well. Of course, they also differentiate into fibroblasts, the major constituent of *lamina propria* of most, if not all, epithelial tissues. This fibroblastic differentiation pathway can take a special form – the carcinoma-associated fibroblasts (CAFs) – providing a supportive stroma found in practically all carcinomas. Another differentiated cell type originating from MSCs is endothelium, a differentiation pathway exploited by tumors of various origins as well, yielding tumor vasculature.

MSCs can be isolated and propagated from a lot of tissues in the body, two prototypical sources being bone marrow and white adipose tissue. These cells are,

nonetheless, not identical and differ in terms of both their relative differentiation abilities and epigenetic genome regulation [9, 10]. These biological differences extend into different nomenclatures: The bone marrow-derived MSCs (BM-MSCs) have been recently proposed to be called skeletal stem cells [11], while the white adipose tissue MSCs are traditionally called adipose tissue-derived stromal cells (ASCs). A notable exception among mesenchymal tissues as to for their exclusive derivation from MSCs is the skeletal muscle, which carries its own stem cell population, the satellite cells. Remarkably, the satellite stem cell niche also adopts a MSCs-like population, again carrying a special name, the fibroblast-adipocyte precursor (FAP) [12]. To make the things even more complicated, there is a separate adult stem cell population, the neural crest-derived stem cells. These cells have descendant cell types, such as specialized neurons, glial cells, and melanocytes, but they can also differentiate into the full spectrum of mesenchymal cell types [13]. In conclusion, there is a pronounced and rather extensive heterogeneity among stem cell populations of normal mesenchymal tissues.

Molecular Biology of MSC Stemness and Differentiation

As introduced above, MSCs have one of the broadest differentiation capacities among adult stem cells, each of the various differentiation programs dominated by specific signals resulting in the activation of specific transcription factors. Transcription factors crucial for osteogenic differentiation are Runx2 and directly downstream positioned Osterix. Among the signals, bone morphogenetic proteins are prominent, resulting in specific Smad activation; notably, a direct Smad-Runx2 protein-protein interaction has been described. Adipogenic differentiation results from the transcription factor succession C/EBPα–C/EBPβ–PPARγ. As to the chondrogenic differentiation, Sox-9 is regarded as a master transcription factor [14].

Crucial from the point of view of sarcoma initiation and development, MSC stemness and differentiation seem to be regulated by an intricate network, whose essential players are classical tumor suppressor proteins p53 and pRb on one hand and key stemness regulators SIRT-1 and Sox-2 on the other (Fig. 7.1). First of all, p53 is a general stemness inhibitor, a function not limited to MSCs [15]. Mechanistically, a part of this stemness inhibition relies on direct as well as indirect transcriptional repression of both *SIRT-1* (two p53 binding sites in the promoter plus a binding site for the p53 downstream transcription factor HIC-1, as well as p53-inducible miRNA34-mediated silencing) [16, 17] and *Sox-2* (mediated mainly by p53-activated miRNA145) [18–20]. *SIRT-1*, a longevity gene, codes for NAD$^+$-dependent protein deacetylase, which, by virtue of this specific posttranslational modification, regulates the activity of numerous cellular proteins. Among them is p53, with deacetylation resulting in blocking of its nuclear translocation and the significant diminution of transcription activation potency, at least in embryonic stem cells [21]. Sox-2 is another direct SIRT-1 target, but in this case, the effect is exactly opposite: Deacetylation promotes the nuclear localization and transcrip-
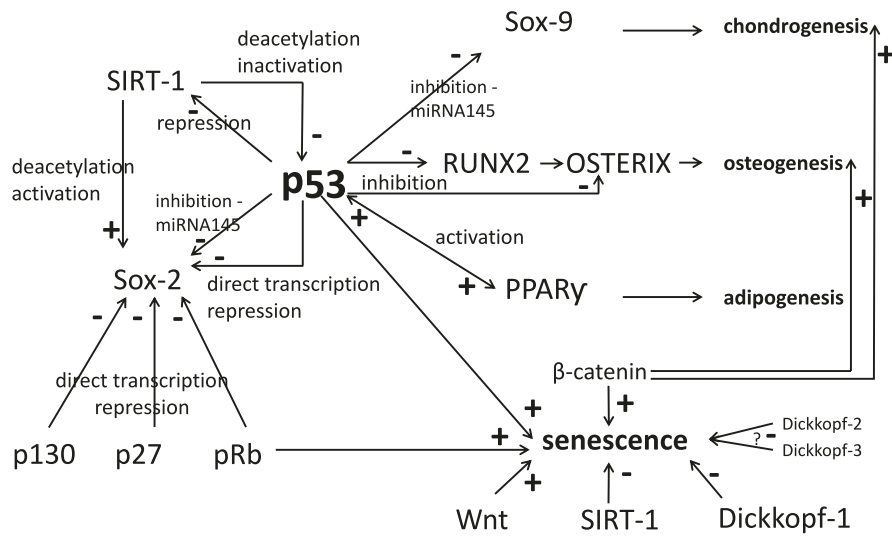
Fig. 7.1 Molecular circuitry operating in stemness regulation in MSCs and sarcoma stem cells. See text for detailed explanation

tional activation of downstream genes [22]. Besides SIRT-1 and p53-mediated regulation, *Sox-2* is transcriptionally repressed in primary fibroblasts by an unusual complex involving cell cycle inhibitor p27 and retinoblastoma family proteins pRb and p130; notably, p53 potentiates this effect [23]. In addition to stemness regulation, p53 is also crucially involved in MSC differentiation. Functional p53 seems to be a necessary prerequisite for successful adipogenic differentiation, in part via mitochondria-generated reactive oxygen species, in part via a direct mutual positive regulation with PPARγ [24]. On the other hand, p53 inhibits both osteogenic (in part by directly repressing the *Runx2* gene and inhibiting Osterix activity through a direct protein-protein interaction) [25] and chondrogenic (via the miRNA145-mediated silencing of Sox-9) differentiations [18, 19, 26].

Some of the tumor suppressor activities of p53 and pRb consist in their actions on cellular life span, restricting it and promoting a special type of cell cycle arrest – senescence. Indeed, MSCs – especially of human origin – are not immortal, at least in vitro, and succumb to senescence arrest sometimes after just a few passages; inasmuch these properties lie in the nature of MSCs or result from culture stress (the bone marrow is a frank hypoxic area, whereas MSCs are usually cultured in normal oxygen conditions) is still not entirely clear. Anyway, senescence could be regarded as an antitumor barrier, overcoming of which could be an important step in tumorigenesis. Interestingly, apart from p53 and pRb, there seems to be one more player impacting both MSC differentiation and senescence, namely, the Wnt/β-catenin pathway. The activation of β-catenin has been reported to be part of both osteogenic and chondrogenic differentiations; on the other hand, this pathway also

accelerates the senescence of MSCs; MSC immortalization can be promoted by Wnt inhibitor Dickkopf-1 (and by SIRT-1) [27, 28].

MSC stemness regulation and sarcomagenesis are associated in various ways. Both SIRT-1 and Sox-2 are poor prognosis factors across various sarcoma types [29, 30]. Diverse sarcomas can be found in increased frequency in affected families suffering from both *p53* (Li-Fraumeni syndrome) and *pRb* (hereditary retinoblastoma) germ line mutation-driven hereditary cancer syndromes [31]. One of the genes carried within the amplified region underlying neochromosome generation in dedifferentiated liposarcoma is *MDM2* coding for a direct p53 inhibitor [32]. Our own transcriptomic analysis of two separate progression models of murine soft tissue sarcoma, the JUN fibrosarcoma progression series [33] and the 3T3-L1 – LM3D liposarcoma progression series [34], revealed that Dickopf-2 and Dickkopf-3, as well as additional published inhibitors of canonical Wnt/β-catenin signaling including Adenomatosis polyposis coli down-regulated 1, Fibulin-5, Maternally expressed 3, and Integrator complex subunit 6, are all upregulated during sarcoma progression. Strikingly, this seems to be accompanied by upregulation of the Receptor tyrosine kinase-like orphan receptor 2 (Ror2), suggesting a switch from the canonical Wnt signaling to the noncanonical Wnt5a-Ror2 pathway [34a].

Sarcoma-Initiating Cells and Sarcoma Stem Cells

Keeping in mind the above-outlined development of mesenchymal tissues reflecting an intrinsic cellular hierarchy that starts from mesenchymal stem cells and follows a given differentiation path through progenitors to terminally differentiating cells, it is quite natural to expect that part of this hierarchy would be preserved in sarcomas. Accordingly, we can assume the existence of sarcoma stem cells that both self-renew and differentiate, much like in carcinomas and leukemias. Of course, only some sarcoma types – for example, osteosarcoma, chondrosarcoma, liposarcoma, leiomyosarcoma, or rhabdomyosarcoma – allow to follow a certain differentiation pathway reminiscent of physiological differentiation. Other sarcoma types – diagnosed as undifferentiated pleomorphic sarcoma or simply just spindle cell sarcoma – do not show any easily recognizable differentiation pattern. In fact, the residual differentiation capacity might not be easily discernible even in high-grade tumors of the former sarcoma types. In such cases, the tumorous (pseudo) differentiation can take the form of diversity in functional aspects, like clonogenicity, tumorigenicity, therapeutic resistance, motility, and invasiveness. Various questions about sarcoma stem cells – like those about their abundance, properties, self-renewal, and differentiation ability – should be clearly separated from questions about sarcoma-initiating cells, which are cells that incur the first mutagenic insult ultimately yielding a sarcoma.

In this respect, the various types of mesenchymal stem cells would be apparent candidates [35–37]. Several reasons support this conclusion. First, again drawing lessons from various carcinoma and leukemia stem cells, the path from a respective

tissue stem cell (mesenchymal for sarcomas) to its derivative cancer stem cell is simpler and more direct than the path assuming cancer initiation in a more differentiated cell, because the various stemness mechanisms are already operating. In addition, the reliance of sarcomas and sarcoma stem cells on Sox-2 and SIRT-1 is a good argument for their derivation from mesenchymal stem cells. We should not forget, however, that MSCs are not a uniform cell type and BM-MSCs clearly differ from ASCs and probably from MSCs isolated from other sources, NCSCs notwithstanding. Another argument is that MSC-specific expression signature has been identified in some sarcomas and it could be especially clearly revealed (together with the restauration of the full multilineage differentiation potential in vitro) by performing an experimental reversion of sarcoma cells, for example, by an shRNA-mediated knockdown of driver fusion oncogenes in translocation-derived sarcomas. Finally, MSCs are amenable to both spontaneous transformation and purposeful genetic manipulation resulting in sarcomas (see below). This last argument should not be overemphasized, however, because a similar outcome could also be arrived at by the in vitro transformation of normal fibroblasts, that is, differentiated mesenchymal cells [38].

In addition, even though it could be feasible to infer the origin of simpler translocation-dependent sarcomas, this task can be much more complicated in karyotypically complex sarcomas. Indeed, available models suggest alternative possibilities. For example, at least in mouse models, a probable osteosarcoma-initiating cell is an osteogenic progenitor, not MSC [39, 40]. What is more, it could be shown that a human fibrosarcoma cell line could be converted to a liposarcoma by a forced expression of a key liposarcoma oncogene *CHOP* (*DDIT3*) [41]. And, of course, rhabdomyosarcomas derive almost certainly from satellite cells [42, 43]. We can thus conclude that there are many potential candidates for the sarcoma cell of origin, including various MSCs and NCSCs and various other mesenchymal cell types.

Modeling Sarcomagenesis in MSCs

Assuming the MSC origin of at least a great part of sarcomas, we can directly use our knowledge of MSC biology – including our ability to differentiate MSCs along a desired path, together with our increasing understanding of underlying biology of diverse sarcomas – to build MSC-based models of sarcoma development. This endeavor can have several forms.

First, we can perform in vitro differentiation of MSCs, identify differentially expressed genes, proteins, or pathways, and relate them to the corresponding sarcoma type. Two studies illustrate well this point. In the first of them, primary human BM-MSCs were subjected to chondrogenic differentiation, and a specific chondrogenesis expression signature was identified. When the gene expression profiles of chondrosarcoma samples of different grades were confronted with the chondrogenesis expression signature, it turned out that all the grade III and grade II

metastatic cases clustered together close to the undifferentiated MSCs, whereas grade I and nonmetastatic grade II chondrosarcomas were more similar to late differentiation stages of MSCs approaching mature chondrocytes [44]. This result rather convincingly shows that stemness preservation (or regain) can represent an important contribution to metastatic competence. In addition, the chondrogenesis gene expression signature identified could be of a direct clinical utility, especially for the prognosis of grade II chondrosarcoma patients.

A conceptually similar approach has been applied to liposarcoma. The liposarcoma itself represents a complex diagnosis consisting of at least four distinct tumor types: dedifferentiated, pleomorphic, myxoid/round cell, and well-differentiated [5]. It could be shown that each of them corresponds, at least in terms of their specific gene expression profile, to a different stage of adipogenic differentiated MSC. Again, this result might have an immediate diagnostic value. Dedifferentiated and pleomorphic liposarcomas thus feature the expression of typical MSC markers – like CD44, CD54, and hepatocyte growth factor – while myxoid/round cell and well-differentiated liposarcomas adopt the expression of typical fat markers, namely, adiponectin, leptin, and lipoprotein lipase [45]. This approach made also possible the identification of genes and pathways typical of either path of liposarcomagenesis. Although their clinical utility has yet to be demonstrated, an intriguing candidate pathway compromised in both dedifferentiated and pleomorphic liposarcoma cases is insulin signaling, a very well-defined proadipogenic signaling pathway, which could be amenable to various pharmacological modulations [46]. It should be stressed, nevertheless, that especially dedifferentiated liposarcoma is a very complicated tumor type, for which the cell of origin is largely unclear (it could be a MSC at an early point of adipogenic differentiation or progressing well-differentiated liposarcoma) and whose genome, as mentioned above, is extremely unstable with unprecedented consequences for gene expression, stemness, and clinical behavior (see below).

If we embrace the idea that most sarcomas may originate from MSCs, a logical next step is to undertake an attempt at deriving sarcoma models by their targeted manipulation. In the last decade, several valuable sarcoma models have been established in this way, revealing several general rules of sarcoma development. First, it turned out that rodent (especially murine) MSCs are distinctly more susceptible to initiate sarcomagenesis than their human counterparts; indeed, murine and rat MSCs are even prone to spontaneous sarcomagenesis upon prolonged in vitro culture, which is practically never observed in human MSCs. We can only speculate about biological reasons for this difference. It is known for quite a long time that mouse adult tissues constitutively express telomerase and the murine cells are thus immortal upon appropriate cell culture conditions, eliminating the senescence barrier (see above). In addition, most – if not all – experiments have been performed on MSCs isolated from various inbred mouse strains, and we can assume a random fixation of various mutant alleles during the inbreeding process. The existing senescence barrier – probably among other mechanisms – makes human MSCs intrinsically resistant to sarcomagenesis, and usually this is the first obstacle to be overcome in order to convert human primary MSCs into desired sarcoma cells. A standard

approach is to introduce viral oncogenes that eliminate the p53- and pRb-mediated senescence arrest (HPV *E6* and *E7* oncogenes or SV40 large T antigen, respectively), complemented by the stable overexpression of the gene coding for catalytic subunit of telomerase (hTERT) [47, 48]. Even these MSC derivative cell lines (called 3 hit MSCs – E6, E7, and hTERT) were not susceptible to spontaneous sarcomagenesis, and two additional genetic steps turned out to be necessary, namely, c-Myc stabilization by virtue of SV40 small t antigen expression and a permanent mitogenic stimulation by the forced expression of a constitutively active *Ha-Ras* oncogene [47, 48]; *Myc-Ras* is a traditional cooperating oncogene pair, defined by its joint ability to transform rat embryonic fibroblasts [49]. The resulting 5 hit MSCs finally yielded undifferentiated pleomorphic sarcomas when injected into a severely immunocompromised mouse [50].

A separate question is which factors promote particular types of sarcomagenesis. This seems to be a very complex issue encompassing several points, such as the source of MSCs (BM-MSCs vs. ASCs), their species origin (mouse or human), and of course the genetic changes either spontaneously accumulated or purposefully introduced. Especially, p53 deficiency (alone or combined with pRb deficiency) can initiate various sarcoma types depending on other factors. In mouse BM-MSCs, spontaneous p53 mutations have been associated with fibrosarcoma development [51], whereas mouse *p53−/−* ASCs were transformed toward leiomyosarcoma [50], and the combined deficiency of both p16^{INK4a} and p19^{ARF} (two tumor suppressor proteins encoded by a single locus and acting via pRb and p53 pathways, respectively [49]) coupled to c-Myc overexpression in mouse BM-MSCs triggered osteosarcoma development [52]. The knowledge and availability of translocation-activated fusion oncogenes provided additional possibilities of specifically directing sarcomagenesis along a desired pathway. The FUS-CHOP oncoprotein, specific for myxoid/round cell liposarcoma, provided a particularly revealing example. A purposeful expression of FUS-CHOP in mouse ASC of *p53−/−* background [50], in 4 hit (HPV E6, E7, hTERT, and SV40 small-t) or 5 hit (+ Ha-Ras^{V12}) human BM-MSC backgrounds [50], or in HT1080 fibrosarcoma cells [41], respectively, was able to divert the pathway of sarcomagenesis from leiomyosarcoma, undifferentiated pleomorphic sarcoma, or fibrosarcoma to liposarcoma. It seems, therefore, that this type of liposarcomagenesis involves at least two principal causal factors: a general tumorigenic transformation of cells (provided by the recipient cells that are already competent to various types of sarcomagenesis) and a limited, corrupt, and incomplete lipomatous differentiation provided by the FUS-CHOP translocation oncoprotein.

Ewing sarcoma provides another example of a sarcoma that relies on a translocation oncogene imposing its effect on target cells. From a certain point of view, its biology seems to be opposite to myxoid/round cell liposarcoma, with sarcomagenesis resulting from a specific dedifferentiation or reprogramming toward a primitive stem cell phenotype. Indeed, in transgenic mice, a conditional *p53* deletion in embryonic limb bud cells led predominantly to osteosarcoma (i.e., a tumor featuring an intrinsic partial differentiation ability) [53], while if combined with *EWS-FLI-1*

translocation oncogene overexpression, this partial differentiation was lost, leading to Ewing sarcoma-like tumors [54]. Like FUS-CHOP, EWS-FLI-1 alone does not transform human adult BM-MSCs (unlike mouse MSCs), but it is able to impose a gene expression profile reminiscent of Ewing sarcoma [55]. Intriguingly, the degree of matching between these gene expression profiles was even greater if pediatric instead of adult BM-MSCs were used. A further increase was achieved when *EWS-FLI-1*-transduced pediatric human BM-MSCs were cultured in medium used to raise induced pluripotent stem cells [20], quite clearly classifying Ewing sarcoma as a stem cell- or reprogramming-type malignancy.

On the other hand, it is not yet clear whether MSCs are the cells of origin for Ewing sarcoma. Independent experiments with *EWS-FLI-1*-transduced NCSCs also showed a strong concordance with the Ewing sarcoma gene expression profile [56], leaving the question of Ewing sarcoma's cell of origin open. A similar question with a very similar dilemma is also pending for synovial sarcoma [57, 58].

Sarcoma Stem Cell Heterogeneity

From all the discussion above, we can take the existence of sarcoma stem cells as, if not certain, then certainly highly probable. Various approaches have been adopted to identify and isolate sarcoma stem cells (Table 7.2), which are, by and large, identical to those applied in various carcinomas, lymphomas, and leukemias, including a group of "obligate" stem cell markers, like CD44, CD90, and CD133 [80]. Such approaches suffer from an inherent weakness that they are based on an *a priori* assumption that positive cells equal stem cells, which is not always true. Specific for certain sarcomas could be cell surface markers that define normal mesenchymal stem cells.

Another possibility would be a marker-free approach essentially aimed at identifying chemoresistant cancer and normal stem cells, like side population (SP) sorting directed toward cells with a high expression of ABC efflux membrane transporters, especially ABCB1 and ABCG2, or Aldefluor assay targeting cells specifically overexpressing detoxification enzymes of aldehyde dehydrogenase family, especially ALDH1A1 and ALDH1A3 [81]. Several experimental models in which sarcomagenesis could be followed in a stepwise manner showed that sarcoma development and progression were associated with an increase in the stem cell fraction, expressed as both SP- [79] and Aldefluor-positive cells [65]. This association could be interpreted as sarcomas representing indeed stem cell tumors. Interestingly in this context, the Wnt inhibitor Dickkopf-1 has been reported not only to be crucial to overcoming senescence but also to increase ALDH1A1 expression and thus to promote sarcoma stemness [82]. In addition, specific stem cell targeting could be one mechanism of action of a relatively new antisarcoma chemotherapeutic drug trabectedin [83].

Table 7.2 A survey of stem cell markers exploited to identify and enrich for sarcoma stem cells

Marker	Biological function	Sarcoma type	References
CD133 (prominin-1)	Surface glycoprotein with five transmembrane domains localizing to membrane protrusions	Synovial sarcoma, osteosarcoma, rhabdomyosarcoma, Ewing's sarcoma, liposarcoma, chondrosarcoma	[59–63]
ALDH(1) (aldehyde dehydrogenase)	Group of enzyme catalyzing the oxidation of intracellular aldehyde to carboxylic acid	Osteosarcoma, Ewing's sarcoma, liposarcoma, fibrosarcoma, synovial sarcoma, chondrosarcoma, rhabdomyosarcoma, myxoid/round cell liposarcoma	[59, 61, 63–66]
Nestin (neuronal stem cell)	Type VI intermediate filaments protein	Rhabdomyosarcoma, osteosarcoma, fibrosarcoma (only in sphere-forming cell subpopulations)	[60, 61, 63]
CD184 (also as C-X-C chemokine receptor type 4 – CXCR4 – or fusin)	Alpha-chemokine receptor specific for stromal-derived factor-1 (SDF-1)	Osteosarcoma, synovial sarcoma	[60, 67]
CD117 (mast/stem cell growth factor receptor—SCFR; c-Kit proto-oncogene)	Receptor tyrosine kinase	Osteosarcoma	[59, 60, 68]
CD29 (integrin beta-1)	Adhesion molecule and extracellular matrix receptor	Osteosarcoma	[69]
CD49f (integrin alpha-6)	Adhesion molecule and extracellular matrix receptor	Osteosarcoma	[60]
STRO-1 (stromal cell precursor surface antigen)	Cell surface marker protein expressed on mesenchymal stem cells	Osteosarcoma	[59, 60, 68]
SSEA-4 (stage-specific embryonic antigen-4)	Glycosphingolipid expressed on embryonic stem cells	Osteosarcoma	[60]
CD57 (HNK1 - human natural killer-1 or LEU7)	Cell surface protein expressed on NK cells and neuroendocrine tumors	Ewing's sarcoma	[60]
LGR5 (leucine-rich repeat-containing G-protein-coupled receptor 5) also as G-protein-coupled receptor 49 (GPR49) or G-protein-coupled receptor 67 (GPR67)	Member of the Wnt signaling pathway; R-spondin receptor	Ewing's sarcoma	[60]

(continued)

Table 7.2 (continued)

Marker	Biological function	Sarcoma type	References
FGFR3 (fibroblast growth factor receptor 3) also as CD333	Receptor tyrosine kinase	Rhabdomyosarcoma	[60]
NANOG	Transcription factor involved in self-renewal of undifferentiated embryonic stem cells	Ewing's sarcoma, osteosarcoma, rhabdomyosarcoma	[60, 70, 71]
Sox2 also as SRY (sex-determining region Y)-box 2	Transcription factor involved in self-renewal of undifferentiated embryonic stem cells	Osteosarcoma, Ewing's sarcoma, rhabdomyosarcoma, synovial sarcoma	[60, 71]
Oct-4 (octamer-binding transcription factor 4) also as POU5F1	Transcription factor involved in self-renewal of undifferentiated embryonic stem cells	Osteosarcoma, Ewing's sarcoma, rhabdomyosarcoma	[60, 66, 70, 72]
CBX3 (chromobox protein homolog 3)	Component of heterochromatin, binds DNA and other proteins and receptors	Osteosarcoma	[73]
c-Myc	Transcription factor activating proliferation and apoptosis	Rhabdomyosarcoma	[71, 74]
Pax3 (paired box gene 3)	Transcription factor involved in muscle development	Rhabdomyosarcoma	[71, 75]
CD105 also as endoglin (ENG)	Involved in TGF-β signaling, cytoskeletal organization, and migration	Osteosarcoma	[76]
CD44	Cell surface glycoprotein expressed on mesenchymal stem cells important in cell-cell interactions and cell adhesion and migration; can interact with many ligands (HA, osteopontin, collagens, etc.)	Osteosarcoma	[69, 76]
CD146 also as melanoma cell adhesion molecule (MCAM) or cell surface glycoprotein MUC18	A surface glycoprotein involved in cell adhesion, a receptor for laminin alpha 4	Fibrosarcoma, undifferentiated pleomorphic sarcoma, osteosarcoma	[77]
ABCG2 (ATP-binding cassette subfamily G member 2)	Protein transporting various molecules across extra- and intracellular membranes	Osteosarcoma, undifferentiated pleomorphic sarcoma	[61]

(continued)

Table 7.2 (continued)

Marker	Biological function	Sarcoma type	References
ABCA5 (ATP-binding cassette, subfamily A member 5)	Protein transporting various molecules across extra- and intracellular membranes	Osteosarcoma	[73]
Side population (dye exclusion)	Multiple ABC efflux pumps, including ABCB1 and ABCG2	Osteosarcoma, Ewing's sarcoma, synovial sarcoma, undifferentiated pleomorphic sarcoma, fibrosarcoma	[59, 78, 79]

Genetic and Epigenetic Plasticity of Sarcoma Stem Cells

An obvious question is inasmuch stemness of potential sarcoma stem cells is a "heritage" from an initiated normal stem cell (in this case most probably a mesenchymal stem cell) or whether it results directly from the action of sarcoma oncogenes. Two karyotypically simple translocation-dependent sarcomas could be rather instrumental to illustrate the latter possibility.

Synovial sarcoma is initiated by t(X;18)(p11;q11) translocation, resulting in a fusion protein between SS18 (whose gene is located on chromosome 18) and one of the translocation partner proteins SS1, SS2, or, rarely, SS4 (collectively called SSX, encoded by multiple homologous genes located on chromosome X) [84]. It has been reported that synovial sarcoma cells, without any sorting or selection, exhibited a high degree of stemness: Clonogenicity (sarcosphere formation) and tumorigenicity were comparable to those achieved by stem cell marker sorted populations in other tumors [85]. The SS18-SSX chimeric proteins encompass several transcription regulatory and protein-protein interaction domains, but, notably, no DNA-binding domain. The actual notion is that SS18-SSX engages a plethora of protein interaction partners, leading to complex changes in gene expression and finally resulting in accentuated stemness. Well-documented protein-protein interaction takes place between SS18-SSX and epithelial-mesenchymal transition (EMT)-triggering transcription repressors Snail and Slug, which prevents their binding to the E-cadherin gene promoter and results in pseudoepithelial transdifferentiation observed in some synovial sarcomas [85a]. Many SS18-SSX interaction partners involve chromatin modifier proteins, with a complex epigenetic reprogramming as a direct consequence. For example, it has been reported that SS18-SS2 directly interacts with the Polycomb-group complex 1 components Bmi1 and Ring1B, resulting in Bmi1 destabilization and the consequent derepression of a large group of Polycomb-silenced developmental genes. SS18 itself is a component of the mSWI/SNF-BAF chromatin remodeling complex, and its replacement by SS18-SSX fusion oncoproteins leads to complex changes in gene expression, among others to the erasure of the repressive histone mark H3K27me3 at the *Sox-2* locus [86, 87].

Strikingly, both of these effects are achieved also by the EWS-FLI-1 fusion oncoprotein underlying Ewing sarcoma, but via different mechanisms. Unlike

SS18-SSX, EWS-FLI-1 acts on its own as a direct transcription factor, via the ETS-DNA-binding domain supplied by the FLI-1 translocation partner [88]. According to recent results, EWS-FLI-1 can directly compete with the Polycomb repressor complex 1 (or, more probably, transcription factors mediating its recruitment, like YY-1) for binding to particular loci – notably certain *HOX* genes, especially posterior *HOXD* genes – resulting in their derepression [89]. In addition, it likely acts as both direct and indirect activator of Sox-2. This latter regulatory function is based on its direct transcriptional repression of miRNA145, encoded by a p53-responsive gene and directly targeting Sox-2 (as well as Oct-4). Intriguingly, EWS-FLI-1 is itself a target of miRNA145-mediated silencing, its repression thus stabilizing EWS-FLI-1 itself as well, a regulatory circuit already described for the relationship between Oct-4 and miRNA145 in embryonic stem cells [20].

Not surprisingly, all the epigenetic regulations crucially depend on the entire regulatory context resulting from signals acting on the cell. In the above-discussed experimental analyses of both synovial sarcoma and Ewing sarcoma, variations in cell culture media played important roles. In vivo, such a regulatory context would probably differ from cell to cell, generating a heterogeneous cell population with variable expressions of stemness traits in each individual sarcoma cell.

What is the situation in karyotypically complex sarcomas? As already mentioned above, dedifferentiated liposarcoma is an example of tumor type with an unusually high degree of genetic and epigenetic instability. This instability manifests at all thinkable levels. Karyotypic instability is mainly represented by neochromosomes, giant or ring chromosomes accumulating amplified segments of various chromosomes. Their origin is not clear, but the consensus is that they are triggered by the originally extrachromosomal amplification of a specific amplicon at 12q. Among the genes amplified are *MDM2* (coding for a direct p53 inhibitor, as mentioned above), *CDK4*, and *YEATS2* (coding for an acetylated and crotonylated histone reader). Via repeated breakage-fusion-bridge cycles, the 12q amplicon triggers a progressive genome destabilization, including structural chromosomal aberrations [90]. Notable among them is the translocation between *HMGA2* and *CPM* genes. *HMGA2* codes for a nonhistone chromatin protein involved in global gene expression regulation. The translocation removes the 3′-part of the *HMGA2* gene, resulting in two principal effects. First, it leads to the production of a shortened protein, and, second, because the removed 3′-part of the gene contains at least three target sequences for the let-7 miRNA, this shortened HMGA2 protein is grossly overexpressed [91]. Intact HMGA2 expressed at a normal level promotes adipogenic differentiation; an overexpressed full-length or shortened protein abolishes it instead, however. In addition, overexpressed HMGA2 has particular gene expression consequences. Among the genes it specifically induces, prominent is the *SS1*, one of the synovial sarcoma translocation partners (see above), eventually promoting stemness [92]. Copy number alterations in dedifferentiated liposarcoma underlie the overexpression of some additional genes with presumed roles in stemness (*c-JUN* oncogene, mesenchymal stem cell factor gene *TUFT1*) or chromatin organization (heterochromatin factor gene *CBX1*) [90]. There can also be more traditional epigenetic aberrations, like the promoter hypermethylation of the gene encoding the

key adipogenic transcription factor C/EBPα or of the *miRNA193b* gene [93]. One of the miRNA193b targets is the fatty acid synthase – an important cancer metabolic enzyme that (as described for leiomyosarcoma) at the same time interacts with various histone modification enzymes and modulates their activity [94], producing a sort of feed-forward loop in epigenome destabilization. Last but not the least, some point mutations found in liposarcoma can produce similarly widespread epigenetic consequences to those caused by more extensive changes described above. About 8% of dedifferentiated liposarcoma cases harbor point mutations (mostly missense) in the gene encoding histone deacetylase 1 [93]; striking in this respect is the finding that HDAC inhibitors might specifically target sarcoma stem cells (as described for the osteosarcoma model) [95].

These various mechanisms of dedifferentiated liposarcoma genome instability create an unprecedented level of genetic and epigenetic plasticity and impacts numerous genes implicated in differentiation and stemness regulation. This situation sets a completely new stage for research on cancer stem cell heterogeneity. Traditionally, it has automatically been assumed that a cancer stem cell achieves its stemness either from an initially mutated normal stem cell or as the direct molecular consequence of an initiating mutation. Once established, cancer stemness can be passed to some daughter cells, resulting in a more or less stable cancer stem cell pool, and it can be lost only by differentiation. Isolated populations of cancer stem cells, like side population cells or stem cell marker sorted cells, thus provide quasi-pure stem cells, but for a certain time only – until they are diluted by differentiation. In the context of the huge genetic and epigenetic plasticity, like that found in dedifferentiated liposarcoma, stemness might be understood in a completely different way. Stem cells might correspond simply to cells that at a given moment accumulate a sufficient number of stemness-promoting and differentiation-inhibiting mutations and epigenetic changes; in other words, stemness can be understood as a defined actual functional state rather than a quasi-fixed cell type. Some of such stem cells may differentiate, others can simply lose their stemness-promoting and differentiation-inhibiting genetic and epigenetic changes as a direct consequence of genetic and epigenetic plasticity, and still others, originally non-stem cells, can regain these changes by the same token. Stem and non-stem cells are thus continuously and bidirectionally changing, mixing, and merging.

Microenvironmental Influence on Sarcoma Stem Cells

All the discussion on sarcoma stem cells pursued by now concentrated largely on cell-autonomous mechanisms. We know, however, that tissue homeostasis is regulated by the cross talk between tissue-specific stem cells and their microenvironment, and, in a similar way, signaling from tumor niches may play relevant roles in the regulation of sarcoma stem cells [96–98]. Among the different subtypes of sarcoma, the relevance of the interaction between microenvironmental components and cancer (stem) cells has been especially well described in osteosarcoma [99].

Osteosarcoma cells closely interact with local microenvironmental cell types, such as stromal cells (MSCs and cancer-associated fibroblasts), osteoblasts, osteocytes, osteoclasts, or chondrocytes, as well as with immune infiltrates mainly composed of T lymphocytes and macrophages [97, 100]. The interaction between these multiple players results in the production of signaling factors that contribute to either favoring or decrease of stemness properties in osteosarcoma [97]. Thus, signaling mediated by fibroblastic growth factor (FGF)-Sox2 axis [101], transforming growth factor β (TGF-β) [102], the Hippo signaling regulator YAP1 [103], or NOTCH1 [40], among others, was reported to promote stemness in osteosarcoma. On the other hand, signals with proven pro-osteogenic activities, like those dependent on bone morphogenetic proteins (BMP) [104] or WNT factors [101], seem to decrease sarcoma stem cell frequency and to promote osteogenic differentiation. In addition, extracellular matrix components of the tumor microenvironment have also been reported to interact with sarcoma stem cells. This is the case of hyaluronan, which may promote stemness properties in tumor cells through the binding with its receptor, the cancer stem cell marker CD44 ([105] – see Table 7.2). We can assume that details of composition of this complex tumor microenvironment differ in each individual tumor, resulting in a wide spectrum of osteosarcoma stemness modulation.

Notice that within the context of osteosarcoma (and possibly other sarcoma types as well), MSCs can thus be viewed not only as possible cells of origin but also as a stromal supporting type. Indeed, MSCs are the cell type with rather precisely described interactions with osteosarcoma stem cell subpopulations. MSCs may be activated by the acidic conditions generated by osteosarcoma cells and these tumor-conditioned MSCs favor osteosarcoma stemness and chemoresistance via IL6-NF-κB signaling [106]. Moreover, MSCs may increase chemoresistance of osteosarcoma cells through the activation of IL6/STAT3 pathway [107].

Several locations within the bone microenvironment where pro-stemness signaling is particularly active have been proposed as suitable niches for osteosarcoma stem cells [96] (Fig. 7.2): (i) the perivascular niche, which was described as the most likely location for the most immature MSCs and therefore may also constitute a niche for sarcoma stem cells originated by transformed MSCs [108]; (ii) the hypoxic niche, which is an important stemness-promoting environmental condition in bones [109]; and (iii) the endosteal niche, which is a signal-rich environment where tumor cells interfere with the bone remodeling process, establishing a "vicious cycle" that favors osteoclast-mediated osteolysis and the subsequent release of calcium and growth factors (FGF, TGF-β, IGF1, BMP, etc.), which support stem and tumorigenic properties [97]. In any case, these three prototypical osteosarcoma niche types differ in their detailed molecular mechanisms of stem cell support, plausibly resulting in a niche-dependent osteosarcoma stem cell heterogeneity.

The detailed knowledge of the microenvironment in maintaining tumor homeostasis has encouraged the development and testing of therapies aimed to counteract pro-tumoral signals, including pro-stemness signals, from the microenvironment [96]. Consequently, several therapeutic strategies have been recently developed to target the role of the tumor-promoting osteoclast activity [110, 111], to reduce the vascularization of tumors [112], and to enhance the immune response against tumors [113, 114].
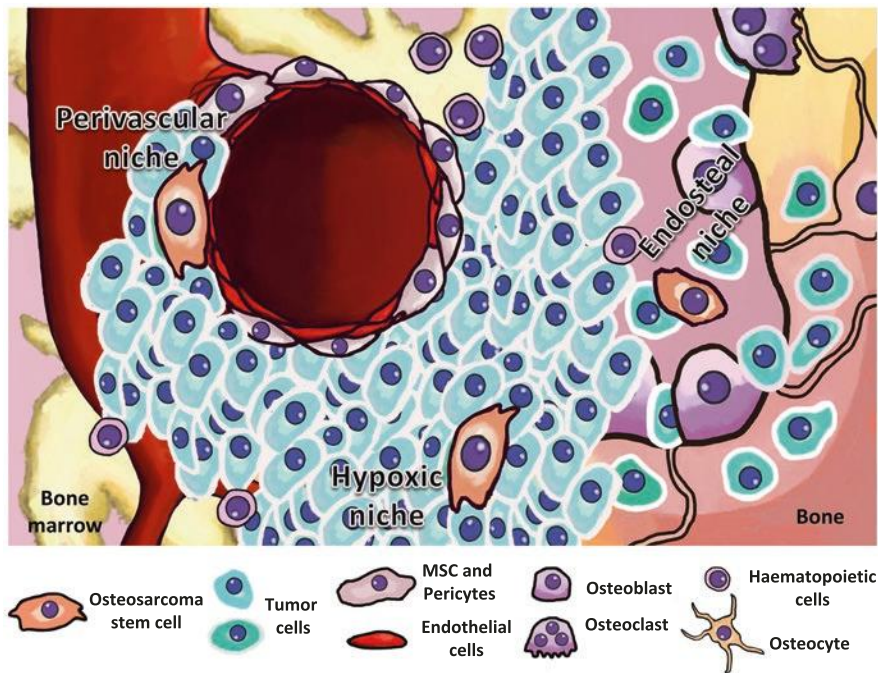
Fig. 7.2 Osteosarcoma stem cell niches. Figure shows the most relevant cell types of the bone microenvironment that may interact with osteosarcoma cells. Suggested locations for osteosarcoma stem cells include the perivascular niche, the endosteal niche, and the areas of poor vascularization (hypoxic niche) (adapted from [96]

References

1. Skubitz KM, D'Adamo DR (2007) Sarcoma. Mayo Clin Proc 82(11):1409–1432
2. Penzel R, Schirmacher P, Renner M, Mechtersheimer G (2011) Molekularpathologie maligner Weichgewebetumoren. In: Schlag PM, Hartmann JT, Budach V (eds) Weichgewebetumoren: Interdisziplinäres Management. Springer, Berlin Heidelberg, Berlin, Heidelberg, pp 23–35
3. Oda Y, Yamamoto H, Kohashi K, Yamada Y, Iura K, Ishii T, Maekawa A, Bekki H (2017) Soft tissue sarcomas: from a morphological to a molecular biological approach. Pathol Int 67(9):435–446
4. Taylor BS, Barretina J, Maki RG, Antonescu CR, Singer S, Ladanyi M (2011a) Advances in sarcoma genomics and new therapeutic targets. Nat Rev Cancer 11(8):541–557

5. Henze J, Bauer S (2013) Liposarcomas. Hematol Oncol Clin North Am 27(5):939–955
6. Papenfuss AT, Thomas DM (2015) The life history of neochromosomes revealed. Mol Cell Oncol 2(4):e1000698
7. Frenette PS, Pinho S, Lucas D, Scheiermann C (2013) Mesenchymal stem cell: keystone of the hematopoietic stem cell niche and a stepping-stone for regenerative medicine. Annu Rev Immunol 31:285–316
8. Schäfer R, Northoff H (2008) Characteristics of mesenchymal stem cells—new stars in regenerative medicine or unrecognized old fellows in autologous regeneration? Transfus Med Hemotherapy 35(3):154–159
9. Guneta V, Tan NS, Chan SKJ, Tanavde V, Lim TC, Wong TCM, Choong C (2016) Comparative study of adipose-derived stem cells and bone marrow-derived stem cells in similar microenvironmental conditions. Exp Cell Res 348(2):155–164
10. Meyer MB, Benkusky NA, Sen B, Rubin J, Pike JW (2016) Epigenetic plasticity drives adipogenic and osteogenic differentiation of marrow-derived mesenchymal stem cells. J Biol Chem 291(34):17,829–17,847
11. Bianco P, Robey PG (2015) Skeletal stem cells. Development 142(6):1023–1027
12. Dinulovic I, Furrer R, Handschin C (2017) Plasticity of the muscle stem cell microenvironment. Adv Exp Med Biol 1041:141–169
13. Shakhova O, Sommer L (2010) Neural crest-derived stem cells. In: The Stem Cell Research Community (ed) StemBook. Harvard Stem Cell Institute, Cambridge, MA
14. Almalki SG, Agrawal DK (2016) Key transcription factors in the differentiation of mesenchymal stem cells. Differ Res Biol Divers 92(1–2):41–51
15. Rivlin N, Koifman G, Rotter V (2015) p53 orchestrates between normal differentiation and cancer. Semin Cancer Biol 32:10–17
16. Chen WY, Wang DH, Yen RC, Luo J, Gu W, Baylin SB (2005) Tumor suppressor HIC1 directly regulates SIRT1 to modulate p53-dependent DNA-damage responses. Cell 123(3):437–448
17. Yamakuchi M, Lowenstein CJ (2009) miR-34, SIRT1 and p53: the feedback loop. Cell Cycle 8:712–715
18. Goeman F, Strano S, Blandino G (2017) MicroRNAs as key effectors in the p53 network. Int Rev Cell Mol Biol 333:51–90
19. Luo Z, Cui R, Tili E, Croce C (2018) Friend or foe: microRNAs in the p53 network. Cancer Lett 419:96–102
20. Riggi N, Suvà M-L, De Vito C, Provero P, Stehle J-C, Baumer K, Cironi L, Janiszewska M, Petricevic T, Suvà D, Tercier S, Joseph J-M, Guillou L, Stamenkovic I (2010) EWS-FLI-1 modulates miRNA145 and SOX2 expression to initiate mesenchymal stem cell reprogramming toward Ewing sarcoma cancer stem cells. Genes Dev 24(9):916–932
21. Han M-K, Song E-K, Guo Y, Ou X, Mantel C, Broxmeyer HE (2008) SIRT1 regulates apoptosis and Nanog expression in mouse embryonic stem cells by controlling p53 subcellular localization. Cell Stem Cell 2(3):241–251
22. Yoon DS, Choi Y, Jang Y, Lee M, Choi WJ, Kim S-H, Lee JW (2014) SIRT1 directly regulates SOX2 to maintain self-renewal and multipotency in bone marrow-derived mesenchymal stem cells. Stem Cells 32(12):3219–3231
23. Vilas JM, Ferreirós A, Carneiro C, Morey L, Silva-Álvarez SD, Fernandes T, Abad M, Croce LD, García-Caballero T, Serrano M, Rivas C, Vidal A, Collado M (2014) Transcriptional regulation of Sox2 by the retinoblastoma family of pocket proteins. Oncotarget 6(5):2992–3002
24. Boregowda SV, Krishnappa V, Strivelli J, Haga CL, Booker CN, Phinney DG (2018) Basal p53 expression is indispensable for mesenchymal stem cell integrity. Cell Death Differ 25(4):677–690
25. Artigas N, Gámez B, Cubillos-Rojas M, Sánchez-de Diego C, Valer JA, Pons G, Rosa JL, Ventura F (2017) p53 inhibits SP7/Osterix activity in the transcriptional program of osteoblast differentiation. Cell Death Differ 24(12):2022–2031
26. Martinez-Sanchez A, Dudek KA, Murphy CL (2012) Regulation of human chondrocyte function through direct inhibition of cartilage master regulator SOX9 by microRNA-145 (miRNA-145). J Biol Chem 287(2):916–924

27. Honoki K, Tsujiuchi T (2013) Senescence bypass in mesenchymal stem cells: a potential pathogenesis and implications of pro-senescence therapy in sarcomas. Expert Rev Anticancer Ther 13(8):983–996

28. Matushansky I, Hernando E, Socci ND, Mills JE, Matos TA, Edgar MA, Singer S, Maki RG, Cordon-Cardo C (2007) Derivation of sarcomas from mesenchymal stem cells via inactivation of the Wnt pathway. J Clin Invest 117(11):3248–3257

29. Kim JR, Moon YJ, Kwon KS, Bae JS, Wagle S, Yu TK, Kim KM, Park HS, Lee J-H, Moon WS, Lee H, Chung MJ, Jang KY (2013) Expression of SIRT1 and DBC1 is associated with poor prognosis of soft tissue sarcomas. PLoS One 8(9):e74738

30. Skoda J, Nunukova A, Loja T, Zambo I, Neradil J, Mudry P, Zitterbart K, Hermanova M, Hampl A, Sterba J, Veselska R (2016) Cancer stem cell markers in pediatric sarcomas: Sox2 is associated with tumorigenicity in immunodeficient mice. Tumour Biol 37(7):9535–9548

31. Plon SE, Malkin D (2010) Childhood cancer and heredity. In: Principles and practice of pediatric oncology, Sixth edition. LWW, Philadelphia, PA, pp 17–37

32. Kanojia D, Nagata Y, Garg M, Lee DH, Sato A, Yoshida K, Sato Y, Sanada M, Mayakonda A, Bartenhagen C, Klein H-U, Doan NB, Said JW, Mohith S, Gunasekar S, Shiraishi Y, Chiba K, Tanaka H, Miyano S, Myklebost O, Yang H, Dugas M, Meza-Zepeda LA, Silberman AW, Forscher C, Tyner JW, Ogawa S, Koeffler HP (2015) Genomic landscape of liposarcoma. Oncotarget 6(40):42,429–42,444

33. Hatina J, Hájková L, Peychl J, Rudolf E, Fínek J, Cervinka M, Reischig J (2003) Establishment and characterization of clonal cell lines derived from a fibrosarcoma of the H2-K/V-JUN transgenic mouse. A model of H2-K/V-JUN mediated tumorigenesis. Tumour Biol 24(4):176–184

34. Mariani O, Brennetot C, Coindre J-M, Gruel N, Ganem C, Delattre O, Stern M-H, Aurias A (2007) JUN oncogene amplification and overexpression block adipocytic differentiation in highly aggressive sarcomas. Cancer Cell 11(4):361–374

34a. Endo M, Nishita M, Fujii M, Minami Y (2015) Insight into the role of Wnt5a-induced signaling in normal and cancer cells. Int Rev Cell Mol Biol 314:117–148

35. Lye KL, Nordin N, Vidyadaran S, Thilakavathy K (2016) Mesenchymal stem cells: from stem cells to sarcomas. Cell Biol Int 40(6):610–618

36. Gaebler M, Silvestri A, Haybaeck J, Reichardt P, Lowery CD, Stancato LF, Zybarth G, Regenbrecht CRA (2017) Three-dimensional patient-derived in vitro sarcoma models: Promising tools for improving clinical tumor management. Front Oncol 7:203

37. Xiao W, Mohseny AB, Hogendoorn PCW, Cleton-Jansen A-M (2013) Mesenchymal stem cell transformation and sarcoma genesis. Clin Sarcoma Res 3(1):10

38. Hahn WC, Counter CM, Lundberg AS, Beijersbergen RL, Brooks MW, Weinberg RA (1999) Creation of human tumour cells with defined genetic elements. Nature 400(6743):464–468

39. Rubio R, Gutierrez-Aranda I, Sáez-Castillo AI, Labarga A, Rosu-Myles M, Gonzalez-Garcia S, Toribio ML, Menendez P, Rodriguez R (2013) The differentiation stage of p53-Rb-deficient bone marrow mesenchymal stem cells imposes the phenotype of in vivo sarcoma development. Oncogene 32(41):4970–4980

40. Tao J, Jiang M-M, Jiang L, Salvo JS, Zeng H-C, Dawson B, Bertin TK, Rao PH, Chen R, Donehower LA, Gannon F, Lee BH (2014) Notch activation as a driver of osteogenic sarcoma. Cancer Cell 26(3):390–401

41. Engström K, Willén H, Kåbjörn-Gustafsson C, Andersson C, Olsson M, Göransson M, Järnum S, Olofsson A, Warnhammar E, Aman P (2006) The myxoid/round cell liposarcoma fusion oncogene FUS-DDIT3 and the normal DDIT3 induce a liposarcoma phenotype in transfected human fibrosarcoma cells. Am J Pathol 168(5):1642–1653

42. Morena D, Maestro N, Bersani F, Forni PE, Lingua MF, Foglizzo V, Šćepanović P, Miretti S, Morotti A, Shern JF, Khan J, Ala U, Provero P, Sala V, Crepaldi T, Gasparini P, Casanova M, Ferrari A, Sozzi G, Chiarle R, Ponzetto C, Taulli R (2016) Hepatocyte growth factor-mediated satellite cells niche perturbation promotes development of distinct sarcoma subtypes. Elife 5:pii: e12116

43. Rubin BP, Nishijo K, Chen H-IH, Yi X, Schuetze DP, Pal R, Prajapati SI, Abraham J, Arenkiel BR, Chen Q-R, Davis S, McCleish AT, Capecchi MR, Michalek JE, Zarzabal LA, Khan J, Yu Z, Parham DM, Barr FG, Meltzer PS, Chen Y, Keller C (2011) Evidence for an unanticipated relationship between undifferentiated pleomorphic sarcoma and embryonal rhabdomyosarcoma. Cancer Cell 19(2):177–191

44. Boeuf S, Kunz P, Hennig T, Lehner B, Hogendoorn P, Bovée J, Richter W (2008) A chondrogenic gene expression signature in mesenchymal stem cells is a classifier of conventional central chondrosarcoma. J Pathol 216(2):158–166

45. Matushansky I, Hernando E, Socci ND, Matos T, Mills J, Edgar MA, Schwartz GK, Singer S, Cordon-Cardo C, Maki RG (2008) A developmental model of sarcomagenesis defines a differentiation-based classification for liposarcomas. Am J Pathol 172(4):1069–1080

46. Borgo C, Milan G, Favaretto F, Stasi F, Fabris R, Salizzato V, Cesaro L, Belligoli A, Sanna M, Foletto M, Prevedello L, Vindigni V, Bardini R, Donella-Deana A, Vettor R (2017) CK2 modulates adipocyte insulin-signaling and is up-regulated in human obesity. Sci Rep 7(1):17,569

47. Funes JM, Quintero M, Henderson S, Martinez D, Qureshi U, Westwood C, Clements MO, Bourboulia D, Pedley RB, Moncada S, Boshoff C (2007) Transformation of human mesenchymal stem cells increases their dependency on oxidative phosphorylation for energy production. Proc Natl Acad Sci U S A 104(15):6223–6228

48. Rodriguez R, Rubio R, Menendez P (2012) Modeling sarcomagenesis using multipotent mesenchymal stem cells. Cell Res 22(1):62–77

49. Schulz W (2005) Molecular biology of human cancers: an advanced student's textbook. Springer, Netherlands

50. Rodriguez R, Tornin J, Suarez C, Astudillo A, Rubio R, Yauk C, Williams A, Rosu-Myles M, Funes JM, Boshoff C, Menendez P (2013) Expression of FUS-CHOP fusion protein in immortalized/transformed human mesenchymal stem cells drives mixoid liposarcoma formation. Stem Cells 31(10):2061–2072

51. Li H, Fan X, Kovi RC, Jo Y, Moquin B, Konz R, Stoicov C, Kurt-Jones E, Grossman SR, Lyle S, Rogers AB, Montrose M, Houghton J (2007) Spontaneous expression of embryonic factors and p53 point mutations in aged mesenchymal stem cells: a model of age-related tumorigenesis in mice. Cancer Res 67(22):10,889–10,898

52. Shimizu T, Ishikawa T, Sugihara E, Kuninaka S, Miyamoto T, Mabuchi Y, Matsuzaki Y, Tsunoda T, Miya F, Morioka H, Nakayama R, Kobayashi E, Toyama Y, Kawai A, Ichikawa H, Hasegawa T, Okada S, Ito T, Ikeda Y, Suda T, Saya H (2010) c-MYC overexpression with loss of Ink4a/Arf transforms bone marrow stromal cells into osteosarcoma accompanied by loss of adipogenesis. Oncogene 29(42):5687–5699

53. Lin PP, Pandey MK, Jin F, Raymond AK, Akiyama H, Lozano G (2009) Targeted mutation of p53 and Rb in mesenchymal cells of the limb bud produces sarcomas in mice. Carcinogenesis 30(10):1789–1795

54. Lin PP, Pandey MK, Jin F, Xiong S, Deavers M, Parant JM, Lozano G (2008) EWS-FLI1 induces developmental abnormalities and accelerates sarcoma formation in a transgenic mouse model. Cancer Res 68(21):8968–8975

55. Riggi N, Suvà M-L, Suvà D, Cironi L, Provero P, Tercier S, Joseph J-M, Stehle J-C, Baumer K, Kindler V, Stamenkovic I (2008) EWS-FLI-1 expression triggers a Ewing's sarcoma initiation program in primary human mesenchymal stem cells. Cancer Res 68(7):2176–2185

56. von Levetzow C, Jiang X, Gwye Y, von Levetzow G, Hung L, Cooper A, Hsu JH-R, Lawlor ER (2011) Modeling initiation of Ewing sarcoma in human neural crest cells. PLoS One 6(4):e19305

57. Mihály D, Matula Z, Changchien Y-C, Papp G, Tátrai P, Sápi Z (2017) First cloned human immortalized adipose derived mesenchymal stem-cell line with chimeric SS18-SSX1 gene (SS-iASC). Cancer Genet 216-217:52–60

58. Tamaki S, Fukuta M, Sekiguchi K, Jin Y, Nagata S, Hayakawa K, Hineno S, Okamoto T, Watanabe M, Woltjen K, Ikeya M, Jr TK, Toguchida J (2015) SS18-SSX, the oncogenic fusion protein in synovial sarcoma, is a cellular context-dependent epigenetic modifier. PLoS One 10(11):e0142991

59. Dela Cruz FS (2013) Cancer stem cells in pediatric sarcomas. Front Oncol 3:168
60. Skoda J, Veselska R (2018) Cancer stem cells in sarcomas: getting to the stemness core. Biochim Biophys Acta 1862(10):2134–2139
61. Veselska R, Skoda J, Neradil J (2012) Detection of cancer stem cell markers in sarcomas. Klin Onkol 25(Suppl 2):2S16–2S20
62. Wu C, Wei Q, Utomo V, Nadesan P, Whetstone H, Kandel R, Wunder JS, Alman BA (2007) Side population cells isolated from mesenchymal neoplasms have tumor initiating potential. Cancer Res 67(17):8216–8222
63. Zhou Y, Zhou Y, Chen D, Chen D, Qi Y, Qi Y, Liu R, Liu R, Li S, Li S, Zou H, Zou H, Lan J, Lan J, Ju X, Ju X, Jiang J, Jiang J, Liang W, Liang W, Shen Y, Shen Y, Pang L, Pang L, Li F, Li F (2017) Evaluation of expression of cancer stem cell markers and fusion gene in synovial sarcoma: insights into histogenesis and pathogenesis. Oncol Rep 37(6):3351–3360
64. Lohberger B, Rinner B, Stuendl N, Absenger M, Liegl-Atzwanger B, Walzer SM, Windhager R, Leithner A (2012) Aldehyde dehydrogenase 1, a potential marker for cancer stem cells in human sarcoma. PLoS One 7(8):e43664
65. Martinez-Cruzado L, Tornin J, Santos L, Rodriguez A, García-Castro J, Morís F, Rodriguez R (2016) Aldh1 expression and activity increase during tumor evolution in sarcoma cancer stem cell populations. Sci Rep 6:27,878
66. Siclari VA, Qin L (2010) Targeting the osteosarcoma cancer stem cell. J Orthop Surg 5(1):78
67. Kimura T, Wang L, Tabu K, Tsuda M, Tanino M, Maekawa A, Nishihara H, Hiraga H, Taga T, Oda Y, Tanaka S (2015) Identification and analysis of CXCR4-positive synovial sarcoma-initiating cells. Oncogene 35(30):3932–3943
68. Adhikari AS, Agarwal N, Wood BM, Porretta C, Ruiz B, Pochampally RR, Iwakuma T (2010) CD117 and Stro-1 identify osteosarcoma tumor-initiating cells associated with metastasis and drug resistance. Cancer Res 70(11):4602–4612
69. Tirino V, Desiderio V, Paino F, De Rosa A, Papaccio F, Fazioli F, Pirozzi G, Papaccio G (2011) Human primary bone sarcomas contain CD133+ cancer stem cells displaying high tumorigenicity in vivo. FASEB J 25(6):2022–2030
70. Suvà M-L, Riggi N, Stehle J-C, Baumer K, Tercier S, Joseph J-M, Suvà D, Clément V, Provero P, Cironi L, Osterheld M-C, Guillou L, Stamenkovic I (2009) Identification of cancer stem cells in Ewing's sarcoma. Cancer Res 69(5):1776–1781
71. Walter D, Satheesha S, Albrecht P, Bornhauser BC, D'Alessandro V, Oesch SM, Rehrauer H, Leuschner I, Koscielniak E, Gengler C, Moch H, Bernasconi M, Niggli FK, Schäfer BW, CWS Study Group (2011) CD133 positive embryonal rhabdomyosarcoma stem-like cell population is enriched in rhabdospheres. PLoS One 6(5):e19506
72. Levings PP, McGarry SV, Currie TP, Nickerson DM, McClellan S, Ghivizzani SC, Steindler DA, Gibbs CP (2009) Expression of an exogenous human Oct-4 promoter identifies tumor-initiating cells in osteosarcoma. Cancer Res 69(14):5648–5655
73. Saini V, Hose CD, Monks A, Nagashima K, Han B, Newton DL, Millione A, Shah J, Hollingshead MG, Hite KM, Burkett MW, Delosh RM, Silvers TE, Scudiero DA, Shoemaker RH (2012) Identification of CBX3 and ABCA5 as putative biomarkers for tumor stem cells in osteosarcoma. PLoS One 7(8):e41401
74. Yang J, Ren Z, Du X, Hao M, Zhou W (2014) The role of mesenchymal stem/progenitor cells in sarcoma: update and dispute. Stem Cell Investig 1:18
75. Zhang L, Wang C (2007) Identification of a new class of PAX3-FKHR target promoters: a role of the Pax3 paired box DNA binding domain. Oncogene 26(11):1595–1605
76. Gibbs CP, Kukekov VG, Reith JD, Tchigrinova O, Suslov ON, Scott EW, Ghivizzani SC, Ignatova TN, Steindler DA (2005) Stem-like cells in bone sarcomas: implications for tumorigenesis. Neoplasia 7(11):967–976
77. Wei Q, Tang YJ, Voisin V, Sato S, Hirata M, Whetstone H, Han I, Ailles L, Bader GD, Wunder J, Alman BA (2015) Identification of CD146 as a marker enriched for tumor-propagating capacity reveals targetable pathways in primary human sarcoma. Oncotarget 6(37):40,283–40,294
78. Trucco M, Loeb D (2012) Sarcoma stem cells: do we know what we are looking for? Sarcoma 2012:291705

79. Wang M-Y, Nestvold J, Rekdal Ø, Kvalheim G, Fodstad Ø (2017) A novel rat fibrosarcoma cell line from transformed bone marrow-derived mesenchymal stem cells with maintained in vitro and in vivo stemness properties. Exp Cell Res 352(2):218–224

80. Fujiwara T, Kawai A, Yoshida A, Ozaki T, Ochiya T (2013) Cancer stem cells of sarcoma. In: Role of cancer stem cells in cancer biology and therapy. CRC Press, Boca Raton, FL, pp 23–78

81. Hatina J, Fernandes MI, Hoffmann MJ, Zeimet AG (2013) Cancer stem cells – basic biological properties and experimental approaches. Encyclopedia of Life Sciences. Chichester, John Wiley & Sons. https://doi.org/10.1002/9780470015902.a0021164.pub2

82. Krause U, Ryan DM, Clough BH, Gregory CA (2014) An unexpected role for a Wnt-inhibitor: Dickkopf-1 triggers a novel cancer survival mechanism through modulation of aldehyde-dehydrogenase-1 activity. Cell Death Dis 5:e1093

83. Martinez-Cruzado L, Tornin J, Rodriguez A, Santos L, Allonca E, Fernandez-Garcia MT, Astudillo A, Garcia-Pedrero JM, Rodriguez R (2017) Trabectedin and campthotecin synergistically eliminate cancer stem cells in cell-of-origin sarcoma models. Neoplasia 19(6): 460–470

84. Stacchiotti S, Van Tine BA (2017) Synovial sarcoma: current concepts and future perspectives. J Clin Oncol 36(2):180–187

85. Naka N, Takenaka S, Araki N, Miwa T, Hashimoto N, Yoshioka K, Joyama S, Hamada K-I, Tsukamoto Y, Tomita Y, Ueda T, Yoshikawa H, Itoh K (2010) Synovial sarcoma is a stem cell malignancy. Stem Cells 28(7):1119–1131

85a. Saito T, Nagai M, Ladanyi M (2006) SYT-SSX1 and SYT-SSX2 interfere with repression of E-cadherin by snail and slug: a potential mechanism for aberrant mesenchymal to epithelial transition in human synovial sarcoma. Cancer Res 66(14):6919–6927

86. Eid JE, Garcia CB (2015) Reprogramming of mesenchymal stem cells by oncogenes. Semin Cancer Biol 32:18–31

87. Zöllner SK, Rössig C, Toretsky JA (2015) Synovial sarcoma is a gateway to the role of chromatin remodeling in cancer. Cancer Metastasis Rev 34(3):417–428

88. Jedlicka P (2010) Ewing Sarcoma, an enigmatic malignancy of likely progenitor cell origin, driven by transcription factor oncogenic fusions. Int J Clin Exp Pathol 3(4):338–347

89. Svoboda LK, Harris A, Bailey NJ, Schwentner R, Tomazou E, von Levetzow C, Magnuson B, Ljungman M, Kovar H, Lawlor ER (2014) Overexpression of HOX genes is prevalent in Ewing sarcoma and is associated with altered epigenetic regulation of developmental transcription programs. Epigenetics 9(12):1613–1625

90. Beird HC, Wu C-C, Ingram DR, Wang W-L, Alimohamed A, Gumbs C, Little L, Song X, Feig BW, Roland CL, Zhang J, Benjamin RS, Hwu P, Lazar AJ, Futreal PA, Somaiah N (2018) Genomic profiling of dedifferentiated liposarcoma compared to matched well-differentiated liposarcoma reveals higher genomic complexity and a common origin. Cold Spring Harb Mol Case Stud 4(2):pii:a002386

91. Mayr C, Hemann MT, Bartel DP (2007) Disrupting the pairing between let-7 and Hmga2 enhances oncogenic transformation. Science 315(5818):1576–1579

92. Henriksen J, Stabell M, Meza-Zepeda LA, Lauvrak SA, Kassem M, Myklebost O (2010) Identification of target genes for wild type and truncated HMGA2 in mesenchymal stem-like cells. BMC Cancer 10:329

93. Taylor BS, DeCarolis PL, Angeles CV, Brenet F, Schultz N, Antonescu CR, Scandura JM, Sander C, Viale AJ, Socci ND, Singer S (2011b) Frequent alterations and epigenetic silencing of differentiation pathway genes in structurally rearranged liposarcomas. Cancer Discov 1(7):587–597

94. Guan M, Wu X, Chu P, Chow WA (2017) Fatty acid synthase reprograms the epigenome in uterine leiomyosarcomas. PLoS One 12(6):e0179692

95. Di Pompo G, Salerno M, Rotili D, Valente S, Zwergel C, Avnet S, Lattanzi G, Baldini N, Mai A (2015) Novel histone deacetylase inhibitors induce growth arrest, apoptosis, and differentiation in sarcoma cancer stem cells. J Med Chem 58(9):4073–4079

96. Abarrategi A, Tornin J, Martinez-Cruzado L, Hamilton A, Martinez-Campos E, Rodrigo JP, González MV, Baldini N, Garcia-Castro J, Rodriguez R (2016) Osteosarcoma: cells-of-origin, cancer stem cells, and targeted therapies. Stem Cells Int 2016:3631764

97. Alfranca A, Martinez-Cruzado L, Tornin J, Abarrategi A, Amaral T, de Alava E, Menendez P, Garcia-Castro J, Rodriguez R (2015) Bone microenvironment signals in osteosarcoma development. Cell Mol Life Sci 72(16):3097–3113

98. Plaks V, Kong N, Werb Z (2015) The cancer stem cell niche: how essential is the niche in regulating stemness of tumor cells? Cell Stem Cell 16(3):225–238

99. Rubio R, Abarrategi A, Garcia-Castro J, Martinez-Cruzado L, Suarez C, Tornin J, Santos L, Astudillo A, Colmenero I, Mulero F, Rosu-Myles M, Menendez P, Rodriguez R (2014) Bone environment is essential for osteosarcoma development from transformed mesenchymal stem cells. Stem Cells 32(5):1136–1148

100. Heymann M-F, Lézot F, Heymann D (2017) The contribution of immune infiltrates and the local microenvironment in the pathogenesis of osteosarcoma. Cell Immunol (17):30,189–30,182

101. Basu-Roy U, Seo E, Ramanathapuram L, Rapp TB, Perry JA, Orkin SH, Mansukhani A, Basilico C (2012) Sox2 maintains self renewal of tumor-initiating cells in osteosarcomas. Oncogene 31(18):2270–2282

102. Zhang H, Wu H, Zheng J, Yu P, Xu L, Jiang P, Gao J, Wang H, Zhang Y (2013) Transforming growth factor β1 signal is crucial for dedifferentiation of cancer cells to cancer stem cells in osteosarcoma. Stem Cells 31(3):433–446

103. Basu-Roy U, Bayin NS, Rattanakorn K, Han E, Placantonakis DG, Mansukhani A, Basilico C (2015) Sox2 antagonizes the Hippo pathway to maintain stemness in cancer cells. Nat Commun 6:6411

104. Wang L, Park P, Zhang H, La Marca F, Claeson A, Valdivia J, Lin C-Y (2011) BMP-2 inhibits the tumorigenicity of cancer stem cells in human osteosarcoma OS99-1 cell line. Cancer Biol Ther 11(5):457–463

105. Avnet S, Cortini M (2016) Role of pericellular matrix in the regulation of cancer stemness. Stem Cell Rev 12(4):464–475

106. Avnet S, Di Pompo G, Chano T, Errani C, Ibrahim-Hashim A, Gillies RJ, Donati DM, Baldini N (2017) Cancer-associated mesenchymal stroma fosters the stemness of osteosarcoma cells in response to intratumoral acidosis via NF-κB activation. Int J Cancer 140(6):1331–1345

107. Tu B, Zhu J, Liu S, Wang L, Fan Q, Hao Y, Fan C, Tang T-T (2016) Mesenchymal stem cells promote osteosarcoma cell survival and drug resistance through activation of STAT3. Oncotarget 7(30):48296–48308

108. Kuhn NZ, Tuan RS (2010) Regulation of stemness and stem cell niche of mesenchymal stem cells: implications in tumorigenesis and metastasis. J Cell Physiol 222(2):268–277

109. Zeng W, Wan R, Zheng Y, Singh SR, Wei Y (2011) Hypoxia, stem cells and bone tumor. Cancer Lett 313(2):129–136

110. Cathomas R, Rothermundt C, Bode B, Fuchs B, von Moos R, Schwitter M (2015) RANK ligand blockade with denosumab in combination with sorafenib in chemorefractory osteosarcoma: a possible step forward? Oncology 88(4):257–260

111. Moriceau G, Ory B, Gobin B, Verrecchia F, Gouin F, Blanchard F, Redini F, Heymann D (2010) Therapeutic approach of primary bone tumours by bisphosphonates. Curr Pharm Des 16(27):2981–2987

112. Sampson VB, Gorlick R, Kamara D, Anders Kolb E (2013) A review of targeted therapies evaluated by the pediatric preclinical testing program for osteosarcoma. Front Oncol 3:132

113. Rainusso N, Brawley VS, Ghazi A, Hicks MJ, Gottschalk S, Rosen JM, Ahmed N (2012) Immunotherapy targeting HER2 with genetically modified T cells eliminates tumor-initiating cells in osteosarcoma. Cancer Gene Ther 19(3):212–217

114. Tarek N, Lee DA (2014) Natural killer cells for osteosarcoma. Adv Exp Med Biol 804:341–353